UNIVERSITY OF OXFORD
DEPARTMENT OF BIOCHEMISTRY

"Exploring a gut-brain axis when immunity is constitutively active"

A thesis submitted for the degree of Doctor of Philosophy
In the University of Oxford Hilary Term 2024

SRISHTI ARORA
STUDENT NUMBER: 1110744
ORIEL COLLEGE

COVID STATEMENT

As I began to find my footing while pursuing my doctoral studies at Oxford, the onset of the global Coronavirus pandemic introduced unforeseen challenges that profoundly impacted my research and, consequently, the progression of my thesis.

The implementation of lockdowns coincided with my visit to my home in India, rendering me unable to return to Oxford for an extended duration due to travel restrictions. This hiatus significantly disrupted my laboratory experiments, particularly affecting the stocks of flies I had carefully maintained. Initially, my research involved working with mutant flies that had been backcrossed into the w^{1118} background. However, the stringent lockdown measures and travel restrictions prevented me from maintaining these stocks, inhibiting my work with these flies. Therefore, once I returned, I continued my research using flies with their original genetic background, resulting in the use of two different controls in this thesis (in **Chapter 2, 3 and 5**). Furthermore, since access to the sequencing lab was limited during this period, two repeat experiments had to be prepared and processed for sequencing together. Due to an unforeseeable error, the number of reads finally sequenced was limited in both repeats and, as a result, had to be eliminated, significantly hampering the results mentioned in **Chapter 5**. This was further exacerbated by a department-wide change in the standard fly food recipe from maize-based to corn due to a lack of availability of raw materials during the lockdown. Since 16S rRNA sequencing is an expensive experiment, repeating the entire experiment was not a viable option. It is due to all these hurdles that I could not delve too deep into the analysis, and the research remains incomplete.

ABSTRACT

A gut-brain axis influenced by host innate immunity and resident microbiota has been implicated in neurological conditions, including Alzheimer's disease and Parkinson's disease. However, the precise connection of innate immunity to neurodegeneration remains unclear. Using Pirk, a negative regulator of the IMD/NF-κB pathway in *Drosophila*, we investigated the neurological phenotypes induced, when genetically predisposing flies to an over-reactive innate immune response. *Pirk* mutants exhibited age-dependent neurological phenotypes, exemplified by reduced locomotion activity and altered sleep patterns. Raising flies in axenic conditions showed that, the absence of gut bacteria only partially rescued the neurological and neurodegenerative phenotypes of *pirk* flies. These results correlate with data obtained by tissue-specific *pirk* RNAi, where silencing *pirk* in gut stem cells and glial cells led to earlier onset of the neurological phenotypes. This, alongside dysbiosis of *pirk* mutants, highlighted a potential early role for the gut-brain axis in the onset of neurodegeneration. These are hallmarks of Alzheimer's in humans, but do not exist in flies. Our results indicate an evolutionarily conserved path to neurodegeneration linked with a predisposition to overactive innate immunity, even in the absence of beta-amyloid aggregation or tau protein tangles.

ACKNOWLEDGEMENTS

The life of a D.Phil. student is not an easy one, and I believe it truly takes a village.
I would like to take this opportunity to thank the people without whom this thesis wouldn't have been possible. First and foremost, I would like to thank my primary supervisor, Prof Petros Ligoxygakis, for not only being an excellent mentor for my work, but also someone who has offered me unprecedented freedom to stoke my intellectual curiosity during my time at the lab. I deeply thank him for always being available to discuss and steer me in the right direction throughout the project.

Next, I would like to thank my secondary supervisor, Prof Lynne Cox. Despite being assigned as my supervisor late into my PhD, professor Cox has always encouraged me and believed in my abilities. Apart from academics, she was a major support during the time of my chronic illness and always had great advice.

I am grateful to Dr. Anissa Kempf for helping me with my initial sleep experimental setup and allowing me to use her equipment for my experiments. Further, I am indebted to Dr. Megan Slone, Dr Jingnu Xia and Shivohum Bahuguna for being a constant source of motivation, encouragement and enthusiasm as lab mates. Thank you for all the weekend rant sessions and the extremely necessary coffee and dessert breaks. I would also like to thank the various members of the Ligoxygakis, Davis and Miesenböck groups with whom I had the opportunity to work and have not already mentioned. During my long time there, the Biochemistry department has provided me with an affable and understanding atmosphere in the lab and helped me with useful feedback as well as insightful comments on my work.

I am forever in debt to my husband, Chaitanya Bishnoi for his wise council and sympathetic ear. Thank you for believing in me, even when I didn't. Dr. Vanshaj Jain and Dr. Aradhana Vadekkethil, who were of great support in deliberating over my problems and findings, as well as providing a happy distraction to rest my mind outside of my research. Ishani Nakra, whose willingness to proofread countless pages of biology without complaining is the only reason this thesis could ever be completed. Thank you for always reminding me that I am doing enough.
Finally my friends and family, without whom this author wouldn't exist or be sane.

LIST OF ABBREVIATIONS

AD	Alzheimer's disease
ALS	Amyotrophic lateral sclerosis
AMP	Antimicrobial peptide
ATM	Ataxia Telangiectasia Mutated gene
Aβ	Amyloid beta
BBB	Blood brain barrier
BDSC	Bloomington *drosophila* stock center
BHI	Brain Heart Infusion agar
BLAST	Basic local alignment search tool
Cdk5	Cyclin-dependent kinase 5
ChIP	Chromatin immunoprecipitation
CI	Cytoplasmic incompatibility
CNS	Central nervous system
CR	Conventionally reared
CR	Conventionally reared
CRISPR	Clustered regularly interspaced short palindromic repeats
CSD	Chronic sleep deprivation
CSF	Cerebrospinal fluid
CUS	Chronic unpredictable stress
CVS	Chorionic villus sampling
CYLD	Conserved cylindromatosis
CYLD	Cylindromatosis
DA	Dopaminergic neurons
DAM	Drosophila Activity monitor
DAP	Diaminopimelic acid
dCYLD	Downstream the cylidromatosis disease homolog
DD	Death domain
dFadd	Drosophila Fas-associated death domain
DGGE	Denaturing gradient gel electrophoresis
Dif	Dorsal- related immune factors
DIF	Dorsal-related immunity factor
Dl	Delta
DNA	Deoxyribonucleic acid
Dnr1	Defense repressor 1
Dpt	Diptericin A
Dredd	Death related ced-3/Nedd2-like
dsRNA	Double-stranded RNA
dTAK1	Growth factor-β-activated kinase 1
dUSP36	*Drosophila* ubiquitin-specific protease 36
dUSP36	Drosophila ubiquitin-specific protease 36
E. coli	*Escherichia coli*
EBs	Enteroblasts

EC	Enterocytes
Ecc15	*Erwinia carotovora carotovora 15*
EE cells	Entero-endocrine cells
EEG	Electroencephalogram
esg	Escargot
FISH	Fluorescence in situ hybridization
Foxo	Forkhead box protein O1
GF	Germ-free
GHRH	Growth hormone-releasing hormone
GI	Gastrointestinal
GNBP	Glucan binding proteins
GNBP1	Gram-negative binding protein 1
GWAS	Genome wide association studies
HD	Huntington's disease
HIV	Human immunodeficiency virus
HMP2	Integrative human microbiome project
hsp90	Heat shock protein 90
Iap2	Inhibitor of apoptosis 2
IBD	Inflammatory bowel disease
IBS	Irritable bowel syndrome
IFN	Interferons
IgA	Immunoglobulin A
iHMP	Integrative human microbiome project
IKK	Inhibitory-κb Kinase
IL	Interleukin
IMD	Immune deficiency
ISC	Intestinal stem cells
ISF	Interstitial fluid
ITGAM	Integrin alpha M
IκBα	Nuclear factor of kappa light polypeptide gene enhancer in B-cells inhibitor, alpha
JNK	C-Jun N-terminal kinases
LAPTM5	Lysosomal protein transmembrane 5
LPS	Lipopolysaccharide
Mag	Magro
MGWAS	Metagenome-wide association studies
miRNA	Microrna
MPTP	1-methyl-4-phenyl-1,2,3,6-tetrahydropyridine
mRNA	Messenger RNA
MRS	Man, Rogosa, and Sharpe
MS	Multiple sclerosis
MyD88	Myeloid differentiation primary-response gene 88
NF-κB	Nuclear factor kappa B
NGS	Next-generation sequencing
NIG	National Institute of Genetics
norpA	No receptor potential

nREM	Non-rapid eye movement
OAS1	Oligoadenylate synthetase 1
OTUs	Operational taxonomic units
P-elements	P transposable elements
PBS	Phosphate buffered saline
PCR	Polymerase chain reaction
PD	Parkinson's disease
PG	Prostaglandins
PGN	Peptidoglycan
PGRP	Peptidoglycan recognition proteins
PGS	Preimplantation genetic screening
PI	Performance index
PIMS	PGRP- LC-interacting inhibitor of IMD signalling
Pirk	Poor Immune Response upon Knock in
PLCG2	1-Phosphatidylinositol-4,5-bisphosphate phosphodiesterase gamma-2
PolyQ	Polyglutamine
POSH	Plenty-of-SH3s
PRRs	Pattern-recognition receptors
PSH	Persephone
pTBI	Penetrating traumatic brain injury
qPCR	Quantitative polymerase chain reaction
RelA	Reticuloendotheliosis viral oncogene homolog A
REM	Rapid eye movement
RHIM	RIP homotypic interaction motif
RHIM	RIP homotypic interaction motif
RISC	RNA-induced silencer complex
RNAi	RNA interference
ROS	Reactive oxygen species
SCFA	Synthesis of short- chain fatty acid
SCN	Suprachiasmatic nucleus
SFA	Short chain fatty acids
shRNAs	Short hairpin RNA
SHY	Synaptic homeostasis hypothesis
siRNA	Small interfering RNA
SkpA	SKP1-related A
SPE	Spätzle-processing enzyme
SPI1	Spi-1 proto-oncogene
Spz	Spätzle
T2D	Type 2 diabetes
Tab2	Tgf-beta activated kinase 1 map3k7) binding protein 2,
Tak1	Transforming growth factor b-activated kinase 1 kinase
TCT	Tracheal cytotoxin
TG	Transglutaminase
TH	Tyrosine hydroxylase
TIR	Toll and interleukin-1 receptor
TISC	Toll-induced signalling complex

TLR	Toll like receptor
TNF	Tumour necrosis factor
TNFR1	Tumour necrosis factor receptor 1
TREM2	Triggering receptor expressed on myeloid cells 2
TRiP	Transgenic RNAi Project
UAS	Upstream activating sequences
VDRC	Vienna drosophila resource center
WntD	Wnt inhibitor of Dorsal
ZT	Zeitgeber time

TABLE OF CONTENTS

LIST OF FIGURES AND TABLES

CHAPTER ONE

Introduction

1.1 INTRODUCTION

Ageing is characterised by the time-dependent deterioration of cellular function and fitness of an organism, accompanied by an increased susceptibility to diseases (Lipsky and King 2015). This decline in function is inexorable and is a key risk factor for a number of human disease pathologies such as diabetes, cancer, cardiovascular disorders, and neurodegenerative diseases (Ferrucci and Fabbri 2018). As the world's geriatric population continues to grow at an exceptional rate (World Population Prospects: the 2019 Revision), a substantial economic burden is placed on the healthcare system to deal with the development of age-related diseases. Therefore, understanding the mechanism of longevity and identifying targets to improve health during ageing is of paramount.

Over the last decade there have been a number of attempts to explain the phenomenon of ageing (Lipsky and King 2015). Different processes that affect ageing can be categorised into nine hallmarks that are shared by ageing and age-related diseases (Kennedy *et al.* 2014). These include altered intercellular communication, stem cell exhaustion, cellular senescence, mitochondrial dysfunction, deregulated nutrient sensing, genomic instability, telomere attrition, loss of proteostasis (protein homeostasis), and epigenetic alterations. These co-occur as an organism ages and are extensively interconnected. However, there are several questions regarding the interconnectedness of these hallmarks. One such question is the role of inflammation and its impact on age-related disorders (Franceschi *et al.* 2018). There is an age-dependent decline in the immune response; a phenomenon termed as "immunosenescence" (Pawelec 2012; Solana *et al.* 2012). This process is marked by a reduction in the adaptive immune response and was initially believed to be a consequence of a progressive rise in low-grade chronic pro inflammatory status known as "inflammageing" (Franceschi et al. 2007, 2018; Frank and Caceres 2015).More precisely, as the thymus releases the last pool of naïve

T-cells and that pool gets depleted each time there is an infection, older people (>65) become progressively weaker in their T-cell responses (Solana *et al.* 2012; Kennedy *et al.* 2014; Franceschi *et al.* 2019). Increase in innate immune pro-inflammatory levels has been seen as a "balancing act" to counter adaptive response reduction. Nevertheless, recent studies have observed that the two processes are mutually maintained and affect one another (Fulop *et al.* 2018). For instance, depletion of adaptive immune cells strengthens the innate immune response, causing inflammageing; similarly, the increased innate immune inflammatory mediators lead to a reduction in the number of adaptive immune cells causing immunosenescence (Tu and Rao 2016). Cumulative studies have also indicated an age-dependent change in the innate immune cell types that leads to an overall decrease in their ability to collaborate in the initiation of the adaptive immune response [reviewed by (Solana *et al.* 2012)]. Inflammageing is often the result of a non-resolving or sterile inflammation and is thought to be a possible underlying basis for most age-related diseases such as infections, cancer, autoimmune disorders, and chronic inflammatory diseases (Salvioli *et al.* 2013). Additionally, cell senescence in other tissues generates cytokines that signal the necessity for these cells to be removed by macrophages, in order to avoid what is called "by-stander senescence", propagating in tissues. This further enhances age-dependent systemic pro-inflammatory activity (Franceschi *et al.* 2007, 2018, 2019; Solana *et al.* 2012; Kennedy *et al.* 2014). The above happens to everyone in the context of healthy ageing

The precise mechanism of the development of neurodegenerative diseases is still unknown. This presents a challenge for the development of treatments and therapies (Hussain *et al.* 2018). Currently, therapies focus only on treating isolated disease symptoms such as protein accumulation, sleep disturbances, memory loss, or behavioural changes. Additionally, disease modifying therapies are largely unsuccessful and there is need for more drug candidates to enter the pipeline. Since most cases of neurodegeneration are only diagnosed after severe

neuronal loss, exploring preclinical symptoms as a potential therapy could facilitate the development of treatments for the early symptoms of the disease. As revealed by genome wide association studies (GWAS), aberrant immune regulation resulting in chronic inflammation long before neurological symptoms manifest themselves may be at the root of these diseases (Salih *et al.* 2019).

1.1.1 Immunity and Neurodegeneration

While the correlation between inflammation and neurodegeneration is well-known (Kim *et al.* 2006) as a consequence of the production of apoptotic factors, whether inflammation is one of its causes or a consequence remains unclear. Inflammation can be triggered and cytokines signalling during neuronal death. However, immune cells produce neurotoxic cytokines that could cause death of neurons (Smith *et al.* 2012a). Initially, the activation of the immune response in the central nervous system (CNS) was believed to be responsible for the elimination of infectious agents and the clearing of debris after injury, suggesting a neuroprotective role of inflammation. A positive role of antimicrobial peptide (AMP) production and ageing has been suggested by Loch et al. (2017). GWAS have reported the activation of numerous genes of the inflammatory pathway during ageing (Jeck, Siebold and Sharpless 2012). Age is the greatest risk factor for neurodegenerative disorders and age-related chronic activation of the immune response is a shared feature among many neurodegenerative disorders (Xia *et al.* 2016). Several GWASs have implicated genetic variants of innate immune genes as risk factors for Alzheimer's disease (AD) (Lambert *et al.* 2010; Li *et al.* 2021; Wang *et al.* 2021b). These studies suggest a potential correlation

Studies in animal models indicate the importance of inflammation in several neurodegenerative disease pathologies (Glass *et al.* 2010). Altering expression of Cdk5 protein kinase (Cdk5α) leads to disruption in autophagy that in turn leads to upregulation of AMP and age-dependent

degeneration of dopaminergic (DA) neurons in *Drosophila* (Shukla *et al.* 2019). Neuroinflammation has been a crucial factor for the pathogenesis of diseases such as AD (Heneka *et al.* 2015)leads to the secretion of multiple neurotoxic agents, such as inflammatory mediators and reactive oxygen species, by glial cells. These aggravate the pathology of the disease (Smith et al. 2012b). Microglia, the resident innate immune cells of the CNS are shown to be chronically activated around these plaques. It is believed that the uncontrolled inflammation of these cells Click or tap here to enter text.It is further demonstrated that mutations in microglial protein TREM2, PLCG2, and ABI3 increase the risk for AD (Dalmasso *et al.* 2019). Additionally, molecular and pathological interaction studies have established glial expression of TREM2/TYROBP as a key factor in Tau-mediated neurodegeneration (Sekiya *et al.* 2018). Activated microglia is suggested as a potential marker to detect AD before the appearance of plaques (Wright *et al.* 2013). Additional risk genes for late onset AD connected to microglia and immunity have been identified recently (Salih *et al.* 2019) identified a transcriptional network of 12 largely microglial genes (Zhang et al. 2013). Genetic analysis of these late-onset AD risk genes Click or tap here to enter text.Six of these (OAS1, LAPTM5, ITGAM, ABI3, PLCG2, SPI1) have good *Drosophila* homologs expressed in the nervous system (our unpublished observations).

Drosophila models illustrate the importance of the Toll receptor-mediated NF-κB response in the neurotoxicity caused by the presence of Aβ42, an isoform of the beta amyloid (Aβ) protein. Down regulation of this immune pathway was shown to reduce the pathological activity of Aβ42 (Tan *et al.* 2008). Evidence in both human and animal model studies have illustrated the correlation between inflammation and Parkinson's disease (PD) (Kannarkat, Boss and Tansey 2013)Mechanisms of neuronal dysfunction, such as mitochondrial impairment and oxidative stress, have been linked to pathogenesis of PD (Dauer and Przedborski 2007). DA neurons in the midbrain are shown to be sensitive to pro inflammatory cytokines, reactive oxygen species,

and chemokines such as TNF-α (tumour necrosis factor alpha) and IFN (interferons) that exacerbate neuronal lesions (Herrera *et al.* 2005). Additionally, there is a rich population of microglia in the substantia nigra, which is the region of the brain that shows the most DA neuron loss in PD patients (Croisier *et al.* 2005). Studies have observed a correlation between deposition microglial activation and α-synuclein, making microglia an attractive therapeutic target (Su *et al.* 2008; Alvarez-Erviti *et al.* 2011). However, PD is considered as a condition that is hypothesised to start in the intestine as chronic inflammation, then may transfer α-synuclein to the brain through the vagus nerve (Kim *et al.* 2019).

Transgenic mice lacking the TNF (tumour necrosis factor)- α receptor demonstrate a reduction in the TH (tyrosine hydroxylase)-immunoreactivity after being exposed to MPTP (1-methyl-4-phenyl-1,2,3,6-tetrahydropyridin). Prolonged use of non-steroidal anti-inflammatory drugs such as ibuprofen is shown to reduce risk of PD (Kannarkat, Boss and Tansey 2013). Consistent with these studies, an increase in circulating cytokines and increased microglial activation have also been linked to early stages of Huntington's disease (HD) (Björkqvist *et al.* 2008; Politis *et al.* 2015). However, production of pro inflammatory molecules is not just limited to microglia. Other types of glia cells such as astrocytes are also used to investigate the progression of inherited amyotrophic lateral sclerosis (ALS) (Yamanaka *et al.* 2008). Studying these processes in humans is extremely challenging, however, model organisms have proven to be an effective tool to help provide critical insights into the cellular and molecular levels of ageing

1.1.2 Drosophila as a model for this study

Over the last two decades, *Drosophila* has developed as a powerful tool to investigate human disease mechanisms. It has orthologs of ~65% of all genes causing heritable diseases in

humans (Yamamoto *et al.* 2014; Ugur, Chen and Bellen 2016) making it an attractive model organism to address novel lines of inquiry for human diseases (Singh and Irvine 2012). Moreover, for every one of these genes, the fly will most of the time have one copy while humans will normally have a group of genes with the same function. The fruit fly is small, has a low cost of rearing and is easy to manipulate in the laboratory. It has a short generation time of 10 days at 25°C, a relatively short lifespan and produces a large number of eggs which boosts statistical relevance of the data obtained. *Drosophila* shows complex behavioural phenotypes including social aggregation, re-enforced learning as well as sleep activity that help address questions of brain function. Transgenic fly lines can be created using numerous sophisticated genetic and molecular tools such as insertions of P-elements (Spradling *et al.* 1999) CRISPR (short for "clustered regularly interspaced short palindromic repeats"), Ribonucleic acid interference (RNAi) silencing, tissue specific and GAL4-upstream activating sequences (UAS) expression system. Additionally, genome-wide genetic screening and analyses with deep sequencers, such as RNA sequencing (RNA-seq) and chromatin immunoprecipitation sequencing (ChIP-seq), allow us to examine the cellular and molecular mechanisms of ageing. Metabolomics analyses further help characterise age-related diseases. Genetic and molecular investigations in model organisms have revealed numerous similarities between the insect host defences and the mammalian innate immune response. Moreover, *Drosophila* has been crucial in the discovery and understanding of innate immune signalling and the development of the nervous system. The fly has traditionally been used to establish key proteins in the nuclear factor kappa-light-chain-enhancer of activated B cells (NF-kB) pathways and further the understanding of microbial pathogenesis (Chamilos, Samonis and P Kontoyiannis 2011). *Drosophila* has demonstrated to be a valuable tool for exploring mucosal immunity and host-microbe interactions (Kuraishi, Hori and Kurata 2013a; Younes *et al.* 2020; Kietz 2021). The digestive tract of the fly, like that of mammals, is divided into functionally distinct segments

and colonised by different bacteria (Miguel-Aliaga, Jasper and Lemaitre 2018). Preventing bacterial systemic invasion requires confining bacteria to the intestinal lumen and preventing bacteria from crossing the gut epithelium.

The fly exhibits multiple physiological changes associated with ageing and age related diseases such as reduced locomotive ability (Gargano *et al.* 2005; Jones and Grotewiel 2011), impaired learning and memory (Tamura *et al.* 2003), progressive decline in intestinal barrier function (Rera, Clark and Walker 2012a), increased inflammation (Kounatidis *et al.* 2017), reduced reproductive capacity, and altered neuronal function (Beaver *et al.* 2002; Piper and Partridge 2018). There are several resemblances between the sleep patterns of *Drosophila* and humans (Chiara Cirelli 2009). Flies are active during the day and usually sleep at night, they are crepuscular. Like in humans, flies have an age dependent increase in sleep fragmentation (Metaxakis *et al.* 2014a). Subsequently, both mechanisms that regulate sleep: circadian rhythm and homeostasis, are evolutionarily conserved. As sleep is a biomarker for cognitive decline in neurodegeneration, the ability to efficiently study sleep in *Drosophila* gives us valuable insights into the progression of neurodegenerative diseases (Keene and Joiner 2015). To summarise, what makes *Drosophila* an ideal candidate for this study is its well-defined nutritional needs (that can easily be manipulated), its genetically accessible tissue systems, anatomical similarities and similar sleep patterns to mammals as well as a defined gut microbiome.

1.1.3 Innate and adaptive immunity

All living organisms are exposed to a great variety of microorganisms that inhabit their surroundings, most of which can cause severe damage to the host if left unchecked. The immune system is responsible for recognising

Jawed vertebrate immunity has several facets but can be categorized into two main categories: the innate and adaptive immune responses. The innate immune system is the non-specific recognition and elimination of a foreign body. The primary goal of the innate immune response is to react promptly and prevent proliferation of infectious pathogen in the host. Whereas the adaptive immune response is extremely specific for particular pathogens (Dempsey, Vaidya and Cheng 2003). Moreover, the adaptive immune response is capable of memory, which means that with every interaction with the same infectious agent the adaptive immune response becomes more efficient. The two key features of adaptive immunity are narrow specificity and memory.

1.1.4 Drosophila Immune Response

1 1.4.1 Systemic innate immunity in *Drosophila*

The innate immune system, or the nonspecific immune system, is an organism's first line of defence. Through this, cells target conserved features of invaders and expeditiously activate themselves to destroy pathogens (Kounatidis and Ligoxygakis 2012). Unlike mammals, insects lack an adaptive immune response and therefore rely on a relatively sophisticated set of innate defences for their survival. The development and function of these reactions are shown to be shared with higher organisms and can be used to study innate immunity and inflammation in humans (Lemaitre and Hoffmann 2007). *Drosophila* utilises a variety of defences to form an effective barrier against pathogens, such as physical barriers, as well as local and systemic immune responses.

The fruit fly has a cuticular exoskeleton that prevents access to potentially pathogenic microbes, in addition to which, a membrane coats the gut and the trachea (Moussian *et al.* 2005). Following the physical barrier lies multiple chemical barriers, first of which is a local immune response. This includes the elimination of incoming pathogens by constitutive

secretion of antimicrobial peptides (AMPs) and reactive oxygen species (ROS) in epithelial tissues that are in direct contact with the environment, including the respiratory, reproductive and the digestive tract. These are also known as the barrier epithelia and are independent of the systemic response as they do not involve the fat body (the fly equivalent of a mammalian liver) (Ferrandon *et al.* 1998; Liehl *et al.* 2006). However, once the physical barrier is breached (by injury or infection), there is a rapid induction of a cellular response, that involves cells of the open circulatory system, of the fruit fly known as hemocytes. These cells are ideal signal mediators in response to infection and wounding and can be divided into three types based on their structural and functional features: plasmatocytes responsible for phagocytic removal of pathogens, crystal cells that mediate melanisation and lamellocytes responsible for encapsulation (Wang, Kounatidis and Ligoxygakis 2014; Ayres and Schneider 2008; Stuart and Ezekowitz 2008). Phagocytosis is an essential cellular mechanism that is responsible for the removal of pathogens and dying cells (Stuart and Ezekowitz 2008). Smaller entities like bacteria can be engulfed directly by phagocytosis, whereas any foreign particles larger than those that can be phagocytosized, such as parasitoid eggs, are encapsulated by lamellocytes instead (Tzou, de Gregorio and Lemaitre 2002). Melanisation is a proteolytic cascade in the hemolymph that is activated immediately against invading pathogens, the degree of which is infection dependent. It is marked by visible blackening of the surface of the pathogen and the site of injury which results from the synthesis and deposition of melanin (Tang 2009). Melanin is also shown to play a role in encapsulation by isolating the pathogen and ultimately killing it by the intermediates of melanisation including hydrogen peroxide (H_2O_2) or nitric oxide (NO) agents (Tang *et al.* 2006). The final response is marked by the systemic production of AMPs in the hemocytes and the fat body. Expression of the AMP genes are regulated by two NF-kB-mediated signalling pathways: The Toll pathway which is homologous to the Toll like receptor

(TLR) in mammals and the immune deficiency (IMD) pathway which is homologous to the tumour necrosis factor receptor 1 (TNFR1) pathway in mammals (Hultmark 2003).

1 1.4.2 Detecting and recognising different classes of pathogens

Infections are detected by the recognition of specific, evolutionary conserved molecules that are present on the pathogen but absent from the host. The *Drosophila* immune system has the ability to differentiate between different classes of pathogens (Pal and Wu 2009). Different NF-kB pathways respond with pathogen specific reactions, the activation of which is regulated by several pattern-recognition receptors (PRRs) (Bland 2023). Most bacterial infection in *Drosophila* are detected by a prominent class of PRRs known as peptidoglycan recognition proteins (PGRPs) that bind to and sometimes cleave different types of peptidoglycans (PGN) (Charroux *et al.* 2009). Gram-positive lysine-type peptidoglycan are recognised (Leulier *et al.* 2003).

Drosophila genome contains 13 PGRP genes that translate into 19 proteins (Royet, Gupta and Dziarski 2011). These are generally classified based on the size of their mRNA transcripts and 5'- untranslated regions - s for short and l for long (Werner *et al.* 2000). Most short PGRP family protein lack a transmembrane domain and are likely to be secreted, whereas most long PGRP proteins have an extended N-terminal and may contain only a transmembrane domain. The PGRP family protein has a characteristic conserved PGRP domain whose structure is similar to N-acetylmuramoyl-L-alanine amidases, such as T7 lysozyme that hydrolyses PGN (Royet and Dziarski 2007). Some of the PGRP family members have retained their ancestral enzymatic activity and are known as catalytic PGRPs; for example, PGRP-SC1B (Mellroth, Karlsson and Steiner 2003), whereas other members of the family have lost their enzymatic activity and act as microbial recognition sensors; these are known as recognition PGRPs

(Werner *et al.* 2000; Ferrandon *et al.* 2007). The catalytic PGRP indirectly influences the transmembrane PGRPS with their ability to process and degrade PGN. The detection of gram-positive bacteria activates the Toll pathway via a circulating recognition complex containing PGRP-SA and GNBP1 (gram-negative binding protein 1) (Michel et al. 2001; Gobert et al. 2006)with the help of PGRP-LC, a transmembrane receptor, and PGRP-LE (Choe et al. 2002; Gottar et al. 2002; Kew et al. 2002; Rämet et al. 2002a). IMD pathway is preferentially induced by gram negative bacteria Click or tap here to enter text.Additionally, PGRP-LE can only activate the IMD pathway by possibly forming heterodimers with PGRP-LC. PGRP-LC can be found in three isoforms: a, x and y (referred to as a, b and c in FlyBase). They are capable of creating heterodimers among themselves and recognising(Takehana *et al.* 2004; Kaneko *et al.* 2006; Neyen *et al.* 2012).

1 1.4.3 The Toll Pathway

The Toll humoral response is prompted by a gram-positive or fungal infection which leads to the activation of two Rel factors, Dorsal and DIF (dorsal-related immunity factor), whose principal target is Drosomycin (**Figure 1**) (Drier, Huang and Steward 1999; Ligoxygakis *et al.* 2002). Apart from its role in the immunity, the toll pathways play a crucial role in the determination of the dorsal ± ventral polarity and wound closure in *Drosophila* embryogenesis (Lemaitre, Nicolas and Michaut 1996; Carvalho, Jacinto and Matova 2014).

Activation of the Toll pathway

In order to initiate the Toll response, bacterial or fungal pathogens first activate PGRP or GNBP receptors that initiate a complex extracellular proteolytic cascade causing a conformational change in the Toll receptor cytokine ligand called Spätzle (Spz) (**Figure 1**) (Schneider *et al.*

1994; Imler and Hoffmann 2001). Spätzle is synthesised as an inactive pre-pro-protein molecule that masks a hydrophobic C- terminus region (Arnot, Gay and Gangloff 2010). Once processed, Spz goes through a conformational change that exposes the Toll binding sites necessary for its signalling activity (Weber *et al.* 2003).

This extracellular proteolytic cleavage of Spz is achieved using different proteins. In embryogenesis, Spz is cleaved by Easter (Chasan, Jin and Anderson 1992), which is activated by the Nudel-Gastrulation Defective-Snake cascade via Pipe (Cho, Stevens and Stein 2010). However, during immune reactions this cleavage is achieved by the Spz- processing enzyme (SPE)(Jang *et al.* 2006). Depending on the PRR, the activation of SPE can be accomplished by one of three protease cascades. Proteases from live Gram-positive bacteria and fungi are sensed by the Persephone (PSH) cascade (Gottar et al. 2002; Ligoxygakis et al. 2002), while PRR binding to cell wall components from Gram-positive bacteria and fungi activates the other two cascades, both of which converge on the same proteolytic cascade (Chamy et al. 2008) (Figure 1).

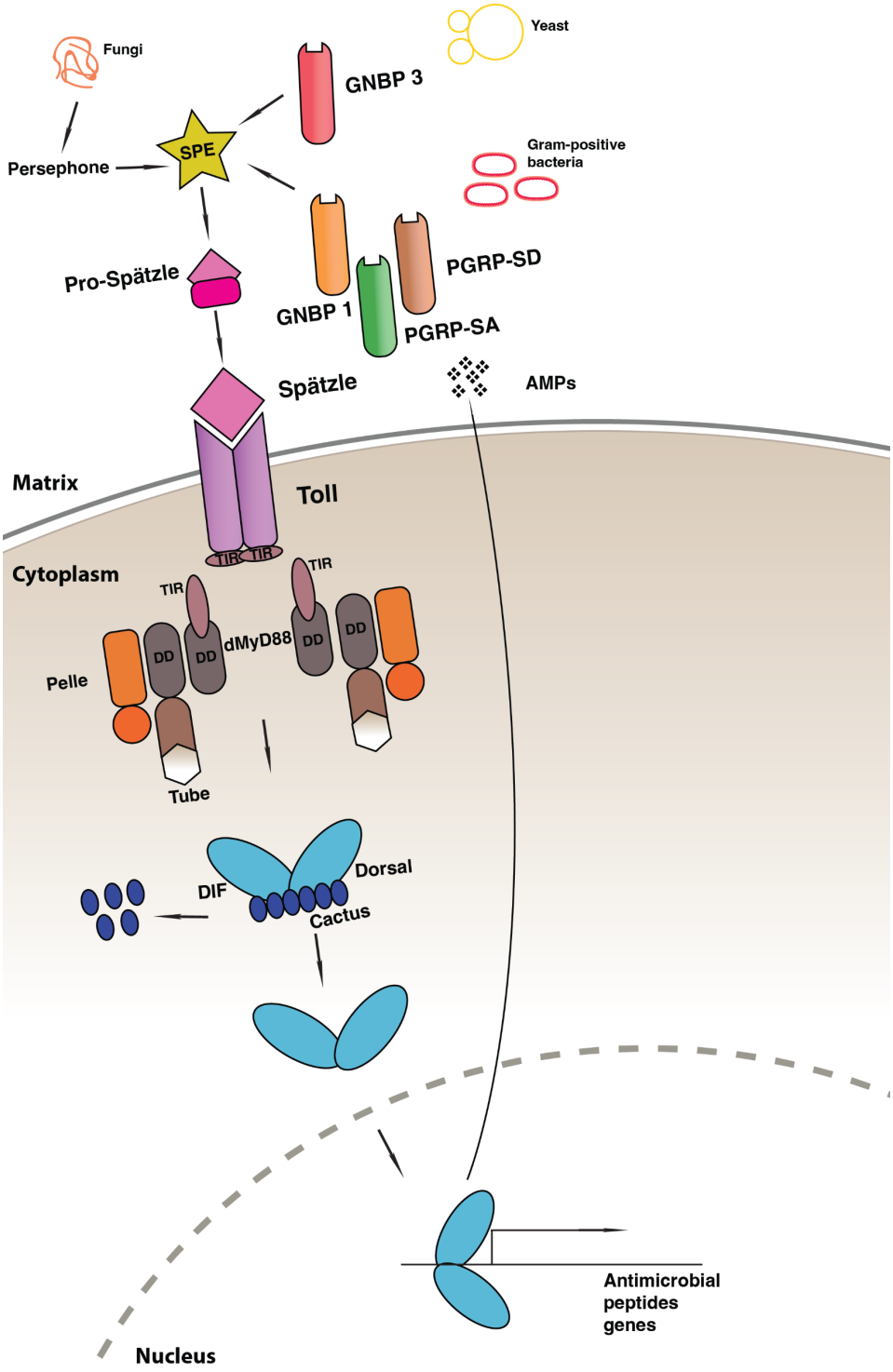

Figure 1: The *Drosophila* Toll pathway. The toll pathway is generally activated by fungi, yeast and gram positive bacteria, that initiate a cascade of reactions leading to the digestion of pro-spätzle into spätzle. Spätzle then binds to the toll reception on the cell surface, leading to the activation of the toll pathway, that further results in the production of antimicrobial peptides. Figure adapted from Valanne, Wang and Rämet (2011)

The Toll pathway-signalling cascade

The cleaved Spz binds with the leucine rich extracellular domain of the transmembrane receptor, called the toll receptor (Hashimoto, Gerttula and Anderson 1991). This leads to the formation of a high affinity crosslink between two toll ectodomains, causing them to form a dimer that leads to a conformational change (Weber *et al.* 2003). The cytoplasmic domain of the toll receptor contains a conserved 150 amino acid region that is similar to the corresponding region of the mammalian interleukin 1 receptor; referred to as the Toll–IL-1R (TIR) domain. This conserved TIR domain interacts with MyD88 (myeloid differentiation primary-response gene 88) leading to a formation of a multivalent complex known as Toll-induced signalling complex (TISC) at the cytoplasmic tail of the Toll receptor. Sherpa, an E3 ubiquitin ligase protein acts as a catalyst and enhances this reaction by binding to Myd88 (Kanoh *et al.* 2015). The MyD88 adaptor protein consists of a TIR domain and a death domain (DD), the former binds to the receptor TIR domain and the latter interacts with the DD of Tube, a second adaptor protein (Warner and Núñez 2013). This adapter protein contains a bivalent DD that further interacts with the DD of Pelle, a protein kinase. Pelle is then phosphorylated by Pellino, which leads to the activation of Pelle kinase activity that ultimately causes rapid phosphorylation and degradation of Cactus (Towb, Bergmann and Wasserman 2001; Haghayeghi *et al.* 2010). Cactus in its basal state is bound to Doral and/or Dorsal- related immune factors (Dif), inhibiting their nuclear localisation(Valanne, Wang and Rämet 2011; Lindsay and Wasserman 2014).

Dysregulation of the Toll Pathway

The Toll pathway was first identified for its role in the dorsoventral patterning in fly embryos. Anderson, Bokla and Nüsslein-Volhard showed that flies lacking the Toll gene produced dorsalised embryos, in which all embryonic cells behave like dorsal cells. During the development of the embryo, WntD (Wnt inhibitor of Dorsal) negatively regulates the pathway by an intracellular negative feedback loop. In the embryo, Wnt blocks the nuclear translocation of Dorsal and is responsible for the establishment of distinct dorsal and ventral domains during dorsoventral patterning. Additionally, WntD functions as a negative regulator for the Toll pathway by downregulating the production of Toll ligand in adults (Misra *et al.* 1998; Lamiable, Meignin and Imler 2016). Mutations in the *wntD* gene have hyperactive immunity and are sensitive to infections with *Listeria monocytogenes* to a greater extent than wild type (Gordon *et al.* 2005).

The role of Toll in the innate immune response was subsequently shown by (Lemaitre, Nicolas and Michaut 1996). Mutations in *toll/cactus/spatzle/dif* made the flies highly susceptible to fungal and gram-positive infections, as they failed to express *drosomycin* (Lemaitre, Nicolas and Michaut 1996; Rutschmann, Kilinc and Ferrandon 2002). Additionally, flies with a loss of function mutations in Toll and 18-Wheeler (Toll2) have severe developmental defects that extend to the larval fat body (Keith and Gay 1990; Eldon *et al.* 1994; Ligoxygakis, Hoffmann and Reichhart 2002). However, mutations in pellino have been shown to reduce Drosomycin secretion and reduce survival against gram-positive bacteria, indicating that pellino acts as a positive regulator of the pathway (Haghayeghi et al. 2010). Towb (2001) further studied the role of Pelle in the feedback loop of Toll. They demonstrated that Pelle downregulated Toll by reducing Tube localisation, highlighting the importance of the Tube-Pelle interaction in this downregulation.

1.1.4.4 The IMD Pathway

Another evolutionarily conserved signalling cascade is the immune deficiency or the IMD pathway which regulates the functioning of the NF-kB transcription factor Relish (Rel) (Marika Hedengren *et al.* 1999; Aggarwal and Silverman 2008). The IMD pathway is initiated with the help of PGRP-LC and PCRP-LE that identify diaminopimelic acid (DAP) - type peptidoglycan (Takehana *et al.* 2004; Kaneko *et al.* 2006). These are usually present on gram-negative bacteria with the exception of a few gram-positive bacteria including Bacillus *spp.* (Stenbak *et al.* 2004; Lemaitre and Hoffmann 2007).

These DAP-type peptidoglycans differ from the Lys-type in that they contain a meso-DAP residue as the third amino acid on the PGN peptidic stems. In Lys-type PGN, generally present in gram-positive bacteria, this position is instead usually occupied by a lysine (Lys) (Humann and Lenz 2009).Click or tap here to enter text. The DAP-PGN is thought to be released from the bacterial cell wall as polymeric and monomeric structures, either during cell proliferation or cell death caused by initial/basal immune response. Highly immunogenic metabolites of the cell wall that are continuously released in the form of monomeric DAP-PGN, known as tracheal cytotoxin (TCT) (Dworkin 2014), have the ability to activate the IMD pathway as potently as polymeric DAP-PGN (Royet, Reichhart and Hoffmann 2005).

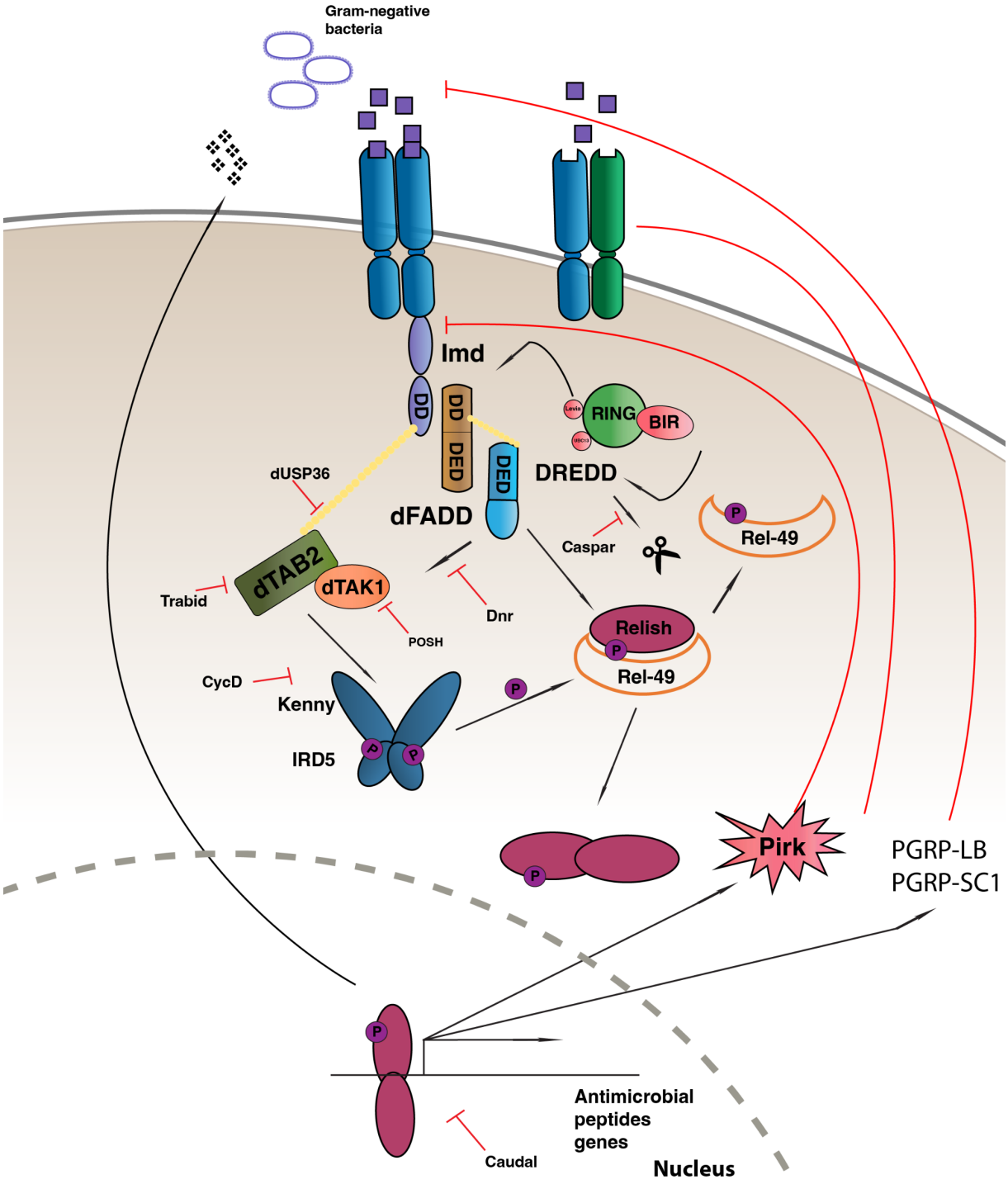

Figure 2: The *Drosophila* IMD pathway. The Drosophila IMD pathway is activated when PGN from gram negative bacteria binds with PGRP receptors present on the cell surface. This binding initiates a signalling cascade that involves the imd-dFADD-Dredd complex leading to the cleavage of Relish and its recruitment into the nucleus. The activated Relish protein acts as NF-kB transcription factor, leading to the transcription of antimicrobial peptides and negative regulators of the pathway to initiate the negative feedback loop. These negative regulators are crucial for immune homeostasis (shown in red). This figure is adapted from Myllymäki, Valanne and Rämet (2014).

Activation of the IMD pathway

Unlike the Toll pathway, the IMD signalling cascade is initiated by transmembrane PGRP receptors, where PGN binds directly to the IMD receptor that acts not only as a recognition protein but also a signalling receptor (**Figure 2**). As mentioned in the previous **Section 1.1.2**, the PGRP receptors responsible for the initiation of the IMD pathway are PGRP-LC and PGRP-LE (Choe *et al.* 2002; Gottar *et al.* 2002; Rämet *et al.* 2002b; Takehana *et al.* 2002). Even though both PGRP receptors belong to the long class of PGRPs and contain a conserved C-terminal along with an extended N- terminal region, knock out experiments suggest that PGRP-LC is the chief receptor of the IMD pathway and PGRP-LE acts alongside and in synergy with PGRP-LC (Kaneko *et al.* 2004; Takehana *et al.* 2004).

The activation of the pathway requires the dimerisation*Listeria* (Yano *et al.* 2008) and is responsible for the recognition of extracellular bacteria that secrete monomeric DAP-PGN in the cytosol (Park and Uehara 2008; Neyen *et al.* 2016a). Furthermore, PGRP-LE plays a key role in the recognition of DAP-PGN in the cytoplasm of insect renal organ, the malpighian tubules (Paik *et al.* 2017) and the prophenoloxidase cascade responsible for melanisation (Takehana *et al.* 2002).

The signalling cascade of the IMD pathway

As illustrated in **Figure 2**, once activated, the cytoplasmic domain of PGRP-LC recruits a signalling complex containing Imd, dFadd, and Dredd via its N-terminal (Lemaitre *et al.* 1995; Georgel *et al.* 2001; Choe *et al.* 2002; Leulier *et al.* 2002). Imd is a death domain protein that resembles the mammalian receptor (RIP1 or receptor interacting protein 1) (Georgel *et al.* 2001), whereas Dredd is homolog to caspase-8 in mammals (Elrod-Erickson, Mishra and Schneider 2000; Leulier *et al.* 2000). Once recruited, Dredd is ubiquinated by the E3 ligase

Iap2 (inhibitor of apoptosis 2) (Meinander *et al.* 2012) and cleaves Imd to expose the Iap2 binding site that allows Iap2 to further ubiquinate Imd. This causes Tab2 and Tak1 (transforming growth factor b-activated kinase 1 kinase) complex to reach the reaction site and phosphorylate the *Drosophila* IKK complex containing *ird5* (a gene encoding a homolog of mammalian IKKβ (Silverman *et al.* 2000; Lu, Wu and Anderson 2001) and Kenny (a homolog of IKK γ/NEMO) (Rutschmann *et al.* 2000; Silverman *et al.* 2000), that activate Rel by phosphorylating multiple sites on its N-terminal (Rutschmann *et al.* 2000; Silverman *et al.* 2000; Lu, Wu and Anderson 2001; Kleino *et al.* 2005). Apart from the phosphorylation, the C terminal of Relish needs to be cleaved, for it to be activated. In vitro studies have illustrated the role of Dredd in this cleavage (Stöven *et al.* 2003). The activated N-terminal (Rel-68) is then translocated into the nucleus and RNA polymerase II is recruited, which ultimately results in the transcription of AMPs (Stöven *et al.* 2000, 2003).

Regulators of the IMD pathway

The improper activation of the immune signalling pathways is associated with inflammation, cancer, and neurodegeneration (Hoesel and Schmid 2013; Kounatidis *et al.* 2017); which leads to developmental defects during ontogenesis (Georgel *et al.* 1995; Bischoff *et al.* 2006; Maillet *et al.* 2008). To prevent the harmful consequences of unwarranted activation, the pathway is firmly regulated by extracellular and intracellular proteins (**Figure 2**, shown with red lines).

The IMD immune response is tightly regulated at many levels, the first of which is the dilution of the activating signal. This is done by the secreted PGRP-SC and PGRP-LB amidase that break down bacterial peptidoglycan into non-stimulatory fragments in the extracellular matrix (Bischoff *et al.* 2006; Charroux *et al.* 2018). On the plasma membrane, the three PGRP-LC isomers interact with each other to suppress spontaneous dimerisation and reduce the number of functioning receptors (Kaneko and Silverman 2005). Additionally, PGRP-LF binds with

PGRP-LC to form non-signalling heterodimers and down regulate the response (Basbous *et al.* 2011). Intracellularly, Pirk (poor Imd response upon knock-in) is a negative regulator that coimmunoprecipitates with Imd protein and blocks the receptor-adaptor interaction and restricting the activity of successive deubiquitination enzymes targeting Imd (Aggarwal *et al.* 2008; Kleino *et al.* 2008; Lhocine *et al.* 2008). Additionally, once ubiquinated Dredd is depleted from the pathway via Dnr1 by ubiquitin-mediated proteolysis, it coimmunoprecipitates with Imd causing a disruption in its association with the cytoplasmic tail of PGRP-LC, receptor leading to its the depletion from the membrane. *Pirk* mutant flies have constitutively activated immune response and are short lived. Moreover, flies over expressing *pirk* have a reduced Imd response (Aggarwal *et al.* 2008; Kleino *et al.* 2008; Lhocine *et al.* 2008). Dnr1 inhibits the activity of Dredd caspase by promoting its proteolytic degradation. *Dnr 1* mutants have shorter lifespans and exhibit age-dependent neuropathology (Cao *et al.* 2013). The activity of the Dredd caspase is also impaired by Caspar, which inhibits Dredd-dependent modification of Relish, further blocking its translocation to the nucleus (Kim *et al.* 2006). The activity of NF-kB is regulated by several ubiquitin-mediated interactions and deregulation of these factors cause chronic inflammation and cancer (Chen and Chen 2013). Further, negative regulators of the Imd pathway include SKP1-related A (SkpA), *Drosophila* ubiquitin-specific protease 36 (dUSP36), cylindromatosis (CYLD), plenty of SH3s (POSH), Trabid, and transglutaminase (TG). *Drosophila* USP36 inhibits the K63-polyubiquitinated Imd build up and promotes its degradation (Lee and Ferrandon 2011). It is a negative regulator of the pathway as silencing dUSP36 constitutively activates the IMD signalling pathway. This activation is lost in GF flies leading to the hypothesis that this interaction might be microbiome dependent (Leulier 2009). K63-linked ubiquitination of *Drosophila* transforming growth factor b-activated kinase 1 (dTAK1), is monitored by another negative regulator of IMD, known as Trabid. Flies lacking this protein show a remarkable increase in the amount of the IMD target,

Diptericin, with a dramatic reduction of the lifespan (Fernando, Kounatidis and Ligoxygakis 2014). A further negative regulator of TAK1, POSH prevents engagement with the c-Jun N-terminal kinase (JNK) scaffold (Tsuda *et al.* 2005). Downstream, the cylidromatosis disease homolog dCYLD, interacts with the *Drosophila* IKKγ homolog Kenny, and disrupts downstream signalling (Tsichritzis *et al.* 2007). In its absence, triglyceride and AMP levels increase (Tsichritzis *et al.* 2007). Finally, at the level of Relish, SkpA, the proteasome-ubiquitin pathway (Khush *et al.* 2002) and Tg (Shibata *et al.* 2013) suppress NF-κB activity.

1 1.5 Predisposition to an overactive immunity causes neurodegeneration

Human genetics and animal model research has illustrated the correlation between innate immunity in the brain and the pathogenesis of neurodegenerative disorders. Increasing amount of evidence suggests that the accumulation of aggregated proteins is only a part of the pathology of neurodegenerative disorders and not the full story [reviewed in (Labzin, Heneka and Latz 2018)]. Increasing evidence suggests the role of the immune system as an aetiological mechanism that influences not only the pathology of the diseases but also modulates basal levels of age dependent neurodegeneration in the context of healthy ageing (Letiembre *et al.* 2007).

In *Drosophila*, Cao et al. (2013) illustrated that chronic activation of the immune response in the wild type *Drosophila* brains causes neurodegeneration. Flies with loss of function mutations in a Relish repressor gene, dnr-1, present signs of early neurodegeneration and an increase in the number of Relish target genes transcripts in the fly brain (Cao et al. 2013). The authors suggest the cause of this neurodegeneration as AMP-associated toxicity caused by constitutive expression of AMPs, or an extremely high-level present in neurons or glial cells. The study also revealed that the overexpression of AMPs in nervous tissue can cause

neurodegeneration and established a causative relationship between neurodegeneration and IMD signalling. They proposed the possibility of a neuroprotective role of negative regulators in neuronal viability (Cao *et al.* 2013).

A similar result was obtained by Kounatidis et al. (2017), who demonstrated an age dependent increase in Relish controlled immune activity in *Drosophila*. They observed that the loss of negative regulators of the IMD pathway in neuronal tissue resulted in the shortening of lifespan, locomotive defects and the formation of brain lesions. This phenotype was rescued once the IMD response was suppressed in glial cells of these flies. In wild type flies, suppressing relish in glial cells resulted in lifespan extension. Genetic predisposition to neurodegeneration was observed with mutation in *trbd, pirk and tg* (Kounatidis *et al.* 2017). Penetrating traumatic brain injury (pbdI) model, shows a greater expression of AMP genes and an over activation of the innate immune response in both young and older flies (Sanuki *et al.* 2019). The positive interaction between pTBI and ageing(Sanuki *et al.* 2019). Additionally, Yorkie, a co-activator of Hippo pathway was also shown to reduce polyglutamine (PolyQ)-mediated neurodegeneration by negatively regulating Toll and Imd pathways via cactus and relish, respectively (Dubey and Tapadia 2018).

Recently, transcription of innate immune genes was observed as the prominent response to paraquat in a *Drosophila* model of PD (Maitra *et al.* 2019). Interestingly, Relish knock down in dopaminergic neurons conferred resistance to paraquat and rescued both motility defects as well as loss of dopaminergic neurons. The study indicates that the immune reaction might not be protective and indicate potential drug targets for preventing neuronal loss during PD (Maitra *et al.* 2019). Immunity induced neurodegeneration can explain the neurodegenerative phenotypes observed in both ataxia– telangiectasia mutated (ATM) gene and retinal degeneration in norpA (no receptor potential) mutants (Chinchore, Gerber and Dolph 2012).

Reduction in the ATM kinase activity in the glial cells may be responsible for the increased innate immune response through protein phosphorylation and cause neurodegeneration in these mutants. Furthermore, retinal degeneration in norpA mutant flies was shown to be dependent on Relish and Dredd (Chinchore, Gerber and Dolph 2012). Ray, Speese and Logan (2017) showed the neuroprotective role of the glial engulfment receptor, Draper, in *Drosophila* model of AD. They further showed that overexpression of glial draper reverses amyloid (Aβ) accumulation along with AD-associated behaviour phenotypes (Ray, Speese and Logan 2017). They also show that protein degradation pathways are expressed downstream to Draper in response to amyloid accumulation. This supports the theory that glial cells may be responsible for the clearance of neurotoxic amyloid peptides in the brain through a Draper/JNK/STAT92E signalling cascade. Draper is also observed to have a significant role in clearance of damaged axons. Purice, Speese and Logan (2016) observed an age dependent decline in the levels of Draper that causes dysfunctional glial engulfment in older flies. Dying neurons activate Toll receptor ligand, Spz in the cortex glia, that further drives the expression of Draper to ensure efficient clearance of the neuron (McLaughlin *et al.* 2019).

Recent studies have also focused on the role of gut- brain crosstalk and neurodegeneration. Wu et al. (2017) highlighted the effect of enteric infection in AD progression. Gut dysbiosis in AD mutant flies caused an increase in hemocyte recruitment to the brain and activation of TNF-JNK mediated neurodegeneration. This neurodegeneration and reduction in lifespan were rescued in flies with genetically depleted Eiger (an activator for JNK pathway) in the brain, further supporting the hypothesis. Westfall et al. (2019) explored how symbiotic and probiotic formulation can influence gut brain signalling and delay the progression of AD.

Gene	*Immune Phenotype*	*Neurological Phenotype*	*Reference*
pirk/rudra/pims (loss of function)	Overactivation of IMD	Locomotion, reduced lifespan, brain neurodegeneration	(Kounatidis *et al.* 2017)
trabid (loss of function)	Overactivation of IMD	Locomotion, reduced lifespan, brain neurodegeneration	(Kounatidis *et al.* 2017)
transglutaminase (loss of function)	Overactivation of IMD	Locomotion, reduced lifespan, brain neurodegeneration	(Kounatidis *et al.* 2017)
dnr1 (loss of function)	Overactivation of IMD	Locomotion, reduced lifespan, brain neurodegeneration	(Cao *et al.* 2013)
cdk5 (loss of function)	Overactive immunity through reduction of autophagy	Loss of DA neurons	(Shukla *et al.* 2019)
Toll and IMD activity increases	Overactive immunity	Age-dependent neurodegeneration in a model of pTBI	(Sanuki *et al.* 2019)
yorkie activity	Suppression of IMD and Toll	Reduction of PolyQ-mediated neurodegeneration	(Dubey and Tapadia 2018)
relish (knock-down in DA neurons)	Suppression of IMD	Increased resistance to paraquat, rescue of motility defects and DA neurons in a *Drosophila* model of PD	(Maitra *et al.* 2019)
relish (loss of function)	Suppression of IMD	Suppression of retinal degeneration in norpA mutants	(Chinchore, Gerber and Dolph 2012)
draper activity	Glial phagocytosis	Better clearance of Aβ-amyloid	(Ray, Speese and Logan 2017)
draper (age-dependent reduction)	Dysfunctional glial-mediated engulfment	Neuronal death	(Purice, Speese and Logan 2016)
spz-5 (in neurons)	Activation of Toll-6 in glia	Neuronal death; dying neurons signal to glia	(McLaughlin *et al.* 2019)

Table 1: Summary of papers at the junction of immunity and neurodegeneration in *Drosophila*. We only list those showing a causative link between immune activity or immune-related signalling and neurological phenotype. This table was also published in Arora and Ligoxygakis 2020.

1.1.6 Gut as a modulator of the immune system

The gut or the gastrointestinal (GI) tract is a major interface between the environment, microbial world and the host (Goto and Kiyono 2012). It is constantly exposed to bacteria and viruses from the food we ingest and is a crucial point of entry for pathogens (Zoetendal, Vaughan and De Vos 2006). It plays a central role in immune homeostasis, because of which it is considered to be the largest immunological organ in the body. The intestinal epithelial barrier is dynamic and interacts strongly with the gut microbiome and immune system cells (Rescigno 2011). This interaction between the epithelial cells of the gut, microbiome and immune cells is responsible for effective antigen-specific immune responses while balancing tolerance and effector immunological activities (Takiishi, Fenero and Câmara 2017). Recent studies have illustrated the importance of a balanced microbiome and its effect on immunological health (Bosco and Noti 2021). Furthermore, studies have focused on the effects of dysbiosis in the gut that has been linked with multiple diseases (Wang and Kasper 2014; Carding *et al.* 2015). A simple example is that of irritable bowel syndrome (IBS), where it is hypothesised(Santana *et al.* 2022). Patients with IBS have reduction in *Lactobacillus* & *Clostridium* genus. Furthermore, changes in diets of patients with IBS have shown to improve symptoms (Malinen *et al.* 2005; Kassinen *et al.* 2007).

1.1.7 The Drosophila Gut

Recent studies have unveiled the invertebrate gut which was once considered as a basic tube required exclusively for digestion, as a major regulator for multiple biological functions (Clark and Walker 2018; Colombani and Andersen 2020). Like other insects, the *Drosophila* gut is made up of a basic epithelium and is enclosed by visceral muscles, nerves and tracheae (Miguel-Aliaga, Jasper and Lemaitre 2018). The epithelial lining is a monolayer consisting of four different types of cells: intestinal stem cells (ISCs), absorptive enterocytes (ECs),

secretory entero-endocrine cells (EE cells), and enteroblasts (EBs). The majority of the cells in the epithelium are EC cells, with hormone-producing EE cells interspersed between them and ISCs at the basal membrane (Miguel-Aliaga, Jasper and Lemaitre 2018) (**Figure 3B**). The ISCs are pluripotent stem cells that are found adjoined to the basal surface of the epithelium and responsible for the rapid cell turnover of the gut epithelium (Micchelli and Perrimon 2006; Ohlstein and Spradling 2006). These cells contain the transcription factor Escargot (*esg*) and the Notch signalling ligand, Delta (Dl). ISC proliferation in young or low-stress flies is relatively slow, with the cells remaining in a 'quiescent state' and undergoing sporadic division to replace the gut epithelium. However, with age or under stress, these cells undergo accelerated proliferation or are in a 'proliferation state' (Biteau, Hochmuth and Jasper 2008; Neophytou and Pitsouli 2022). The ISCs differentiate into an immature diploid cell known as the enteroblasts, which do not divide; instead, these increase in size and relocate towards the lumen forming a brush border. These further differentiate into absorptive ECs or secretory EE cells. The EC cells are large and polyploid whereas the EE cells are small, diploid and express the transcription factor Prospero. Like the ISC, the EB cells express the *esg* markers and have increased Notch signalling activity which is crucial in successful differentiation (Micchelli and Perrimon 2006; Ohlstein and Spradling 2006). The decision of differentiating into absorptive ECs or secretory EE cells is determined by Notch Signalling, where the elevated Notch activity trigger the differentiation into ECs, and reduced signalling stimulates the differentiation to EEs (Ohlstein and Spradling 2006). The apoptotic cells are eventually lost by delamination of cells into the lumen. Finally, the peritrophic matrix in flies provides a cushion between the lumen and the epithelium; this matrix is analogous to the mammalian mucus layer and protects the epithelium from possible invasion.

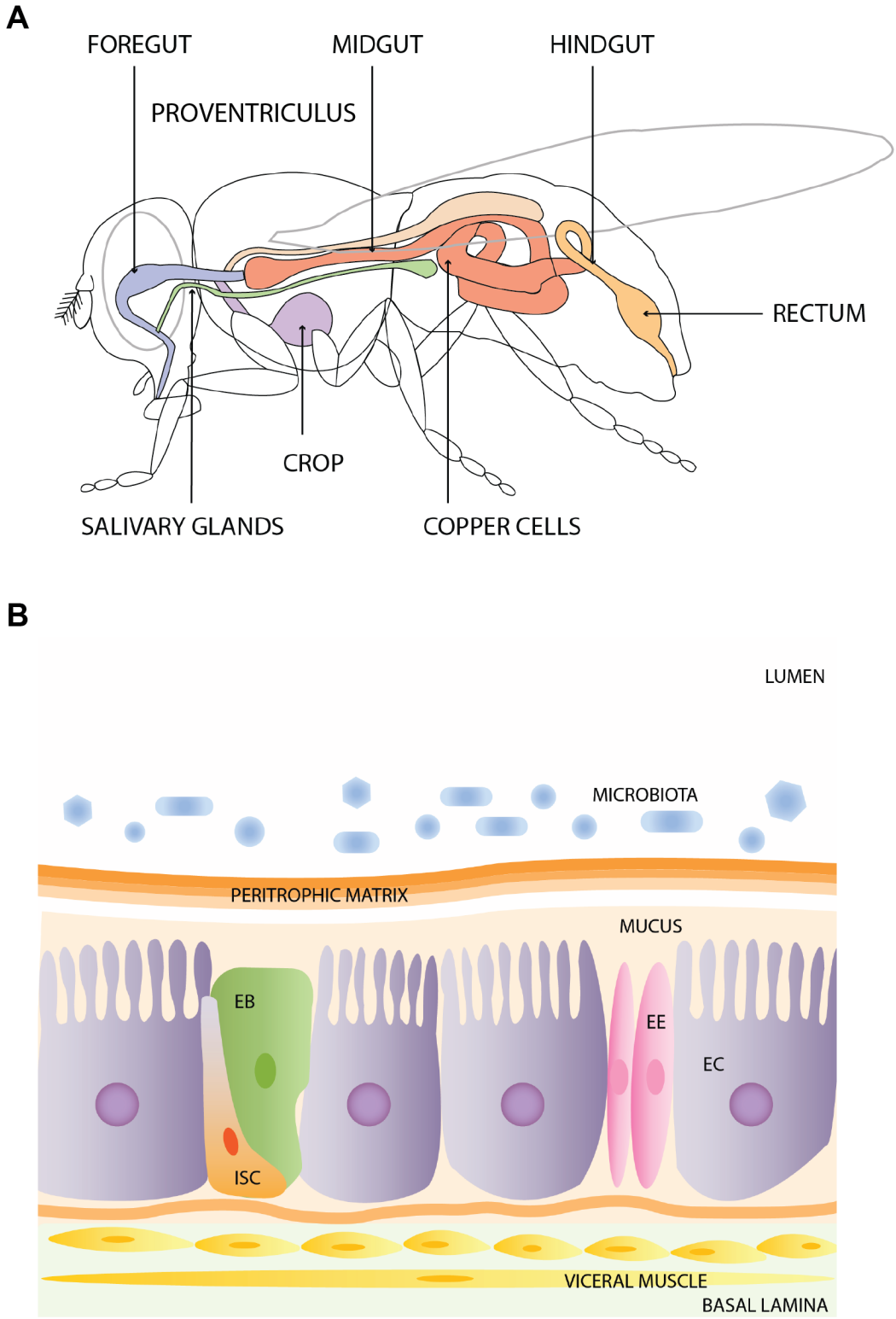

Figure 3: The *Drosophila* gut, (A) A schematic illustration of different organs and sections of the digestive system of an adult Drosophila. The fly intestine is a tubular organ and is separated into foregut, midgut and hind gut. Once ingested, the food is stored in the crop from where it enters the foregut, followed by the midgut, containing most of the gut microbiome and finally excreted via the hindgut. **(B).** A cross section of the midgut epithelium containing several types of cells including the pluripotent intestinal stem cells (ISCs) that differentiate into the enteroblasts (EBs) and then into either absorptive enterocytes (ECs) or secretory entero-endocrine cells (EE cells). Adapted from (Kuraishi, Hori and Kurata 2013; Kitani-Morii et al. 2021).

1.1.7.1 Different sections and their origins

The gut is compartmentalised into three anatomical segments: the foregut, midgut and hindgut (Demerec 1950; Hakim, Baldwin and Smagghe 2010). In an adult fly, the foregut consists of the pharynx, the oesophagus and the crop. The crop is unique to Diptera; this diverticulated structure includes a sophisticated array of muscles, including pumps and sphincters responsible for regulating the movement of food into/within the crop, and then into the alimentary canal (Stoffolano Jr and Haselton 2013). The crop is suggested to be responsible for a number of functions other than in early digestion such as detoxification, microbial control, and food storage (Stoffolano Jr and Haselton 2013). The epithelium of the foregut is of ectodermal origin and lined by an impermeable cuticle on its apical side. At the end of the foregut is a complex bulb-shaped structure known as the cardia (also known as the proventriculus), found in the foregut-midgut junction (Buchon *et al.* 2013). The cardia is made up of three epithelial layers and is a crucial site of the production of AMPs (Tzou *et al.* 2000). It is said to also function as a gastric valve, similar to the mammalian sphincter (Singh *et al.* 2011), and is responsible for the secretion of the peritrophic matrix (King 1988; Eisemann, Wijffels and Tellam 2001).

The cardia also marks the beginning of the midgut that is of endodermal origin and is regarded as the main site for nutrient absorption (Demerec 1950; King 1988; Karasov and Douglas 2013). Unlike the foregut and hindgut that are protected with the cuticle, the midgut is protected by the peritrophic matrix on the luminal side of the tube (Lemaitre and Miguel-Aliaga 2013). The lumen and the epithelia are separated by the peritrophic matrix and layer of mucus that is responsible for protecting the enterocytes from damage caused by abrasive particles or pathogens (Kuraishi *et al.* 2011; Kuraishi, Hori and Kurata 2013a). The midgut is roughly divided into six main regions (R0-R5) that further have subdivisions. Each region is characterisedand cellular features, or distinct gene expression patterns (Murakami *et al.* 1994; Strand and Micchelli 2011; Buchon *et al.* 2013; Marianes and Spradling 2013). This

regionalisation is not limited to the epithelium, but is also observed in the surrounding muscles, trachea and neurons (Cognigni, Bailey and Miguel-Aliaga 2011; Buchon *et al.* 2013; Marianes and Spradling 2013; Linneweber *et al.* 2014). This intricate compartmentalisation enables the *Drosophila* digestive tract to enable efficient digestion and maintenance of homeostasis (Karasov and Douglas 2013). Although studies have demonstrated the presence of several populations of ISCs, the R3 region has been shown to contain specialised copper cells which produce gastric acid, these are renewed by specific ISC population that are usually quiescent (Strand and Micchelli 2011).

The Malpighian tubules (tubular excretory organs) are present between the midgut and hindgut junction (Demerec 1950). These function analogously to the mammalian kidneys and are responsible for water reabsorption prior to excretion (Cognigni, Bailey and Miguel-Aliaga 2011). The midgut-hindgut border also contains the hindgut proliferation zone, which is the site for specialised hindgut stem cells (Takashima *et al.* 2008). The hindgut is responsible for reabsorption of water and discharge of waste. It is ectodermal in origin and can be divided into pylorus (a second valve-like structure), ileum, and rectum (Demerec 1950; Karasov and Douglas 2013). Like the foregut, the hindgut is also protected by an impermeable cuticle on its apical side (Demerec 1950; Gartner 1985; King 1988; Cognigni, Bailey and Miguel-Aliaga 2011; Lemaitre and Miguel-Aliaga 2013). Although the regenerative properties of the ectodermal regions of the gut have not been extensively evaluated, it is assumed that the tissue turnover of the foregut and hindgut is relatively slower than the endodermal midgut (Fox and Spradling 2009).

1.1.7.2 Ageing of the *Drosophila* Gut

As an organism ages, a wide variety of damage accumulates over time in its organs resulting in the loss of its physiological function. This is usually followed by the depletion of regenerative capacity in tissues with high turn-over. In the case of the fly gut, this damage includes the loss of regenerative potential of the gut in old age. Interestingly, this is not a result of the inability of stem cells to self-renew, instead, because of improper differentiation of its progeny(Morrison *et al.* 1996; Rossi *et al.* 2005, 2007; Rossi, Jamieson and Weissman 2008). During ageing. the ISCs hyperproliferate and result in an increased number of ISC daughter cells that missdifferentiate and express both stem cell and progenitor cell markers along with differentiation markers (Biteau, Hochmuth and Jasper 2008; Choi *et al.* 2008; Buchon *et al.* 2009; Hochmuth *et al.* 2011). The misdifferentiation of ISCs during ageing is thought to be the product of the gut's defensive signalling processes. In older flies, it causes several challenges, including the development of gastric metaplasia, in which the acidity of the region is compromised because of incomplete differentiation of copper cells (Li, Qi and Jasper 2016). This alteration in the acidity of the midgut causes disturbances in the intestinal compartmentalisation and changes in the composition of the commensal microbiota, further leading to dysbiosis and immune deregulation in the epithelium.

The pathway responsible for regulating ISC division and cytoprotection is the JNK pathway, whereas ISC proliferation is limited by Notch signalling to ensure proper differentiation of the daughter cells. Stress induced elevation of the JNK pathway induces overproliferation (Biteau, Hochmuth and Jasper 2008) and defective differentiation caused by ectopic N activation, due to an inability to properly repress Dl expression in ISC daughter cells. This disfunction results in the loss of epithelial barrier function leading to shortening of lifespan (Rera, Clark and Walker 2012a). Additionally, chronic activation of the JNK pathway is also known to be responsible for raised ROS levels in the gut during ageing and causes epithelial cell

sensescence (Biteau, Hochmuth and Jasper 2008). The resulting epithelial dysplasia is responsible for age-related loss of lipid homeostasis (Karpac, Biteau and Jasper 2013).

The overactivation of the JNK signalling pathway causes chronic activation of the insulin-signalling-repressible transcription factor Foxo, which represses expression of the lipase Magro (Mag) (Gáliková and Klepsatel 2018), the key lipase required for digestion of triacylglycerol (Heier et al. 2021). This prolonged repression of lipase expression disrupts lipid metabolism. Aged flies are associated with higher bacterial loads (Ren *et al.* 2007; Buchon *et al.* 2009; Broderick, Buchon and Lemaitre 2014; Guo *et al.* 2014), whereas axenic flies display dysplasia, validating the confounding role of gut microbiome in intestinal senescence (Ren *et al.* 2007; Buchon *et al.* 2013).

1.1.8 The Gut Microbiome

It is now well established that the digestive tract (or the gut) of metazoans is colonized by several benign or beneficial microorganisms collectively known as the gut microbiome or commensal microbiota. Not only does the microbiome vary in diversity between species but also among individual hosts, and further within the same host over the course of its lifespan (Dethlefsen, McFall-Ngai and Relman 2007; Consortium 2012; David *et al.* 2014). It is known to influence several host traits (McFall-Ngai *et al.* 2013; Douglas 2015) and its metabolites play a critical role in homeostasis of the host.

However, the idea that the microbiome influences host health is not new. Elie Metchnikoff (1845–1916), a Russian scientist hypothesised the role of gut homeostasis as an essential modulator for host physiology over a century ago (Gordon 2016). However, the relationship between deregulation of gut physiology and host health was not explored until recently. There

has been a surge in the number of gut and gut microbiome related studies which is in line with the development of gnotobiotic animal models and genomic techniques that have allowed us to represent the entire microbial diversity and its function (Zoetendal, Vaughan and De Vos 2006; Rajilić-Stojanović, Smidt and De Vos 2007).

The human gut contains a large amount of microbes that has been shown to play a pivotal role in immune function (Cahenzli, Balmer and McCoy 2013; Schuijt *et al.* 2013), nutrient processing and several other host functions (Gilbert *et al.* 2018a). The mammalian lower intestine harbours approximately 10^{14}-10^{15} microbial cells. This vast community not only matches the approximate number of eukaryotic cells in the human body, but contains significantly more genes than the human genome (Frank and Pace 2008; Nicholson *et al.* 2008). Development of molecular and metagenomic studies have enabled scientists to recognise(Alves *et al.* 2018). Arumugam et al. (2011) sequenced 22 European faecal samples and observed that a large part of the sequences were bacterial, along with 5.8% viral and 0.8% archaeal. Although the human gut has a large diversity of over a 1000 different species or species- like taxa; most of them can be classified into three prominent phyla: Firmicutes, Bacteroides and Actinobacteria (Dicksved *et al.* 2009; Delgado *et al.* 2013). Firmicutes are gram positive anaerobes with low G+C content, Actinobactieria are gram positive aerobes with high G+C content and Bacteroides are gram-negative anaerobes. Apart from these, phyla such as Proteobacteria, Fusobacteria, and Verrucomicrobia are also present in low abundance (Ranjan *et al.* 2018).

The gut microbiome is dynamic in nature. Tts composition has been shown to depend on the internal intestinal physiology, including intestinal architecture, flux and pH; and therefore are different in different parts of the digestive track, such as the ileum and the colon. In addition to this, factors such as host genetics, diet, and environmental factors have also been shown to

influence composition between individuals. Therefore, an individual's metabolic profile might provide an insight into their environmental history and can further help us understand the progression of complex diseases. Cryan et al. (2019) reviews several of these factors including effects of antibiotics, prebiotics and fermented food on host microbial population. Additionally, the review gives into the changes in gut microbial diversity in humans from infancy to old age and speaks about the current challenges in microbiome research (Cryan *et al.* 2019).

1.1.9 How does the microbiome affect the host?

The Integrative Human Microbiome Project (iHMP; also known as HMP2), was established in 2004 with the aim to understand gut dysbiosis and microbiome functionality in health and disease states. Schirmer et al. (2018) profiled over 100 individuals with Crohn's disease, ulcerative colitis and non IBD controls. They found that IBD specific signals altered the expression profile of patients leading to increase inflammatory responses and altered oxidative state of the gut, along with a reduced mucosal layer (Naughton *et al.* 2014).

Over the last decade, studies illustrating the influence of microbial variation on the phenotype of the host have substantially increased (Belkaid and Hand 2014; Kohl *et al.* 2014; Rooks and Garrett 2016; Sampson *et al.* 2016; Surana and Kasper 2017; Visconti *et al.* 2019; Liberti and Engel 2020; Van Treuren and Dodd 2020). Furthermore, its effect on complex behavioural traits such as learning and memory, social behaviour, reproductive isolation and mood have also been explored (Vuong *et al.* 2017a). The results for these behavioural effects have been inconsistent (Forsythe, Kunze and Bienenstock 2016; Johnson and Foster 2018).

This has only been possible by studying and comparing various axenic / gnotobiotic animals to their conventionally reared counterparts. Therefore, traditional lab models such as *Mus*

musculus (mouse), *Danio rerio* (zebrafish), *Drosophila* (fruit fly) and *Caenorhabditis elegans* (worm) are now being recognised as appropriate models to study the foundation of animal–gut microbiome interactions (Douglas 2019). As mentioned earlier (**Section 1.1.2**), *Drosophila* has several advantages as a model system, as it is fairly simple to generate microbe-free / germ-free flies.

1.1.10 Drosophila Microbiome

Like most insects, *Drosophila* harbours a rich and diverse microbiome community. This is partly due to transfer of diverse bacteria via maternal transmission, and due to the fact that fruit flies spend most of their life in and around decomposing fruits (Broderick and Lemaitre 2012). In contrast with other intracellular symbionts, such as *Wolbachia* and *Spiroplasma* that are transmitted from within the embryo, the gut bacteria is obtained from the chorion and the environment after birth (Clark *et al.* 2005; Riegler *et al.* 2005; Haselkorn, Markow and Moran 2009). Moreover, like humans, the gut flora in flies vary between individuals / strains because of varying food habits that result in dissimilar gut structures and function (Arumugam *et al.* 2011; Cryan *et al.* 2019). The gut microbiome in flies potentially provides its host with bioactive compounds such as antimalarial, antiviral or even antitumoral peptides (Dharne, Patole and Shouche 2006).

The *Drosophila* microbiome consists of 20 different species, the most abundant of which are four to five dominant species belonging to the *Acetobacter* and *Lactobacillus* genus (Chandler *et al.* 2011; Ludington and Ja 2020a). However, unlike humans, *Drosophila* gut flora mostly contains aerobic bacteria and particularly lacks the main colonising species of the human gut: the Bacteroidetes species (Charroux and Royet 2012). Techniques such as pyrosequencing have enabled us to perform comprehensive analysis of the commensal gut community in

Drosophila that can enable us to understand the influence of these microbes on the host (Yun *et al.* 2014; Bahuguna *et al.* 2022).

1.1.11 Age related changes of the microbiome

The gut microbiome in *Drosophila* stock is observed to differ greatly between laboratories and even between stocks within the same laboratory (Heys *et al.* 2018). This illustrates the possibility of vertical transfer of bacteria from parents to the offspring, as stocks in the laboratory are maintained on identical standard medium (Sabat and Johnson 2015). Bakula (1969) established that the *Drosophila* gut community is diverse and varies from its environment. Like humans, the *Drosophila* microbiome also changes with age (Dmitrieva *et al.* 2021). Bakula deduced that the embryos were essentially sterile and contained bacteria on the egg shells through the use of culture techniques to check the density and diversity of different bacteria. She estimated that the adult faeces contaminated the eggshell (Bakula 1969). This observation led to the development of the protocol used to obtain axenic flies till date which is removal of the chorion (or eggshell) with the help of bleach that is still used to generate germ free flies (Sabat and Johnson 2015). In addition to this, embryos stained with methylene blue were used to verify the hypothesis that the chorion is consumed by the larva and acquires the bacteria coating it (Bakula 1969).

Recently, by using molecular techniques, scientists have been able to monitor the changes in composition and diversity of bacteria as the fly ages (Dmitrieva *et al.* 2021). It has been shown that eggshells contain a high diversity of bacteria, but in low density (Broderick and Lemaitre 2012; Wong *et al.* 2015). However, after feeding, the quantity of bacteria rises significantly and reaches a plateau in the wandering larva stage. Twenty-four hours after pupation, metamorphosis causes a dramatic drop in bacterial density, which rises after 48 hours.

(Broderick and Lemaitre 2012). This reduction in numbers is corelated with an increase in AMP production during the pupal stage (De Reggi and Cailla 1975). It is also estimated to be a protective mechanism to shield the developing tissue from potential bacterial infection (Broderick and Lemaitre 2012). Interestingly, during pupation the larval gut is the only organ that is not completely histolyzed. It is contained within a transient pupal epithelium around which the adult midgut develops. This larval midgut is said to be the source of progenitor cells which form the foundation of the adult gut (Broderick and Lemaitre 2012). The larval/pupal gut, often known as the "yellow body," develops into the first adult faeces and is easily identifiable because of its distinct green colour. Additionally, this meconium is also believed to be a reservoir of the gut microbiome (Broderick and Lemaitre 2012).

The bacterial counts in the adult stages are also dynamic: young adults have a low abundance of bacteria (ranging from 40 to 1,000 cells) (Bakula 1969; Buchon et al. 2009; Storelli et al. 2011). However, as the fly ages, there is a significant increase in the bacterial load (10–1,000 fold) (Ren *et al.* 2007; Buchon *et al.* 2009). Along with this, there is also a shift in the composition of the gut, where the dominant species are also observed to change with age. Young flies are dominated with *Lactobacillus fructivorans,* whereas, older flies are mostly colonised by *Acetobacter pomorum* (Wong, Ng and Douglas 2011). The authors theorised that this change in composition could be due to changes in the oxidative state on the ageing gut.

1.1.12 What happens when this balance is lost?

The gut microbiome is responsible for providing the host with nutritional information, enabling production of essential short-chain fatty acids, vitamins and digestion of complex plant sugars for absorption (Ramakrishna 2013). The ability to differentiate between the resident microbes and pathogens is a result of years of coevolution of the host and the commensal microbiome

(Macke *et al.* 2017). It has a significant impact on the immune system and is responsible for maintaining homeostatic balance and response to incoming infection (Ahluwalia, Magnusson and Öhman 2017).

The real question is, how does the host know what microorganism is commensal, and what is pathogenic. Vertebrates have developed strategies to allow both its adaptive and innate immune responses to tolerate commensal bacteria (Jarchum and Pamer 2011). This tolerance is created by multiple strategies, first of which is the ability of the commensal bacteria to avoid immune recognition. Since the immune system recognises key virulence factors, non-pathogenic bacteria have evolved to evade recognition (Hornef *et al.* 2002). An example of this is the evolution of lipid A present in *Bacteroidetes* to its pentacylated version that cannot be sensed by the human (h) TLR4 and help the bacteria avoid detecting (Coats *et al.* 2007; Sansonetti and Puhar 2010) As lipid A is the hydrophobic component of lipopolysaccharide (LPS), it is responsible. for the endotoxic activity of gram-negative bacteria (Wang and Quinn 2010). Furthermore, lipid A is also the key in the pathogenetic recognition of the bacteria via TLR4 (Saha *et al.* 2022). In contrast to *Bacteroidetes*, the lipid A is hexacylated in *Proteobacteria* making it a stronger endotoxin and leading to prompt recognition (Munford and Varley 2006). This might explain the reason why Bacteroidetes are more prevalent than Proteobacteria.

However, the strong recognition effect of Proteobacteria lipid A might be diluted by the presence of Bacteroidetes species. A study conducted by Lupp et al. (2007) observed a decrease in Bacteroidetes and Firmicutes species and an increase in Proteobacteria during infection or inflammation associated with IBS, that may lead to an increase in intestinal inflammation (Lupp *et al.* 2007).

The second method by which the host creates tolerance is active suppression of the host response (Schneider and Ayres 2008). The gut microbiome has been shown to reinforce the

gut epithelial barrier physically and immunologically (Barbara *et al.* 2021). It occupies physical space in the gut and exerts the right of "first occupancy" and makes it harder for invading pathogen to attach to the epithelial barrier (Sekirov *et al.* 2010). Guts with higher microbiome diversity are considered more stable and reduce the risk of subsequent colonisations (Obadia *et al.* 2017). Additionally, studies have indicated the capability of some commensal bacteria to supress NF-κB mediated immune responses. These include non-pathogenic *Salmonella* that blocks IκBα ubiquitination and prevents its degradation further blocking the degradation of NF-κB (Collier-Hyams and Neish 2005) and *Bacteroides thetaiotaomicron* that enhances the export of RelA from the nucleus and prevents the transcription of the proinflammatory gene (Kelly *et al.* 2004). As mentioned earlier, the immune pathways are tightly regulated in the gut. Basal levels of AMP secretion are known as physiological inflammation, however, once interrupted the gut epithelium causes a more aggressive inflammatory response (pathological inflammation) responsible for keeping the microbiome "in check" (Schneider and Ayres 2008).

1.1.13 The Gut- microbiome- Brain Crosstalk

Our understanding of the gut microbiome and its role in physiology is rapidly expanding (Jovel *et al.* 2017a). The realisation that the gut is not an ordinary organ but holds the capability of influencing the body has been the focal point for several studies (Foster and McVey Neufeld 2013; Aidy, Dinan and Cryan 2014; Mayer, Padua and Tillisch 2014; Liang, Wu and Jin 2018; Kowalski, Mulak and Words 2019; Menozzi, Macnaughtan and Schapira 2021; Blackmer-Raynolds and Sampson 2022; O'Riordan *et al.* 2022a). The gastrointestinal (GI) tract, CNS, and microbiome are tightly linked by a network of signalling pathways known as the gut–brain axis, more recently termed as the gut-microbiota-brain axis (Osadchiy, Martin and Mayer 2019). The two organs communicate via several different mechanisms; these are: neuronal (via

vagal afferents), endocrine (via gut hormones), and immune pathways (via cytokines) (Cryan and Dinan 2012; Forsythe, Bienenstock and Kunze 2014; Burokas *et al.* 2015). The axis's primary role is to ensure gut homeostasis and to connect the brain's cognitive and affective centres to peripheral GI processes and mechanisms such as an enteric reflex, immunological activation, entero-endocrine communication, and intestinal permeability (Carabottia *et al.* 2015).

The microbiome communicates the nutritional information of ingested food to the CNS, that reflects the nutritional and energy state of the gut via a systemic response (Romaní-Pérez *et al.* 2021). Studies have illustrated that dysbiosis in the gut environment leads to stress signals that cause chronic low-grade inflammation which potentially contributes to altered permeability of the blood-brain barrier (BBB) and neuroinflammation (Parker, Fonseca and Carding 2020; Tang *et al.* 2020; Wen *et al.* 2020). The latter of which is low grade inflammation that results in increased oxidative stress, unbalanced energy homeostasis and a general increase in cellular degeneration, that is thought to play a role in the pathogenesis of a variety of neurological disorders, including depression, anxiety, and neurodegeneration (reviewed by (Zhu *et al.* 2020)). Additionally, several early symptoms of neurodegenerative disorders are now being observed in the GI tract, indicating the role of gut dysbiosis in the pathogenesis of neurodegenerative diseases (Pellegrini *et al.* 2018).

A potential mechanism by which the microbiome could cause neuroinflammation is by the significant increase in the production of LPS, amyloids, and other pro-inflammatory molecules during dysbiosis (Doifode *et al.* 2021). These are hypothesised to leak through the intestine and start accumulating in the body (including the brain) and potentially cause age-related changes in the inflammatory status of the body and neurodegeneration (Kahn *et al.* 2012; Zhao and Lukiw 2015; Lukiw 2016). Amyloids are also hypothesised to travel through the vagus

nerve and get accumulated in the brain and manifest neurological disorders (Sun *et al.* 2020). Additionally, the gut flora plays a pivotal role in the activation of microglia and regulate neuroimmune activation via the synthesis of short-chain fatty acid (SCFA) (Silva, Bernardi and Frozza 2020).

The gut microbiome is also responsible for the secreting of neurotransmitters such as acetylcholine, gamma-aminobutyric acid, adrenaline, serotonin and dopamine (Dicks 2022). Changes in the composition of the microbiome have been shown to alter the levels of SCFAs, that potentially causes dysregulation of gut metabolism and in turn, affects immune regulation, mitochondrial functioning and the oxidative balance of the gut (Tomasello *et al.* 2016; Marciano and Vajro 2017; Gonçalves, Araújo and Di Santo 2018; Anderson and Maes 2020). Furthermore, this increase in oxidative stress in the gut has also been shown to increase pro inflammatory activity in the body and as a result, causes increased permeability in the BBB (Shandilya *et al.* 2022). Similar to that of mammals, changes in the oxidative state of the fly gut have also been shown to affect several behavioural phenotypes and lifespan (Ha *et al.* 2005; Schretter *et al.* 2018; Jia *et al.* 2021). As this connection is bidirectional, brain injuries and certain psychological states have been shown to impact the composition of the gut flora and potentially influence pathogenicity of diseases (Sundman *et al.* 2017). For example, a study demonstrated the changes in gut microbiome of mice after experimental strokes. This change in composition consisted of changes in *Peptococcaceae* and *Prevotellaceae* that were injury dependent (Houlden et al. 2016). Furthermore, in 2022 a review that investigated 14 clinical trials, identified changes in the gut microbiome of patients after a stroke. These changes included higher prevalence of 62 taxas including *Streptococcus*, *Lactobacillus, Escherichia* and reduced prevalence of 29 taxas between stroke patients and healthy patients (Peh et al. 2022).

Therefore exploring the microbiome-gut-brain axis further could lead to development of therapies and prevention of several inflammatory and neurodegenerative disorders.

1.2 THE AIMS OF THIS THESIS

This thesis builds upon the foundational work conducted by Kounatidis et al. (2017) in the Ligoxygakis laboratory; highlighting the causative effects of the loss of negative regulators of the IMD pathway on age-dependent neurodegeneration. The study revealed that the loss of IMD negative regulation is linked to NF-κB-dependent upregulation of AMP genes in the brain, resulting in locomotion defects, brain lesions and ultimately, a reduced lifespan. The study identified Pirk, a protein shown to be expressed in the presence of commensal bacteria, as one of those key negative regulators. Furthermore, Kounatidis et al. (2017) demonstrated that the brain lesions and shortened lifespan exhibited by pirk mutants were rescued by generating germ-free mutants, indicating a potential role for the gut microbiota in age-dependent neurodegeneration.

In this thesis, we aimed to delve deeper into the relationship between immunity and age-dependent neurodegeneration, with a specific focus on exploring the potential role of the gut-brain axis in age-related neuronal decline.

Our hypothesis was that a dysbiotic gut can cause neurogenerative disorder. We chose sleep, as a neurological marker correlating with neurodegenerative disease to understand the extent of Pirk involvement in both the gut as well as the brain. Furthermore, we hypothesised that the neurodegeneration observed, Kounatidis et al. (2017) in *pirk* mutants was likely caused by the dysbiotic microbiome and could potentially be rescued by the generation of germ-free animals. In addition to this, we aimed to understand the Pirk protein further by examining its tissue-specific effects on lifespan, sleep, and locomotion. Finally, we investigated the microbiome of *pirk* mutant flies and transfer of this microbiome (by co-housing) to controls and observe if the

neurodegeneration observed was caused by the microbiome. By extending the insights derived from prior research, this thesis aims to contribute to the broader understanding of the complex interplay between immunity, gut microbiota, and the neurology of age-dependent neurodegeneration.

We carefully selected both 6-day and 28-day intervals within the lifecycle of the flies with the intention to represent a young and a relatively older time point. While 6-days signifies early development, we acknowledge that 28-days isn't typical for older flies. However, we based this decision on previous lifespan data reported by Kounatidis et al. (2017), wherein we observed that the chronological and biological ages of both experimental and control flies were the same up to 30-days. Therefore, 28-day is an ideal time point to ensure strong sample size, considering the inherently abbreviated lifespan characteristic of *pirk* mutant flies.

CHAPTER TWO

Exploring the neurological phenotypes of pirk mutants

CHAPTER TWO:

EXPLORING THE NEUROLOGICAL PHENOTYPES OF PIRK MUTANTS

The sleep assay executed in this chapter was performed in Professor Gero Meissenbok's laboratory at the Centre for Neural Circuits and Behaviour (CNCB) in the Department of Physiology Anatomy and Genetics, University of Oxford. However, even though the initial set up and experimental design was created under the guidance of Dr Anissa Kemp, a former post doc at the lab, all the experimental setup and analysis were performed by the author.

This chapter aims to investigate the neurological phenotypes observed in both 6 and 28-days old female and male *pirk* mutant flies with respect to their controls.

Section 2.1: This section focuses on Pirk protein and how it can be used to explore the gut brain axis. We dive into understanding sleep and its association with the immune system and neurodegenerative disorders.

Section 2.2: In this section we examine the climbing ability, sleep and activity profiles, and intestinal permeability of both male and female *pirk* ^{EY00723} flies at 6 and 28-days with respect to their w^{1118} controls.

Finally, **section 2.3** provides a brief summary of the phenotypes observed and their potential significance.

2.1 BACKGROUND

This chapter focuses on Pirk protein, a negative regulator for the IMD pathway (discussed briefly in **Chapter 1 Section 1.4.4**.). Previous studies have demonstrated that the basal expression of *pirk* is dependent on the presence of commensal microbiome (Lhocine *et al.* 2008) and the absence of Pirk protein causes neurodegeneration by histology (Kounatidis *et al.* 2017) (in detail below). The aim of this chapter is to use sleep and locomotive ability of *Drosophila* to establish the extent of neurodegeneration observed in mutant *pirk* flies. Additionally, we explore the intestinal barrier permeability of these flies using the intestinal permeability assay, also known as "the smurf assay" (Rera, Clark and Walker 2012).

2.1.1 Pirk Mutant

Pirk (**P**oor **I**mmune **R**esponse upon **K**nock in) was identified by three independent studies. First; via a yeast two-hybrid screen with the cytoplasmic domain of PGRP-LC as bait by Aggarwal et al. (2008), who chose to address it as "Rudra", and other, during a large scale microarray analysis used to study genes that are upregulated following a gram negative infection Kleino et al. (2008); who called it "Pirk" and by Lhocine et al. (2008); who called this protein "PIMS (PGRP- LC-interacting inhibitor of IMD signalling)". The gene was eventually named *pirk.* All three studies demonstrated the role of Pirk as a crucial component of the negative feedback loop for IMD signalling. Flies deficient in Pirk were shown to have a significantly enhanced IMD response and elevated basal levels of diptericin (*Dpt*) (Lhocine *et al.* 2008). In wild type flies, *pirk* has been shown to be predominantly expressed in the adult guts, with the highest levels in the adult midgut (Chintapalli, Wang and Dow 2007).

At the protein level, Pirk has been shown to coimmunoprecipitate with the cytoplasmic tail of PGRP-LCx, disrupting the availability of the signalling receptor and there by leading to the

suppression of IMD signalling (Kleino *et al.* 2008). The Pirk protein contains 197 amino acids and lacks any discernible domains or motifs. It includes a repeating region in its central portion between location 51 and 136, along with a non-conserved putative RHIM region that was computationally predicted (Kajava *et al.* 2014). Pirk is shown to interact directly with PGRP-LC and PGRP-LE cRHIM motifs along with Imd and is responsible for regulating both system activation in response to infection and immune tolerance in response to gut commensal bacteria (Kallio *et al.* 2005; Aggarwal *et al.* 2008; Kleino *et al.* 2008; Lhocine *et al.* 2008).

RNAi mediated knock down of Pirk protein (IR-Gal4) has been shown to cause hyperactivation of IMD signalling, leading to greater AMP production upon gram negative bacterial infection (Lhocine *et al.* 2008). Similarly, flies overexpressing Pirk (UAS *pirk*) have been shown to be more susceptible to gram negative infections compared to wild type flies (Aggarwal *et al.* 2008). Lhocine et al. (2008) illustrated that mutant flies raised in germ free conditions have low basal levels of *Dpt* expression in their guts when compared to their wild type controls. Moreover, flies deficient in Pirk not only have a stronger local AMP response against the commensal bacteria, but also hyperactivate AMP secretion in response to oral and systemic infection (Aggarwal *et al.* 2008). Lhocine et al. (2008) found that the *Dpt* expression level in *pirk* mutants was 2-3 fold above the control levels following E. coli (*Escherichia coli)* or Ecc15 (*Erwinia carotovora carotovora 15*) infection after 2, 6 and 24-hours. However, these levels were shown to eventually decrease from 48 to 72 hours and reach control levels, illustrating the importance of multiple negative regulators that compensate for the lack of Pirk protein. The role of Pirk in clearing membrane receptors and targeting them into vesicular compartments potentially for lysosomal degradation (Lhocine *et al.* 2008) or via endosomal recycling (Neyen et al. 2016) has also been suggested.

Finally, the basal expression of *pirk* has been shown to depend on the presence of commensal flora (Lhocine *et al.* 2008). Flies lacking gut flora (germ free/axenic) do not express *pirk* in their midgut, illustrating the protein's role in developing immune tolerance of commensal flora in fruit flies (Lhocine *et al.* 2008). Additionally, Kounatidis *et al.* (2017) demonstrated the role of IMD/NF-κB negative regulators (including *pirk*) in predisposing flies to early onset neurodegeneration. These studies make Pirk an ideal candidate to explore the gut brain axis.

The Pirk mutant strain used in this study is $pirk^{EY0072}$, a null mutant that is viable and fertile with a reduced lifespan (Kounatidis *et al.* 2017). Pirk's gut specific expression was entirely eliminated in homozygous or hemizygous (EY00723/Df(2R)ED3923) $pirk^{EY00723}$ mutants and the transcription expression levels were comparable to wild type flies when raised in germ-free conditions (Lhocine *et al.* 2008). In this thesis $pirk^{EY00723}$ is referred to as *pirk* unless stated otherwise.

2.1.2 Sleep

Sleep is a critical physiological process and is responsible for various functions such as the maintenance of synaptic homeostasis, memory reconsolidation and tissue regeneration (Cirelli and Tononi 2008). It is characterised by a reversible reduction of responsiveness to external stimuli and is generally divided into three major stages: the wakeful state, rapid eye movement (REM) sleep and non-REM (NREM) sleep (Sehgal and Mignot 2011). The different stages of sleep have distinctive readings and can be measured using an electroencephalogram (EEG). In humans, the wakeful state shows up as alpha waves on the EEG that slowly decrease when the individual enters light sleep. The NREM sleep shows up as slow waves and spindles, whereas the EEG of REM sleep is similar to that of an awake individual (Ondo 2014). Even though the

reason why humans need two sleep states is up for debate, the fact that both these stages are important is not.

An organism goes through several metabolic and physiological changes while asleep. These changes include cellular repair, and the regulation of processes such as body temperature, memory restoration, blood pressure, heart rate, hormone secretions, and immunological defences (Luyster *et al.* 2012). Apart from being associated with a general increase in sleep pressure leading to daytime sleepiness, fatigue, impaired vigilant attention (Hudson, Van Dongen and Honn 2020) and cognitive decline (Aidman, Jackson and Kleitman 2019), sleep deprivation has been associated with an increased risk of several disorders including cardiovascular (Cappuccio and Miller 2017; Tobaldini *et al.* 2017), respiratory (Rault *et al.* 2020), metabolic disorders including obesity (Beccutia and Pannain 2011) and type 2 diabetes (Grandner *et al.* 2012). Furthermore, sleep deprivation can lead to several psychopathological and psychiatric disorders, including depression (Pandi-Perumal *et al.* 2020), psychosis (Davies *et al.* 2017; Reeve, Sheaves and Freeman 2019), anxiety (Lader 2016) and suicidal behaviour (Bernert and Joiner 2007; Liu *et al.* 2020). In addition to this, sleep deprivation has been corelated with an increased risk of certain cancer (Kakizaki *et al.* 2008), stroke (Ruesten *et al.* 2012), deregulated immune responses and neurological disorders such as AD (Ahmadian *et al.* 2018) & PD (Bishir *et al.* 2020). Finally, due to its association with development of several diseases, sleep deprivation has been shown to reduce quality of life and increase mortality (Grandner *et al.* 2010).

The two independent processes that have been shown to regulate sleep, are the circadian cycle and the homeostatic mechanism (Borbély 1982; Cirelli 2009). The circadian cycle is an adaptive feature that enables living organisms to regulate their cellular processes, physiological functions and behaviours with the external changes caused by the 24h dark-light cycle on Earth.

In the context of sleep, the circadian cycle provides ecologically appropriate time to sleep. Studies using microarray analysis have shown that gene expression of around 5- 10% of total genes in different vertebrate tissues are regulated with the circadian cycle (Storch *et al.* 2002; Keller *et al.* 2009). Additionally, the homeostatic mechanism is responsible for the accumulation of sleep pressure because of which prolonged periods of wakefulness result in an increase in drowsiness, reduction in performance and finally rebound sleep (Borbély and Achermann 1999; Goldschmied *et al.* 2022).

There are two widely accepted theories that try to explain the importance of sleep; the "synaptic homeostasis hypothesis (SHY)" by Giulio Tononi and Chiara Cirelli (Tononi and Cirelli 2003, 2006) and "restorative theories" (Adam 1980; Hauglund, Pavan and Nedergaard 2020). According to SHY, being awake comes at a metabolic cost, at both cellular and system levels as a result of increased energy consumption required for synaptic plasticity, whereas, sleep is the renewing response to maintain synaptic homeostasis. The authors describe sleep as "the price we pay for plasticity" as it reduces the metabolic burden that the brain goes through when awake. However, the alternative group of theories, known as the restorative theories, focus on the nourishing nature of the body and its need to repair and restore cellular components of the brain. There are multiple theories under the restorative hypothesis, some that focus on the depletion of neuronal components while awake, while others that focus on the aggregation of toxic metabolic bi-products that need to be cleared out during sleep (Xie *et al.* 2013). One such study conducted by Xie et al. (2013) demonstrates the important role of sleep in metabolite clearance in mice. The study showed that Aβ plaques and ^{14}C-inulin was cleared two-fold faster in sleeping mice than awake. Additionally, the study showed that sleep led to a 60% increase in interstitial space that may be the reason for increased neurotoxin clearance (Xie *et al.* 2013).

Finally, it is also believed that sleep homeostasis likely involves production of sleep regulatory substances, including immune factors such as interleukin (IL)-1, TNF-α and could be responsible for aiding the brain in keeping track of its sleep/wake cycle history thereby establishing an important link between sleep and the immune system (Krueger, Rector and Churchill 2007).

2.1.3 Sleep and the immune system

Studies have shown that lack of sleep affects the endocrine, metabolic, and immune systems (Aldabal and Bahammam 2011). In terms of the immune system, sleep deprivation has been shown to cause unresolved inflammation, leading to chronic diseases (Hu *et al.* 2003; Foley *et al.* 2004; Frey, Fleshner and Wright 2007). It has also been shown to lead to a chronic inflammatory state that further increases risk of cardiometabolic, neoplastic, autoimmune and neurodegenerative diseases (Garbarino *et al.* 2021). Additionally, chronic sleep deficiency (or short sleep) has also been linked to inflammatory diseases such as cardiovascular disease (CVS) (Buxton and Marcelli 2010), type 2 diabetes (T2D) and certain cancers (Verkasalo *et al.* 2005).

Molecules that regulate sleep have been shown to influence several inflammatory pathways (Krueger 2008). Immune system components such as muramyl peptide, endotoxin lipopolysaccharide (LPS), cytokines IL-1, TNF-α, prostaglandins (PGs), growth hormone-releasing hormone (GHRH) and growth factors have been associated with NREM sleep (Krueger 2008). It is hypothesised that the regulation of sleep in a few cases could potentially be a result of enhanced cytokine production (Churchill *et al.* 2008; Jewett *et al.* 2015). IL1 and TNFα are examples of cytokines that are shown to regulate NREM (Krueger, Rector and Churchill 2007). The expression of IL-1 beta and IL-18 within different areas of the brain have

been shown to align with the circadian cycle, further strengthening the theorical association between the immune system and sleep patterns (Krueger 2008). In addition to this, an over improvement in NREM sleep duration was observed in animals after a systemic or central administration of IL-1beta, and, this observation was also seen in animals treated with IL-18 (Zielinski and Krueger 2013). Mutant mice that lack TNF1 have been shown to have low spontaneous NREM and REM sleep durations when compared to their respective controls (Krueger 2008). Pathogenic diseases caused by influenza, bacteria, and human immunodeficiency virus (HIV) have been shown to modify sleep behaviours through inflammatory processes (Majde and Krueger 2005). Additionally, dysregulation of inflammatory pathways has been shown to be corelated with sleep disorders such as obstructive sleep apnea and insomnia (Kapsimalis *et al.* 2008). Finally, disbalanced sleep has been shown to increase risk of infection and inflammatory disorders (Kripke, Garfinkel and Wingard 2002; Mallon, Broman and Hetta 2002; Dew et al. 2003; Vgontzas et al. 2007). This is likely associated with low grade neuro-inflammation by increasing pro-inflammatory cytokines in sleep deprived mice (Manchanda *et al.* 2018). Additionally, studies have reported changes in the slow wave NREM sleep, leading to a reduction in REM sleep during acute infection with non-neurotropic agents. The role of cytokines is associated with the regulation of both regular and infection associated sleep (Majde and Krueger 2005).

2.1.4 Sleep and Neurodegeneration

Since sleep plays an important role in the development of the brain, sleep deprivation during developmental stages has been shown to disrupt neuronal homeostasis, alter behaviour and reduce brain size (Mirmiran *et al.* 1983). EEG studies have illustrated the role of sleep deprivation in increasing seizure episodes by enhancing interictal epileptiform discharges and neuronal excitability (Halász 2013).

Circadian disruptions are common in several psychiatric and neurodegenerative disorders (Wulff *et al.* 2010). Moreover, there is an age dependent decline in circadian rhythmicity of sleep leading to the disruption of sleep architecture (Redline *et al.* 2004). These are thought to be caused by the intrinsic clock's impaired performance or a decrease in the suprachiasmatic nucleus's (SCN) entraining signals (Mattis and Sehgal 2016). The disruptions in the sleep architecture include reduction and fragmentation of total sleep time and poor sleep quality that leads to poor cognitive performance. Additionally, other sleep disorders such as sleep apnea, di-synchronisation of neuronal membrane potential, insomnia and periodic leg movements are also common in ageing(Pace-Schott and Spencer 2011). However, it is worth noting that the effect of sleep and circadian variations on cognitive function is challenging in ageing

Nevertheless, there are several correlations(Wang and Holtzman 2020), PD (Stefani and Högl 2020), multiple sclerosis (MS) (Braley and Boudreau 2016) and Huntington's disease (HD) (Zhang *et al.* 2019). Chronic sleep deprivation (CSD) has been shown to increase risk of AD. Zhao et al. (2017), sleep-deprived mice. CSD is also known conducted a study on mice that illustrated altered Aβ protein precursor processing in to increase pathogenesis of AD in wild type mice by increasing cortical deposits of Aβ plaques. Additionally, sleep has been demonstrated to improve the bulk flow of interstitial fluid to cerebrospinal fluid and boost Aβ clearance (Ooms *et al.* 2014). Sleep deprivation on the other hand, has been shown to increase Aβ burden, resulting in AD (Spira *et al.* 2013; Ooms *et al.* 2014; Tarasoff-Conway *et al.* 2015). In PD patients, improved sleep quality has been associated with enhanced cognitive and mental function (Stavitsky *et al.* 2012). However, in humans, the loss of nigrostriatal DA neurons or the dorsal striatum, has been shown to alter the sleep-wake cycle (Kim *et al.* 2010)

2.1.5 Sleep in Drosophila

Drosophila by two independent studies (Hendricks et al. 2000; Shaw et al. 2000). circadian rhythms studies have clearly shown that fruit flies are active and move around during the day, but considerably less so at night. However, its viability as a model was only established in 2000 To demonstrate sleep behaviour in flies, they used three criteria: ocular observation, an ultrasonic activity monitoring system and an automated infrared system. The studies concluded that *Drosophila* including homeostatic regulation and the decline in learning and memory that occurs when sleep is lost (Borbély 1982)., like mammals, have immobility periods during night-time that can last up to a few hours during which they rest in a certain sleep posture and have decreased reaction to external stimuli combined with an increased arousal threshold. After two decades of study, we now understand that flies meet all the essential characteristics of sleep, Furthermore, stimulants such as caffeine (Hendricks *et al.* 2000; Shaw *et al.* 2000), modafinil (Hendricks *et al.* 2003), amphetamines (Andretic, Van Swinderen and Greenspan 2005) and antihistamines (Shaw *et al.* 2000) have shown to affect sleep in flies. Moreover, there is a high degree of consistency in the quantity of daily sleep and the timing of the main sleep phases from day to day; similar to that of mammals (Cirelli 2003). In addition to this, the same parameters have high interindividual variability, even when age and breeding conditions are kept constant (Cirelli and Bushey 2008). Although there are significant differences between the anatomy of flies and humans, they are crucial in identifying signals integrated in sleep circuits and circuit concepts that underpin sleep state control. Flies have been integral in the identification of genes, chemicals and neuroanatomical loci crucial for controlling sleep duration (Cirelli and Bushey 2008).

Additionally, *Drosophila* is a useful tool for examining the impact of elements like stress (Lenz *et al.* 2015), availability of food (Zimmerman *et al.* 2012), mating (Isaac *et al.* 2010), social experience (Ganguly-Fitzgerald, Donlea and Shaw 2006; Bushey, Tononi and Cirelli 2011; Liu

et al. 2015; Lone et al. 2016), along with environmental factors such as light (Shang, Griffith and Rosbash 2008), temperature (Parisky *et al.* 2016), feeding (Keene *et al.* 2010; Thimgan *et al.* 2010), age (Koh et al. 2006; Seugnet et al. 2011; Kayser, Yue and Sehgal 2014; Metaxakis et al. 2014) and infection (Kuo et al. 2010; Kuo and Williams 2014), on sleep phenotype. These factors also affect complex behaviours such as learning and memory, courtship, and aggression.

2.1.6 Aims of the Chapter

From **section 2.1.1**, we know that the expression of Pirk depends on the presence of gut microbiota. In order to establish a gut brain axis, in this chapter we aim to determine the neurological phenotype of Pirk mutant flies.

First, we assess the role of Pirk protein in influencing the climbing ability of the flies, and then dive into an in-dept evaluation of the sleep profiles of both male and female mutant flies. We know that flies lacking Pirk protein have neurodegeneration that may be the cause of their early deaths. Therefore, we use sleep as a marker to study the extent of this neurodegeneration and try to rescue this phenotype in the next chapter (**Chapter 3**). Along with this, we also evaluate the intestinal permeability of the guts of the mutant flies, to understand the gut brain axis in these flies. The mutant flies used in this chapter were back six generations of backcrossing in a w^{1118} background. Consequently, w^{1118} flies serve as our controls, providing a robust basis for comparison.

2.2 RESULTS

2.2.1 Pirk Mutant:

The mutant used in this study is the *pirk*^{EY00723} (hereby addressed as *pirk*), that was created as a part of the Berkeley *Drosophila* Genome Project (Bellen *et al.* 2004). An intron less yellow gene marker was inserted next to a mini-*white* gene resulting in *P{EPgy2}* element that was inserted in wild type flies **(Figure 4 (A))**. In the initial study, the genomic sequence of the mutant was determined by direct sequencing of inverse PCR products (Liao, Rehm and Rubin 2000).

We analysed the flanking sequence provided by Liao, Rehm and Rubin (2000), against the *pirk* gene sequence (obtained from FlyBase) **(Figure 4 (B))**. Our analysis demonstrated that the mutant flies carry a transposon- inserted 62 bp upstream of the translational start site, which is in line with the result shown by Lhocine et al. (2008). The study illustrated that the gut specific expression of pirk was completely eliminated in *pirk*^{EY00723} mutant flies.

A.

B.

aaacaaacaggctcgtgaagcatctagaggaaatcattgcctccgtttcacagatctcacttggcaactgcgtaa
atatttatcaatttctagtgcttaaaactttatcatcggttatcgtcggttattacccctttaggttggggttgg
tgggtttttgactccgcgtttacgactcccaaaaatggaaatcagcaactatatcagtggacttattaatgataa
gagaagttaacaaaaatccccatcaaagttgggtctgtactgcataagttgataacagtctacacagcgaaaagt
tacaatgcgtaagtaaataaattccactttgatgggtcaagacccgaataacacccattactattagggataaga
ctataagcacatcattttaggagaaactataaaacgataagatacagtaataatgtttgaatttactggtgctgt
taactaaatatatatttaaactttattactatatgctgaagatttggctagctcaagtcgatggacgagcccatt
gcgagggcaccaacaggtggacattactcatgccgaataaattcggcgacccaatcaaaggtctccccagatggc
gagatgcctttaagttcgcgactctcatgcatacgaggtgattttcgtgccggccctcgggcgaaataaaaaagc
cccggcgctagactctccggcggatataaaagcggttcccgagcggcattagcgttcaatagccaaagtgccagc
gagcgagcgagcagtaagcacggcgaaagcgataccagagatcgccaaactcaacgcacaataaaagttcagaaa
acagagggagttcccctggcggaagcagacgatcccccagcgctgaattgaatacaaaaacaacacacacaattg
gatatctttgaccttagccatccggattgctcatcattcggagtcttcccccagcgacagagacggagatagaga
taggaaaaagagttggagaatgagctaaccgacagactggacggtgatttttacgagtgattagcagcggaaaga
aacgataccggcggtaattcacaccaaaatgggcgttcgtgtgatagaaaccgattcggcgagcgattcgtatga
cgatgacgagtgctccacttgccagaaagagcacgagcagggtaaatcccccaataagagcaagaaaagttccac
gccgccggagacaaccatctacgccagcaaggatctggtgggcaactgcaaggagtaccgcattgagaacaacac
gcgcgatctcaggatcatcggcaatggcaaccgcatacggattgtgaacaactccgggcaactgcaagtaatcgg
caatagcaccagactcaagatccagaacaatagcggagccctcaagtacacgggtaacgacggaaggatctacct
gggcagcagctccacgcagcaggtggtcgactacacgggctgcaatggactgctcaaggtggtcaagtccctgga
tcttagcggcgatgccaagaaaaggcccagctctcgatcgaaaaacgccaagccaacgccaacggatgctggcca
aggcaagtccggcggcattgagatcgacagcaatctaacgatacggcacggagccgggaacattgtgatcaagaa
tgccatcaacgtgagcatctgagaatcttgagctctctaagtcatctttggccaaagattaaggattaatgtaac
gaaactcttgccaccgaacgcaaaggttcctattgactgcaaaatagtcacttagtcttaatgtgtctttcgact
gctaccaatattaacatcaccctgcacattcagcaatgtcaagtattaaacgccacgtcgctagtctaaaaatcc
attactattcacaaaacacacccactgattagggaaatatatgtattgtatgtatatgtttagtcgtaacgcaga
agcgcagtgtgaacaaagcctaaacttcattccgagaatgaataatctgattaaaaaatacaactatatgtctaa
atat

peach: genomic untranslated
pink: insertion sequence connected to insertion recovered via reverse PCR
purple: site of insertion based on 8bp P-element target sequence
green: coding sequence for proteint

Pirk protein sequence:

MGVRVIETDSASDSYDDDECSTCQKEHEQGKSPNKSKKSSTPPETTIYASKDLVGNCKEYRI
ENNTRDLRIIGNGNRIRIVNNSGQLQVIGNSTRLKIQNNSGALKYTGNDGRIYLGSSSTQQV
VDYTGCNGLLKVVKSLDLSGDAKKRPSSRSKNAKPTPTDAGQGKSGGIEIDSNLTIRHGAGN
IVIKNAINVSI

Figure 4: *Pirk* mutant sequence analysis (A) a schematic diagram inspired from Lhocine et al., 2008, representing the position of insertion of the P-element in the *pirk* gene. (B) A detailed analysis of the genomic region of *pirk* gene. The base highlighted in blue is the insertion site go the P-element and is shown to lie outside the coding sequence of the gene. The black arrow indicates the direction of transcription, the yellow is the untranslated region of the pirk gene and the green is the protein coding sequence. Additionally, the blue marks the start site for transcription and the red indicates the insertion sequence of the p element.

2.2.2 Effects on Negative Geotaxis

The climbing assay or the negative geotaxis assay relies on the tendency of *Drosophila* to climb upwards against the force of gravity, also known as the negative geotactic response (Le Bourg and Lints 1992). In this section, we study the climbing ability, as this innate behaviour has been shown to diminish with age and in neurodegenerative *Drosophila* models (Sofola *et al.* 2010).

15 flies per tube were introduced into the climbing tubes and allowed to acclimate in the incubator. Subsequently, the tubes were uniformly tapped, prompting the flies to descend to the lowest compartment. After a 30-second climbing period, the number of flies in each section was recorded (n=5 vials of 15 flies per genotype). To minimize procedural variability, the experiment was conducted four times, with the initial repeat excluded, and the average of the remaining three repetitions was calculated (**Chapter 7 Section 7.1.6)**. We measured the climbing behaviour in both male and female *pirk* mutant and w^{1118} adult flies at 6-days and 28-days of age.

Further, we calculated the performance index (PI) defined as:

$$½(ntot + ntop - nbottom)/ntot)$$

An unpaired Mann Witney Rank sum test was performed, and the data was plotted on a bar graph to show mean (± SEM).

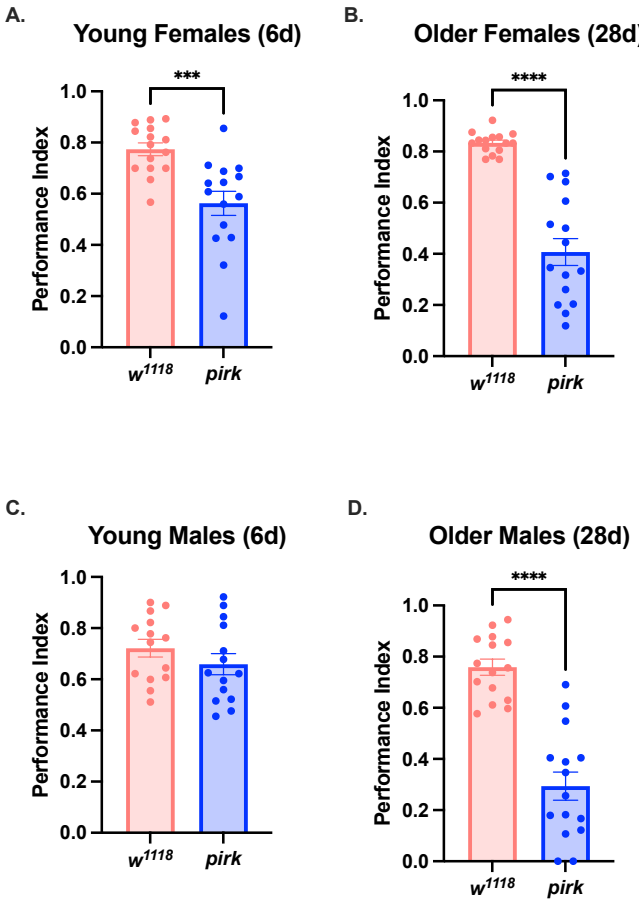

Figure 5: A negative geotaxis or climbing assay of 6-day and 28-day *pirk* mutant flies vs w^{1118}. Both female **(A-B)** and male **(C-D)** flies *pirk* mutant flies along with their w^{1118} were used to conduct the experiment. 5 vials containing 15 flies each (X3 repeats) were examined, and an unpaired Mann Witney Rank sum test was performed. The data was averaged and plotted using GraphPad Prism plotted to show the mean (± SEM), non-significant results were not marked and p≤ 0.05 (*), ≤ 0.01 (**), ≤ 0.001 (***), ≤ 0.0001 (****).

We observed a substantial reduction in the performance index in female *pirk* mutants compared to their controls in both 6 and 28-day old flies **(Figure 5 (A-B))**. A significant reduction of 0.18 was noted in 6-day old (p=0.0002, n=15) **(Figure 5A)** and that of 0.48 was observed in 28-day old (p=0.8333, n=15) *pirk* female flies **(Figure 5B)**. However, no significant change was detected in 6-day old male mutants (p=0.3009, n=14) **(Figure 5C)**, but a reduction of 0.5 (p<0.0001, n=15) was observed in 28-day old male *pirk* flies **(Figure 5D)**.

2.2.3 Effects on Sleep and Locomotion

After examining the effects of the *pirk* mutation on climbing ability, we tested whether the *pirk* adult flies aged 6 and 28-days had an effect on sleep and activity behaviour of the flies and whether this effect is exacerbated with age.

We assessed the effects of *pirk* mutant adult flies aged 6 and 28 on sleep and activity behaviours using Drosophila Activity Monitors (DAMs). Thirty-two flies were loaded onto a single DAM in 10 mm-long tubes. The flies were allowed to acclimate, and data from 2 days (excluding day 1) were averaged. This procedure was repeated 3 times, and a random selection of 32 flies was made to represent the genotype and, inactivity for longer than 5 minutes was calculated as sleep.

Finally, the data was evaluated to check if it followed normal distribution by performing a D.Agostino & Pearson test, after which a Mann-Whitney Rank Sum Test was performed and p values less that 0.05 was considered statistically significant. The median differences were calculated using the Hodges-Lehmann estimator and data was then presented in the form of an individual value column graph with +SEM error bars.

2.2.3.1 Effects on Females

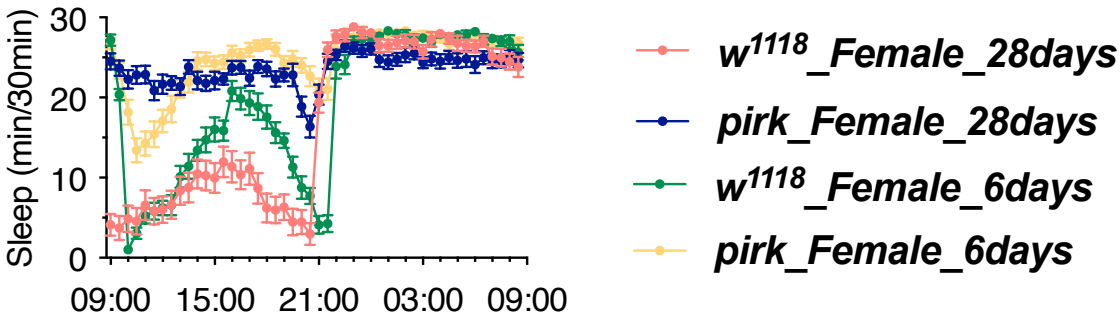

Figure 6: An illustration to suggest the effect of Pirk protein on sleep of 6-day and 28-day old female mutant flies compared to their w^{1118} controls. Three independent repeats were conducted for each genotype, and 32 flies were randomly selected from these repeats, resulting in a total sample size (n) of 32. Sleep was defined as inactivity for longer than 5 minutes.

As anticipated, the flies in the experiment have predictable circadian rhythm **(Figure 6)**. Female w^{1118} flies exhibit peak activity near lights on Zeitgeber time 0 (ZT0) and lights off (ZT12) and were more active during the light phase (9am to 9pm) than dark (9pm to 9am). Zeitgeber time (ZT) is a standardised 24-hour notation and is referred to as any environmental cue capable of acting as circadian time cues. The most common ZT is the light/dark cycle, where ZT 0 represents the start of the day, or the light phase, while ZT 12 marks the beginning of the night, or the dark phase.

In wild type (w^{1118}) flies, an age dependent reduction is observed in sleep during the light phase or daytime sleep. It is evident that there is an increase in daytime sleep in *pirk* female flies at both ages; however, 28-days *pirk* flies have the highest daytime sleep with a short peak right before lights off.

Sleep Profile

Total Sleep duration is calculated as total minutes of sleep during a set period of time. We observe that absence of Pirk protein has a significant effect on the total sleep duration of female flies at both 6-days and 28-days ($p<0.0001$, $n=32$) **(Figure 7A)**. The median sleep of 6 and 28-day *pirk* flies were 1226 and 1192 minutes respectively, as opposed to 1002 and 806.5 minutes for 6-days and 28-days w^{1118} flies respectively, illustrating a significant increase in the total sleep duration of the mutant flies **(Figure 7A)**.

Total sleep per day can further be divided into total duration of sleep during the day and total duration of sleep at night. Similar to total sleep duration, we observed a significant rise in total sleep during the day in *pirk* flies at both 6 and 28-daytime point compared to their respective controls ($p<0.0001$, $n=32$) **(Figure 7B)**. Moreover, a slightly significant increase in night-time

sleep in 6-day *pirk* females (p=0.0341, n=32) and a significant decrease in night-time sleep in 28-days (p=0.0172, n=32) was also observed **(Figure 7C)**. This leads us to believe that *pirk* flies are sleeping significantly more during the day, that may slightly be compensated at night in 28-day flies but not in 6-day old flies.

To examine whether the increase of sleep is because of an increase in sleep quantity (number of sleep episodes) or sleep quality (duration of sleep episodes), we analysed other sleep parameters. We did not observe any significant fluctuation in the number of sleep episodes in 6-day old *pirk* flies (p=0.7819, n=32) (**Figure 7D**). However, we did observe a stark increase in the number of sleep episodes in 28-day old *pirk* female flies compared to their controls (p<0.0001, n=32) with a median difference of 16 episodes (Hodges-Lehmann estimator) (**Figure 7D**). Since *pirk* mutants likely sleep more during the day (**Section 2.2.3.1**), we further divided our analysis into daytime and night-time. Similar to the total number of episodes for 24-hours, we observed a significant increase in the number of sleep episodes during the day in 28-day old (**Figure 7E**) female *pirk* mutant (p<0.0001, n=32) and no significant association at day 6 (p=0.5591, n=32) (**Figure 7E**). Furthermore, a similar yet less significant observation was made during night-time with 28-day old flies (p=0.0044, n=32) (**Figure 7F**).

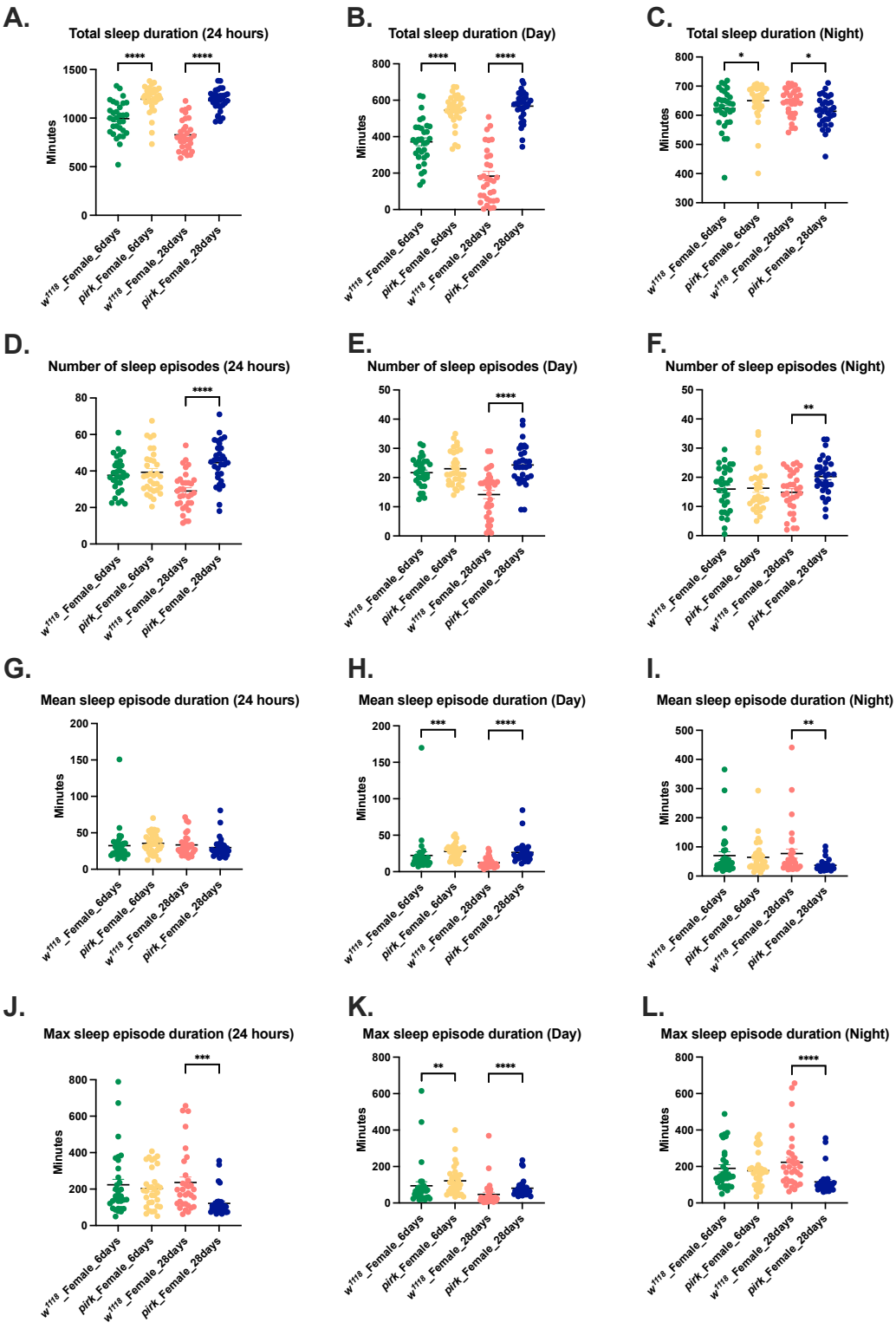

Figure 7: The effect of Pirk protein on sleep profiles of 6-day and 28-day old *pirk* female flies compared to their w^{1118} controls. Three independent repeats were conducted for each genotype, and 32 flies were randomly selected from these repeats, resulting in a total sample size (n) of 32. These 32 flies were then analysed, and a Mann Witney Rank sum test was performed between mutant flies and their respective controls, without consideration of age-dependent analysis. Non-significant results were not marked and $p \leq 0.05$ (*), ≤ 0.01 (**), ≤ 0.001 (***), ≤ 0.0001 (****).

To understand if the increased daytime sleep is due to poor sleep quality, we analysed the mean sleep episode duration/rest bout length. Even though we did not observe any notable interaction in the mean sleep episode duration throughout the day **(Figure 7G)**, we did observe a strong association between mean sleep episodes and the absence of Pirk protein during daytime at both 6-day ($p=0.0004$, $n=32$) and 28-day ($p<0.0001$, $n=32$) old female flies with a median difference of 9.90 and 11.84 respectively **(Figure 7H)**. In contrast to this, we did not observe any significant changes in the mean sleep episode during night-time at 6-days ($p=0.6383$, $n=32$) but a significant reduction during night-time at 28-days of age ($p=0.0065$, $n=32$) **(Figure 7I)**.

We observed no significant association with the absence of Pirk protein and the maximum sleep episode duration over the course of the day in 6-day old Female *pirk* flies ($p=0.7975$, $n=32$) **(Figure 7J)**. However, we saw a significant decline in 28-day old female mutant flies with the median value dropping from 187.5 minutes in control flies to 102.3 minutes in mutant ($p=0.0001$, $n=32$) **(Figure 7J)**. In contrast to this observation, we detected an increase in the maximum sleep episode duration in the day in 6-day old female mutant flies, with a median difference of 36 minutes ($p=0.0054$, $n=32$) and in 28-day old mutants, with an increase of 41.25 minutes ($p=0.0054$, $n=32$) **(Figure 7K)**. Additionally, we did not observe any significant fluctuation in 6-day old mutant females at night ($p=0.9601$, $n=32$), but observed a significant decline in 28-day old female flies ($p<0.0001$, $n=32$) as compared to their controls **(Figure 7L)**.

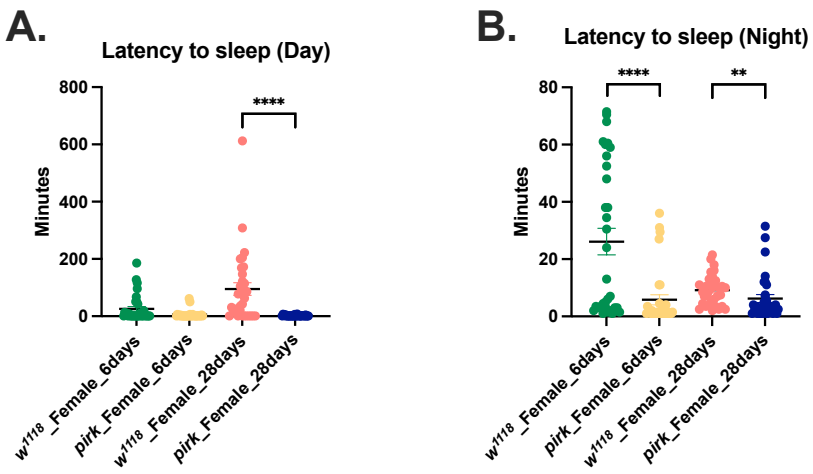

Figure 8: The effects of the absence of Pirk protein on the latency to sleep of 6-day and 28-day old *pirk* mutant female flies with respect to their w^{1118} controls. Latency is defined as the time taken by flies to fall asleep once lights are off, since the latency to sleep is the same over the course of 24-hours and during daytime sleep. Three independent repeats were conducted for each genotype, and 32 flies were randomly selected from these repeats, resulting in a total sample size (n) of 32, non-significant results were not marked and $p \leq 0.05$ (*), ≤ 0.01 (**), ≤ 0.001 (***), ≤ 0.0001 (****).

In the context of both daytime and night-time, this denotes the time elapsed before the fly experiences its initial sleep episode after the lights are turned off or on, respectively. Finally, latency to sleep is characterised as the duration it takes for flies to fall asleep once the lights are turned off. During daytime sleep, we observed a significant decrease in latency to sleep in *pirk* 28-day old female flies compared to their controls ($p<0.0001$, $n=32$) **(Figure 8A)**. Additionally, we observed a sharp decline in the latency to sleep at night in both 6-day ($p<0.0001$, $n=32$) and 28-day ($p=0.0015$, $n=32$) old female *pirk* mutant with a median difference of 5.5 and 4 minutes respectively **(Figure 8B)**.

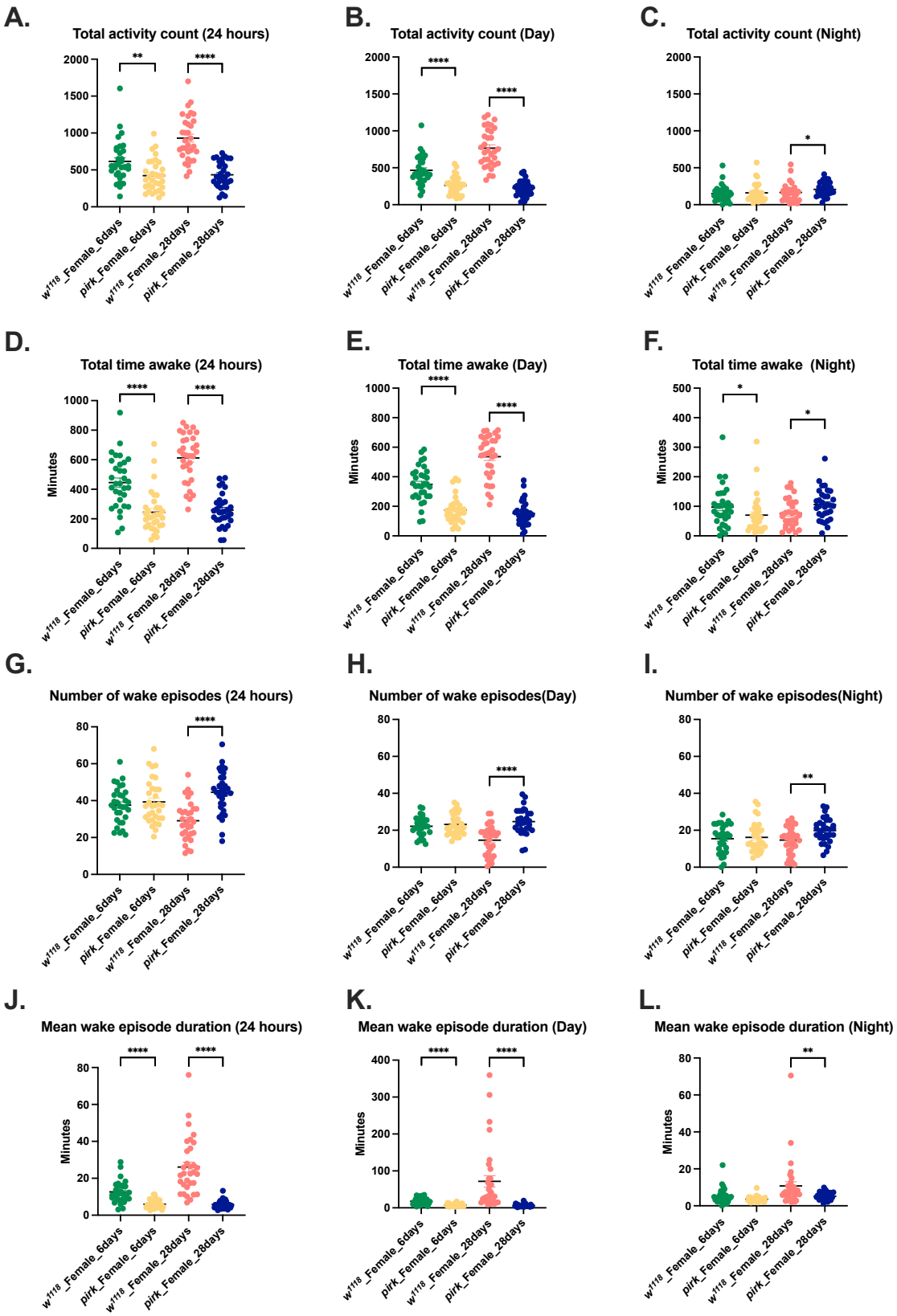

Figure 9: The effect of Pirk protein on activity parameters of 6-day and 28-day old *pirk* female mutant flies compared to their w^{1118} controls. Three independent repeats were conducted for each genotype, and 32 flies were randomly selected from these repeats, resulting in a total sample size (n) of 32. These 32 flies were then analysed, and a Mann Witney Rank sum test was performed between mutant flies and their respective controls, without consideration of age-dependent analysis. Non-significant results were not marked and $p \leq 0.05$ (*), ≤ 0.01 (**), ≤ 0.001 (***), ≤ 0.0001 (****).

Activity Profiles

Since sleep duration is largely affected by the activity of the flies, we analysed the total activity count of these flies or total beam crossing, to determine if there were overall activity differences between groups. This is defined as the number of times the flies crossed the beam for a defined period of time. We found that total activity count per day was significantly affected by the absence of Pirk protein at both 6-days ($p=0.0017$, $n=32$) and at 28-days ($p<0.0001$, $n=32$) **(Figure 9A)**. Further, we noted a sharp decline in the total activity count between *pirk* mutant and w^{1118} female flies at both 6-days ($p=0.0017$, $n=32$) and at 28-days ($p<0.0001$, $n=32$). This effect was stronger in 28-day flies with median activity count of 402.5 for *pirk* flies and 864.5 for w^{1118} flies **(Figure 9A)**.

Like total sleep, total activity count can be further divided into daytime activity count and night-time activity count. As expected, we observed a significant reduction in the total activity count during the day as compared to at night. Furthermore, this reduction was equally significant at both the ages ($p<0.0001$, $n=32$) **(Figure 9B)**. The median activity count values during the day were as follows: 260 for *pirk* 6-days females, 424.3 for w^{1118} 6-days females, 219.8 for *pirk* 28-day flies and 727.3 for w^{1118} 28-days flies. Additionally, we found a notable reduction in the total activity count at night in 28-day female *pirk* flies ($p=0.0335$, $n=32$) where the median difference was 51.50, but not in 6-day old female flies ($p=0.9708$, $n=32$) **(Figure 9C)**.

A difference in the total activity count or total beam crossing is not enough to draw any significant conclusion without understanding other parameters of activity such as mean / max wake episodes and total time awake.

We observed a significant reduction in the total time the flies were awake (measured in minutes) in both 6-day ($p<0.0001$, n=32) and 28-day old ($p<0.0001$, n=32) *pirk* mutant female flies **(Figure 9D)**. This decline in total time awake was consistent during the day in both ages ($p<0.0001$, n=32 for both) **(Figure 9E)**, but was less significant during night-time for both 6-days ($p=0.0341$, n=32) and 28-day old flies ($p=0.0172$, n=32) **(Figure 9F)**. In summary, the total activity count along with total time asleep shows a possibility that the mutant flies sleep more during the day.

Similar to the parameters of sleep episodes, the wake episodes can be divided further into the number of wake episodes, max wake episodes and mean wake episodes **(Figure 9(G-I))**. No significant association was observed in the number of wake episodes and the absence of Pirk protein in 6-day old female flies ($p=0.7666$, n=32) during the course of the day **(Figure 9G)**. However, a strong effect was observed in 28-day old mutant flies ($p<0.0001$, n=32), with a stark increase in median value of 16 episodes. A similar result was detected in the number of wake episodes during both daytime and night-time, with no significant differences in 6-day old flies, ($p=0.7564$ during the day and 0.9389 at night (n=32)) **(Figure 9(H-I))**. Additionally, a strong increase in 28-day old flies was observed during the day, $p<0.0001$, with a median increase from 17 episodes in control flies to 24.25 in pirk females (n=32) and a median increase from 16 episodes to 20 episodes at night ($p=0.0048$, n=32) **(Figure 9(H-I))**.

We found a stark decline in the mean wake episode duration throughout the day in *pirk* female flies at both ages compared to their controls ($p<0.0001$, n=32 for both) **(Figure 9J)**. This effect was also observed during daytime with a median reduction of 9.15 minutes for 6-day old ($p<0.0001$, n=32) and that of 27.15 minutes for 28-day old female *pirk* flies compared to their w^{1118} controls **(Figure 9K)**. However, we did not observe any significant change in 6-day old

flies (p=0.1031, n=32) during night-time, but a slight lowering of 2.42 minutes in 28-day old flies (p=0.0053, n=32) **(Figure 9L)**.

Similarly, we observed a significant reduction in the max wake episode duration over the course of the day in both ages (p<0.0001, n=32 for both) **(Figure 10A)**, which corelated with an increase in the duration of the max wake episode during daytime. A median decline of 41.25 minutes was observed in 6-day old flies (p<0.0001, n=32) and that of 127.3 minutes was observed in 28-day of flies (p<0.0001, n=32) **(Figure 10B)**. Similar to that of mean wake episode duration, no notable changes were observed in 6-day old *pirk* flies (p=0.0602, n=32) but a significant median decrease of 24 minutes was observed at the age of 28-days (p=0.0021, n=32) in *pirk* female flies compared to their controls **(Figure 10C)**.

An important question to ask when using the DAM system to study flies that potentially have neurodegeneration is if they are truly in sleep / rest, or appear immobile because of neuromuscular damage. One parameter within the sleep setup that helps us answer this question is the activity count / time awake. It is defined as the activity rate of flies when awake. Flies with neuromuscular damage have lower wake activity compared to that of the controls.

We observe a significant increase in the activity count / time awake in mutant *pirk* flies at both 6-days (p=0.0002, n=32) and 28-days (p=0.0164, n=32) **(Figure 10D)**, compared to their controls. Moreover, this effect was not observed during the day at either of the ages. Additionally, a significant increase is observed during night-time in 6-day old *pirk* mutant flies (p<0.0001, n=32) but not in 28-day old flies (p=0.8992, n=32) **(Figure 10(E-F))**.

Since we don't observe any reduction in activity count / time awake, it is safe to say that these flies might not have neuromuscular damage and are truly affected by sleep. Young mutant flies show a significant increase in activity count / time awake at night which could likely be an overcompensation of the lack of sleep.

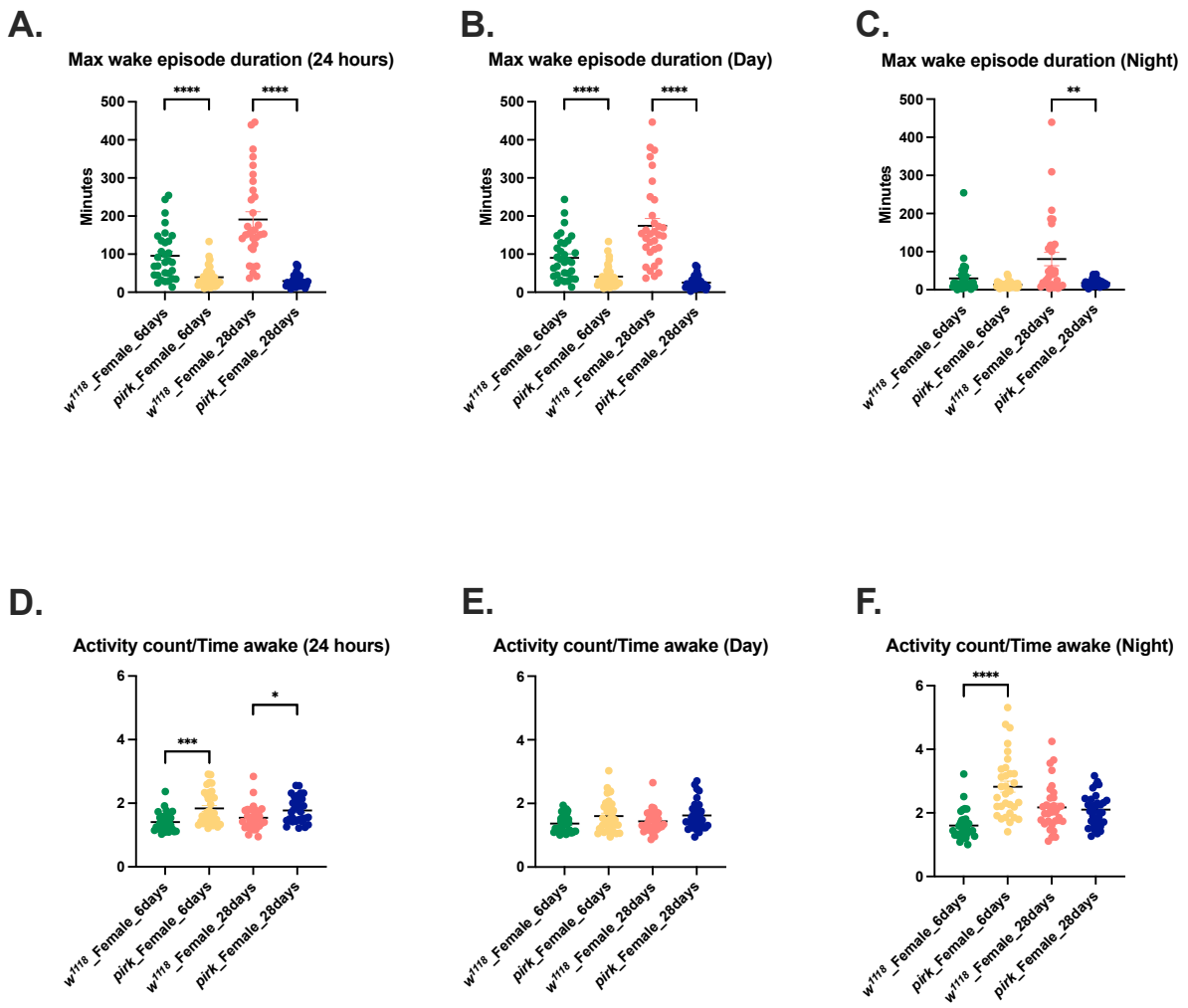

Figure 10: The effect of Pirk protein on maximum wake episode duration and rate of activity of 6-day and 28-day old *pirk* female mutant flies compared to their controls. Three independent repeats were conducted for each genotype, and 32 flies were randomly selected from these repeats, resulting in a total sample size (n) of 32. These 32 flies were then analysed, and a Mann Witney Rank sum test was performed between mutant flies and their respective controls, without consideration of age-dependent analysis. Non-significant results were not marked and $p \leq 0.05$ (*), ≤ 0.01 (**), ≤ 0.001 (***), ≤ 0.0001 (****).

2.2.3.2 Effects on Males

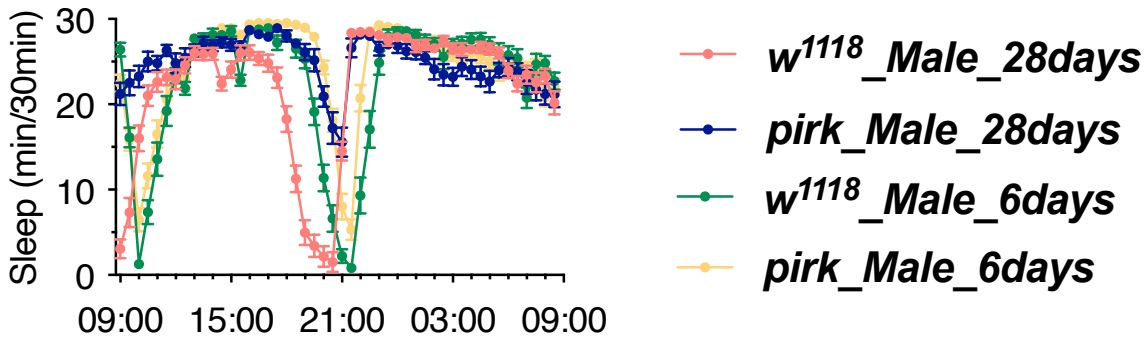

Figure 11: An illustration to suggest the effect of Pirk protein on sleep of 6-day and 28-day old male mutant flies compared to their w^{1118} controls. Three independent repeats were conducted for each genotype, and 32 flies were randomly selected from these repeats, resulting in a total sample size (n) of 32. Sleep was defined as inactivity for longer than 5 minutes.

Like female flies, male w^{1118} flies display a predictable circadian rhythm. Male w^{1118} flies exhibit maximum activity near lights on (ZT0) and lights off (ZT12) **(Figure 11)**. However, unlike female flies, w^{1118} flies seem to sleep more during the day at both ages. Additionally, we still observe an age dependent increase in daytime sleep in both w^{1118} and *pirk* males. Overall, we can deduce that older *pirk* males might be sleeping more during the day. However, this needed to be confirmed by other sleep profiles. For this, we divided total sleep (and all other parameters) into daytime (ZT0 - ZT12) and night-time (ZT12 - ZT24).

Sleep Profiles

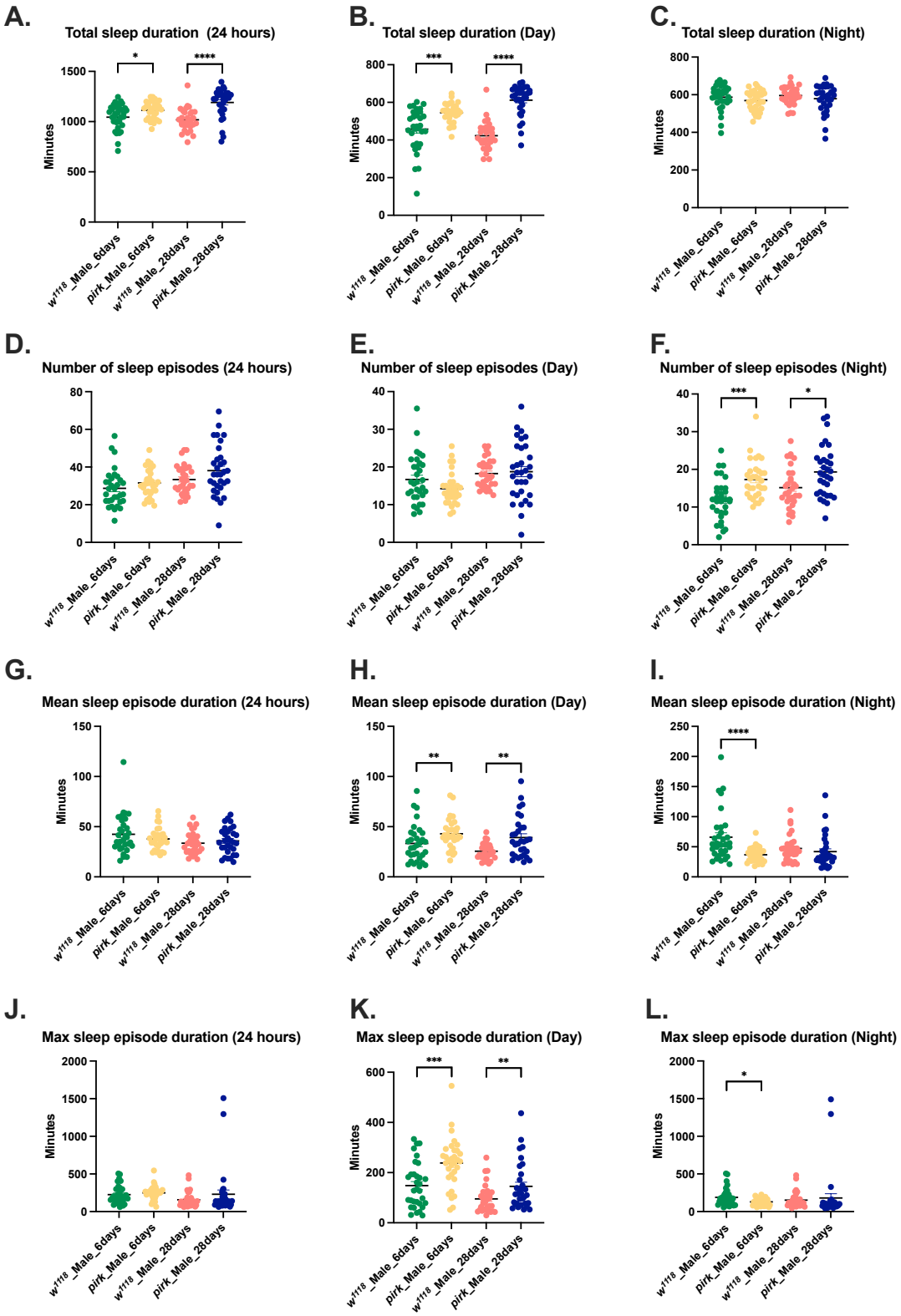

Figure 12: The effect of Pirk protein on sleep parameters of 6-day and 28-day old *pirk* male flies compared to their w^{1118} controls. Three independent repeats were conducted for each genotype, and 32 flies were randomly selected from these repeats, resulting in a total sample size (n) of 32. These 32 flies were then analysed, and a Mann Witney Rank sum test was performed between mutant flies and their respective controls, without consideration of age-dependent analysis. Non-significant results were not marked and $p \leq 0.05$ (*), ≤ 0.01 (**), ≤ 0.001 (***), ≤ 0.0001 (****).

We observed a significant increase in the total duration of sleep in both 6-day (p=0.0258, n=32) and 28-day old (p<0.0001, n=32) male *pirk* flies with a median increase in sleep of 56.75 minutes in younger flies and an increase of 199 minutes in older ones **(Figure 12A)**. However, once we divided them into daytime and night-time sleep, it was evident that there was an increase in daytime sleep which was not compensated for during the night. A substantial increase in total sleep during the day was observed in both 6-day (p=0.0006, n=32) and 28-day (p<0.0001, n=32) old male *pirk* mutant as compared to their w^{1118} controls **(Figure 12B)**; whereas, no remarkable change was observed during the night in both the ages with p=0.1174 for 6-day old and p=0.6547 for 28-day old flies (n=32 for both) **(Figure 12C)**.

We did not observe any solitary effect of absence of *pirk* and the total number of sleep episodes in either 6-days (p=0.0926, n=32) or 28-days (p=0.1506, n=32) old male flies compared to their controls **(Figure 12D)**. Similarly, no significant association was detected during daytime, with median differences of 2 (p=0.1302, n=32) in 6-day old males and that of 0.25 (p=0.8671, n=32) in 28-day old flies **(Figure 12E)**. Nevertheless, a substantial increase in the number of sleep episodes was detected in both ages during night-time. A median increase of 5 episodes was observed in 6-day old flies (p=0.0001, n=32) and a median increase of 4 was observed in 28-day old male *pirk* mutants compared to their controls (p=0.0132, n=32) **(Figure 12F)**.

To understand the sleep phenotype further, we inspected the quality of sleep by looking into the mean and max sleep episode duration. We noted no significant differences in the mean sleep episode duration in both 6 (p=0.4919, n=32) and 28-day old (p=0.5019, n=32) male *pirk* flies compared to their controls **(Figure 12G)**. However, examining the effects during daytime, we found a significant increase in the number sleep episodes in either of the ages, with a median difference of 11.22 minutes in 6-day old (p=0.0050, n=32) and that of 9.91 minutes in 28-day old (p=0.0057, n=32) male mutant flies compared to their controls **(Figure 12H)**. In contrast,

we observed a stark decrease in the mean sleep episode duration of 18.11 minutes in 6-day old flies at night-time (p<0.0001, n=32) and no significant change in 28-day old males (p=0.0870, n=32) **(Figure 12I)**. Similar to the other measurements of sleep episodes, we did not observe any notable changes in the maximum sleep episode duration during the day in both 6-day (p=0.1488, n=32) and 28-day (p=0.5319, n=32) old male *pirk* flies **(Figure 12J)**. However, we found a significant increase during daytime in both ages, with an increase of 95 minutes at 6-day (p=0.0005, n=32) and an increase of 30.75 minutes (p=0.0098, n=32) at 28-days of age **(Figure 12K)**. Furthermore, a slight decrease of 33.25 minutes was observed in 6-day old *pirk* male flies (p=0.0424, n=32) during night-time but no significant fluctuations were observed in 28-day old flies **(Figure 12L)**.

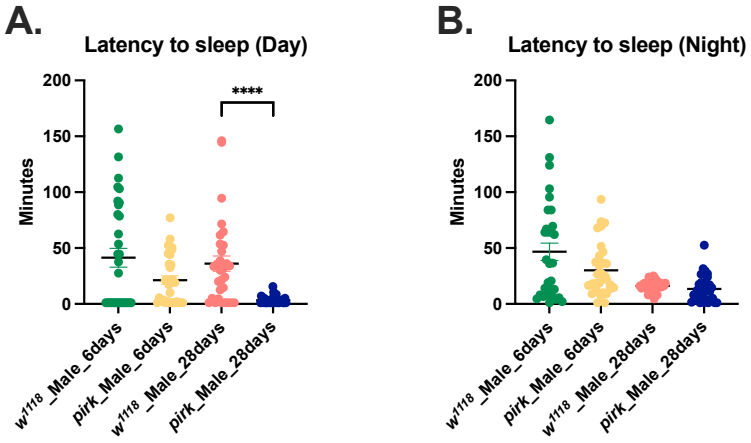

Figure 13: The effects of the absence of Pirk protein on the latency to sleep of 6-day and 28-day old *pirk* mutant male flies with respect to their w^{1118} controls. Latency is defined as the time taken by flies to fall asleep once lights are off, since the latency to sleep is the same over the course of 24-hours and during daytime sleep. Three independent repeats were conducted for each genotype, and 32 flies were randomly selected from these repeats, resulting in a total sample size (n) of 32, non-significant results were not marked and p≤ 0.05 (*), ≤ 0.01 (**), ≤ 0.001 (***), ≤ 0.0001 (****).

Latency to sleep during daytime sleep was shown to be significantly affected by the presence of Pirk protein in 28-day old male *pirk* mutant fly (p<0.0001, n=32) **(Figure 13A)**.

We did not observe any significant changes in the latency to sleep at night for both 6-day (p=0.5152, n=32) and 28-day old (p=0.0541, n=32) *pirk* male flies compared to their w^{1118} counterparts **(Figure 13B)**.

Activity Profiles

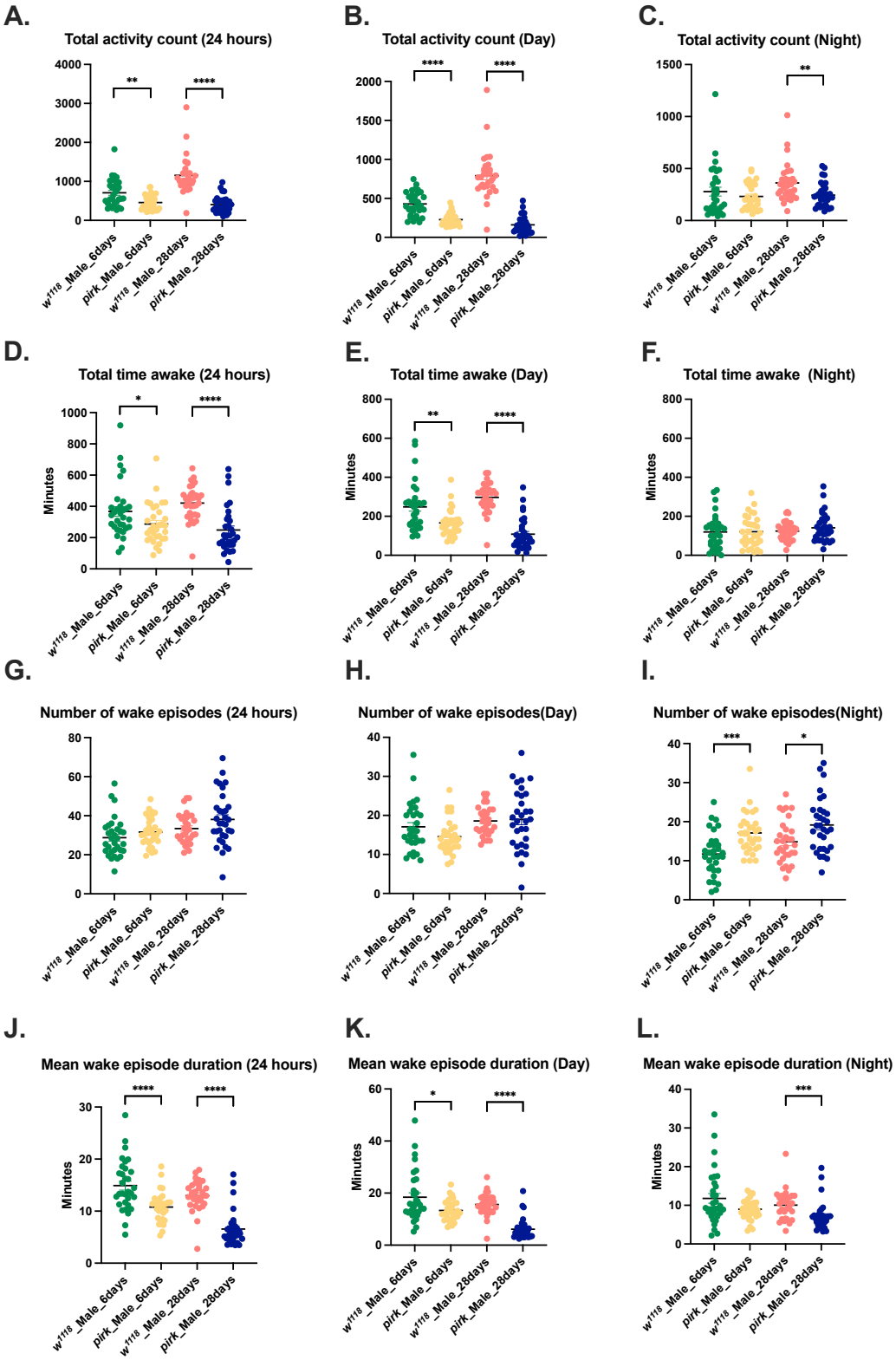

Figure 14: The effect of Pirk protein on activity parameters of 6-day and 28-day old *pirk* male mutant flies compared to their w^{1118} controls. Three independent repeats were conducted for each genotype, and 32 flies were randomly selected from these repeats, resulting in a total sample size (n) of 32. These 32 flies were then analysed, and a Mann Witney Rank sum test was performed between mutant flies and their respective controls, without consideration of age-dependent analysis Non-significant results were not marked and $p \leq 0.05$ (*), ≤ 0.01 (**), ≤ 0.001 (***), ≤ 0.0001 (****).

We found a significant association between total activity count and absence of Pirk protein over the course of the day at both 6-days ($p=0.0014$, $n=32$) and 28-days ($p<0.0001$, $n=32$) of age **(Figure 14A)**. A median decline of 201.3 was observed in 6-day old mutant male flies ($p<0.0001$, $n=32$) and that of 601.8 was observed in 28-day old flies ($p<0.0001$, $n=32$) during daytime activity **(Figure 14B)**. Additionally, no significant change was observed in 6-day old *pirk* mutants at night-time ($p=0.9177$, $n=32$) but a significant reduction of 99.25 was noted in 28-day old flies ($p=0.0016$, $n=32$) **(Figure 14C)**.

Activity count or the number of times the fly crosses the beam is not enough to understand the activity profile of a fly line. Therefore, we examine other parameters such as total time awake, max and min wake episodes and activity count / time awake to get a more comprehensive understanding of the activity profiles.

We noted a slight median decline of 67 minutes in the total time awake of mutant *pirk* male flies at 6-days ($p=0.0397$, $n=32$) and a more significant decline of 199 minutes in 28-day old flies ($p<0.0001$, $n=32$) compared to their w^{1118} controls throughout the day **(Figure 14D)**. Additionally, a similar effect was observed during daytime in both 6-day and 28-day old mutants ($p=0.0022$, $n=32$ and $p<0.0001$, $n=32$ respectively) **(Figure 14E)**. However, no significant association was detected during night-time in both ages with p equal to 0.7616 for 6-day old flies and p equal to 0.6547 in 28-day old flies **(Figure 14F)**.

Despite observing a reduction in the total time awake, we did not note any remarkable change in the number of wake episodes in both ages throughout the day with $p=0.0913$ for 6-day old and $p=0.1546$ for 28-day old *pirk* mutant flies ($n=32$ for both) **(Figure 14G)**. In addition to this, we did not find any significant changes in the number of wake episodes during daytime in both 6 and 28-day ($p=0.0885$ and $p=0.9049$ respectively, $n=32$) **(Figure 14H)**. However, we

found a significant rise of 5.5 wake episodes in 6-day old (p=0.0001, n=32) and a median rise of 4 episodes in 28-day (p=0.0143, n=32) old mutants during night-time **(Figure 14I)**. We noted a striking decrease in the mean wake episode duration in both ages throughout the day (p<0.0001, n=32 for both) **(Figure 14J)**. Additionally, a median decline of 2.89 minutes in 6-day old *pirk* mutants (p=0.0913, n=32) and that 10.15 minutes in 28-day old (p<0.0001, n=32) during daytime was detected **(Figure 14K)**. This effect was not observed in 6-day old mutants during night-time with p=0.2012 (n=32) but was detected in 28-day old flies, with a median reduction of 3.41 minutes and p=0.0004 (n=32) **(Figure 14L)**.

Like the mean wake episode duration, the maximum duration of the wake episode was significantly associated with the absence of Pirk. We observed a significant reduction in the max wake episode duration in both young and old flies (p<0.0001, n=32 for both) **(Figure 15A)**. Furthermore, a significant median reduction of 38.25 minutes was observed during the day for 6-day old *pirk* mutant flies (p=0.0001, n=32) and that of 84.5 minutes in 28-day old (p<0.0001, n=32) male flies, compared to their controls **(Figure 15B)**. However, no notable difference was observed in 6-day old flies during night-time (p=0.2247, n=32) but a decline of 16 minutes in 28-day old (p=0.0037, n=32) flies compared to w^{1118} **(Figure 15C)**.

A median decline of 0.66 was observed in 6-day old (p<0.0001, n=32), we noted a significant decline in the activity rate of male mutant flies compared to their controls. In the 24-hour period, and that of 0.94 in 28-day old (p<0.0001, n=32) males **(Figure 15D)**. A comparable effect was also observed in flies during day and night-time. With a significant reduction of 0.83 and 1 in young and old flies respectively during daytime (p<0.0001, n=32 for both) **(Figure 15E)**. Furthermore, a decrease of 0.49 (p=0.0001, n=32) and 1.07 (p<0.0001, n=32) in 6-day and 28-day old male *pirk* flies was observed during night-time **(Figure 15F)**.

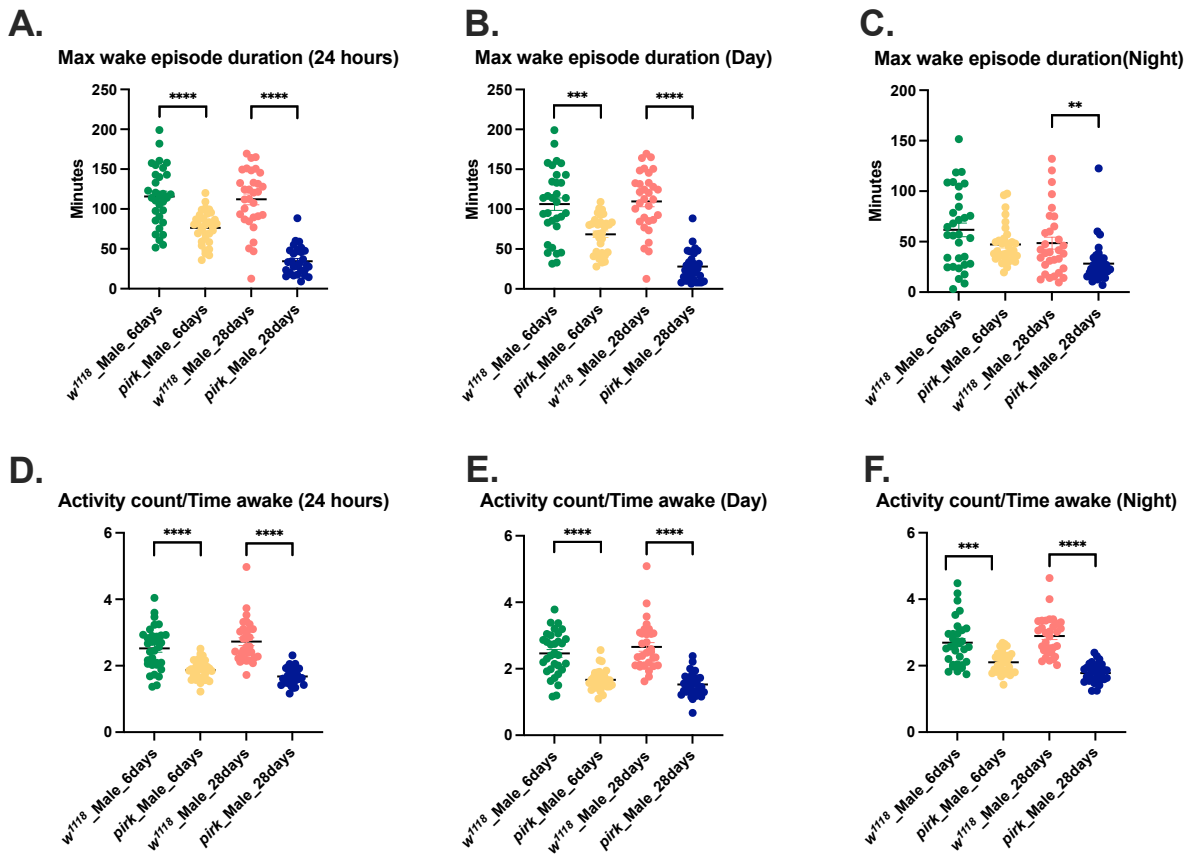

Figure 15: The effect of Pirk protein on maximum wake episode duration and rate of activity of 6-day and 28-day old *pirk* male mutant flies compared to their controls. Three independent repeats were conducted for each genotype, and 32 flies were randomly selected from these repeats, resulting in a total sample size (n) of 32. These 32 flies were then analysed, and a Mann Whitney Rank sum test was performed between mutant flies and their respective controls, without consideration of age-dependent analysis. Non-significant results were not marked and p≤ 0.05 (*), ≤ 0.01 (**), ≤ 0.001 (***), ≤ 0.0001 (****).

2.2.4 Effects on Intestinal Permeability

The intestinal permeability assay or "the smurf assay" is non-invasive technique developed by Rera et al. (2011), used to study the intestinal integrity of fly lines. It relies on the capability of the fly to restrict large molecules to the digestive track after feeding. The flies are fed with a nonabsorbable blue food dye (FD&C blue dye #1) and are left for observation. After 6 hours, the flies with the blue dye outside the track or "smurfs" are recorded. In this study, this assay is used to examine the intestinal integrity of flies with constitutively active immune response in the gut ($pirk^{EY00723}$ mutants).

We manually counted the number of blue flies at the end of the day and flies that were completely blue (as shown in the paper, Rera, Clark and Walker (2012a) were marked as smurfs. A two tailed Wilcoxon matched-pairs signed rank test was performed and p value of 0.05 or lower was considered significant.

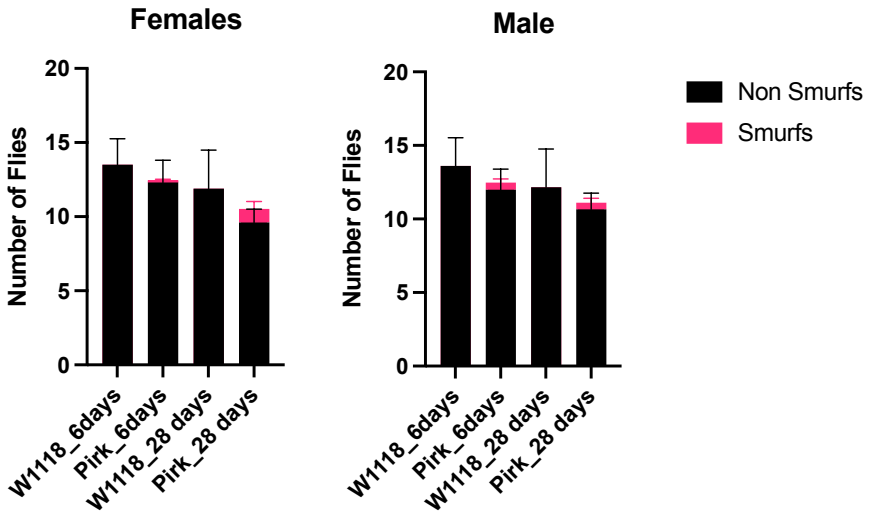

Figure 16: The effect of Pirk protein on intestinal permeability of both male and female flies at 6 and 28-days of age compared to their controls. Three independent repeats were conducted for each genotype, and 4 vials of 15 flies very analysed per repeat, these very then averaged out. Resulting in a total sample size (n) of 45, a Wilcoxon matched-pairs signed rank test was performed and $p < 0.05$ was considered significant.

Despite observing a slight trend in the number of smurfs, our analysis found no statistically significant differences in the number smurfs observed in both 6-day or 28-day old female or male *pirk* mutant flies with respect to their w^{1118} controls **(Figure 16(A-B))**.

Similar to that of females, we found no noteworthy changes in the total number of smurfs in male mutants at either of the ages. The lack of smurfs could mean that the intestinal barrier is intact in mutant flies and is likely not the cause of death in these flies. However, it is worth noting that even though we do not observe any significant changes in the number of smurfs, there seems to be a trend towards higher number of smurfs in pirk mutant flies than controls.

Summary of Results

After analysing several behavioural parameters, it is safe to say that constitutive inflammation in the gut has a significant effect on sleep and locomotion of *Drosophila*. This effect was shown to be more significant in female flies than their male siblings and is shown to get progressively worse as the flies age.

We initially observed a significant decline in climbing ability among female flies at both 6 and 28-days of age, whereas this decline was only evident in male flies aged 28-days. Analysis of sleep profiles revealed that *pirk* mutant flies, particularly females, displayed increased daytime sleep, a trend consistent across both age groups. This finding was corroborated when sleep parameters were segregated into daytime and night-time periods. Further investigation into the potential drivers of increased daytime sleep revealed a likely augmentation in sleep duration rather than frequency, as evidenced by an increase in mean sleep episode duration. Additionally, examination of latency to sleep revealed that female *pirk* flies exhibited quicker sleep onset in response to light changes at both 6 and 28-days. Interestingly, while sleep phenotypes were predominantly observed during the day at 6-days, they extended to night-time as the flies aged to 28-days. All these effects were further validated by examining several activity parameters.

Similar trends were observed in male *pirk* mutant flies, with increased total sleep duration observed throughout the day and during daytime sleep across both age groups. This increase was primarily attributed to longer mean sleep episode durations during daytime sleep. However, no significant changes in latency were observed in male flies at either age.

Finally, we examined whether flies with consistently active immune systems displayed any signs of impaired intestinal barrier permeability, using the "Smurf assay." Surprisingly, our observations revealed no noteworthy change in the occurrence of smurfs among either male or female *pirk* mutant flies at 6 or 28-days.

However, it's important to recognise*pirk* mutant background indicates a potential factor that may contribute to gut leakage. Although the effect seems statistically subtle from this perspective, it's essential to approach the conclusion cautiously and refrain from dismissing any impact entirely.

CHAPTER THREE

Exploring the sleep phenotypes of Axenic pirk mutants

CHAPTER THREE:

EXPLORING THE SLEEP PHENOTYPE OF AXENIC *PIRK* MUTANTS

This chapter aims to investigate the neurological phenotypes observed in both 6 and 28-days old female and male *pirk* mutant flies that have been treated with bleach and antibiotics to be made germ free or axenic.

Section 3.1: This section focuses on why *Drosophila* is a good model to study the gut microbiome and its advantages in understanding the physiological role of the commensal microbiome on host physiology.

Section 3.2: Here we talk about the various methods of generating germ free flies and further examine the sleep and activity profiles of both male and female germ free *pirk* ^{EY00723} flies at 6 and 28-days with respect to their controls.

Finally, **section 3.3** provides a brief summary of the phenotypes observed and their potential significance.

3.1 BACKGROUND

Drosophila melanogaster has been widely used as a model organism in biological sciences, but recently has gained attention as a suitable model to study human gut related disorders (Apidianakis and Rahme 2011; Chiang et al. 2022). The fly gut shares several conserved features with the mammalian intestines, and they are said to be homologous to each other. These features include similarities in intestinal pathophysiology and regeneration, as well as signalling pathways that regulate the gut (Cryan and Dinan 2012; Capo, Wilson and Di Cara 2019). In addition to this, the role of commensal microbiome in maintaining gut homeostasis and morphology is a phenomenon that is observed in both vertebrates and invertebrates (Buchon *et al.* 2009; Sekirov *et al.* 2010; Broderick, Buchon and Lemaitre 2014). The commensal microbiome has been associated with several physiological aspects of host physiology (See **Chapter 1** for more detail). These include the metabolism of lipids and carbohydrates (Cho and Blaser 2012; Gilbert et al. 2018), as well as the manifestation of a number of gastrointestinal conditions, including metabolic abnormalities, colorectal cancer, irritable bowel syndrome (IBS) and inflammatory bowel disease (IBD) (Garrett *et al.* 2010). Dysbiosis in the gut has also been associated with several systemic illnesses, such as type 2 diabetes, and obesity (See **Chapter 1** for more detail).

Drosophila has proven to be a model of choice to examine the role of microbes in lifespan extension, improved lifespan, intestinal stem cell activity and regulation, metabolic and developmental homeostasis, and the effects of dietary habits on microflora improvement (Jiang and Edgar 2011; Wong, Vanhove and Watnick 2016; Liu, Hodgson and Buchon 2017; Lee *et al.* 2019). It is noteworthy that the gut microbiome has exhibited a complex bidirectional relationship that influences an individual's behaviour via the gut brain axis, and is responsible

for stimulating inflammation, regulating the immune system, mid-gut regeneration and protection against pathogens (Pédron and Sansonetti 2008; Ryu *et al.* 2008; Fraune and Bosch 2010; Sharon *et al.* 2010; Griffith 2012; Jones *et al.* 2013; Kapsetaki *et al.* 2014; Venu *et al.* 2014). One of the main tools for examining the impact of a changed microbiome on a host's physiology is the use of germ-free (GF) model organisms. What makes the fly a good model for intestinal research is its vast genetic and genomic resources combined with easy maintenance, along with simple microbiome manipulation protocols. This allows germ free / microbiologically sterile flies to be generated in large numbers and makes *Drosophila* a useful alternative to rodents in microbiome research (Douglas 2018).

The interest in GF organisms is not a new one; in 1885, Louis Pasteur predicted that life would be impossible without commensal microbes (Pasteur 1885) because of which microbes became a topic of popular discussion after the discovery of antibiotics (Luczynski *et al.* 2016). The term germ free / axenic refers to an animal that harbours no cultivable organism or is devoid of microbes throughout its lifetime. For example, bacteria, viruses, fungi, protozoa, and parasites (Coates 1968; Kirk 2012). The term "gnotobiotic" refers to GF animals that have been colonised by one or more selective species (Al-Asmakh and Zadjali 2015). These help in examining the impacts of a specific strain or a particular microbial genus on the host and has potential to further help understand the complex host-microbe interactions. The guinea pig was the first animal to be produced GF; it was born by aseptic C-section and kept microbiologically sterile for two weeks (Basic and Bleich 2019). However, the largest application of the technology was the development of bio bubbles to protect immunocompromised humans (Barnes, Tuffrey and Cook 1968; Barnes *et al.* 1969; Lawrence 1985).

Despite its multiple applications GF technology is yet to be used outside of the laboratory and therefore, since it was first developed, the current procedure of generation GF animals has remained unaltered (Reyniers and Sacksteder 1959; Gustafsson and Maunsbach 1971; Macpherson and Harris 2004; Luczynski *et al.* 2016; Zhou *et al.* 2021). It includes aseptic delivery of progeny using C-section and their transfer into a sterile isolator where they will be reared (Basic and Bleich 2019). Subsequent generations of animals are made GF by inbreeding the germ-free animals and allowing them to deliver in isolation (Gordon 1960). Further, the germ-free status is confirmed by bacterial culture techniques via weekly cage swabs and faecal matter analysis (Bibiloni 2012; Williams 2014). Needless to say, there are several logistical limitations in raising germ free vertebrates. These limitations include high cost of rearing, confounding behavioural effects of keeping animals in isolator units and reduced reproducibility. Therefore, due to its low cost and ease of rearing, *Drosophila* is often used as the model to investigate GF animals (Sabat and Johnson 2015).

3.1.1.1 Different methods of generating axenic Flies

There are several techniques used to generate axenic/GF flies, such as removal of chorion of newly laid eggs (dechorionation), rearing flies on an antibiotic cocktail mixed into the food and raising flies on autoclaved sterile food.

During the dechorionation process, eggs are gathered using cages and plates, then delicately collected using a sterile paintbrush. They undergo a meticulous treatment sequence, starting with a hypochlorite solution, followed by ethanol, miliQ water, and PBS washes to ensure sterility. Subsequently, eggs devoid of their protective eggshell (chorion) are carefully transferred either into autoclaved food, as described by Kounatidis et al. (2017), or into food

supplemented with antibiotics. Typically, either individual or a combination of broad-spectrum antibiotics, such as tetracycline, penicillin, streptomycin, and rifamycin, are added (Sharon *et al.* 2010; Heys *et al.* 2018; Jacqueline, Parvy and Faugère 2019) to achieve GF status in flies, which can persist across multiple generations. The control group undergoes a thorough sterilisation process involving washing with sterile water, followed by rinsing with PBS, before being introduced to standard fly food. Similarly, the generation of gnotobiotic flies involves a parallel approach, where axenic food is supplemented with single or a combination of bacterial species, facilitating the exploration of species-specific host-microbe interactions.

Verification of the germ-free status of both eggs and flies is achieved through PCR amplification of the 16srRNA gene region or via conventional culture techniques on selective media such as MRS (Man, Rogosa, and Sharpe), BHI (Brain Heart Infusion agar), and LB (Luria Broth agar) (Sabat and Johnson 2015; Kounatidis et al. 2017; Mistry, Kounatidis and Ligoxygakis 2017).

3.1.1.2 Aims of this chapter

This chapter seeks to explore the impact of the microbiome on the sleep phenotype seen in **Chapter 2**. Lhocine et al. (2008) illustrated that the basal expression of *pirk* in the fly gut is microbiota dependent. We hypothesise that the observed sleep defects in **Chapter 2**, could potentially be rescued in GF conditions.

As noted in the **Covid Statement**, disruptions caused by the pandemic resulted in the loss of our w^{1118}:$pirk^{EY00723}$ stock during lockdowns. As a result, we chose to continue our research utilising*yw*) as the control for this chapter.

3.2 RESULTS

3.2.1 Generation of Axenic Flies

Germ Free flies were generated using the method of dechorionation following rearing the flies on a cocktail of antibiotics as outlined in Sharon et al.'s (2010) methodology (Sharon *et al.* 2010). The vials and bottles were prepared fresh (twice a week) and germ-free status was confirmed using MRS plating weekly **(S1)**. Finally, control flies raised in standard laboratory food were addressed as CR or conventionally reared flies and were generated by treating the eggs with miliQ water and PBS, and raising them in the same incubator as the GF flies. Please refer to Material and Method **Chapter 7 Section 7.1.8** for more details.

It is worth noting that in the following chapter, the terms 'microbe-free', 'germ free' and 'axenic' are used interchangeably, and the term 'conventional reared' is used for *Drosophila* with unmanipulated gut microbiomes.

3.2.2 Effects on Sleep and Locomotion

3.2.2.1 Sleep Profiles of Females

As expected, the sleep profiles of female flies follow a predictable circadian rhythm with an activity peak near lights on (Zeitgeber time (ZT) 0, 09:00) and lights off (ZT12, 21:00) **(Figure 17)**. Additionally, both young and old female *yw* and *pirk* flies are more active during the lights on phase or daytime (09:00 to 21:00) than lights off or night-time (21:00 to 09:00).

We observe an age dependent increase in daytime sleep in all the fly lines. Additionally, *pirk* mutant flies are visibly seen to have increased daytime sleep, compared to their controls. Young *yw* flies show a microbiome dependent increase in activity during the light phase. However, this effect is not as visibly significant in 28-day old female flies **(Figure 17(A-B))**.

Since sleep profiles are only a graphical representation, there is a need to examine the various sleep parameters before drawing any conclusions.

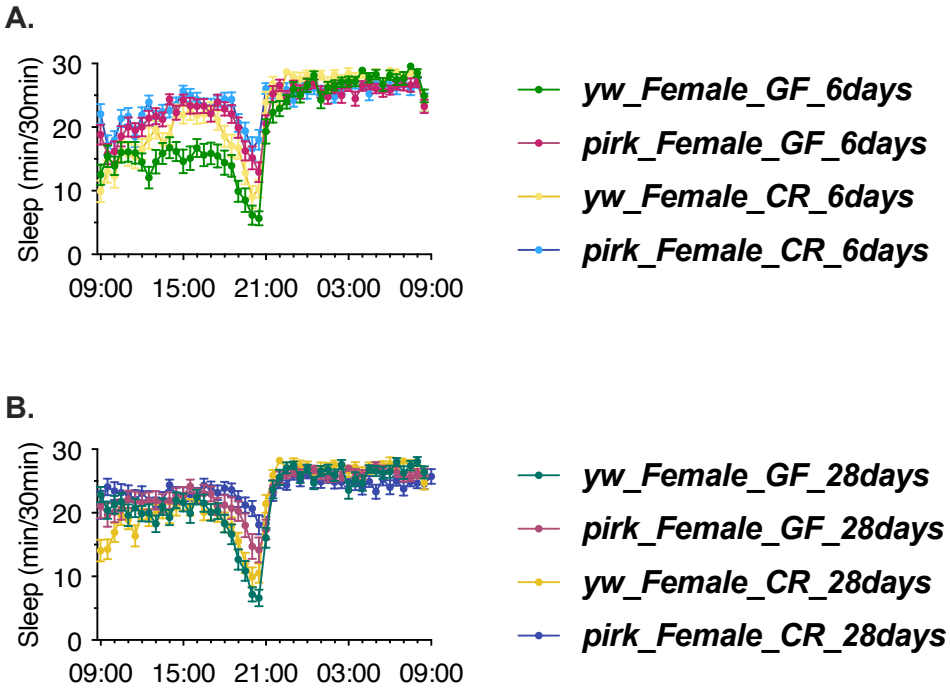

Figure 17: Sleep profiles for female GF vs CR *pirk* mutant flies with respect to their *yw* controls at both 6-days (A) and 28-days (B) of age. Three independent repeats were conducted for each genotype, and 32 flies were randomly selected from these repeats, resulting in a total sample size (n) of 32. Sleep was defined as inactivity for longer than 5 minutes. No statistical analysis was performed.

3.2.2.2 Effects on Young Females

To examine whether the microbiome composition of dysbiotic *pirk* female mutant guts contributes to the neurological phenotypes observed in **Chapter 2**, a parallel sleep experiment was conducted. However, unlike the previous chapter, a two-way ANOVA was applied to the dataset, supplemented by Šídák's correction to address multiple comparisons. Specifically, we analysed the data to investigate the effect of the presence of pirk, germ-free (GF) status, and

age-related differences in mutant flies compared to their controls. Significance within the data is denoted by an asterisk (*) in the diagram, while non-significant findings remain unmarked.

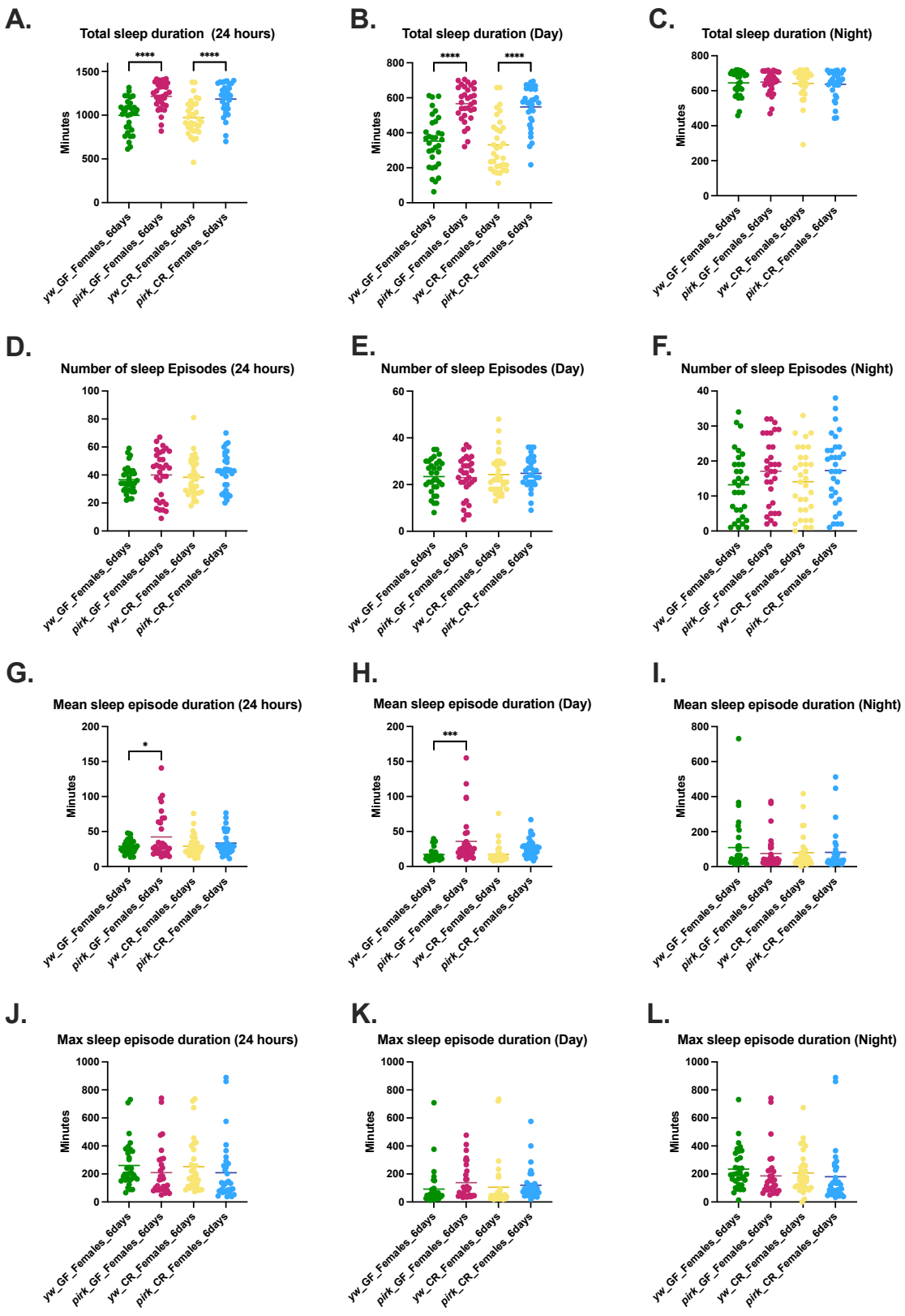

Figure 18: Sleep parameters of 6-day old *pirk* vs *yw* flies in both germ free and conventionally reared conditions. Three independent repeats were conducted for each genotype, and 32 flies were randomly selected from these repeats, resulting in a total sample size (n) of 32. Individual groups of flies were compared to each other and were analysed using a two-way ANOVA along with Šídák's correction. Non-significant results were not marked and p≤ 0.05 (*), ≤ 0.01 (**), ≤ 0.001 (***), ≤ 0.0001 (****).

Total Sleep

We observed no significant differences in the total sleep of 6-day old female germ-free flies, compared to their conventionally reared controls in all three data points (GF versus CR) **(Figure 18(A-C))**. However, we did observe a significant increase in the total minutes of sleep through the day in 6-day old *pirk* flies, compared to their *yw* counterparts **(Figure 18A)** A rise of 212 minutes was observed in 6-day old conventionally reared (CR) pirk flies compared to their yw control. ($p<0.0001$, n=32) and a similar increase of 218.4 minutes was observed in young GF *pirk* female flies compared to *yw* ($p<0.0001$, n=32) **(Figure 18A)**. Just like in **Chapter 2 Section 2.2.3.1.1.** This increase was due to an increase in daytime sleep in both groups ($p<0.0001$, n=32 for both 6-day old GF and CR flies), with a rise of 213.5 minutes in GF flies and 216.5 minutes in CR flies **(Figure 18B).** Furthermore, no significant deviation was observed in either fly lines at night-time with p=0.9999, n=32 in germ free flies and $p>0.9999$, n=32 in 6-day old CR *pirk* flies compared to their wild type controls **(Figure 18C)**.

Number of sleep episodes

We found no significant difference in the number of sleep episodes in both 6-day old *pirk* GF versus *pirk* CR (p=0.9912, n=32), and *yw* GF as well as *yw* CR flies (p=0.9969, n=32) **(Figure 18(D-F))**. We found no notable change in the number of sleep episodes during a 24-hour period in 6-day old female *pirk* GF flies versus their control with p=0.8975, n=32 and in female *pirk* CR flies versus CR *yw* flies with p=0.8459, n=32 **(Figure 18D)**. Similarly, no significant variation was observed during both daytime GF ($p>0.9999$, n=32) and CR (p=0.9999, n=32) **(Figure 18E)** and night-time GF (p=0.4759, n=32); and CR (p=0.6860, n=32) 6-day old *pirk* female flies **(Figure 18F)** compared to their respective controls.

Mean Sleep Episode duration

Similar to the results above, we found no noticeable fluctuation in average sleep episode duration or mean sleep episode duration between germ free and conventionally reared in 6-day old GF, versus CR flies in both *pirk* and *yw* flies **(Figure 18(G-I))**. An increase of 13.28 minutes in the mean sleep episode for 24-hours was observed in young GF *pirk* versus GF *yw* flies (p=0.0325, n=32) **(Figure 18G)**. However, no noticeable change was observed in young *pirk* CR flies relative to their controls (p=0.9235, n=32) **(Figure 18G)**. As expected, this increase in mean sleep episode duration was because of increased sleep during daytime, and a rise of 18.73 minutes was observed in young GF *pirk* female flies compared to *yw* (p=0.0008, n=32), and no distinguishable variation was observed in young CR *pirk* flies compared to their controls **(Figure 18H)**. Finally, we saw no noticeable change in the mean sleep episode duration in both GF and CR 6-day old *pirk* female flies at night-time **(Figure 18I)**.

Interestingly, we observed no changes in the maximum sleep episode duration in CR and GF 6-day old *pirk* female flies during a 24-hour period (p=0.9181, n=32 and p=0.8346, n=32 respectively) **(Figure 18J)**. Additionally, there was no significant differences in the maximum sleep episode values during both day and night-time as well **(Figure 18K)**. This leads us to believe that the increased sleep might not be caused due to a single long sleep episode but perhaps an overall increase in the duration of sleep episodes **(Figure 18L)**.

Latency of Sleep

We observed no notable changes in latency to sleep during daytime in GF *pirk* flies compared to their controls (p=0.0643, n=32). However, we observed a significant decline in latency during daytime sleep in conventionally reared *pirk* flies versus *yw* (p=0.0001, n=32) **(Figure**

19A). Additionally, we saw no significant increase in the latency to sleep during night-time, with p=0.9103 (n=32) in 6-day old *pirk* GF flies and p=0.9781 (n=32) in 6-day old CR flies with respect to their respective controls **(Figure 19B)**.

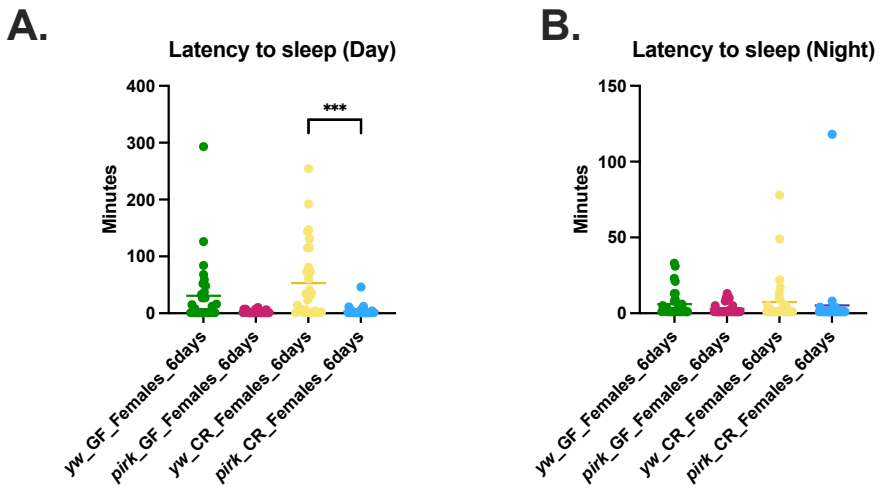

Figure 19: Effects of presence of the microbiome on latency to sleep of 6-day old *pirk* vs *yw* flies in both germ free and conventionally reared conditions Latency is defined as the time taken by flies to fall asleep once lights are off, since the latency to sleep is the same over the course of 24-hours and during daytime sleep. Three independent repeats were conducted for each genotype, and 32 flies were randomly selected from these repeats, resulting in a total sample size (n) of 32, non-significant results were not marked and p≤ 0.05 (*), ≤ 0.01 (**), ≤ 0.001 (***), ≤ 0.0001 (****).

Total Activity count

We examined the total number of times the fly crosses the beam, also known as the total activity count, in 6-day old *pirk* GF and CR flies along with their controls. As expected, we observed a significant reduction in the activity counts of both *pirk* GF (p<0.0001, n=32) **(Figure 20A)** and CR (p<0.0001, n=32) **(Figure 20A)** versus *yw* flies during the course of the day. Like total sleep, this reduction in activity count was due to a drop in activity during daytime (likely due to increase in daytime sleep), with a decrease of 414 (p<0.0001, n=32) in 6-day old GF flies and that of 370.1 (p<0.0001, n=32) in 6-day old CR flies versus their respective controls **(Figure 20B)**. Moreover, no observable change was seen during night-time **(Figure 20C)**.

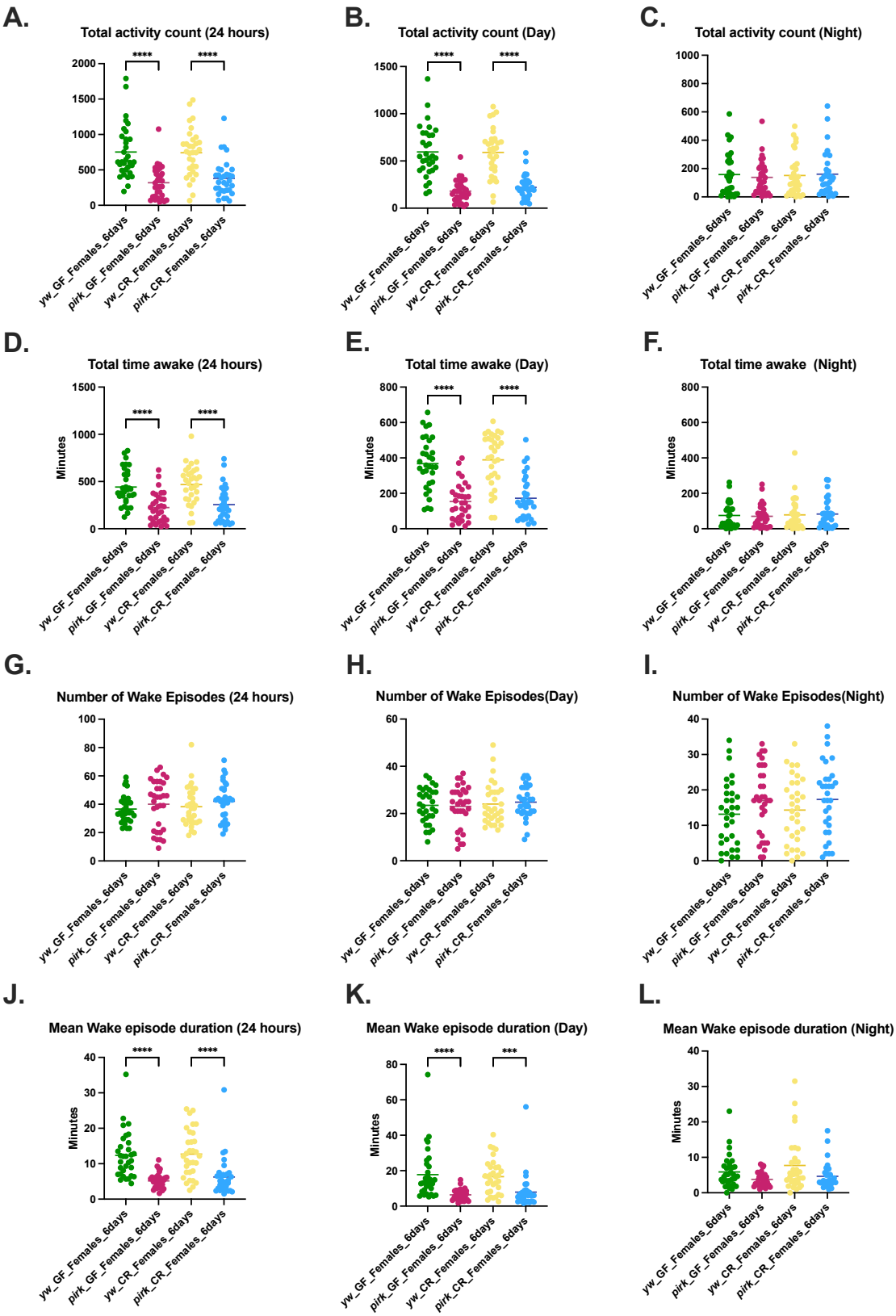

Figure 20: Activity parameters of 6-day old *pirk* vs *yw* flies in both germ free and conventionally reared conditions. Three independent repeats were conducted for each genotype, and 32 flies were randomly selected from these repeats, resulting in a total sample size (n) of 32. Individual groups of flies were compared to each other and were analysed using a two-way ANOVA along with Šídák's correction. Non-significant results were not marked and p≤ 0.05 (*), ≤ 0.01 (**), ≤ 0.001 (***), ≤ 0.0001 (****).

Total Time Awake

Similar to the total activity count, the number of minutes of wakefulness or total time awake was reduced by 218.4 minutes in GF *pirk* flies ($p<0.0001$, n=32) with respect to their controls and a significant drop of 212 minutes in *pirk* CR flies versus *yw* ($p<0.0001$, n=32) **(Figure 20D)**. Like other parameters, this reduction was likely caused due to an increase in daytime sleep. We observed a significant decrease in the total time awake during the daytime in both GF ($p<0.0001$, n=32) and CR ($p<0.0001$, n=32) *pirk* mutant flies versus their controls **(Figure 20E)**. Additionally, no significant fluctuation in the number of minutes of wakefulness was observed in either GF ($p=0.9999$, n=32) or CR ($p>0.9999$, n=32) raised flies at night-time **(Figure 20F)**.

Number of Wake Episode duration

There were no observable differences in the number of wake episodes in either GF ($p=0.8986$, n=32) or CR ($p=0.8374$, n=32) **(Figure 20G)** raised *pirk* flies with respect to their respective controls during the course of the day. Similarly, we saw no significant changes in the number of episodes in 6-day old *pirk* GF and CR flies during the day ($p>0.9999$, n=32 and $p=0.9998$, n=32 respectively) **(Figure 20H)** or night-time ($p=0.4769$, n=32 and $p=0.7399$, n=32 respectively) **(Figure 20I)**.

Mean Wake Episode duration

The mean wake episode duration or the average wake episode duration of young *pirk* flies over the course of the day was significantly affected in both GF and CR flies, with an increase of 7.177 minutes in *pirk* GF flies ($p<0.0001$, n=32) versus GF *yw* **(Figure 20J)** and that of 6.469 minutes in CR flies ($p<0.0001$, n=32) versus their respective controls **(Figure 20J)**. This is also postulated due to the reduction in the mean wake episode duration during daytime, as we

observed a significant reduction of 11.44 and 8.724 minutes in GF ($p<0.0001$, n=32) and CR ($p=0.0003$, n=32) 6-day old *pirk* flies with respect to their *yw* counterparts **(Figure 20K)**. Finally, no significant observations were made during night-time in either GF or CR flies ($p=0.3577$, n=32 and $p=0.0533$, n=32 respectively) **(Figure 20L)**.

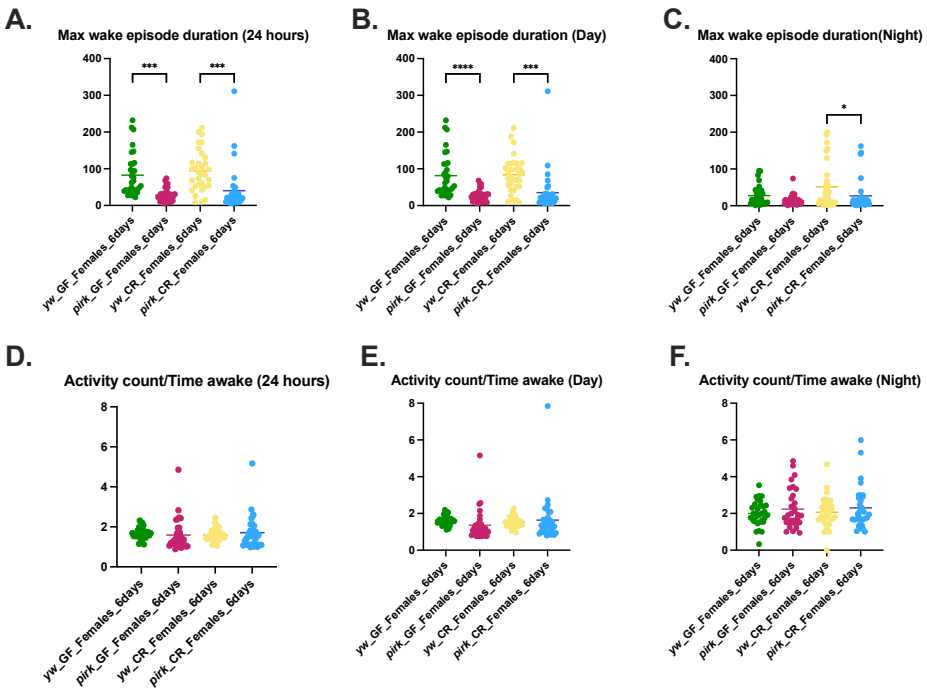

Figure 21: Effects of presence of the microbiome on maximum wake episode duration (A-C) and rate of activity (D-F) of 6-day old *pirk* and *yw* flies in both germ free and conventionally reared conditions. Three independent repeats were conducted for each genotype, and 32 flies were randomly selected from these repeats, resulting in a total sample size (n) of 32. Individual groups of flies were compared to each other and were analysed using a two-way ANOVA along with Šídák's correction. Non-significant results were not marked and $p \leq 0.05$ (*), ≤ 0.01 (**), ≤ 0.001 (***), ≤ 0.0001 (****).

Maximum Wake Episode duration

Interestingly, we detected a notable reduction in the duration of the max wake episode in young *pirk* flies during the course of the day **(Figure 21A)**. A decline of 53.73 minutes ($p=0.0001$, n=32) was observed in GF and of 53.73 minutes ($p=0.0001$, n=32) in CR young *pirk* flies versus *yw*. Additionally, a reduction of 54.7 minutes in GF ($p<0.0001$, n=32) and that of 48.64 minutes in CR ($p=0.0002$, n=32) **(Figure 22B)** was observed during daytime. Finally, a

significant dip of 24.67 minutes in the max wake episode was observed in *pirk* CR versus *yw* CR flies during night-time (p=0.0484, n=32) **(Figure 23C)**.

Activity Count/ Time Awake

Like in *pirk* mutant flies, we looked at the movement of flies per minute of wakefulness (or activity count per time awake) to examine if the sleep effects observed are due to neuro-muscular damage or true sleep phenotypes. We found no significant change in the activity count / time awake in 6-day old *pirk* female flies, despite how they were raised, (GF or CR) in either of the three time points (over 24-hours, daytime and night-time) **(Figure 23(D-F))**.

3.2.2.2 Effects on Older Females

Next, we examined sleep phenotypes of 28-day old female *pirk* and *yw* flies that were either raised in germ free or conventionally reared conditions, to examine the role of the microbiome on age dependent neurodegeneration.

Total Sleep duration

Total minutes of sleep over the course of the day or total sleep duration (24-hours) was not affected by the absence of Pirk protein or the presence of the microbiome in 28-day old flies **(Figure 22A)**. We observed no noticeable changes in overall sleep duration in both GF (p=0.7246, n=32) or CR *pirk* flies (p=0.8576, n=32) compared to their controls **(Figure 22A)**. Even though we did not observe any change in GF flies (p=0.4611, n=32), a significant increase of 114.7 minutes was noted in CR flies with p=0.0096 (n=32) **(Figure 22B)**. However, this effect seems to be somewhat compensated at night where we saw a decrease of 61.78 minutes (p=0.0060, n=32) in mean difference but no noticeable differences in GF flies (p>0.9999, n=32) **(Figure 22C)**. It is noteworthy that while no significant differences were observed in

GF conditions, a trend towards increased sleep duration was evident in GF *pirk* flies compared to the *yw* control group, across both 24-hour and daytime periods.

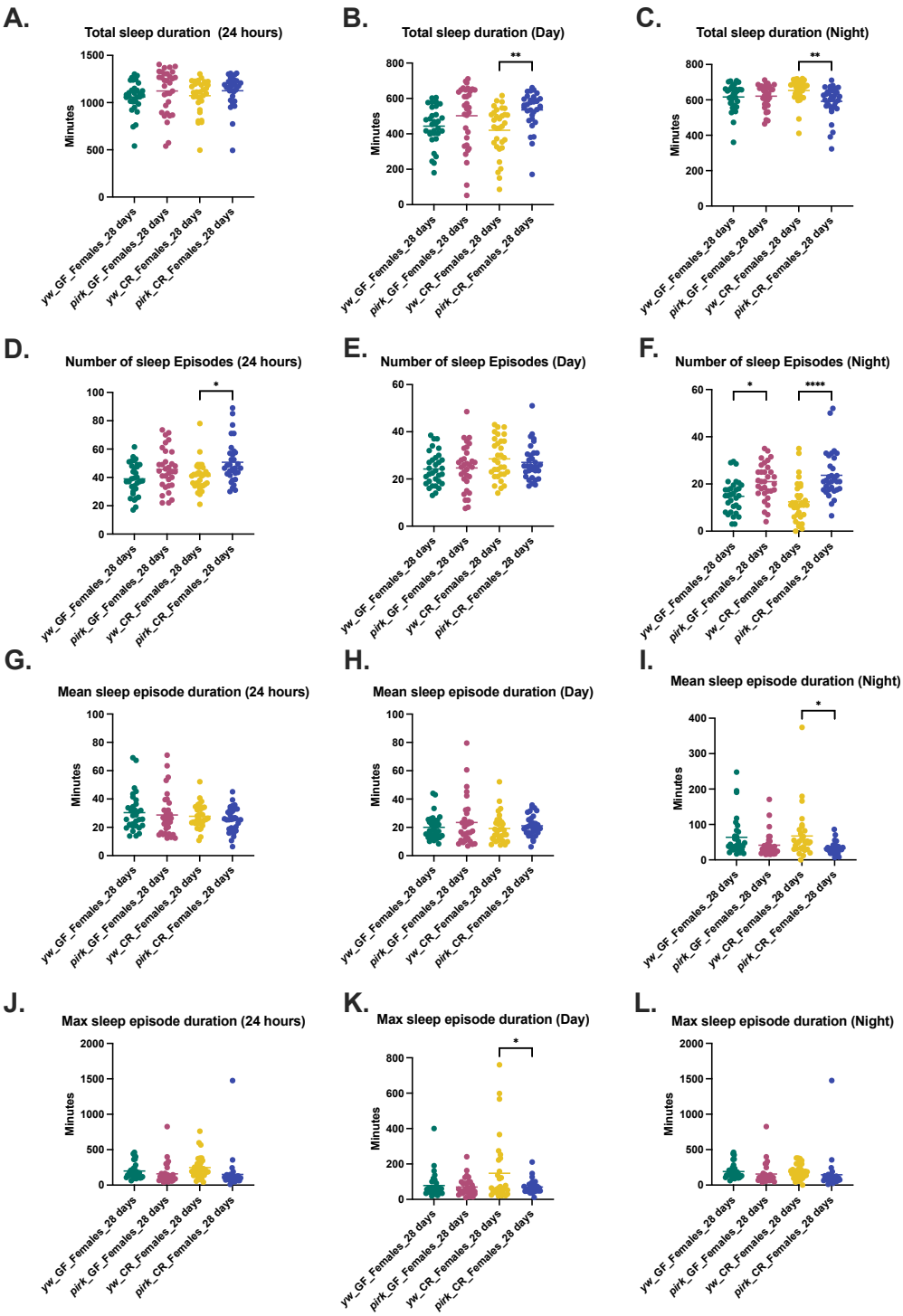

Figure 22: Sleep parameters of 28-day old *pirk* vs *yw* flies in both GF and CR conditions. All the parameters are divided in 24-hours, daytime sleep and night-time sleep. Three independent repeats were conducted for each genotype, and 32 flies were randomly selected from these repeats, resulting in a total sample size (n) of 32. Individual groups of flies were compared to each other and were analysed using a two way ANOVA along with Šídák's correction. Non-significant results were not marked and p≤ 0.05 (*), ≤ 0.01 (**), ≤0.001 (***), ≤ 0.0001 (****).

Number of Sleep episodes

Similarly, we saw no observable change in the number of sleep episodes in GF *pirk* versus *yw* flies (p=0.2519 (n=32) thought-out a 24-hour period **(Figure 22D)**. However, we observed a mean increase of 9.73 episodes in CR flies (p=0.0235, n=32) **(Figure 22D)**. No significant fluctuations were observed once we analysed the number of sleep episodes during lights on / daytime in either GF (p>0.9999, n=32) or CR flies (p=0.9730, n=32) **(Figure 22E)**. Interestingly, a strong correlation**(Figure 22F)** flies in 28-day old *pirk* mutant versus *yw* flies with a mean increase of 6.18 and 11.27 respectively.

Mean Sleep Episode duration

To try and understand sleep quality, we asses mean sleep or average sleep episode duration of the flies. Compared to their respective controls, the *pirk* flies do not have any increase or decrease in the mean sleep episode duration throughout the day in both GF and CR conditions with p=0.9944 (n=32) in GF flies and p=0.9570 in CR **(Figure 22G)**. Additionally, we saw no observable change in the mean sleep episode value during the day of both GF and CR flies (p=0.8005 and p=0.9877, n=32 respectively) **(Figure 22H)**. We observed a slightly significant decline of 34.99 minutes in CR flies (p=0.0257, n=32) during the night but no significant change in GF flies (p=0.3306, n=32) **(Figure 22I)**. Similar to total sleep duration, germ-free (GF) flies also exhibited a trend towards an increased mean sleep episode duration over a 24-hour period and during daytime sleep intervals.

Maximum Sleep Episode duration

No notable change was detected in the duration of the max sleep episode throughout the day in both CR (p=0.1928, n=32) and GF (p=0.9379, n=32) 28-day old *pirk* flies with respect to their controls **(Figure 22J)**. Nevertheless, we did notice a significant reduction of 77.98 minutes in CR 28-day old flies (p=0.0194, n=32) but no observable differences in GF flies (p=0.9997, n=32) during daytime **(Figure 22K)**. Finally, no association between the maximum sleep episode duration and our two parameters (presence or Pirk and absence of the microbiome) was observed in either GF (p=0.9500, n=32) or CR (p=0.9214, n=32) 28-day old flies versus their respective controls during night-time sleep **(Figure 22L)**.

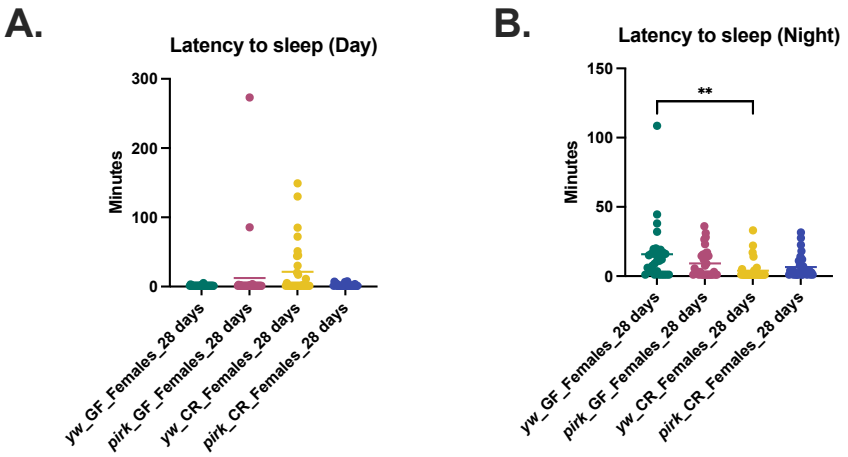

Figure 23: Effects of presence of the microbiome on latency to sleep of 28-day old *pirk* vs *yw* flies in both germ free and conventionally reared conditions. Latency is defined as the time taken by flies to fall asleep once lights are off, since the latency to sleep is the same over the course of 24-hours and during daytime sleep. Three independent repeats were conducted for each genotype, and 32 flies were randomly selected from these repeats, resulting in a total sample size (n) of 32, non-significant results were not marked and $p \leq 0.05$ (*), ≤ 0.01 (**), ≤ 0.001 (***), ≤ 0.0001 (****).

Latency of Sleep

We observed no significant changes in latency to sleep during the day in either GF (p=0.6728, n=32) or CR GF (p=0.1028, n=32) *pirk* female flies compared to their control.

In **Figure 23(A)**, we see that the latency to sleep is not significantly affected by the presence of *pirk* in 28-day old mutant flies raised in both GF (p=0.2232, n=32) and CR (p=0.9603, n=32)

conditions. However, we do see a slight reduction in latency between *yw* GF and *yw* CR (p=0.0018, n=32) indicating a potential effect of the GF treatment on sleep in *yw* flies **(Figure 23B)**.

Total Activity count

Total activity count or the number of times a fly crosses the centre of the tube over a period of 24-hours was observed to be affected by the absence of Pirk protein in 28-day old female flies in both GF and CR conditions, with a significant decrease of 226.5 counts in GF (p=0.0148, n=32) and that of 218 counts in CR *pirk* flies versus their controls (p=0.0210, n=32) **(Figure 24A)**. However, this effect is estimated to be because of a greater decrease in the total activity count during daytime in both GF (p=0.0003, n=32) and CR (p<0.0001, n=32) conditions **(Figure 24B)**. In addition to this, no observable changes were detected in 28-day old *pirk* mutant flies raised in both GF (p=0.8460, n=32) and CR (p=0.9986, n=32) conditions with respect to their controls **(Figure 24C)**.

Total Time Awake

Interestingly, this decrease in activity did not corelate to any change in the total minutes of wakefulness or total time awake in *pirk* mutant flies raised in either GF or CR conditions, with the p value of 0.7246 (n=32) for GF and p value of 0.8576 (n=32) in 28-day old CR *pirk* flies **(Figure 24D)**. Additionally, we did not observe any significant changes in the total time awake during the day of flies GF raised *pirk* flies with p of 0.4611 (n=32), but saw a stark decline of 114 minutes during the day in CR raised flies (p=0.0096, n=32) **(Figure 24E)**. This effect seems to be somewhat compensated during night-time with an increase of 61.78 minutes (p=0.0060, n=32), with no significant change in GF flies (p>0.9999, n=32) **(Figure 24F)**.

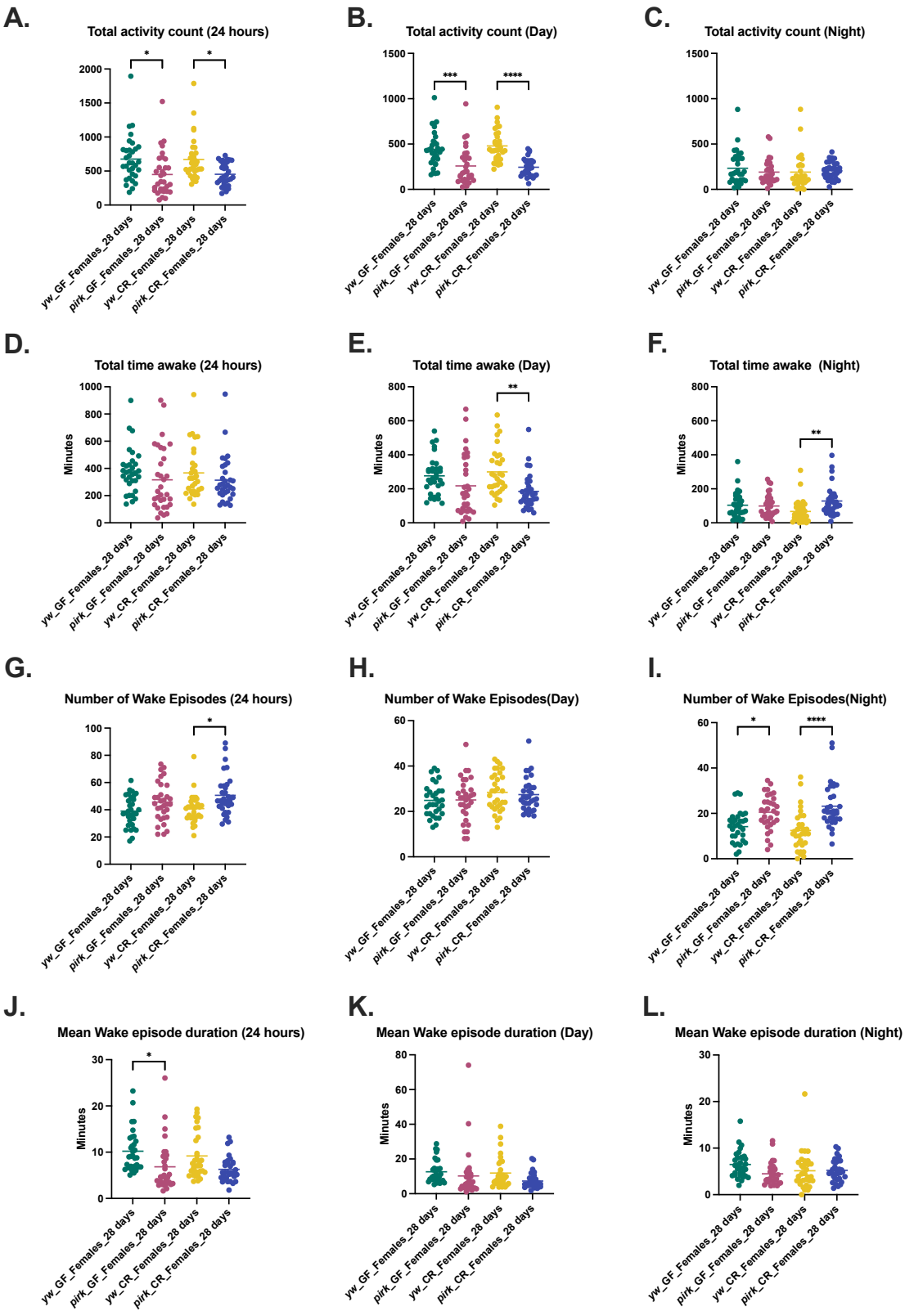

Figure 24: Activity parameters of 28-day old *pirk* vs *yw* flies in both germ free and conventionally reared conditions. All the parameters are divided in 24-hours, daytime sleep and night-time sleep. Three independent repeats were conducted for each genotype, and 32 flies were randomly selected from these repeats, resulting in a total sample size (n) of 32. Individual groups of flies were compared to each other and were analysed using a two-way ANOVA along with Šídák's correction. Non-significant results were not marked and $p \leq 0.05$ (*), ≤ 0.01 (**), ≤ 0.001 (***), ≤ 0.0001 (****).

Number of Wake Episode duration

Like sleep episodes, packets of wakefulness are termed as “wake episodes”. We observed no noticeable change in the total number of wake episodes in GF raised 28-day old *pirk* flies with respect to their controls (p=0.2664, n=32) **(Figure 24G)**. However, we observed an increase of 9.736 episodes (p=0.0234, n=32) in CR 28-day flies **(Figure 24G)**. Additionally, the decrease in activity observed in previous parameters did not translate into any change in the number of wake episodes during daytime in either GF (p>0.9999, n=32) or CR (p=0.9973, n=32) raised 28-day old Female *pirk* flies versus their respective controls **(Figure 24H)**. A rise in the number of wake episodes was seen during night-time in both conditions, with an increase of 6.328 episodes in GF (p=0.0172, n=32) in GF and that of 10.72 episodes in CR raised flies (p<0.0001, n=32) **(Figure 24I)**.

Mean Wake Episode duration

In contrast, we observed a significant decline in the average wake episode duration during a 24-hour period in 28-day old *pirk* flies raised in GF conditions (p=0.0243, n=32) but no change in CR raised flies (p=0.0786, n=32) **(Figure 24J)**. Moreover, we did not observe any noticeable difference in either GF (p=0.8917, n=32) and CR (p=0.2780, n=32) flies during daytime **(Figure 24K)**. Similarly, no effect was seen during night-time with p=0.0519 (n=32) in GF and p>0.9999 (n=32) in CR *pirk* flies with respect to their *yw* controls **(Figure 24L)**.

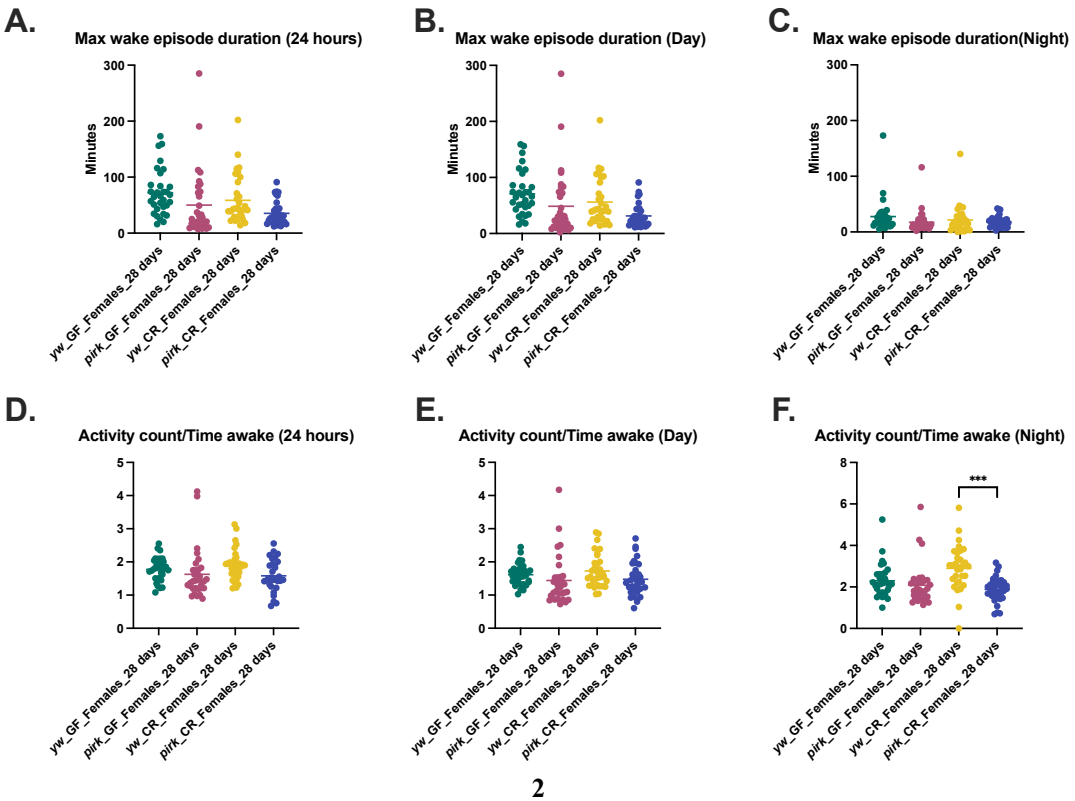

2

Figure 25: Effects of presence of the microbiome on maximum wake episode duration (A-C) and rate of activity (D-F) of 28-day old *pirk* vs *yw* flies in both germ free and conventionally reared conditions. Three independent repeats were conducted for each genotype, and 32 flies were randomly selected from these repeats, resulting in a total sample size (n) of 32. Individual groups of flies were compared to each other and were analysed using a two-way ANOVA along with Šídák's correction. Non-significant results were not marked and $p \leq 0.05$ (*), ≤ 0.01 (**), ≤ 0.001 (***), ≤ 0.0001 (****).

Maximum Wake Episodes duration

No observable changes were noted in the duration of the largest wake episode over the course of the day in either GF (p=0.2782, n=32) and CR (p=0.2228, n=32) **(Figure 25A)** raised 28-day old *pirk* flies. A similar observation was made when breaking up the 24-hours into day and night-time sleep with p=0.2673 and, p=0.4163 respectively (n=32 for both) for GF flies along with p=0.1613 and, p=0.9927 respectively (n=32 for both) for CR *pirk* flies versus their *yw* controls **(Figure 25(B-C))**.

Activity Count/ Time Awake

It is known that a significant reduction in the activity count per minute during wakefulness can be a symptom of neuromuscular damage. Therefore, it is an important parameter to understand whether the sleep effects we observe stem from genuine sleep defects or from neuromuscular damage.

Even though, we saw no significant changes in either *pirk* GF (p=0.8791, n=32) or CR (p=0.1175, n=32) flies over the course of the day **(Figure 25D)** and during daytime (p=0.7832, n=32 for GF and p=0.4281, n=32 for CR flies) **(Figure 25E)**. We saw a significant reduction in the activity count / time awake in CR *pirk* flies during night-time with p=0.0001 (n=32) but no changes in GF *pirk* f*lies* with p=0.9207 (n=32) versus their *yw* controls **(Figure 25F)**.

3.2.2.3 Sleep Profiles of Males

As expected, the sleep profiles of male flies follow a predictable circadian rhythm, exhibiting an activity peak near lights on (ZT0, 09:00) and lights off (ZT12, 21:00) at both 6-days and 28-days of age **(Figure 26(A-B))**. Similar to female flies, both young and old male *yw* and pirk flies display higher activity levels during the lights-on phase or daytime (09:00 to 21:00) than during lights-off or night-time (21:00 to 09:00). We observe an age-dependent increase in daytime sleep in all fly lines, along with a slight increase in daytime sleep in young *yw* versus conventionally *pirk* flies in both GF and CR conditions. However, since sleep profiles serve as only a graphical representation, a statistical examination of other sleep parameters is necessary to draw any conclusions.

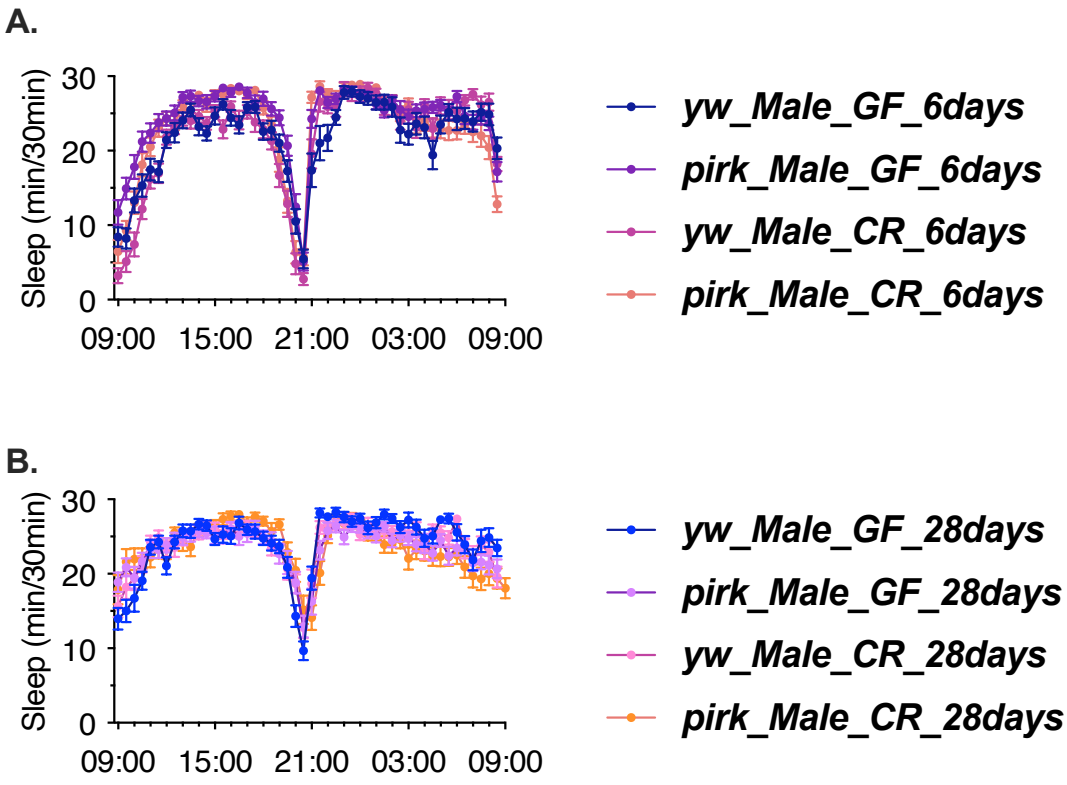

Figure 26: Sleep profiles for male GF vs CR *pirk* mutant flies with respect to their *yw* controls at both 6-days (A) and 28-days (B) of age. Three independent repeats were conducted for each genotype, and 32 flies were randomly selected from these repeats, resulting in a total sample size (n) of 32. Sleep was defined as inactivity for longer than 5 minutes. No statistical analysis was performed.

3.2.2.4 Effects on Young Males

We proceeded to analyse the effects of the presence or absence of the microbiome and Pirk protein in 6-day-old *pirk* male mutant flies in comparison to 6-day-old male *yw* control flies **(Figure 27)**. Like female flies, the *pirk* mutant selected was in the *yw* background, and therefore, *yw* flies were used as genetic control. Three repeats of 32 flies each was independently analysed and random 32 flies were chosen. These flies were then analysed using a two-way ANOVA with Šídák's correction using Graph Pad prism. P value less than 0.05 was considered significant and was marked by and asterisk '*' and the graph was plotted with SEM **(Figure 27)**.

Total Sleep duration

The duration of sleep throughout the day was significantly affected by the absence of Pirk in *pirk* GF versus *yw* GF flies, with a mean increase of 119.6 minutes (p=0.0039, n=32) **(Figure 27A)**. However, no significant fluctuation was observed in CR flies with p=0.3818 (n=32) **(Figure 27A)**. Once the analysis with split into daytime and night-time sleep, we observed a stark increase in daytime sleep in both CR and GF 6-day old male *pirk* flies versus their respective controls; with a mean rise of 81.2 minutes in GF (p<0.0001, n=32) and that of 74.5 minutes in CR flies (p=0.0003, n=32) **(Figure 27B)**. This effect was not detected in both GF (p=0.3793, n=32) and CR (p=0.9873, n=32) flies during night-time **(Figure 27C)**.

Number of Sleep episodes

To further understand the quality of sleep we looked at the number of sleep episodes throughout the day and then during daytime and night-time. We noticed an overall increase in the frequency of sleep episodes in *pirk* CR flies but not in *pirk* GF flies compared to their controls over a 24-hour period **(Figure 27D)** with a significant increase of 7.3 episodes in CR (p=0.0228, n=32) flies **(Figure 27D)**. Nevertheless, a notable decline of 5.6 episodes was seen in GF flies (p=0.0046, n=32) during daytime sleep and no effect was seen in male CR *pirk* 6-day old flies with p=0.9849 (n=32) with respect to their *yw* controls **(Figure 27E)**. An opposite result was observed during night-time with a significant increase in number of sleep episodes in both GF (p=0.0005, n=32) and CR (p=0.0017, n=32) flies **(Figure 27F)**.

Mean Sleep Episode duration

However, the duration of average sleep episodes was not affected by the presence or absence of Pirk protein over the course of the day in either *pirk* GF (p=0.6040, n=32) or CR (p=0.9368, n=32) 6-day old male flies versus GF and CR *yw* flies respectively **(Figure 27G)**. During

daytime, we observed a rise of 16.34 minutes in the mean sleep episode duration of GF flies (p=0.0006, n=32) but no noticeable change in CR flies (p=0.9570, n=32) **(Figure 27H)**. In contrast to this, a drop of 27.07 minutes was observed in GF flies during night-time, but no significant observation was made in CR flies (p=0.1645, n=32) in *pirk* 6-day old male mutant flies during night-time versus their controls **(Figure 27I)**.

Maximum Sleep Episodes duration

The duration of the largest sleep episode was not significantly affected by the presence or absence of Pirk protein. We observed no notable changes in either GF (p=0.9364, n=32) or CR (p=0.7673, n=32) *pirk* flies versus *yw,* during the course of the day (24-hours) **(Figure 27J)**. But observed a significant reduction during daytime sleep in 6-day old GF *pirk* flies (p=0.0435, n=32) and no change in CR flies (p>0.9999, n=32) **(Figure 27K)**. A similar observation was made during night-time where we saw a decline of 84.6 minutes (p=0.0006, n=32) in GF flies and no significant observation in 6-day male *pirk* CR (p=0.1442, n=32) flies with respect to their individual controls **(Figure 27L)**.

Latency of Sleep

During daytime sleep, latency was significantly reduced in *pirk* GF male mutant flies compared to their *yw* controls (p<0.0001, n=32). Additionally, a notable decrease in latency was observed in conventionally reared (CR) male flies (p=0.0082, n=32) **(Figure 28A)**. Intriguingly, there was an increase in latency to sleep in *pirk* GF versus *pirk* CR flies (p=0.0120, n=32), suggesting a potential side effect of the germ-free fly generation protocol. Notably, latency to sleep at night was significantly affected by the presence of Pirk in GF flies, showing an observable decline of 18.50 minutes during night-time (p=0.0011, n=32), while this effect was not observed in CR conditions (p=0.3465, n=32) **(Figure 28B)**.

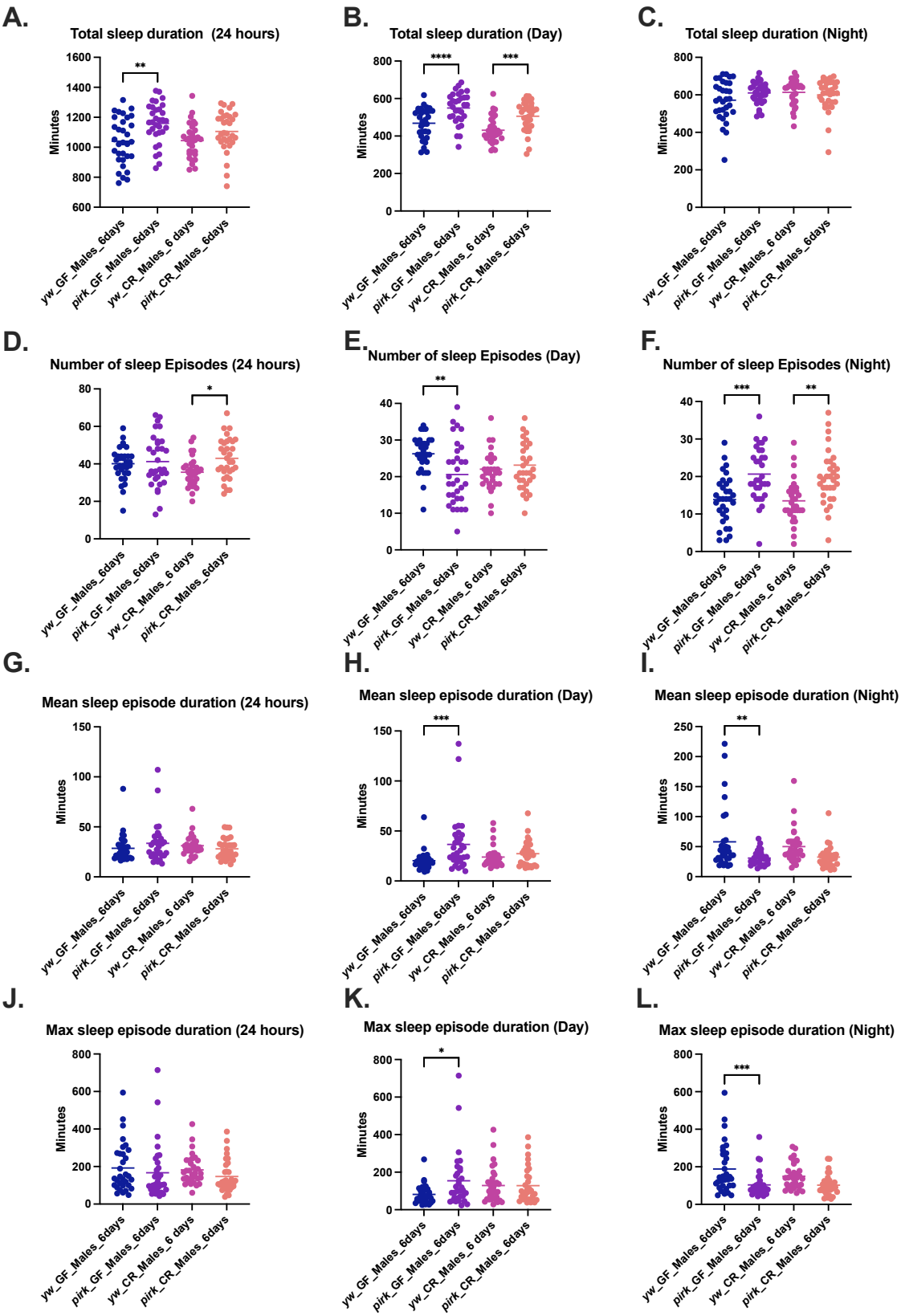

Figure 27: Sleep parameters of 6-day old male *pirk* vs *yw* flies in both germ free and conventionally reared conditions. Three independent repeats were conducted for each genotype, and 32 flies were randomly selected from these repeats, resulting in a total sample size (n) of 32. Individual groups of flies were compared to each other and were analysed using a two-way ANOVA along with Šídák's correction. Non-significant results were not marked and p≤ 0.05 (*), ≤ 0.01 (**), ≤ 0.001 (***), ≤ 0.0001 (****).

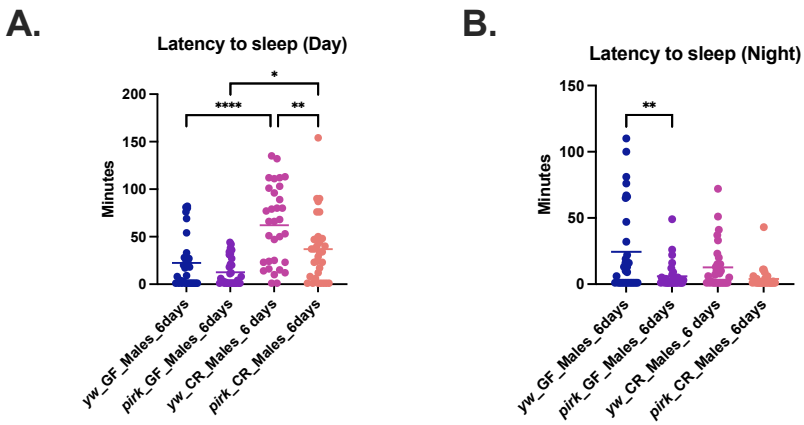

Figure 28:Effects of presence of the microbiome on latency to sleep of 6-day old male *pirk* and *yw* flies in both germ free and conventionally reared conditions. Three independent repeats were conducted for each genotype, and 32 flies were randomly selected from these repeats, resulting in a total sample size (n) of 32, non-significant results were not marked and p≤ 0.05 (*), ≤ 0.01 (**), ≤ 0.001 (***), ≤ 0.0001 (****).

Total Activity count

Total activity count or the number of times the fly crosses the middle of the tube was not affected in 6-day old male *pirk* flies over the course of the day in either GF or CR conditions (p=0.1152, n=32 and p=0.6897, n=32 respectively) **(Figure 29A)**. However, there was a strong dip in activity during daytime in both GF and CR flies, with a mean decline of 141.8 times in GF flies (p=0.0020, n=32) and that of 126.8 times in CR flies (p=0.0074, n=32) **(Figure 29B)**. However, no significant observation was noted during night-time **(Figure 29C)**.

Total Time Awake

The total minutes of wakefulness over the course of the day was affected by the presence of Pirk protein in GF conditions, where a decline of 119.6 minutes (p=0.0039, n=32) was observed but not in CR flies (p=0.3818, n=32) **(Figure 29D)**. However, total time awake was significantly affected during daytime in both CR and GF flies (p=0.0003 and p<0.0001 (n=32) respectively) **(Figure 29E)**. No notable differences were observed during night-time with p=0.3793 (n=32) for GF and p=0.9873 (n=32) for CR *pirk* 6-day old male flies with respect to their genetic controls **(Figure 29F)**.

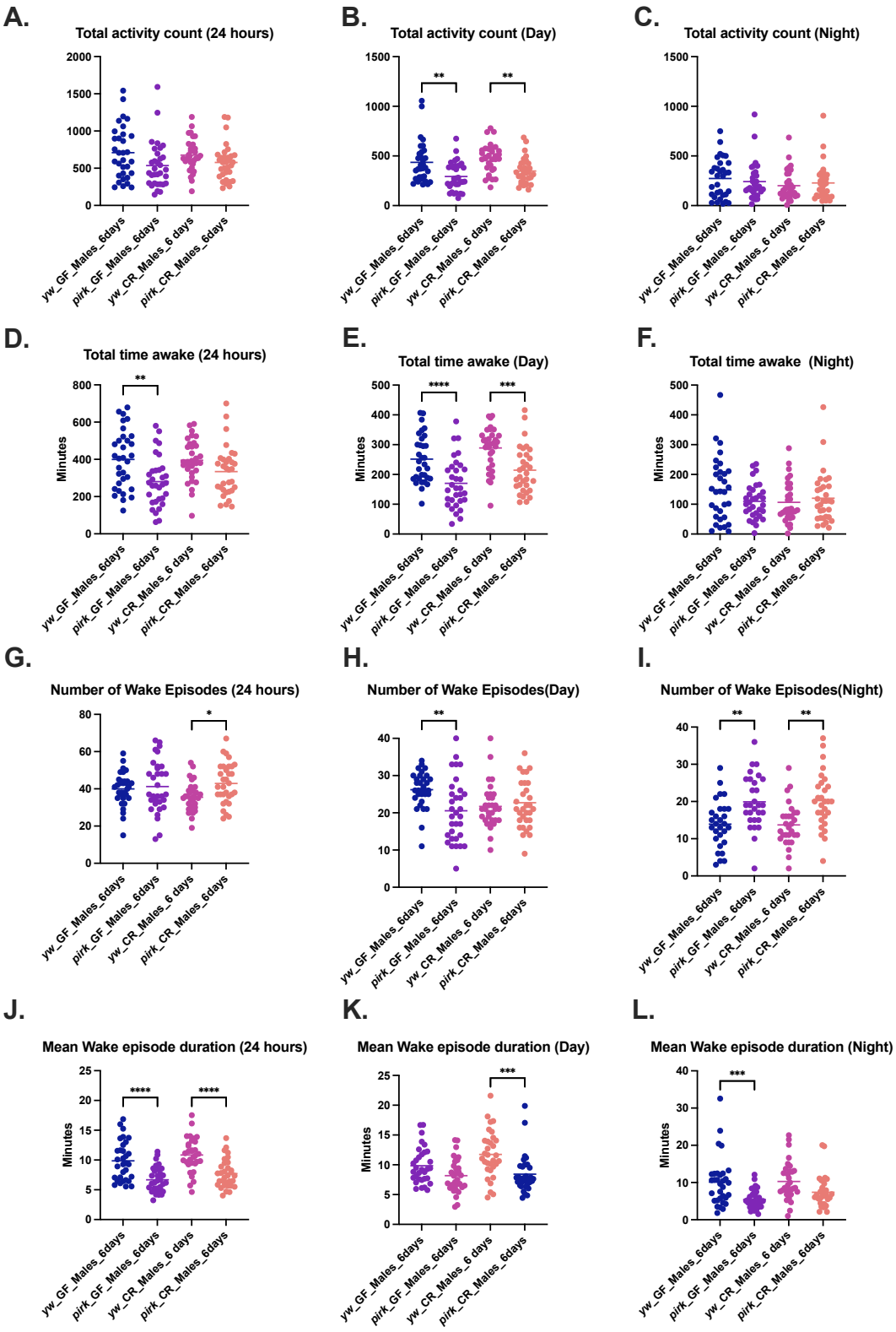

Figure 29: Activity parameters of 6-day old male *pirk* vs *yw* flies in both germ free and conventionally reared conditions. All the parameters are divided in 24-hours, daytime sleep and night-time sleep. Three independent repeats were conducted for each genotype, and 32 flies were randomly selected from these repeats, resulting in a total sample size (n) of 32. Individual groups of flies were compared to each other and were analysed using a two-way ANOVA along with Šídák's correction. Non-significant results were not marked and $p \leq 0.05$ (*), ≤ 0.01 (**), ≤ 0.001 (***), ≤ 0.0001 (****).

Number of Wake Episode duration

Interestingly, we did not observe a significant correlation*pirk* 6-day old male flies. However, a slight increase of 7.438 episodes (p=0.0230, n=32) was observed in CR flies **(Figure 29G)**. Contrary to this, a mean decrease of 5.656 episodes was observed during daytime in GF flies (p=0.0042, n=32) but no significant observation was made in CR flies (p=0.9902, n=32) **(Figure 29H)**. At night-time, a significant rise of 6 episodes in GF flies (p=0.0058, n=32) and that of 6.517 in CR (p=0.0022, n=32) young *pirk* male flies versus *yw* was observed **(Figure 29I)**.

Mean Wake Episode duration

in both GF and CR flies throughout the course of the dayWe saw a notable change in the average wake episode duration , a reduction of 3.180 minutes in *pirk* GF flies (p<0.0001, n=32) and that of 3.143 minutes in *pirk* CR flies (p<0.0001, n=32) in 6-day old *pirk* male flies versus their respective controls **(Figure 29J)**. During daytime, we saw a significant reduction of 3.311 minutes in CR flies (p=0.0006, n=32) but no observable fluctuation in GF flies (p=0.2351, n=32) **(Figure 29K)**. In contrast, we observed a significant drop in GF flies (p=0.0008, n=32) but no significant observation in CR flies (p=0.0906, n=32) **(Figure 29L)**.

Maximum Wake Episodes duration

In a 24-hour period, we observed a significant decline in the duration of the maximum wake episode in GF young male *pirk* flies with a decline of 27.72 minutes (p=0.0149, n=32) but no change in the *pirk* CR flies (p=0.2070, n=32) versus their *yw* controls **(Figure 30A)**. Additionally, a significant increase was observed between *pirk* GF and *pirk* CR flies (p=0.0397, n=32), over the course of a 24-hour period, indicating the potential effects of the antibiotics on sleep behaviour. A similar observation was seen during the daytime with a stark reduction of

25.97 minutes in GF flies (p=0.0110, n=32) and no notable changes in the CR flies (p=0.1824, n=32) **(Figure 30B)**. However, no changes were noted during night-time in either GF (p=0.6506, n=32) or CR (p=0.9900, n=32) 6-day old male *pirk* flies versus their controls **(Figure 30C)** but a p value of 0.0323 (n=32) was noted when comparing *pirk* GF versus *pirk* CR flies during night-time.

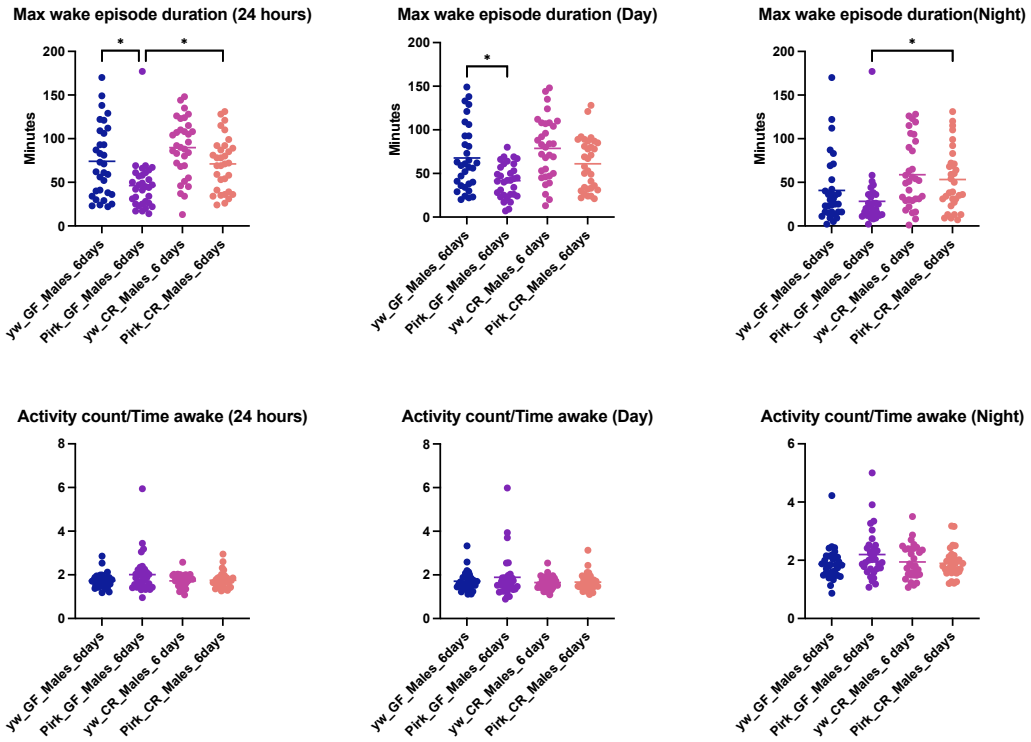

Figure 30: Effects of presence of the microbiome on maximum wake episode duration (A-C) and rate of activity **(D-F)** of 6-day old male pirk vs *yw* flies in both GF and CR conditions. Three independent repeats were conducted for each genotype, and 32 flies were randomly selected from these repeats, resulting in a total sample size (n) of 32. Individual groups of flies were compared to each other and were analysed using a two-way ANOVA along with Šídák's correction. Non-significant results were not marked and p≤ 0.05 (*), ≤ 0.01 (**), ≤ 0.001 (***), ≤ 0.0001 (****).

Activity Count/ Time Awake

We did not observe any notable difference in the activity count per time awake in either GF (p=0.2232, n=32) and CR (p>0.9999, n=32) flies over the course of the day **(Figure 30D)**. A similar effect was observed during both day and night-time, with no significant effect observed in either GF (p=0.8039, n=32, p=0.1888, n=32 respectively) or CR flies (p>0.9999, n=32, p=0.9997, n=32 respectively) **(Figure 30(E-F))**.

3.2.2.5 Effects on Older Males

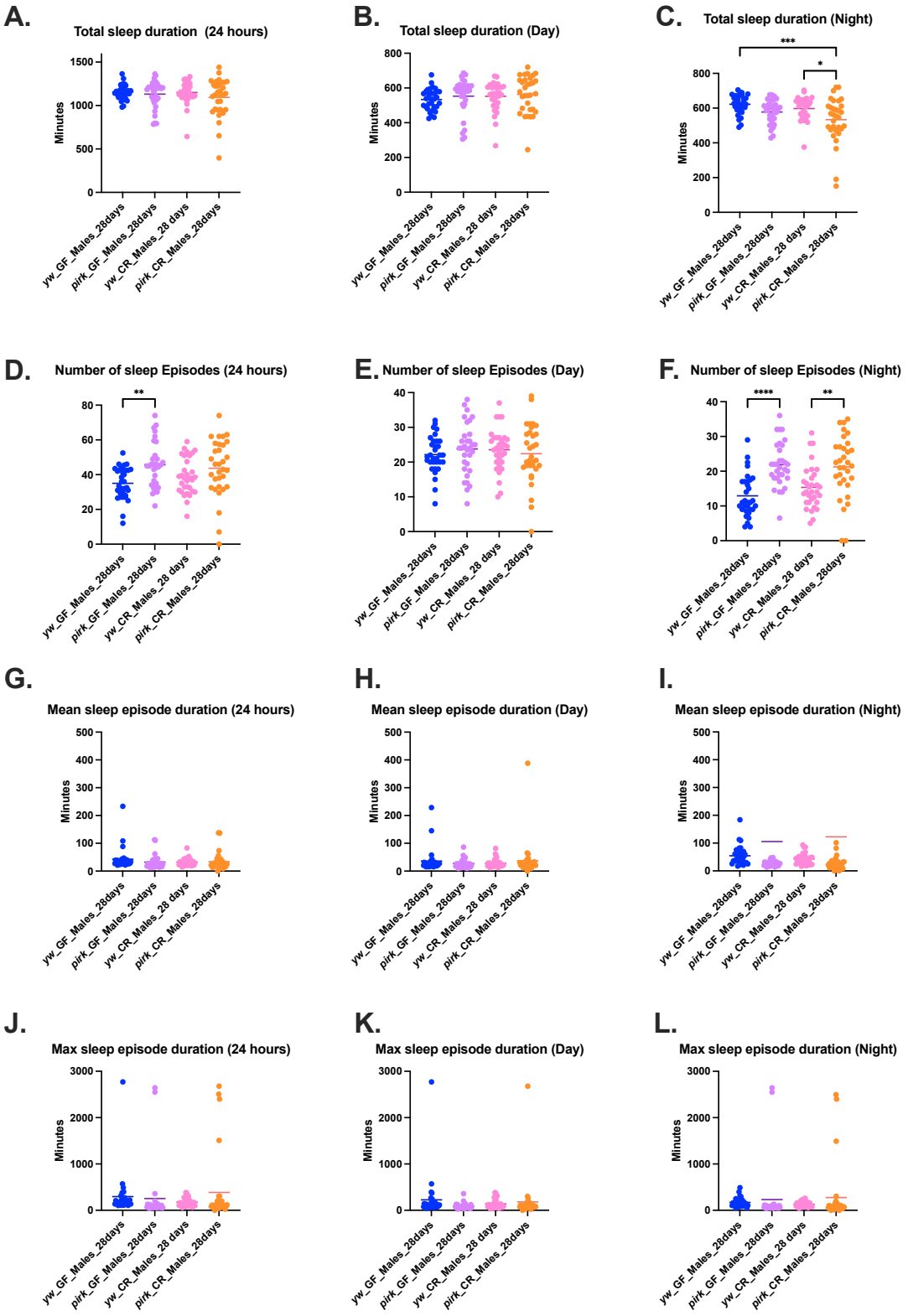

Figure 31: Sleep parameters of 28-day old male *pirk* vs *yw* flies in both germ free and conventionally reared conditions. Three independent repeats were conducted for each genotype, and 32 flies were randomly selected from these repeats, resulting in a total sample size (n) of 32. Individual groups of flies were compared to each other and were analysed using a two-way ANOVA along with Šídák's correction. Non-significant results were not marked and $p \leq 0.05$ (*), ≤ 0.01 (**), ≤ 0.001 (***), ≤ 0.0001 (****).

Total Sleep duration

In 28-day old *pirk* mutant male flies, the total minutes of sleep was not affected by the absence of *pirk* protein in both GF and CR raised *pirk* flies compared to their controls, with p=0.9869 (n=32) in GF and p=0.6287 (n=32) in CR flies over a 24-hour period **(Figure 31A)**. Similarly, no significant effects were observed during daytime sleep in either GF (p=0.9440, n=32) or CR (p=0.9970, n=32) old male *pirk* flies versus *yw* controls **(Figure 31B)**. However, a notable effect was observed in *pirk* CR flies during night-time, with a dip of 64.19 minutes (p=0.0196, n=32) but no effect in GF *pirk* flies (p=0.2043, n=32) versus their respective controls **(Figure 31C)**.

Number of Sleep episodes

A stark increase in the total number of sleep episodes throughout the day was observed, with an increase of 10.61 episodes in *pirk* GF flies (p=0.0045, n=32) but not in *pirk* CR raised flies where p=0.5372 (n=32) *(pirk* versus *yw*) **(Figure 31D)**. However, no significant fluctuations were observed during either *pirk* GF (p=0.9155, n=32) or CR (p=0.9852, n=32) flies versus *yw* during daytime sleep **(Figure 31E)**. However, an increase of 8.969 episodes was noted in GF flies (p<0.0001, n=32) and that of 5.906 episodes in CR flies (p=0.0048, n=32) in older male *pirk* flies with respect to their respective controls **(Figure 31F)**.

Mean Sleep Episode duration

The average sleep episode duration was not affected by the presence of the *pirk* protein throughout the day in both GF (p=0.6283, n=32) and CR (p>0.9999, n=32) conditions **(Figure 31G)**. Additionally, no effects were also observed during daytime in either of the conditions, with p=0.9327 (n=32) in *pirk* GF flies and p=0.9113 (n=32) in CR conditions versus their respective genetic controls **(Figure 31H)**. During night-time, we observed no notable changed

in either GF (p=0.9546, n=32) or CR (p=0.7262, n=32) conditions in older *pirk* male mutant flies with respect to their controls **(Figure 31I)**.

Maximum Sleep Episodes duration

Similar to that of the mean sleep episode duration, we observed no significant changes in the duration of the largest sleep episode in 28-day old male mutant flies versus their respective control in both *pirk* GF and CR conditions. During daytime sleep, no noticeable change was observed in both *pirk* GF (p=0.9997, n=32) and CR (p=0.4867, n=32) flies **(Figure 31J)**. Moreover, the same result was observed during night-time with p=0.4601 (n=32) in GF during daytime and p=0.9920 (n=32) at night-time, along with p=0.9951 (n=32) in CR during daytime and p=0.6520 (n=32) at night-time **(Figure 31(K-L))**.

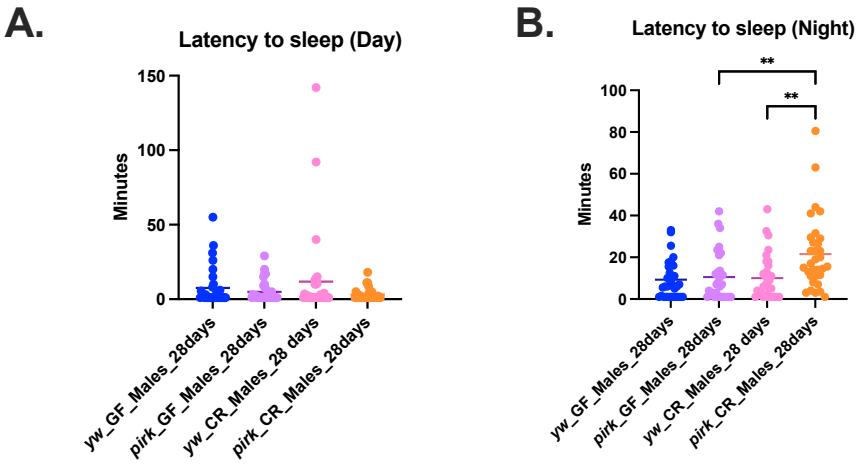

Figure 32: Effects of presence of the microbiome on latency to sleep of 28-day old male *pirk* vs *yw* flies in both germ free and conventionally reared conditions. Latency is defined as the time taken by flies to fall asleep once lights are off, since the latency to sleep is the same over the course of 24-hours and during daytime sleep. Three independent repeats were conducted for each genotype, and 32 flies were randomly selected from these repeats, resulting in a total sample size (n) of 32, non-significant results were not marked and p≤ 0.05 (*), ≤ 0.01 (**), ≤ 0.001 (***), ≤ 0.0001 (****).

Latency of Sleep

No notable changes were observed in the latency of sleep in 28-day-old *pirk* mutant flies compared to *yw* controls in both germ-free (GF) and conventionally reared (CR) conditions

(p=0.9899, n=32, and p=0.2115, n=32, respectively) **(Figure 32A)**. Likewise, no significant differences were found in the latency to sleep during night-time in CR flies (p=0.9991, n=32), but a significant increase of 11.47 minutes was identified in GF-raised (p=0.0031, n=32) 28-day-old *pirk* mutant flies compared to *yw* controls **(Figure 32B)**. Finally, a significant change in latency was observed between *pirk* GF and *pirk* CR flies (p=0.0014, n=32) **(Figure 32B)**.

Total Activity count

Total activity count was not affected by the absence of Pirk protein over the course of the day in both GF (p>0.9999, n=32) and CR (p=0.9062, n=32) 28-day old mutant *pirk* flies versus their controls **(Figure 33D)**. A significant drop-in activity was observed during daytime with p=0.0270 (n=32) for GF but no notable observation was made in CR flies (p=0.1128, n=32) **(Figure 33E)**. Similarly, during night-time we observed a rise of 108.8 in activity for old *pirk* male flies in GF condition (p=0.0050, n=32) but no significant changes in CR flies (p=0.8948, n=32) **(Figure 33F)**.

Total Time Awake

No significant observations were made in the total time awake throughout the day in either GF (p=0.9969, n=32) or CR (p=0.6955, n=32) raised old *pirk* male flies versus their genetic controls **(Figure 33A)**. A similar effect was observed during daytime where p=0.9363 (n=32) for GF and p=0.9994 (n=32) for CR male mutant flies **(Figure 33B)**. However, a stark increase of 64.19 minutes was noted during night-time in mutant flies raised in CR conditions (p=0.0205, n=32) with respect to their controls but no changes were seen in GF flies with p=0.2228 (n=32) **(Figure 33C)**.

Number of Wake Episode duration

A significant rise in the total number of wake episodes was observed in GF flies (p=0.0049, n=32) during the course of the day but no notable difference was observed in CR flies (p=0.5652, n=32) **(Figure 33G)**. Interestingly, this effect was not observed during the day where no significant observation was made in either GF or CR flies with p=0.9187 (n=32) and p=0.9910 (n=32) respectively in 28-day old *pirk* male flies, with respect to their controls **(Figure 33H)**. However, during night-time a significant increase of 8.92 episodes was observed in GF flies (p<0.0001, n=32) and that of 5.71 episodes was seen in CR (p=0.0075, n=32) old *pirk* mutant flies versus their controls **(Figure 33I)**.

Mean Wake Episode duration

The average duration of wake episodes or mean wake episode duration over the course of the day was unaffected by the absence of Pirk protein in both GF (p=0.2119, n=32) and CR (p>0.9999, n=32) 28-day old *pirk* male flies compared to their *yw* controls **(Figure 33J)**. A similar effect was observed in both day and night-time sleep, with p=0.3739 (n=32) in GF flies during the day and p=0.7019 (n=32) during night and p> 0.9999 (n=32) in CR flies during the day and p=0.9334 (n=32) during night-time **(Figure 33(K-L))**.

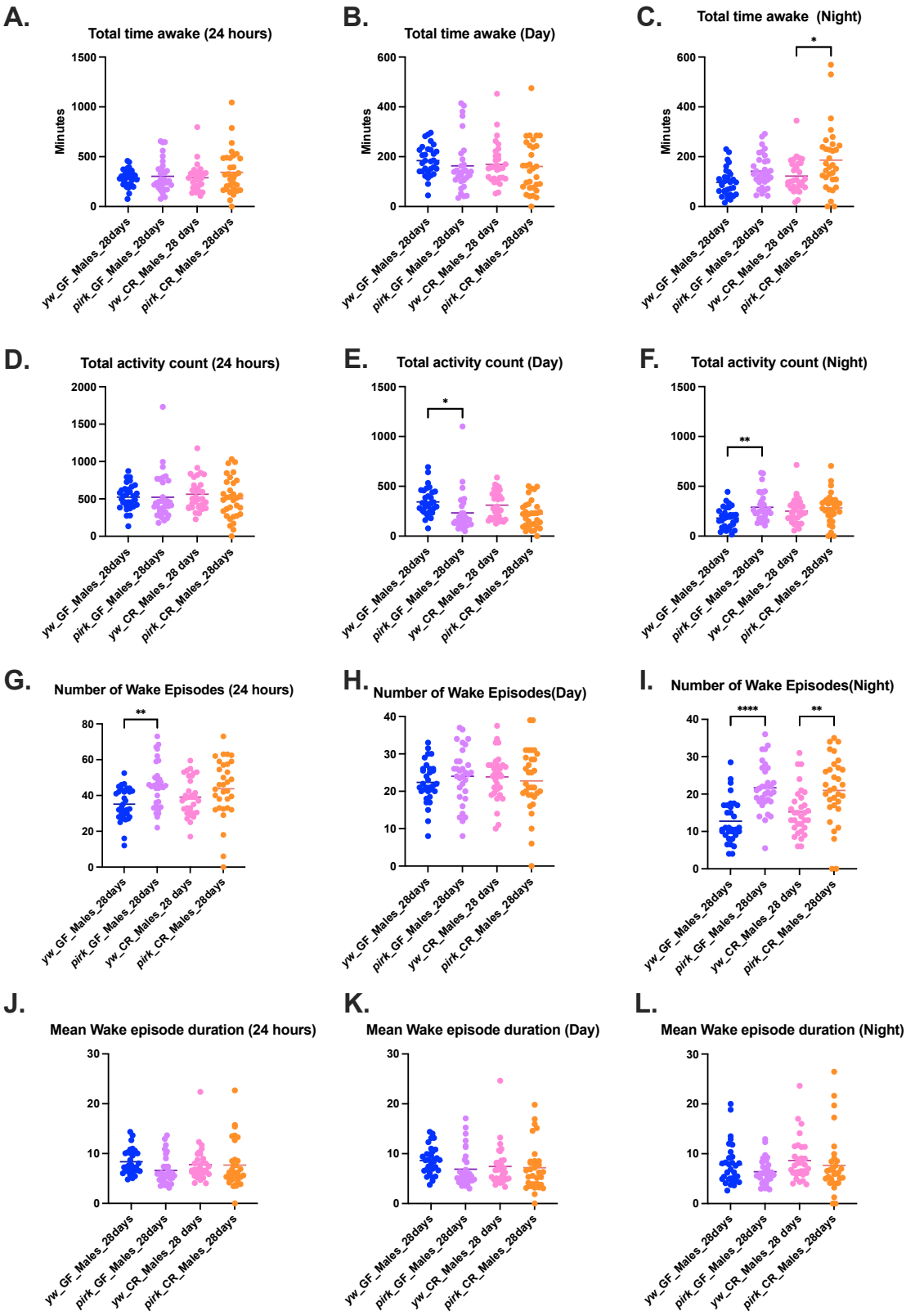

Figure 33:Activity parameters of 28-day old male *pirk* vs *yw* flies in both germ free and conventionally reared conditions. All the parameters are divided in 24-hours, daytime sleep and night-time sleep. Three independent repeats were conducted for each genotype, and 32 flies were randomly selected from these repeats, resulting in a total sample size (n) of 32. Individual groups of flies were compared to each other and were analysed using a two-way ANOVA along with Šídák's correction. Non-significant results were not marked and $p \leq 0.05$ (*), ≤ 0.01 (**), ≤ 0.001 (***), ≤ 0.0001 (****).

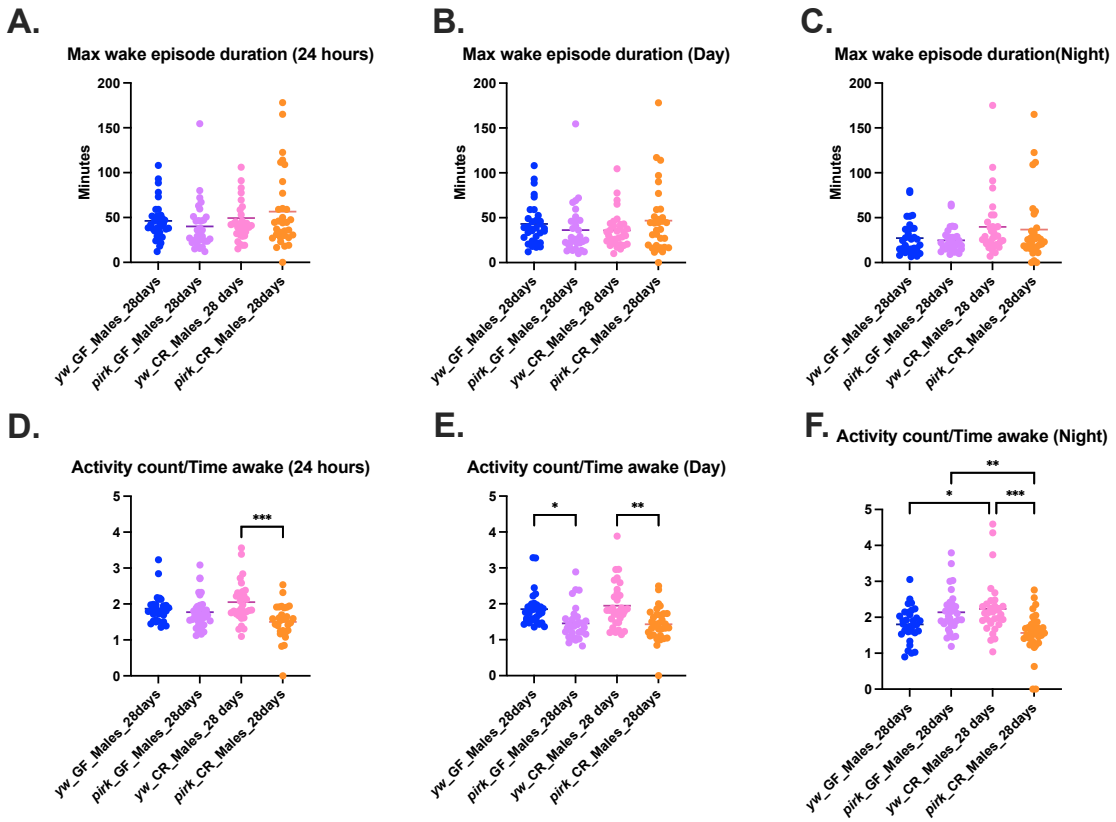

Figure 34: Effects of presence of the microbiome on maximum wake episode duration (A-C) and rate of activity (D-F) of 28-day male old *pirk* vs *yw* flies in both germ free and conventionally reared conditions. All the parameters are divided in 24-hours, daytime sleep and night-time sleep. Three independent repeats were conducted for each genotype, and 32 flies were randomly selected from these repeats, resulting in a total sample size (n) of 32. Individual groups of flies were compared to each other and were analysed using a two-way ANOVA along with Šídák's correction. Non-significant results were not marked and p≤ 0.05 (*), ≤ 0.01 (**), ≤ 0.001 (***), ≤ 0.0001 (****).

Maximum Wake Episode duration

Similar to that of mean wake episode duration, we observed no significant changes in the duration of the maximum wake episode in older *pirk* male flies in both CR and GF conditions compared to their respective controls, with p=0.9764 (n=32) in GF flies and p=0.9461 (n=32) in CR flies during a 24-hour period **(Figure 34A)**. Moreover, no notable change in either day or night-time wakefulness was observed in either GF (p=0.9241, n=32 and p=0.9996, n=32 respectively) or CR (p=0.5945, n=32 during daytime and p=0.9989 n=32 during night-time) *pirk* mutant flies versus *yw* **(Figure 34(B-C))**.

Activity Count/ Time Awake

Interestingly, we found a significant decline in the rate at which the fly crosses the beam or in 28-day old *pirk* mutant flies versus their controls raised in CR conditions over the course of the day (p=0.0001, n=32), but no observable difference in GF flies (p=0.9711, n=32) **(Figure 34D)**. During daytime, a dip was observed in both GF (p=0.0222, n=32) and CR (p=0.0011, n=32) conditions **(Figure 34E)**. However, at night-time this effect was only seen in CR flies with a mean difference of 0.6703 and p=0.0002 (n=32) and not in GF (p=0.1693, n=32) old male mutant flies) **(Figure 34F)**. Additionally, significant changes were observed between both *pirk* and *yw* flies raised in GF and CR conditions, indicating potential effects of the process of generating germ free flies in the activity count per time awake of older male flies.

3.2.3 Summary of Results

In our investigation, we initially examined the sleep and activity patterns of 6-day-old GF and CR female mutant flies alongside their controls. We noted that both GF and CR *pirk* mutant flies exhibited an augmented total sleep duration in comparison to their *yw* controls, along with a rise in mean sleep episode duration specifically in GF *yw* versus *pirk* flies.

Our findings regarding 6-day-old female flies revealed an increase in total sleep across both GF and CR conditions, which likely stemmed from disturbances in wake episodes, evidenced by reductions in both mean and maximum wake durations. Conversely, for 28-day-old female flies, we didn't discern any significant changes in sleep patterns. However, we did observe a slight increase in daytime sleep among CR flies, which could be linked to longer durations of the largest sleep episode. Additionally, a noteworthy decrease in total activity count, both over a 24-hour period and during daytime, was observed.

Similarly, in 6-day-old male flies, the outcomes were not as pronounced as in the previous chapter, although a rise in daytime sleep was evident in both GF and CR flies, possibly due to changes in wake episodes. However, in 28-day-old male flies, contrary to expectations, we did not detect any significant changes in sleep profiles in either GF or CR flies, save for an increase in the number of wake episodes at night. Our overarching finding suggests that the stark changes observed previously may potentially be attributed to differences in control strains (w^{1118} versus *yw*).

Finally, while raising GF *pirk* flies, we observed only a marginal influence on sleep patterns analogous to those of CR *pirk* flies. Unfortunately, the anticipated rescue was not observed. Nevertheless, it's intriguing to note that the evidence falls short of substantiating a significant effect on the sleep patterns of *pirk* CR and GF. The constitutive activation of immunity likely supersedes the influence of microbiota. Despite our efforts to measure the impact of microbiota on sleep behaviours, the findings were notably limited.

CHAPTER FOUR

Exploring the tissue specific effects of **Pirk** *in Drosophila melanogaster*

CHAPTER FOUR:

EXPLORING THE TISSUE SPECIFIC EFFECTS OF PIRK IN DROSOPHILA

Section 4.1: The introductory section starts with a brief introduction into the techniques used in the chapter (UAS/GAL4 and RNAi) to achieve tissue specific knockdowns of Pirk protein in the digestive and nervous systems of *Drosophila* and ends with a list of fly lines along with controls used in this chapter.

Section 4.2: The results section is divided into three parts: first by tissue, then by the various GAL4 and RNAi lines used, and finally by age. This section covers several behavioural analyses including lifespan, climbing assays, sleep and activity assays. It aims to understand the tissue specific effects of Pirk protein to further understand the role of a deregulated immune response on sleep and phenotypes.

Finally, **section 4.3** provides a brief summary of the results.

4.1 BACKGROUND

4.1.1 UAS Gal4 System

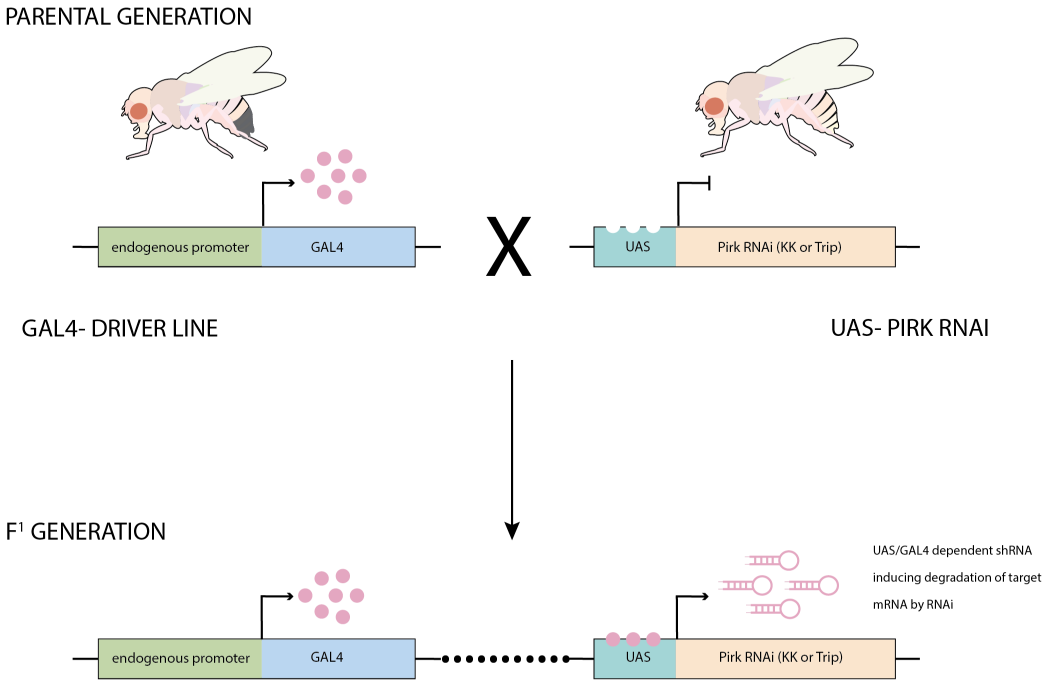

Figure 35: UAS-GAL4 system is used for tissue specific expression of the gene of interest.
The gene of interest present downstream of UAS is only activated in the presence of the GAL4 protein. Adapted from: Yamamoto-Hino and Goto (2013)

As mentioned in previous chapters, *Drosophila* melanogaster has a rich arsenal of genetic tools available, making it an indispensable model organism for functional genomic studies. However, what makes *Drosophila* the most genetically tractable metazoan is the development of the UAS/GAL4 system (Duffy 2002) that is critical for tissue and cell specific expression of genes (Brand and Perrimon 1993). This technique requires the use of two types of transgenes (generally present in two different flies): a driver gene (GAL4 protein) and a GAL4 responsive UAS vector gene **(Figure 35)**. These flies are then crossed together to get progeny with selective activation of any desired genes. The UAS or Upstream Activating Sequences are analogous to enhancers that contain various binding sites for the GAL4 protein, and are

designed to only drive expression of the inserted sequences in the presence of it (rFischer et al. 1988; Brand and Perrimon 1993).

Furthermore, a tissue specific GAL4 driver that is usually present downstream of a gene promoter is used to regulate the expression of the desired genes to specific tissues (Phelps and Brand 1998; Osterwalder *et al.* 2001). For example, in this study we achieved conditional expression of Pirk protein in the pan neuronal system (among others) using the *elav* promoter. The GAL4 system can be used to either knock down or increase gene expression. Transgene containing an extra gene copy can be used to increase the expression of a desired gene, and transgenes containing RNAi can be used to knock down/ reduce gene expression in the whole fly or in tissue specific manner (Duffy 2002).

4.1.2 RNAi fly lines

RNAi or RNA interference is an endogenous cellular mechanism first discovered in *Caenorhabditis elegans* that is responsible for the guided degradation of mRNA transcripts from a double stranded RNA (dsRNA) trigger (Ameres and Zamore 2013). Fire et al. (1998) silenced genes in C elegans by injecting long dsRNA or feeding the worm bacteria expressing dsRNA, illustrating its potential application in characterising gene function. In *Drosophila* studies, the exogenous dsRNA trigger forms a complex that consists of Dicer-2 and R2D2, that slices the dsRNA into 19-bp single- stranded RNA (Tomari and Zamore 2005). This complex is further incorporated into the RISC (RNA-induced silencer complex) containing Ago2, along with several accessory proteins including hsp90. The RISC identifies siRNA complementary mRNA and is responsible for its cleavage and degradation (Carthew and Sontheimer 2009).

While this technique is essential in examining functions of several genes, studies have shown intrinsic limitations of transgenic RNAi lines including “leaks” or significant levels of expression in tissue along with several off-target effects (McClure et al. 2022). Irrespective of this, with the current RNAi data base libraries containing over 50,000 fly lines, RNAi transgenic flies have been of utmost importance in evaluating gene function along with understanding gene activities and regulation of developmental and physiological processes.

With collaborative efforts amongst researchers in the industry, we have seen a steady increase of transgenic RNAi fly strains, especially in the recent past (Birmingham *et al.* 2009). Various stock centres contain vast collection of RNAi- fly lines regulated by UAS that allow tissue specific knockdown experiments (Brand and Perrimon 1993). These include the VDRC collection (the Transgenic RNAi Project (TRiP)), the Bloomington *Drosophila* Stock Center (BDSC), and the National Institute of Genetics (NIG) (Dietzl *et al.* 2007). FlyBase has a credible list of relevant literature and proves to be a strong asset for *Drosophila* experiments (Hu et al. 2013; St. Pierre et al. 2014).

The VDRC collection is responsible for distributing flies from the GD library generated in early 2007 (Dietzl *et al.* 2007); as of January 2017 the stock centre contained 16,763 GD (P-Element) RNAi library lines, 9,822 (phiC31) KK RNAi lines and 372 small hairpin RNA (shRNA) fly lines that together cover over 12,671 genes representing almost 91% of known *Drosophila* protein coding regions (https://shop.vbc.ac.at/vdrc_store/faq). The flies in the GD library were constructed by using gene-specific inverted repeats 300bp downstream of the UAS vector. These constructs were introduced into flies by using of P- element-mediated transposition, leading to random insertion sites in the *Drosophila* genome, further leading to varying site dependent expression levels (Dietzl *et al.* 2007). An upgrade to the GD library was

the KK library, which was designed to target 9646 genes. The library construction was based on PhiC31-mediated site-specific integration that contain precisely designed *attP* sites and allow transgenes to be inserted into predetermined locations into the *Drosophila* genome (Bischof et al. 2007; Green et al. 2014).

Another RNAi fly stock resource was developed at the Harvard Medical School in 2008 known as the Transgenic RNAi Project or TRiP. It is distributed by BDSC and is said to contain around 13610 RNAi fly lines (Perkins *et al.* 2015). The vector design of these lines is said to be constantly evolving because of which they are not categorised into separate libraries. Early vector designs included inverted repeats that are 400-600 bp long integrated using the PhiC31-mediated site-specific integration. Recently, these designs have focused around shRNAs that contain a 21-nucleotide target sequence inserted into the miRNA scaffold. This has shown to effectively supress gene expression in all tissue including the germline. Ultimately, the shorter length of the shRNAs allows them to reduce off target effects (Perkins *et al.* 2015).

Final RNAi stock resource is found in NIG in Kyoto, who were the first to start distribution of stock lines. The centre currently contains about 12,400 of NIG-RNAi lines, containing transgenes that have long inverted repeats that have been randomly inserted within genome using P-element-mediated transposition (https://shigen.nig.ac.jp/fly/nigfly/).

Aims of this Chapter

The primary aim of this chapter was to characterise*pirk* RNAi lines and study the effect of this knock down (silencing) on sleep, activity and lifespan in *Drosophila*. The *pirk* gene was knocked down in the following tissues:

1. Pan neural network (CNS) via *elav* GAL4
2. Glial cells via *repo* GAL4
3. Gut enterocytes via *np1* GAL 4
4. Gut progenitor cells (enteroblasts and stem cells) via *esg* GAL4

The gene was knocked down in various tissues using the GeneSwitch system. However, we used different RNAi lines to account for any off-site or "leaking" effects commonly observed in RNAi lines. Additionally, the control flies were crossed to GAL4 lines to create appropriate controls **(Chapter 7 Section 7.1.4)**.

Considering the more finely regulated sleep cycle observed in female flies and the more pronounced sleep phenotype documented in **Chapter 2**, all flies used in this chapter are exclusively females.

4.2 RESULTS

The results section is structured into distinct subsections. Initially, the four GAL4 lines are categorised based on the specific organ tissues they impact, namely, brain and gut. Within each subsection, the results of individual GAL4 lines are further categorised by age. Additionally, to reinforce the validation of our findings, we present results from a pair of RNAi lines (KK and Trip), keeping them together for comparative analysis.

To find optimal controls for the RNAi lines, we analysed the lifespan data across various control options. Ultimately, the Background X GAL4 line was selected as the control group for all behavioural assays **(Chapter 7 Section 7.1.4)**.

4.2.1 Effect of pirk knock down on the brain

4.2.1.1. Effects on Lifespan

To investigate the impact of neuronal knockdown of pirk on lifespan, female flies, obtained after crossing the desired GAL4 to *pirk* RNAi (KK and Trip) lines, were divided into groups of 10 and placed on standard food alongside their background X GAL4 controls. Ten vials, each containing 10 flies, were transferred to new food three times a week, and manual scoring was performed by recording the number of deceased flies during each change. This data was then input into GraphPad Prism for statistical analysis and graph generation. To assess the effect on lifespan, the survival of each fly line was calculated, and the data was plotted as survival curves. Subsequently, it was tested for significant differences using the Log-Rank (Mantel-Cox) Test.

Pirk KK RNAi

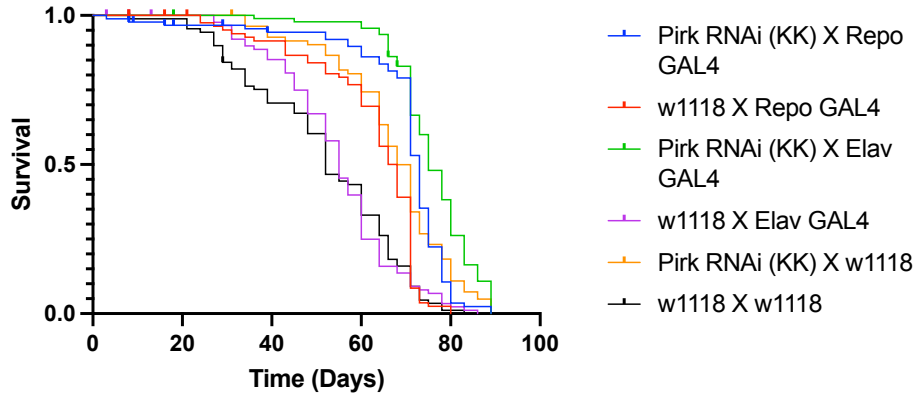

Figure 36:Lifespan analysis of *pirk*^{KK} RNAi female flies crossed with *repo* and *elav* GAL4. Flies from each genotype were randomly split into standard food vials, 10 vials containing 15 flies each were tipped onto new food thrice a week and scored for the number of dead flies during each tip. Survival of each fly line was calculated and the data was plotted as survival curves and tested for significant differences using the Log-Rank (Mantel-Cox) Test. P<0.05 was considered significant.

An unexpected increase in median lifespan was observed in *pirk*^{elav} RNAi KK from 55 days in control flies (*w*^{1118} X *elav*) to 75 days in *pirk* RNAi KK *elav* GAL4 flies (p<0.0001) **(Figure 36)**. Similarly, a rise in the median lifespan in *pirk*^{repo} RNAi KK female flies was seen in flies with reduced expression of Pirk protein in glial cells, from 67 days in control flies to 73 days in RNAi KK flies (p<0.0001) **(Figure 36)**.

Pirk Trip RNAi

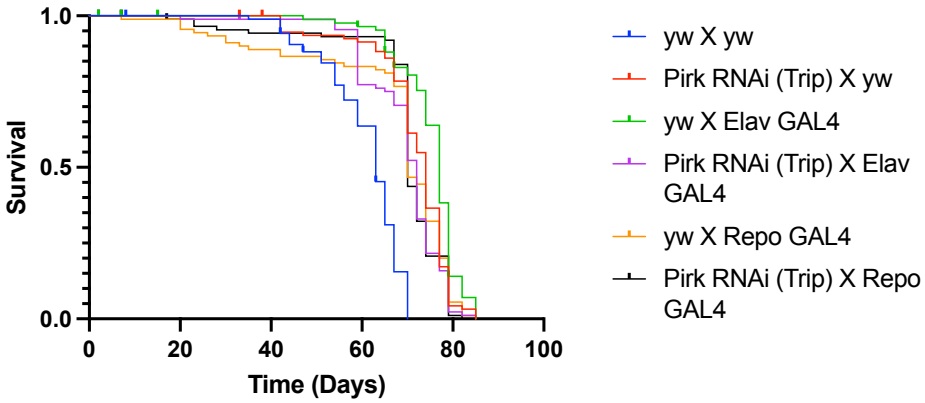

Figure 37: Lifespan analysis of Pirk Trip RNAi female flies crossed with *repo* and *elav* GAL4. Flies from each genotype were randomly split into standard food vials, 10 vials containing 15 flies each were tipped onto new food thrice a week and scored for the number of dead flies during each tip. Survival of each fly line was calculated and the data was plotted as survival curves and tested for significant differences using the Log-Rank (Mantel-Cox) Test. P<0.05 was considered significant.

We observed a significant decline in median lifespan in *pirk*^{elav} RNAi Trip female flies, with a median decline from 77 days in control flies to that of 72 days RNAi Trip flies flies (p=0.0006) **(Figure 36)** when Pirk protein was knocked down in the pan neuronal network via *elav* protein. However, this change in median lifespan was not observed when *pirk*^{repo} RNAi Trip female flies was knocked down in glial cells via *repo* protein (p=0.3068) **(Figure 36)**.

4.2.1.2. Effect of *pirk* knock down on sleep and locomotion in the pan-neuronal system (*elav* Gal4)

Effects on Climbing Ability

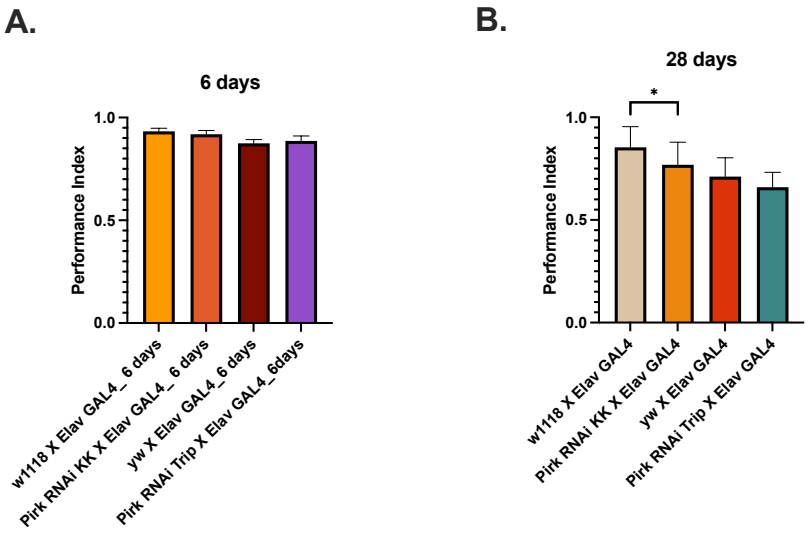

Figure 38: Climbing Analysis of 6-day and 28-day *pirk* Female in pirk RNAi lines with *pirk* silenced in the pan neuronal network via *elav* GAL4 in (A) 6-days (B) 28-days of age. 5 vials containing 15 flies each (X3 repeats) were examined, and an unpaired Mann Witney Rank sum test was performed. The data was then plotted using GraphPad Prism plotted to show the mean (± SEM), non-significant results were not marked and p≤ 0.05 (*), ≤ 0.01 (**), ≤ 0.001 (***), ≤ 0.0001 (****).

The pan neuronal knockdown of Pirk protein in either of the two (*pirk*^{elav} KK or *pirk*^{elav} Trip) RNAi lines did not affect the performance index of young female flies compared to their respective controls, with p=0.6748 (n=15) in *pirk*^{elav} KK RNAi flies and p=0.5736 (n=15) in *pirk*^{elav} Trip RNAi female flies **(Figure 38A)**. As the flies aged, we observed a significant

reduction in the climbing ability of 6-day old *pirk*^{elav} RNAi KK female flies (p=0.0397, n=15) but not in *pirk*^{elav} RNAi Trip flies (p=0.0996, n=15) when crossed with *elav* GAL4 flies **(Figure 38B)**.

Effects on Locomotion and Sleep

Young Flies

We found no significant variation in total sleep time during the day in either of the 6-day old *pirk*^{elav} RNAi type flies as compared to their respective controls, with p=0.2657 (n=32) in *pirk*^{elav} KK RNAi flies and p=0.4406 (n=32) in *pirk*^{elav} Trip RNAi female flies **(Figure 39A)**. Additionally, this effect (or lack of) was also seen when the day was divided into daytime sleep and night-time sleep in both KK RNAi (p=0.1307, n=32 & p=0.8077, n=32 respectively) and Trip RNAi (p=0.1646, n=32 & p=0.4648, n=32 respectively) 6-day old female flies compared to their controls **(Figure 39(B-C))**. However, it is worth noting that even though we did not find significant differences in flies *pirk*^{elav} Trip and KK flies versus their controls, a trend towards lower sleep duration was observed in both genotypes during a 24-hour period and during daytime sleep.

A similar effect was observed in the total number of sleep episodes observed during the course of the day (24-hour period) in both KK (p=0.5593, n=32) and Trip (p=0.0801, n=32) young *pirk*^{elav} RNAi flies **(Figure 39D)**. However, a slight reduction of 6 minutes is observed in the frequency of the sleep episodes during the day in *pirk*^{elav} Trip RNAi flies (p=0.0039, n=32) but not in *pirk*^{elav} KK RNAi flies (p=0.3512, n=32) **(Figure 39E)**. Similar to total sleep duration, we observed no significant changes in mean sleep episode durations in either of the RNAi lines in a 24-hour period or during daytime or night-time sleep **(Figure 39(G-I))**.

Similar to other sleep parameters, we found no observable differences in the latency to sleep in either day or night-time sleep in both *pirk*^{elav} RNAi KK or *pirk*^{elav} RNAi Trip flies **(Figure 40(A-B))**. Even though we found no significant changes in activity count / time awake in 6-day old *pirk*^{elav} Trip RNAi female flies in either of the three time points **(Figure 40(C-E))**, we observed a slight reduction in *pirk*^{elav} KK RNAi during a 24-hour period ($p=0.0042$, $n=32$) **(Figure 40C)**, during daytime ($p=0.036$, $n=32$) **(Figure 40D)** and night-time ($p=0.0371$, $n=32$) **(Figure 40E)** activity count per time awake in 6-day old female flies versus their controls.

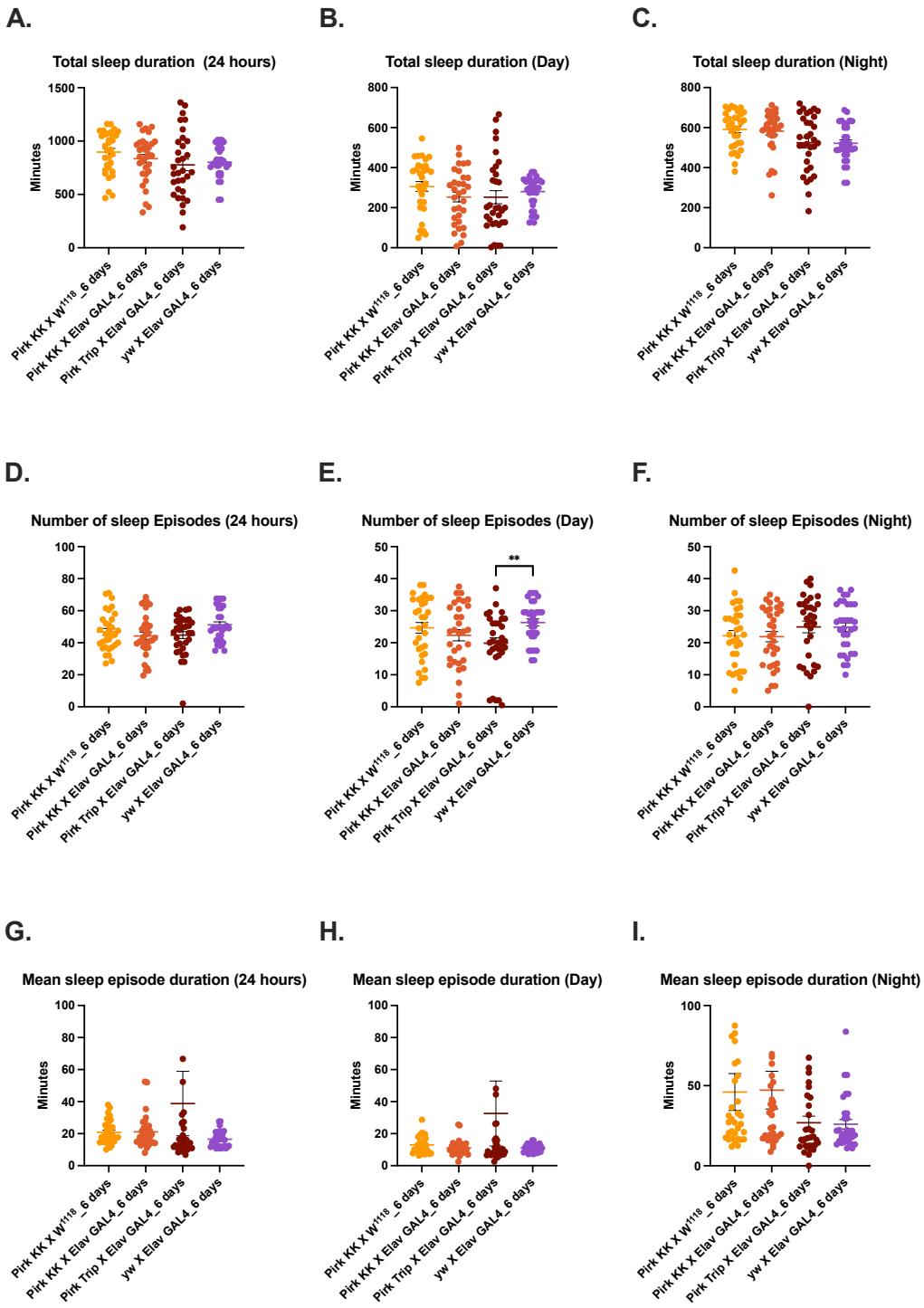

Figure 39: The effect of pan neuronal specific knock down of *pirk* on sleep profiles of 6-day old *pirk^{elav}* female flies compared to their controls. Three independent repeats were conducted for each genotype, and 32 flies were randomly selected from these repeats, resulting in a total sample size (n) of 32. These 32 flies were then analysed, and a Mann Witney Rank sum test was performed between mutant flies and their respective controls, without consideration of age-dependent analysis. Non-significant results were not marked and $p \leq 0.05$ (*), ≤ 0.01 (**), ≤ 0.001 (***), ≤ 0.0001 (****).

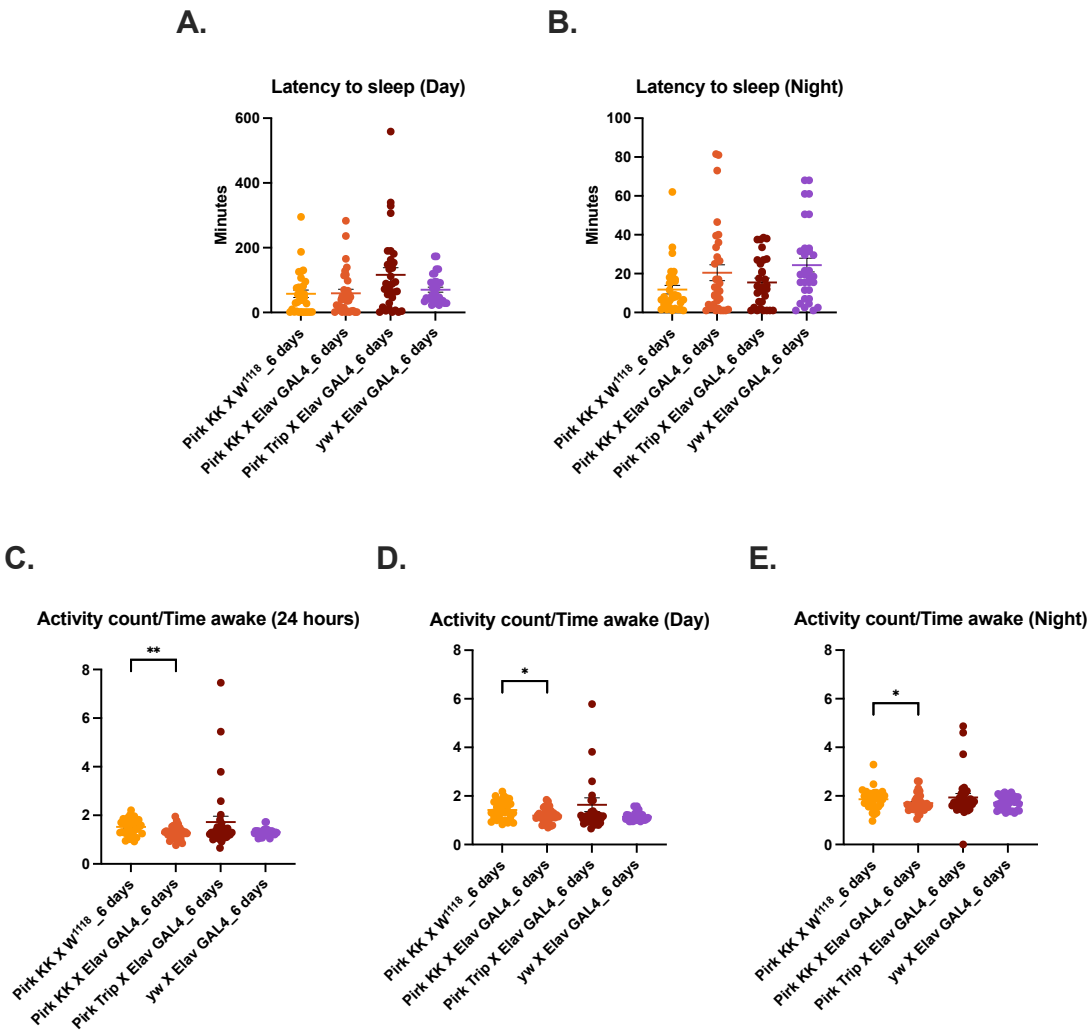

Figure 40: The effect of pan neuronal specific knock down of *pirk* on latency to sleep and activity count / time awake of 6-day old *pirk*^{elav} female flies compared to their controls. Three independent repeats were conducted for each genotype, and 32 flies were randomly selected from these repeats, resulting in a total sample size (n) of 32. These 32 flies were then analysed, and a Mann Witney Rank sum test was performed between mutant flies and their respective controls, without consideration of age-dependent analysis. Non-significant results were not marked and p≤ 0.05 (*), ≤ 0.01 (**), ≤ 0.001 (***), ≤ 0.0001 (****).

Older Flies

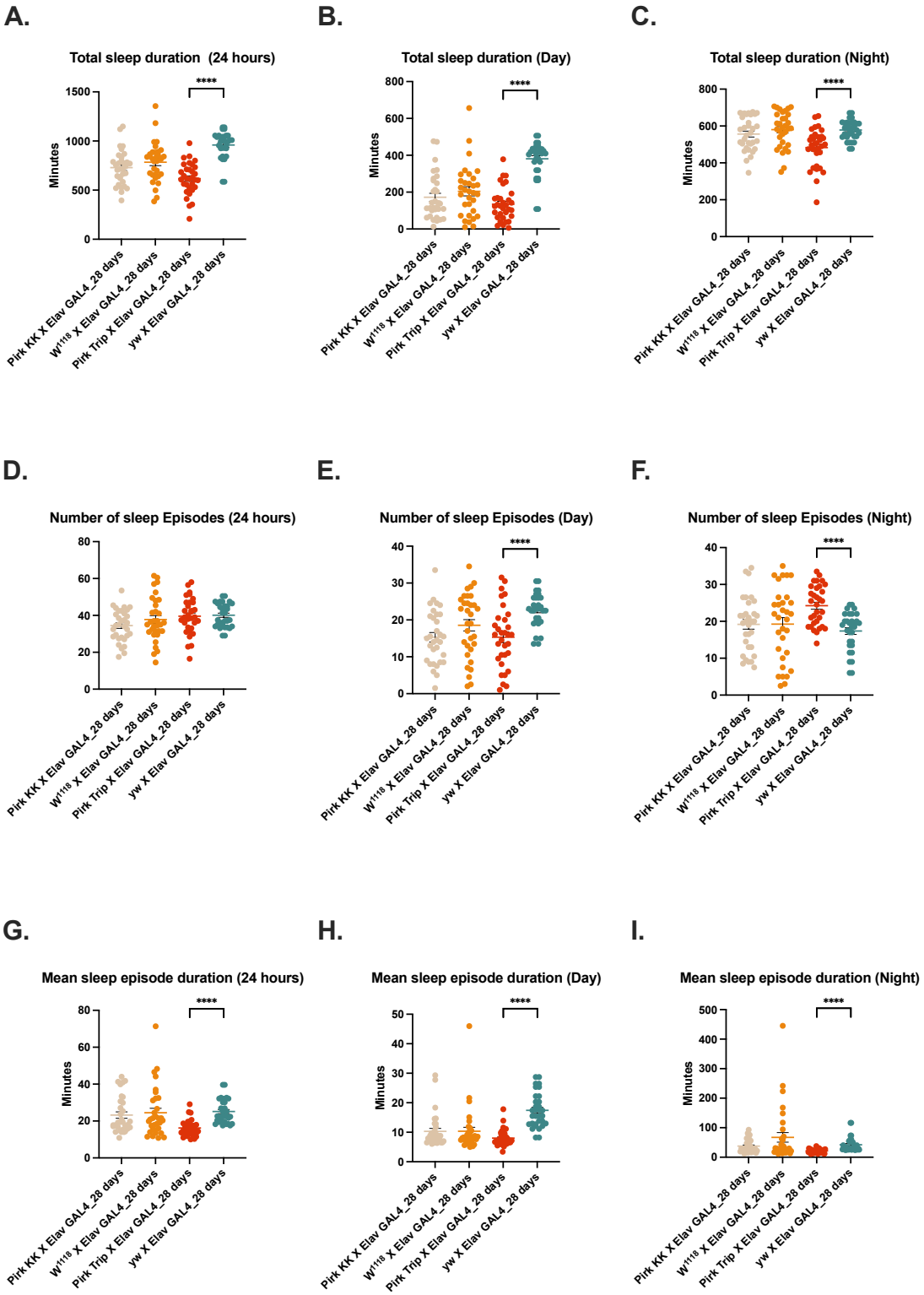

Figure 41: The effect of pan neuronal specific knock down of pirk on sleep profiles of 28-days old *pirk^{elav}* female flies compared to their controls. Three independent repeats were conducted for each genotype, and 32 flies were randomly selected from these repeats, resulting in a total sample size (n) of 32. These 32 flies were then analysed, and a Mann Witney Rank sum test was performed between mutant flies and their respective controls, without consideration of age-dependent analysis. Non-significant results were not marked and $p \leq 0.05$ (*), ≤ 0.01 (**), ≤ 0.001 (***), ≤ 0.0001 (****).

Like that of total sleep, the number of sleep episodes showed fluctuations in only *pirk*^{elav} Trip RNAi female flies and not in *pirk*^{elav} RNAi KK flies. Interestingly, this change in *pirk*^{elav} Trip RNAi was not observed during the 24-hour period (p=0.9495, n=32) **(Figure 41D)** but a significant median reduction of 7 episodes was observed during daytime sleep (p<0.0001, n=32) **(Figure 41E)** and an equal but opposite stark increase of 7 episodes was observed at night-time (p<0.0001, n=32) in 28-day old female *pirk*^{elav} Trip RNAi female flies**(Figure 41F)**. Similar to other sleep parameters, no significant observations were made in older *pirk*^{elav} KK RNAi female flies versus their controls.

Similarly, a notable drop in the average sleep episode duration was observed only in older *pirk*^{elav} RNAi Trip female flies (p<0.0001, n=32) and not in *pirk*^{elav} RNAi KK flies (p=0.9098, n=32). **(Figure 41G)** This was also seen during daytime and night-time sleep where mean sleep episode duration was significantly affected in *pirk*^{elav} Trip RNAi flies (p<0.0001, n=32 for both) and not in *pirk*^{elav} KK RNAi older female flies compared to their controls **(Figure 41(H-I))**.

Latency to sleep during the day was affected in older female *pirk*^{elav} RNAi Trip flies (p=0.0045, n=32) but not in *pirk*^{elav} KK RNAi flies (p=0.1188, n=32) **(Figure 42A)**. Surprisingly, a significant increase in latency to sleep at night-time was observed in both KK and Trip *pirk*^{elav} RNAi female flies, with p=0.0005 (n=32) in older KK females and p <0.0001 (n=32) in older Trip females with respect to their controls **(Figure 42B)**. We observed a notable rise in the activity count per time awake in 28-day old female *pirk*^{elav} KK RNAi flies (p=0.0040, n=32) but not in *pirk*^{elav} RNAi trip flies (p=0.6525, n=32) during a 24-hour period **(Figure 42C)**. However, a significant increase in both KK (p=0.0002, n=32) and Trip line (p=0.0003, n=32) rate of activity was noted during daytime **(Figure 42D)**. This observation seems to have been compensated with an equal but opposite decrease in activity count per time awake in 28-day

old female *pirk*^{elav} Trip RNAi flies during night-time (p=0.0001, n=32) but not in KK RNAi flies, where no significant observation was noted (p=0.6169, n=32) **(Figure 42E)**.

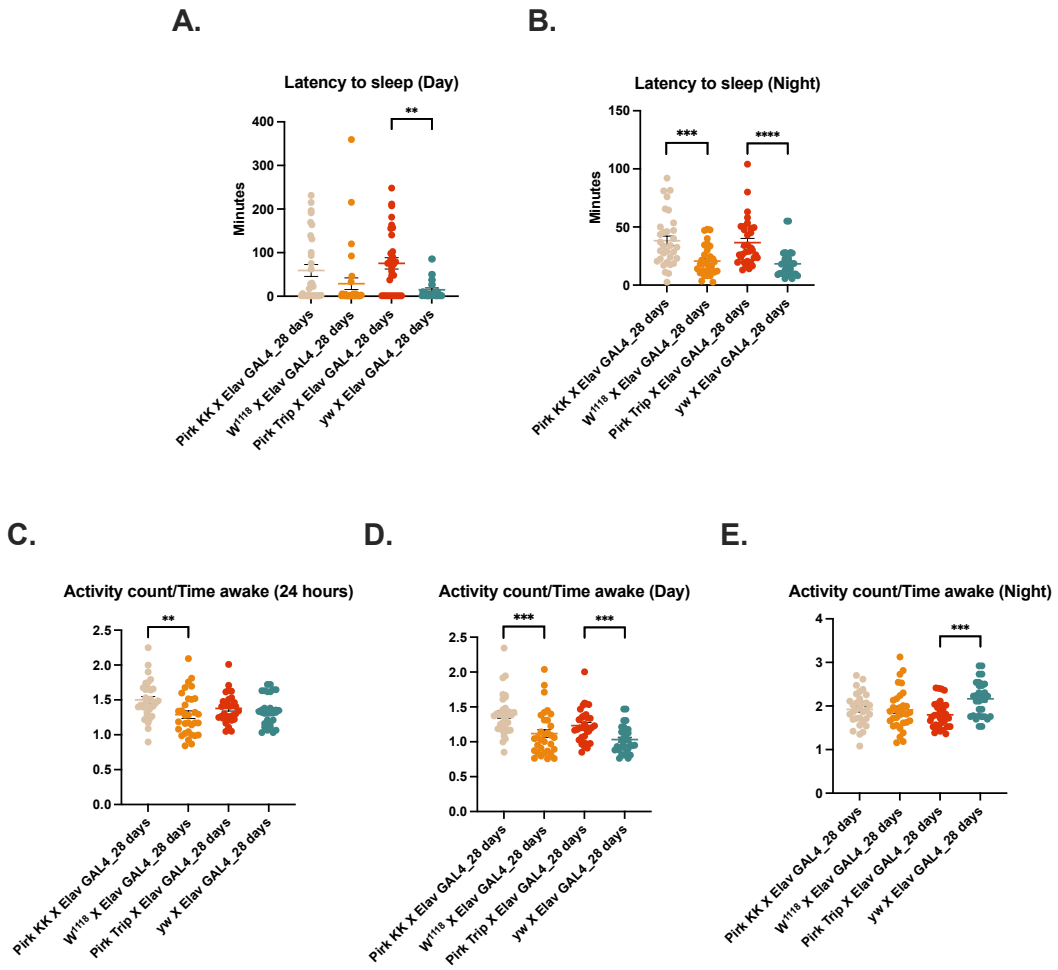

Figure 42: The effect of pan neuronal specific knock down of pirk on latency to sleep and activity count/time awake of 28-day old *pirk*^{elav} female flies compared to their controls. Three independent repeats were conducted for each genotype, and 32 flies were randomly selected from these repeats, resulting in a total sample size (n) of 32. These 32 flies were then analysed, and a Mann Witney Rank sum test was performed between mutant flies and their respective controls, without consideration of age-dependent analysis non-significant results were not marked and p≤ 0.05 (*), ≤ 0.01 (**), ≤ 0.001 (***), ≤ 0.0001 (****).

4.2.1.4. Effect of *pirk* knock down on sleep and locomotion in glial cells (*repo* GAL4)

Effects on climbing ability

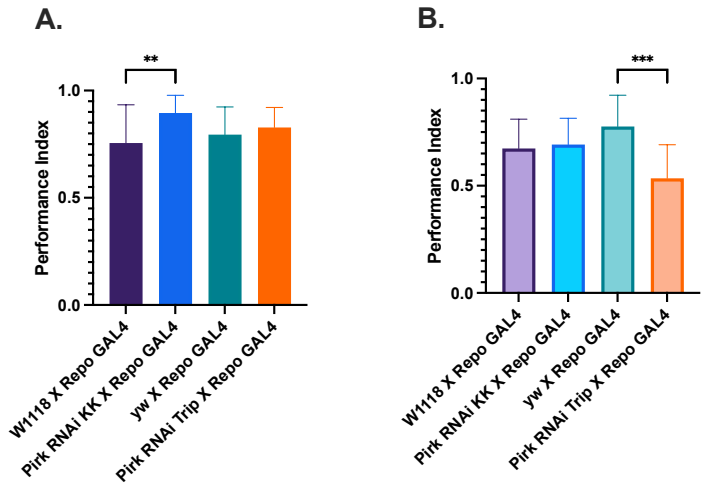

Figure 43: Climbing Analysis of 6-day and 28-day *pirk* Female in *pirk* RNAi lines with *pirk* silenced in the glial cells via *repo* GAL4 in (A) 6-days (B) 28-days of age. 5 vials containing 15 flies each (X3 repeats) were examined, and an unpaired Mann Witney Rank sum test was performed. The data was then plotted using GraphPad Prism plotted to show the mean (± SEM), non-significant results were not marked and p≤ 0.05 (*), ≤ 0.01 (**), ≤ 0.001 (***), ≤ 0.0001 (****).

Pirk^{repo} RNAi KK flies showed a notable increase in the performance index in 6-day old female flies versus their control (p =0.0024, n=15). However, this effect was not observed in *pirk*^{repo} RNAi Trip *repo* female flies (p=0.6747, n=15) **(Figure 43A)**. Unlike their younger counterpart, 28-day old *pirk* RNAi KK female flies crossed with *repo* GAL4 did not show any notable changes (p=0.5742, n=15) **(Figure 43B)**. A significant decline in the performance index was observed in older *pirk*^{repo} Trip RNAi flies with p=0.0005 (n=15) versus their control **(Figure 43B)**.

Effects on Locomotion and Sleep

Young Flies

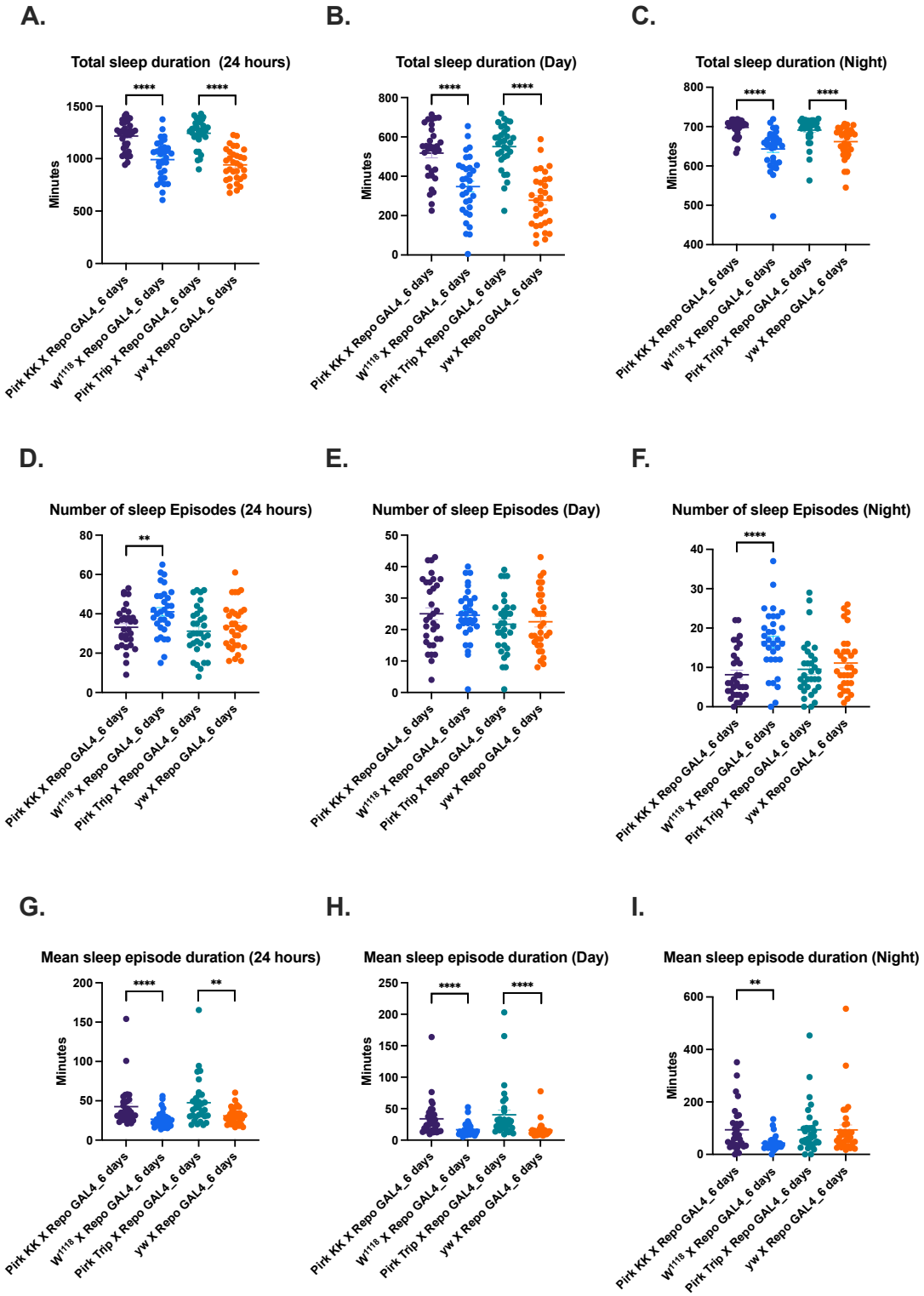

Figure 44: The effect of glial knock down of *pirk* on sleep profiles of 6-days old *pirk* female flies compared to their controls. Three independent repeats were conducted for each genotype, and 32 flies were randomly selected from these repeats, resulting in a total sample size (n) of 32. These 32 flies were then analysed, and a Mann Witney Rank sum test was performed between mutant flies and their respective controls, without consideration of age-dependent analysis. Non-significant results were not marked and p≤ 0.05 (*), ≤ 0.01 (**), ≤ 0.001 (***), ≤ 0.0001 (****).

Total duration of sleep was deeply affected by knocking down Pirk protein in only glial cells (via *repo* GAL4). We observed a significant increase in total sleep during a 24-hour period with $p<0.0001$ (n=32) in both KK and Trip $pirk^{repo}$ RNAi young female flies **(Figure 44A)**. This increase in sleep was due to an increase in both daytime and night-time sleep observed in both RNAi lines. A median increase of 170 minutes was observed in young $pirk^{repo}$ RNAi KK flies ($p<0.0001$, n=32) and that of 283 minutes was observed in $pirk^{repo}$ RNAi Trip flies during daytime sleep ($p<0.0001$, n=32) **(Figure 44B)**. Furthermore, a median increase of 49 minutes was observed in $pirk^{repo}$ RNAi KK flies and that of 25 minutes in Trip RNAi female flies ($p<0.0001$, n=32 for both) during night-time sleep **(Figure 44C)**.

As mentioned in previous chapters, the number of sleep episodes is one of the parameters that helps investigate if the increase in total sleep is due to a change in sleep quality or quantity. Here we observed a significant reduction in the total number of sleep episodes over the course of the day in $pirk^{repo}$ KK RNAi flies with respect to their controls ($p=0.0095$, n=32) but no change in the $pirk^{repo}$ Trip RNAi flies ($p=0.5020$, n=32) **(Figure 44D)**. This effect is likely due to a reduction in the number of sleep episodes during night-time sleep in $pirk^{repo}$ KK RNAi flies ($p<0.0001$, n=32). Additionally, we observed no notable changes in daytime sleep in either of the young $pirk^{repo}$ RNAi female flies ($p=0.9495$, n=32 in KK and $p=0.9654$, n=32 in Trip) or in night-time sleep in $pirk^{repo}$ Trip RNAi flies ($p=0.3171$, n=32) **(Figure 44(E-F))**.

To assess the quality of sleep, we examined the mean sleep episode duration of the flies. It was observed that 6-day old female flies with Pirk protein knocked down in glial cells have significantly less mean sleep episode duration than their controls over a 24-hour period. This is seen in both types of RNAi lines, with a median decrease of approximately 10.88 minutes in young $pirk^{repo}$ KK RNAi female flies ($p<0.0001$, n=32) and that of 10.53 minutes in young

pirk^{repo} Trip RNAi female flies (p=0.0042, n=32) **(Figure 44G)**. This effect was also observed during daytime sleep with p<0.0001 (n=32) in both *pirk*^{repo} KK and *pirk*^{repo} Trip RNAi 6-day old female flies compared to their controls **(Figure 44H)**. Additionally, a median rise of 27.5 minutes was observed during night-time sleep in *pirk*^{repo} RNAi KK flies (p=0.0023, n=32) but no significant change was seen in *pirk*^{repo} Trip RNAi flies (p=0.6621, n=32) **(Figure 44I)**.

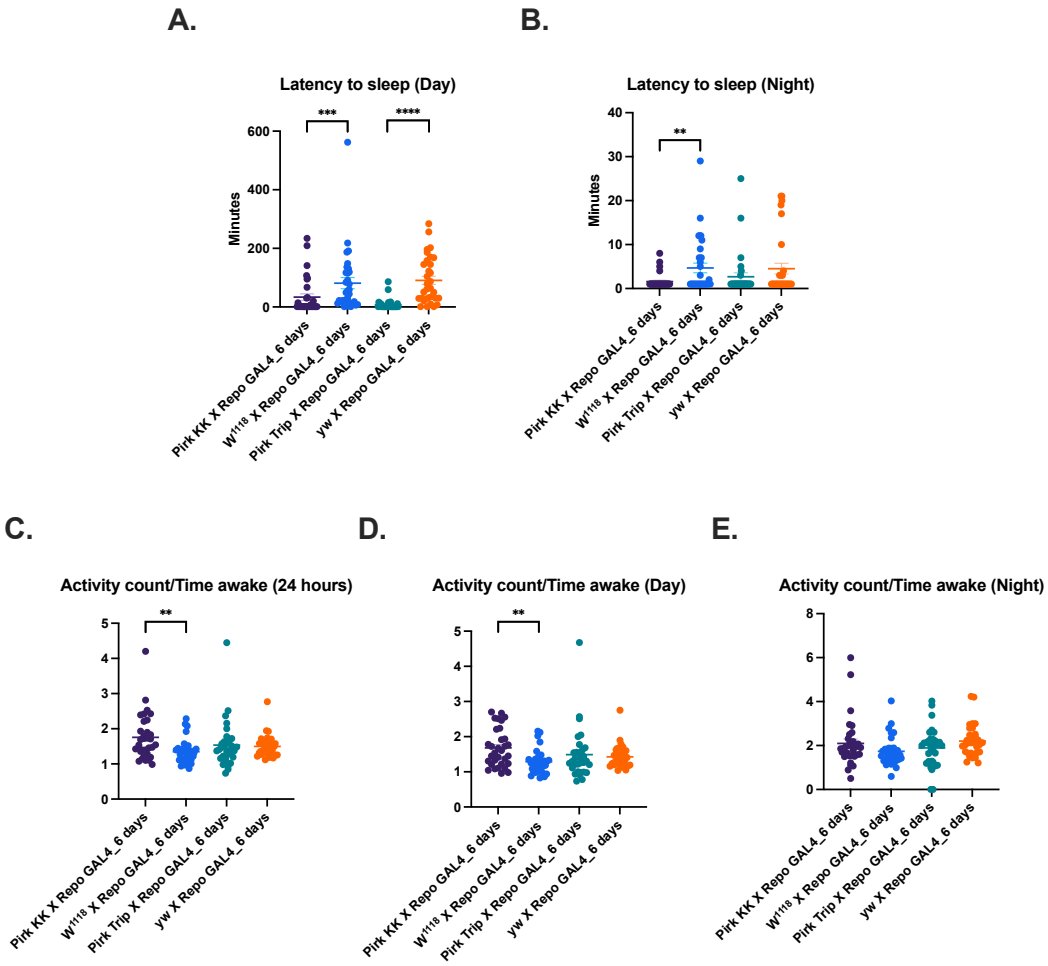

Figure 45: The effect of glial specific knock down of pirk on latency to sleep and activity count / time awake of 6-day old pirk female flies compared to their controls. Three independent repeats were conducted for each genotype, and 32 flies were randomly selected from these repeats, resulting in a total sample size (n) of 32. These 32 flies were then analysed, and a Mann Witney Rank sum test was performed between mutant flies and their respective controls, without consideration of age-dependent analysis Non-significant results were not marked and p≤ 0.05 (*), ≤ 0.01 (**), ≤ 0.001 (***), ≤ 0.0001 (****).

We observed a significant decline in the number of minutes the flies take to have their first sleep episode after light on (latency to sleep during daytime) in both young *pirk*^{repo} RNAi female flies, with p=0.0002 (n=32) in *pirk*^{repo} RNAi KK flies and p <0.0001 (n=32) in young *pirk*^{repo} RNAi Trip female flies **(Figure 45A)**. During night-time sleep, this effect was only

observed in KK flies (p=0.0056, n=32) and not in Trip female flies (p=0.1780, n=32) **(Figure 45B)**.

To understand if any sleep related observation is caused due to neuromuscular damage or not, we examined the activity count per time awake. Young *pirk*^{repo} RNAi KK flies show a slight increase in the rate of activity over the course of the day (p=0.0021, n=32) **(Figure 45C).** This effect is likely due to a rise in the rate of beam crossing during daytime wakefulness (p=0.0019, n=32) **(Figure 45D)**, as we noted no significant changes during night-time (p=0.0724, n=32) **(Figure 45E)**. Furthermore, we observed no significant changes in either of the time points in 6-day old *pirk*^{repo} RNAi Trip female flies compared to their controls.

Older Flies

Unlike the younger flies, we only observed a noteworthy rise in the total sleep in 28-day old *pirk*^{repo} RNAi KK female flies during a set 24-hour period (p<0.0001, n=32), and no observable difference in *pirk*^{repo} RNAi Trip flies (p=0.1862, n=32) **(Figure 46A)**. Similar observations were noted during both daytime and night-time sleep, with a significant median increase of approximately 185 minutes in *pirk*^{repo} RNAi KK flies during daytime (p=0.0002, n=32), and that of 42 minutes during night-time (p=0.0012, n=32). However, no significant changes were observed in 28-day old pirk^{repo} RNAi Trip female flies versus their controls, but an obvious trend towards increased sleep across all three timepoints was noted **(Figure 46(B-C))**.

The above graphs indicate that no significant changes in number of sleep episodes are observed in *pirk*^{repo} RNAi KK female flies over a period of 24-hours (p=0.4129, n=32) **(Figure 46D)**. However, a notable increase is observed in 28-day old *pirk*^{repo} RNAi Trip female flies with a median increase of 8 episodes and p=0.0097 (n=32) **(Figure 46D)**. Furthermore, we observe a significant increase in both *pirk*^{repo} RNAi KK female flies and *pirk*^{repo} RNAi Trip female flies

during daytime sleep, with a median increase of 8 episodes in *pirk*^{repo} RNAi KK female flies (p=0.0048, n=32), and that of 6 episodes in 28-day old *pirk*^{repo} RNAi Trip female flies (p=0.0021, n=32) **(Figure 46E)**. Interestingly, no notable change was observed *pirk*^{repo} RNAi Trip flies during the night-time (p=0.3241, n=32), while on the other hand, a stark median decline of 11 sleep episodes at night-time was observed in *pirk*^{repo} RNAi KK flies, compared to their controls (p<0.0001, n=32) **(Figure 46F)**.

We see a significant reduction in the mean sleep episode duration in *pirk*^{repo} RNAi KK flies when observed during a 24-hour period as well as during day and night-time sleep. In the 24-hour period, a median decline of 7.5 minutes is observed (p=0.0008, n=32) **(Figure 46G)**. Further, during daytime sleep, a median decline of 4.3 minutes is observed (p=0.0003, n=32) and during the night-time sleep, a median decline of 23.08 min was noted (p=0.0005, n=32) **(Figure 46(H-I))**.

Conversely, no change is observed in *pirk*^{repo} RNAi Trip flies, where the sleep episodes are the same when observed in a 24-hour span (p=0.0607, n=32), during daytime sleep (p=0.6622, n=32) as well as during night-time sleep (p=0.2158, n=32) **(Figure 46(G-I))**.

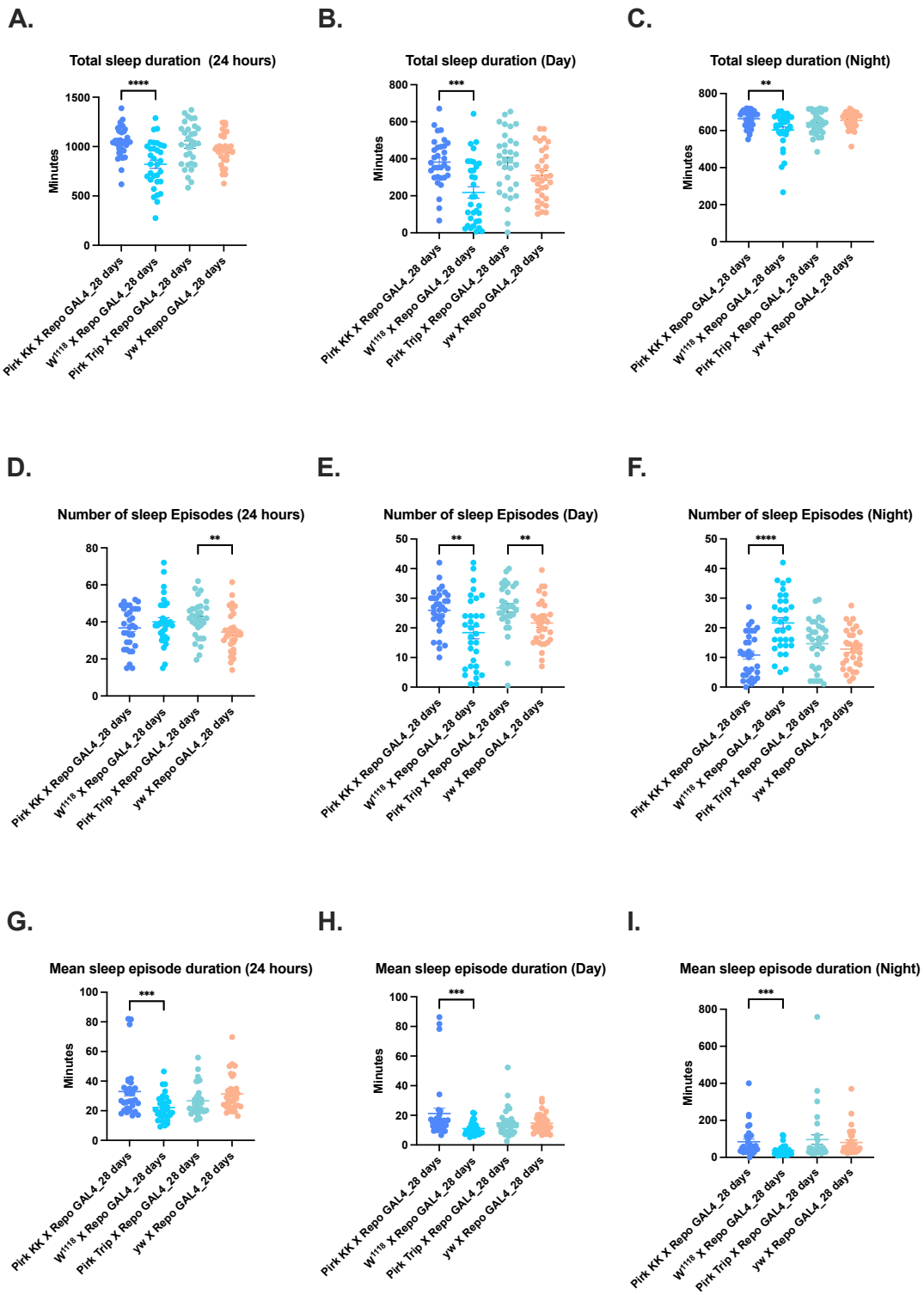

Figure 46: The effect of glial knock down of pirk on sleep profiles of 28-days old Pirk female flies compared to their controls. Three independent repeats were conducted for each genotype, and 32 flies were randomly selected from these repeats, resulting in a total sample size (n) of 32. These 32 flies were then analysed, and a Mann Witney Rank sum test was performed between mutant flies and their respective controls, without consideration of age-dependent analysis. Non-significant results were not marked and $p \leq 0.05$ (*), ≤ 0.01 (**), ≤ 0.001 (***), ≤ 0.0001 (****).

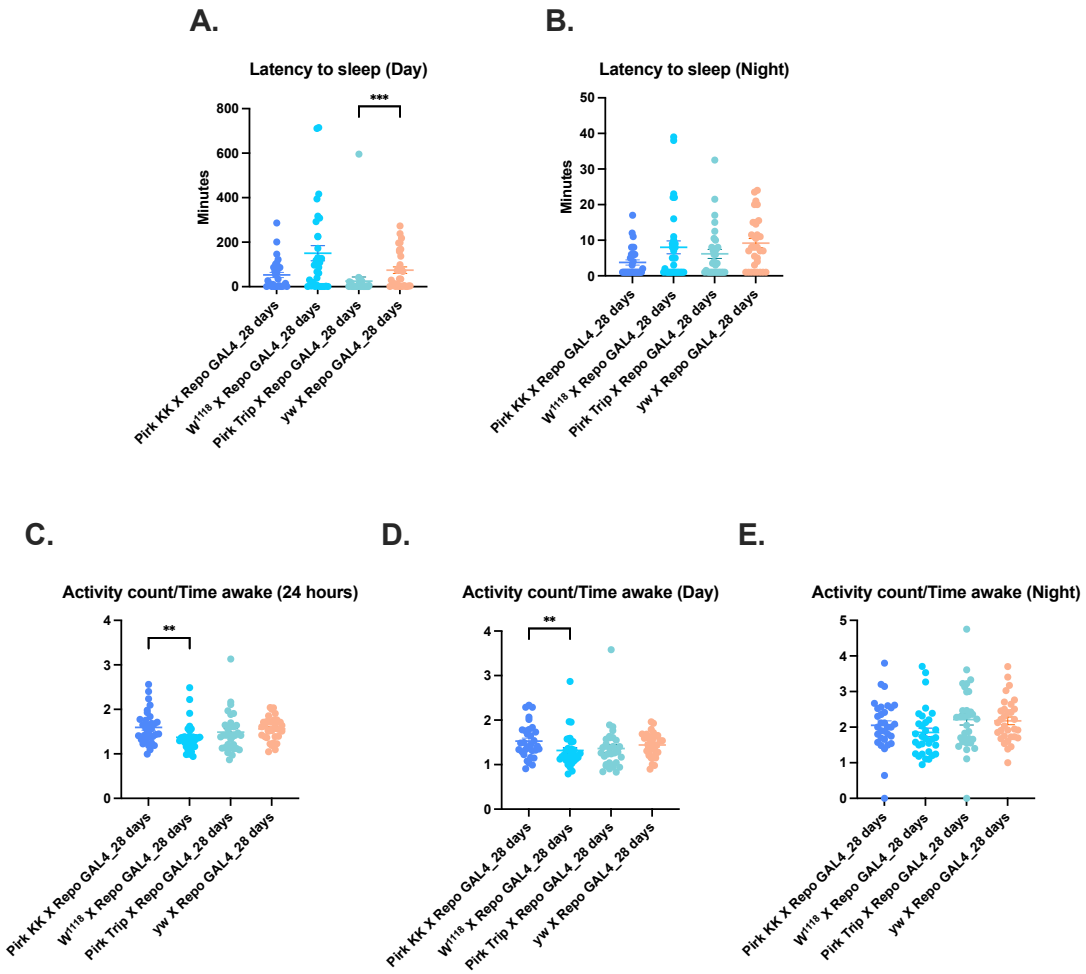

Figure 47: The effect of glial specific knock down of pirk on latency to sleep and activity count/time awake of 28-day old pirk female flies compared to their controls. Three independent repeats were conducted for each genotype, and 32 flies were randomly selected from these repeats, resulting in a total sample size (n) of 32. These 32 flies were then analysed, and a Mann Witney Rank sum test was performed between mutant flies and their respective controls, without consideration of age-dependent analysis. Non-significant results were not marked and p≤ 0.05 (*), ≤ 0.01 (**), ≤ 0.001 (***), ≤ 0.0001 (****).

We observed no notable changes in latency to sleep in 28-day old *pirk*^{repo} RNAi KK female flies during daytime sleep compared to their controls (p=0.0544, n=32) as well as during the night (p=0.1331, n=32) **(Figure 47(A-B))**. However, in contrast to that we see a stark decline in latency to sleep in *pirk*^{repo} RNAi Trip flies during daytime with a median reduction of 29 minutes (p=0.0002, n=32) but not during night-time (p=0.0521, n=32) **(Figure 47(A-B))**.

When observed over a 24-hour period, we see that older *pirk*^{repo} Trip female flies do not show any significant change in activity count per time awake (p=0.1060, n=32), whereas *pirk*^{repo} KK flies show an increase in activity count (p=0.0016, n=32) when compared to their respective controls **(Figure 47C)**. Further, when observed during daytime, *pirk*^{repo} KK flies show a slight reduction in activity count (p=0.0074, n=32), whereas *pirk*^{repo} Trip flies do not show any notable change (p=0.0870, n=32) **(Figure 46D)**. Lastly, when observed during the night-time, both *pirk*^{repo} RNAi KK flies and *pirk*^{repo} Trip KK flies show no observable changes (p=0.0666 (n=32) and p=0.8887 (n=32) respectively) **(Figure 46E)**.

4.2.2 Effect of Pirk Knock down on Gastrointestinal tissue

4.2.2.1. Effects on Lifespan

To study the effect of *pirk* RNAi (KK and Trip) knock down in gut tissue on lifespan, survival of each fly line was calculated. 10 vials containing 10 females each were flipped onto new vials containing new food. Survival was then manually scored by recording the number of dead flies during food changing. The data was then recorded in GraphPad Prism and Log Rank (Mantel-Cox) was performed to calculate probability of survival.

We analysed lifespan of flies with *pirk* knocked down in enterocytes (via *np1* GAL4) and gut stem cells (via *esg* GAL4). After analysing various controls, we finally selected Background X GAL4 as the ideal control for this study.

Pirk KK RNAi

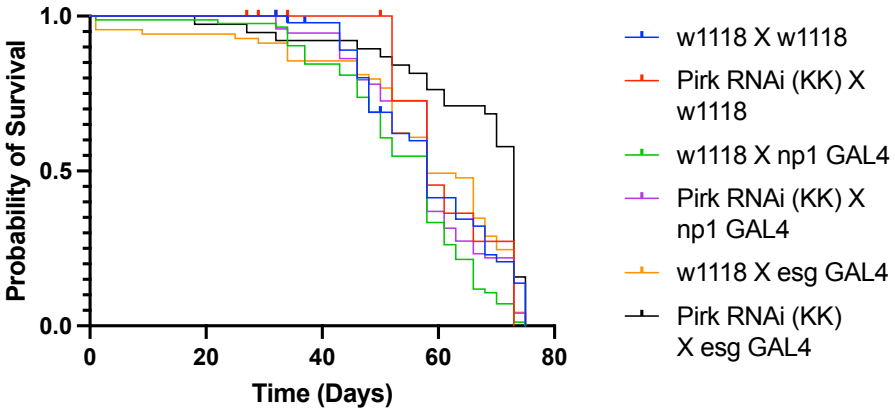

Figure 48: Lifespan analysis of pirk KK RNAi female flies crossed with *np1* and *esg* GAL4. Flies from each genotype were randomly split into standard food vials, 10 vials containing 15 flies each were tipped onto new food thrice a week and scored for the number of dead flies during each tip. survival of each fly line was calculated, and the data was plotted as survival curves and tested for significant differences using the Log-Rank (Mantel-Cox) Test. P<0.05 was considered significant.

We observed a significant increase in the median lifespan in *pirk* RNAi KK flies with Pirk protein knocked down in the gut progenitor cells (*esg*-GAL4) (p=0.0006) with respect to their controls (w^{1118} X esg GAL4). In addition to this, a notable change was observed in KK flies where *pirk* expression was reduced in the enterocytes (via *np1*-GAL4) (p=0.0191)

Pirk Trip RNAi

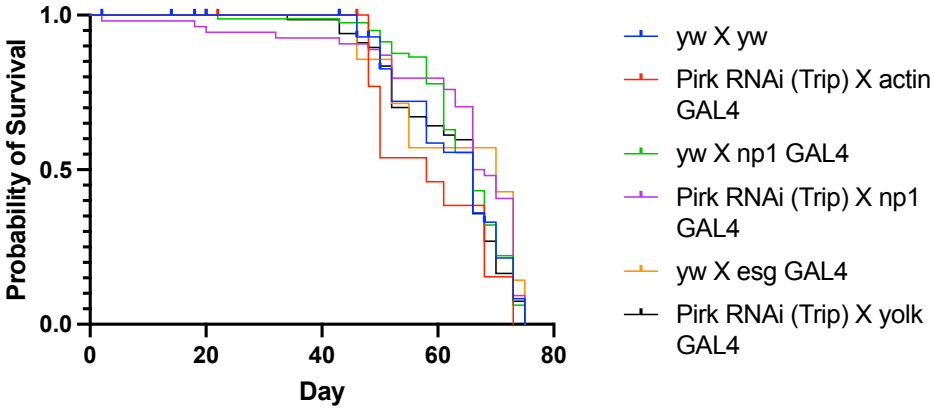

Figure 49: Lifespan analysis of pirk KK RNAi female flies crossed with *np1* and *esg* GAL4. Flies from each genotype were randomly split into standard food vials, 10 vials containing 15 flies each were tipped onto new food thrice a week and scored for the number of dead flies during each tip. survival of each fly line was calculated, and the data was plotted as survival curves and tested for significant differences using the Log-Rank (Mantel-Cox) Test. P<0.05 was considered significant.

No notable changes in the median lifespan of *pirk* RNAi Trip that have Pirk protein knocked down either in the enterocytes via *np1*- GAL4 (p=0.0751) or in the intestinal stem cells via *esg*- GAL4 (p=0.3165) were observed.

4.2.2.1. Effect of *pirk* knock down on sleep and locomotion in the gut progenitor cells *(via esg Gal4)*

Effects on Sleep and locomotion

Young Flies

Here we see a median rise of 93.01 minutes in total minutes of sleep in 6-day old $pirk^{esg}$ KK RNAi (p<0.0001, n=32) but not in $pirk^{esg}$ Trip RNAi female flies (p=0.0953, n=32) **(Figure 50A)**. This increase in sleep was also observed during daytime sleep in both KK and Trip RNAi flies, with a median rise of 72 minutes in KK flies (p=0.0004, n=32) and that of 50 minutes in Trip flies (p=0.0444, n=32) **(Figure 50B)**. During night-time sleep we see a median increase of 23.54 minutes in $pirk^{esg}$ KK flies (p=0.0011 n=32), and once again, not in $pirk^{esg}$ Trip flies (p=0.9814, n=32) **(Figure 50C)**.

We see that when examined over a period of 24-hours, a median decline of 15.96 episodes is observed in $pirk^{esg}$ RNAi KK flies (p<0.0001, n=32) with respect to their controls, and a less striking but significant median reduction of 7.154 $pirk^{esg}$ Trip flies (p=0.0086, n=32) is observed **(Figure 50D)**. With the number of daytime sleep episodes, we see a median fall of 10 episodes in $pirk^{esg}$ KK flies (p<0.0001, n=32) and that of 9 episodes in young $pirk^{esg}$ RNAi Trip female flies (p<0.0001, n=32) **(Figure 50E)**. Lastly, with the number of night-time sleep episodes, we see a median decline of 5 episodes in $pirk^{esg}$ KK flies (p=0.0001, n=32). However, no noteworthy change is observed in $pirk^{esg}$ Trip flies (p=0.6519, n=32) **(Figure 50F)**.

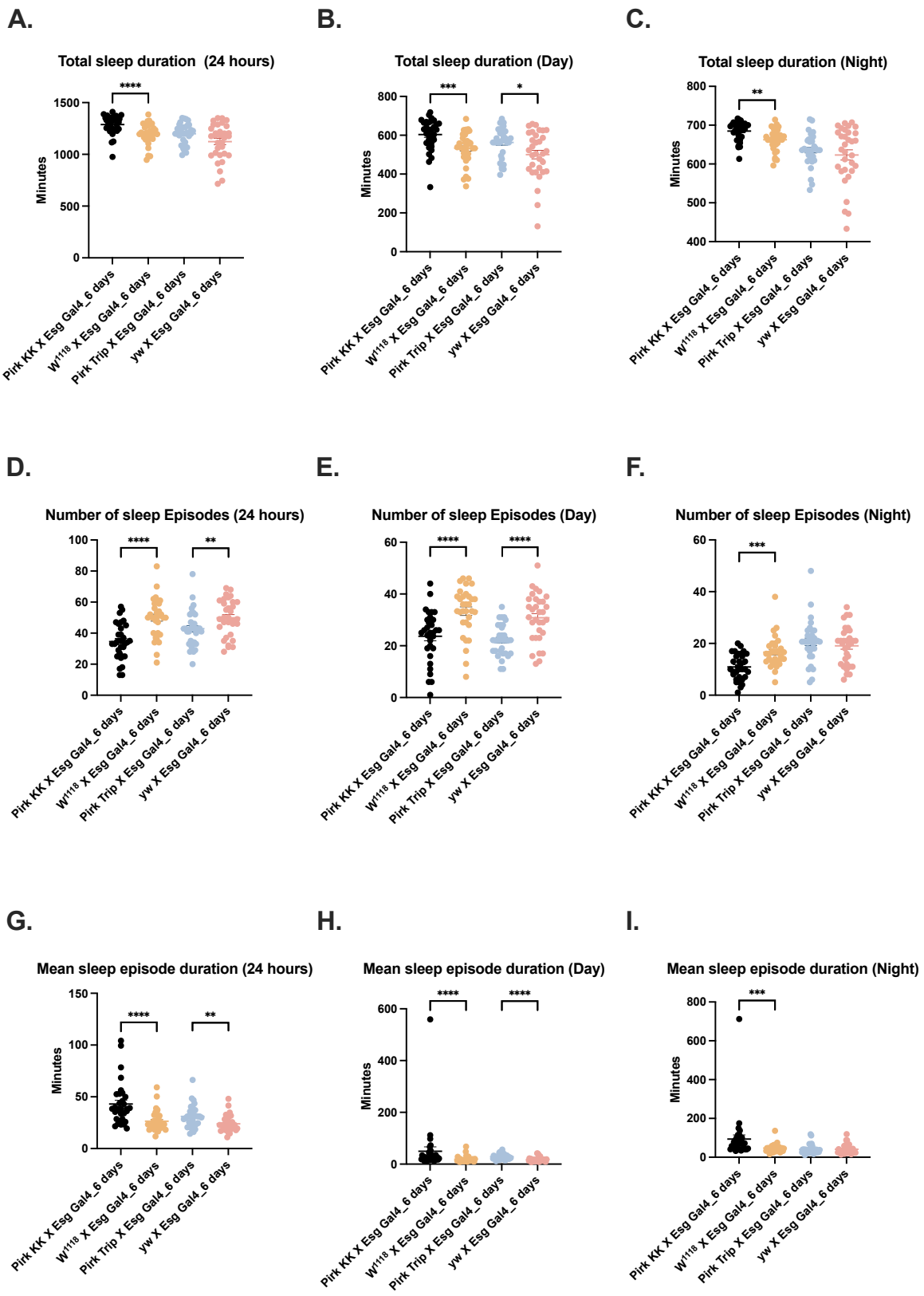

Figure 50: The effect of gut progenitor cells knock down of pirk on sleep profiles of 6-days old Pirk female flies compared to their controls. Three independent repeats were conducted for each genotype, and 32 flies were randomly selected from these repeats, resulting in a total sample size (n) of 32. These 32 flies were then analysed, and a Mann Witney Rank sum test was performed between mutant flies and their respective controls, without consideration of age-dependent analysis. Non-significant results were not marked and $p \leq 0.05$ (*), ≤ 0.01 (**), ≤ 0.001 (***), ≤ 0.0001 (****).

When it comes to mean sleep episodes, a significant increase is observed in *pirk*^{esg} RNAi KK flies during the 24-hour period ($p<0.0001$, $n=32$), during daytime ($p<0.0001$, $n=32$), as well as during night-time ($p=0.0005$, $n=32$) **(Figure 50(G-I))**. However, in contrast, no notable change is observed in *pirk*^{esg} RNAi Trip flies, during night-time sleep ($p=0.9442$, $n=32$), but a significant increase is observed during a 24-hour period ($p=0.0015$, $n=32$) and daytime sleep ($p<0.0001$, $n=32$) compared to their controls **(Figure 50(G-I))**.

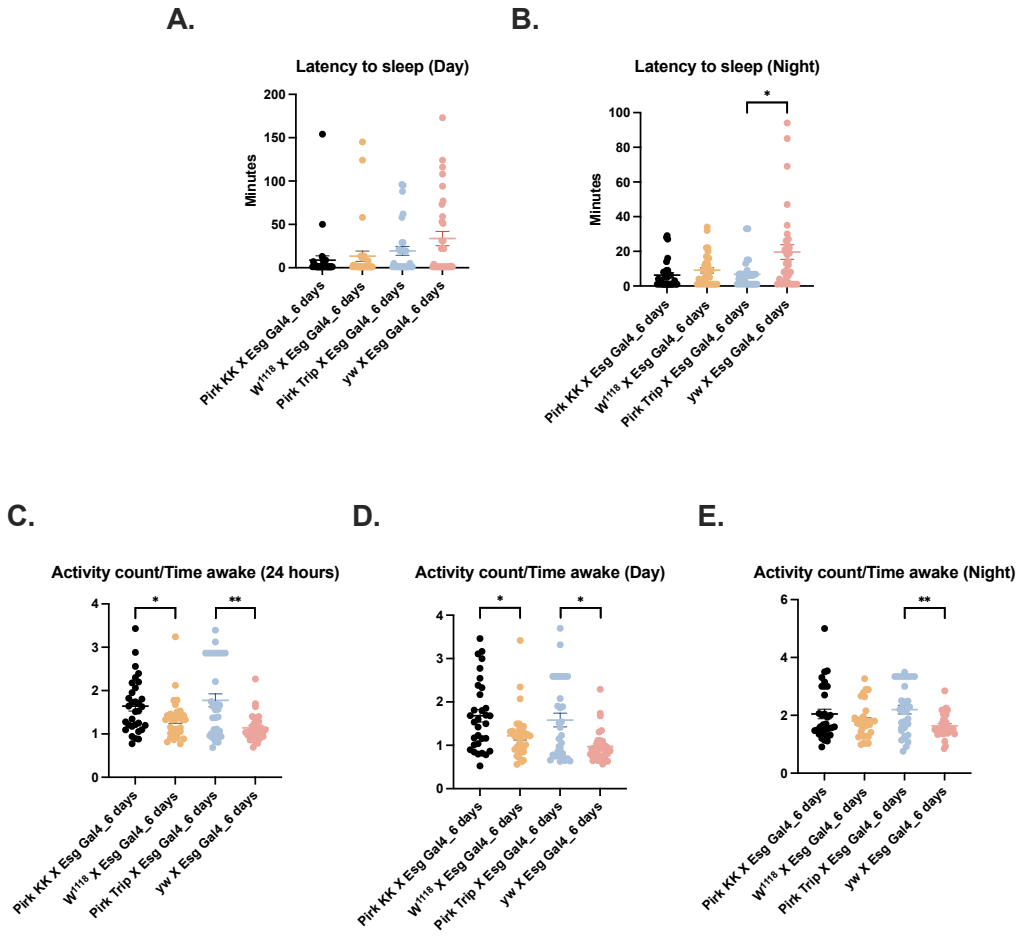

Figure 51: The effect of in gut progenitor cells specific knock down of *pirk* on latency to sleep and activity count / time awake of 6-day old *Pirk* female flies compared to their controls. Three independent repeats were conducted for each genotype, and 32 flies were randomly selected from these repeats, resulting in a total sample size (n) of 32. These 32 flies were then analysed, and a Mann Witney Rank sum test was performed between mutant flies and their respective controls, without consideration of age-dependent analysis. Non-significant results were not marked and $p \leq 0.05$ (*), ≤ 0.01 (**), ≤ 0.001 (***), ≤ 0.0001 (****).

Latency to sleep was not significantly affected by the knock down of Pirk protein in the gut progenitor cells via *esg* GAL4 in either 6-day old *pirk* KK flies (p=0.2761, n=32) or $pirk^{esg}$ Trip female flies (p=0.4069, n=32) during daytime sleep **(Figure 51A)**. Additionally, no noteworthy observation was made in $pirk^{esg}$ RNAi KK flies during night-time sleep (p=0.1076, n=32). However, we observed a slight increase in latency during night-time sleep in 6-day old $pirk^{esg}$ RNAi female flies compared to its respective control (p=0.0119, n=32) **(Figure 51B)**.

We observe a significant rise in rate of activity in both 6-day old $pirk^{esg}$ RNAi KK flies (p=0.0282, n=32) and Trip flies (p=0.0029, n=32) during a 24-hour period **(Figure 51C)**. Similar to this, a significant increase in activity count per time awake in both 6-day old $pirk^{esg}$ RNAi KK flies (p=0.0151, n=32) and Trip flies (p=0.0106, n=32) was also recorded **(Figure 51D)**. However, no notable change was observed in KK flies during night-time sleep (p=0.5504, n=32) but a notable rise in rate of activity in Trip flies with p=0.0065 (n=32) **(Figure 51E)**.

Older flies

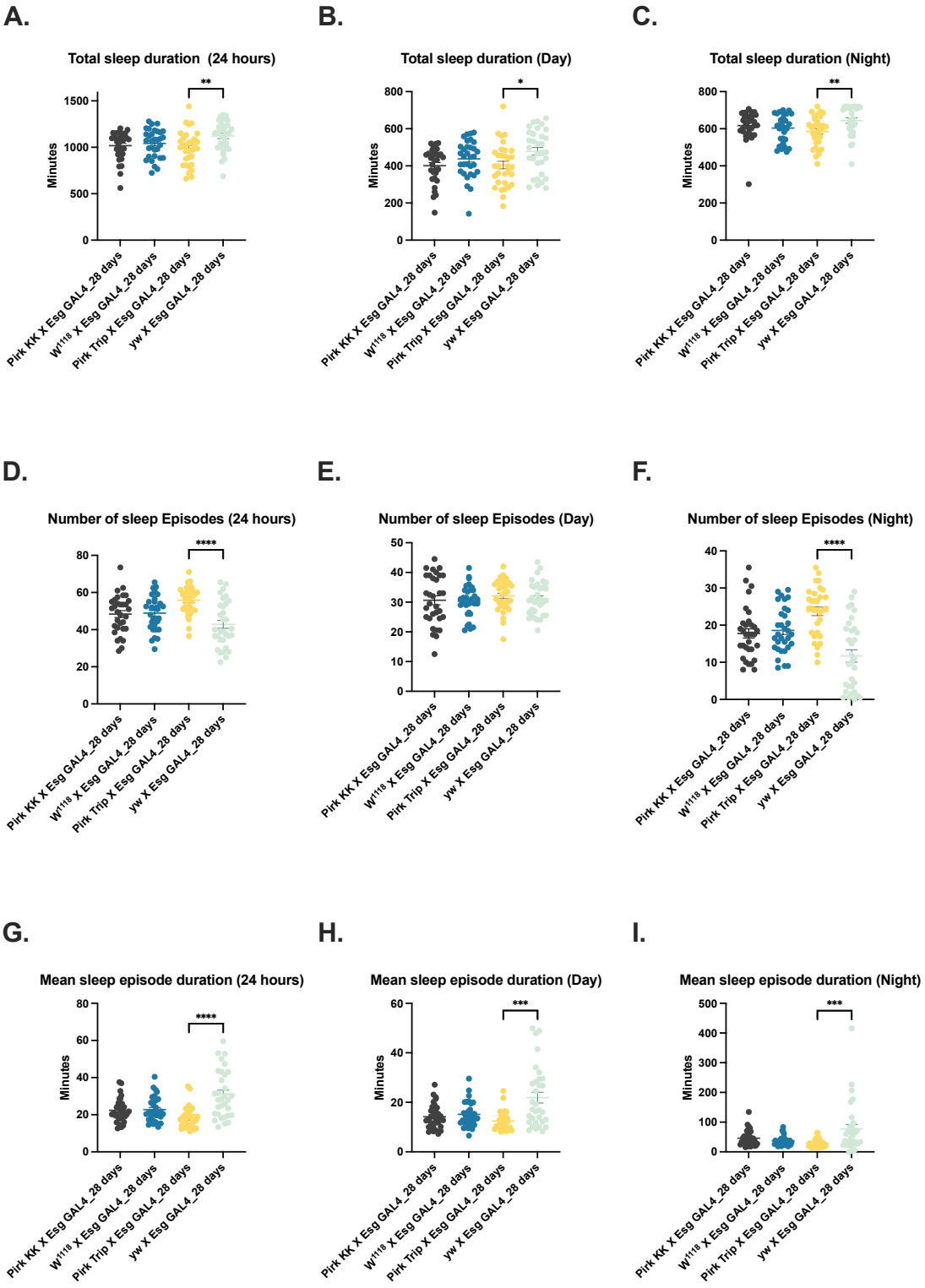

Figure 52: The effect of gut progenitor cells knock down of *pirk* on sleep profiles of 28-days old *pirk* female flies compared to their controls. Three independent repeats were conducted for each genotype, and 32 flies were randomly selected from these repeats, resulting in a total sample size (n) of 32. These 32 flies were then analysed, and a Mann Witney Rank sum test was performed between mutant flies and their respective controls, without consideration of age-dependent analysis. Non-significant results were not marked and $p \leq 0.05$ (*), ≤ 0.01 (**), ≤ 0.001 (***), ≤ 0.0001 (****).

With respect to total sleep, no significant change was observed in 28-day old *pirk*^{esg} KK Flies in a 24-hour period (p=0.6005, n=32), during the day (p=0.1112, n=32) or during the night (p=0.4367, n=32) **(Figure 52(A-C))**. Further, 28-day old *pirk*^{esg} Trip flies display decreased sleep duration during the 24-hour period (p=0.0028, n=32) with a median fall of 14.3 minutes as well as an increase in sleep time during the day (p=0.0158, n=32) with a median decline of 77 minutes **(Figure 52(A-C))**. Lastly, the median reduction at night (p=0.0030, n=32) is 62.50 minutes was also observed.

When looking at number of sleep episodes in 28-day old *pirk*^{esg} KK flies, no significant difference is observed in the 24-hour period (p=0.8388, n=32) or during the day (p=0.9071, n=32), but an increase is noticed at night (p=0.5910, n=32) **(Figure 52(D-F))**. However, when looking at number of sleep episodes in 28-day old *pirk*^{esg} Trip flies, median increase of 14 episodes was noted during the 24-hour observation period (p<0.0001, n=32) and that of 12.5 episodes was observed during night-time sleep (p<0.0001, n=32) but not during daytime sleep (p=0.3721, n=32) **(Figure 52(D-F))**.

With respect to mean sleep duration in 28-day old *pirk*^{esg} KK flies, no significant difference is seen in the 24-hour observation period (p=0.8572, n=32) **(Figure 52G)** or during the day (p=0.4912, n=32) **(Figure 52H)**. An increase, however, is observed at night (p=0.2642, n=32) **(Figure 52I)**.

Conversely, a stark decline in mean sleep episode duration is observed in the 28-day old *pirk*^{esg} Trip flies in the 24-hour period (p<0.0001, n=32) with a median reduction of 10.8 minutes, during the day (p=0.0003, n=32) with a median drop of 5.692 minutes, as well as at night (p=0.0003, n=32) with a median decrease of 24.34 minutes versus their controls (**Figure 52(G-I)**).

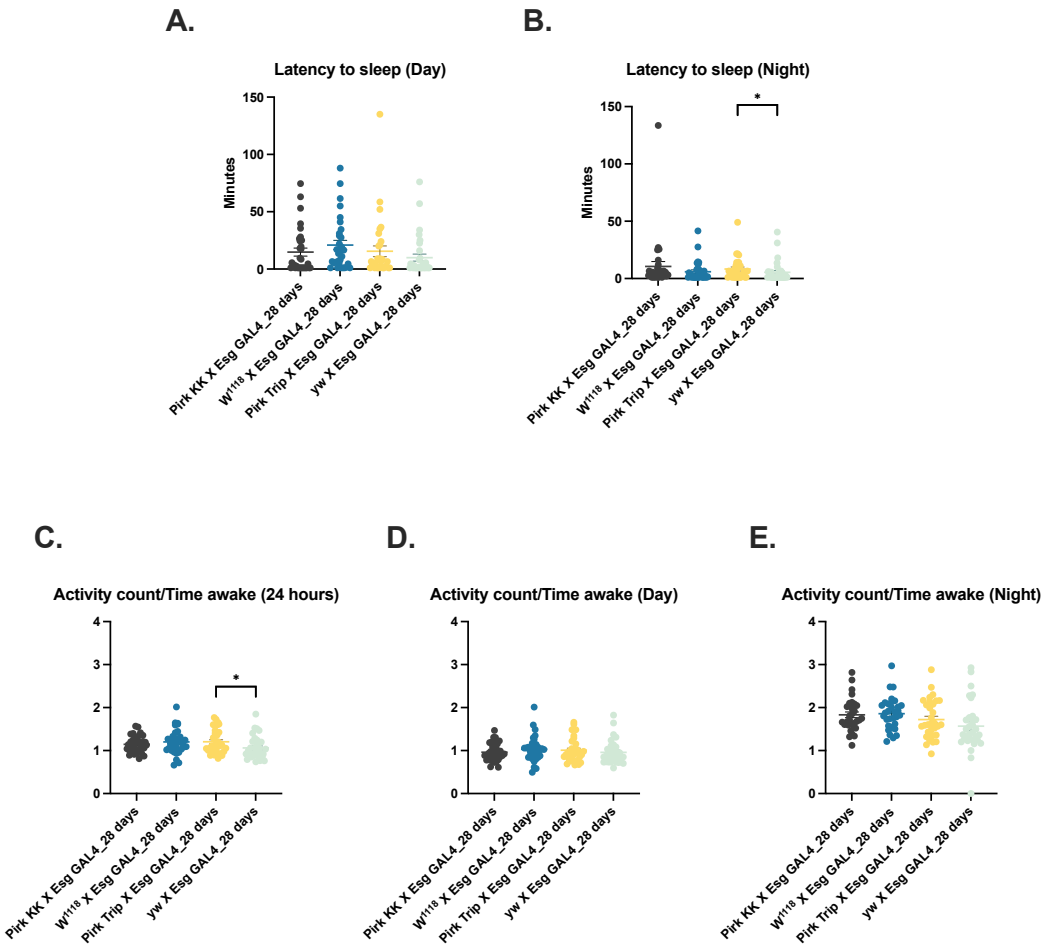

Figure 53: The effect of in gut progenitor cells specific knock down of *pirk* on latency to sleep and activity count/time awake of 28-day old *pirk* female flies compared to their controls. Three independent repeats were conducted for each genotype, and 32 flies were randomly selected from these repeats, resulting in a total sample size (n) of 32. These 32 flies were then analysed, and a Mann Witney Rank sum test was performed between mutant flies and their respective controls, without consideration of age-dependent analysis. Non-significant results were not marked and p≤ 0.05 (*), ≤ 0.01 (**), ≤ 0.001 (***), ≤ 0.0001 (****).

Latency to sleep was not significantly affected by knock down of $pirk^{esg}$ protein in gut enterocytes (via *esg* GAL4) in older $pirk^{esg}$ RNAi KK female flies with p=0.1049 (n=32) during daytime sleep and p=0.1010 (n=32) during night-time sleep **(Figure 53 (A-B))**. Even though we did not see any notable change in latency during daytime of 28-day old $pirk^{esg}$ RNAi Trip flies (p=0.1305, n=32) we recorded a median rise of 2 minutes during night-time (p=0.0467, n=32) **(Figure 53 (A-B))**.

When observing activity count in 28-day old *pirk*^{esg} KK female flies, we do not see any significant difference in either of the three time periods: the 24-hour period (p=0.4059, n=32) **(Figure 53 C)**, or during the day (p=0.3050, n=32) **(Figure 53 D)**, or at night (p=0.7238, n=32) **(Figure 53 E)**. However, when observing activity count in 28-day old *pirk*^{esg} Trip female flies, a slight increase is observed in the 24-hour period (p=0.0206, n=32) but no notable effect was observed during the day (p=0.3195, n=32), or at night (p=0.1953, n=32) **(Figure 53 (D-E))**.

4.2.1.3. Effect of pirk Knock down on sleep and locomotion on gut enterocytes (*np1* GAL4)

Young Flies

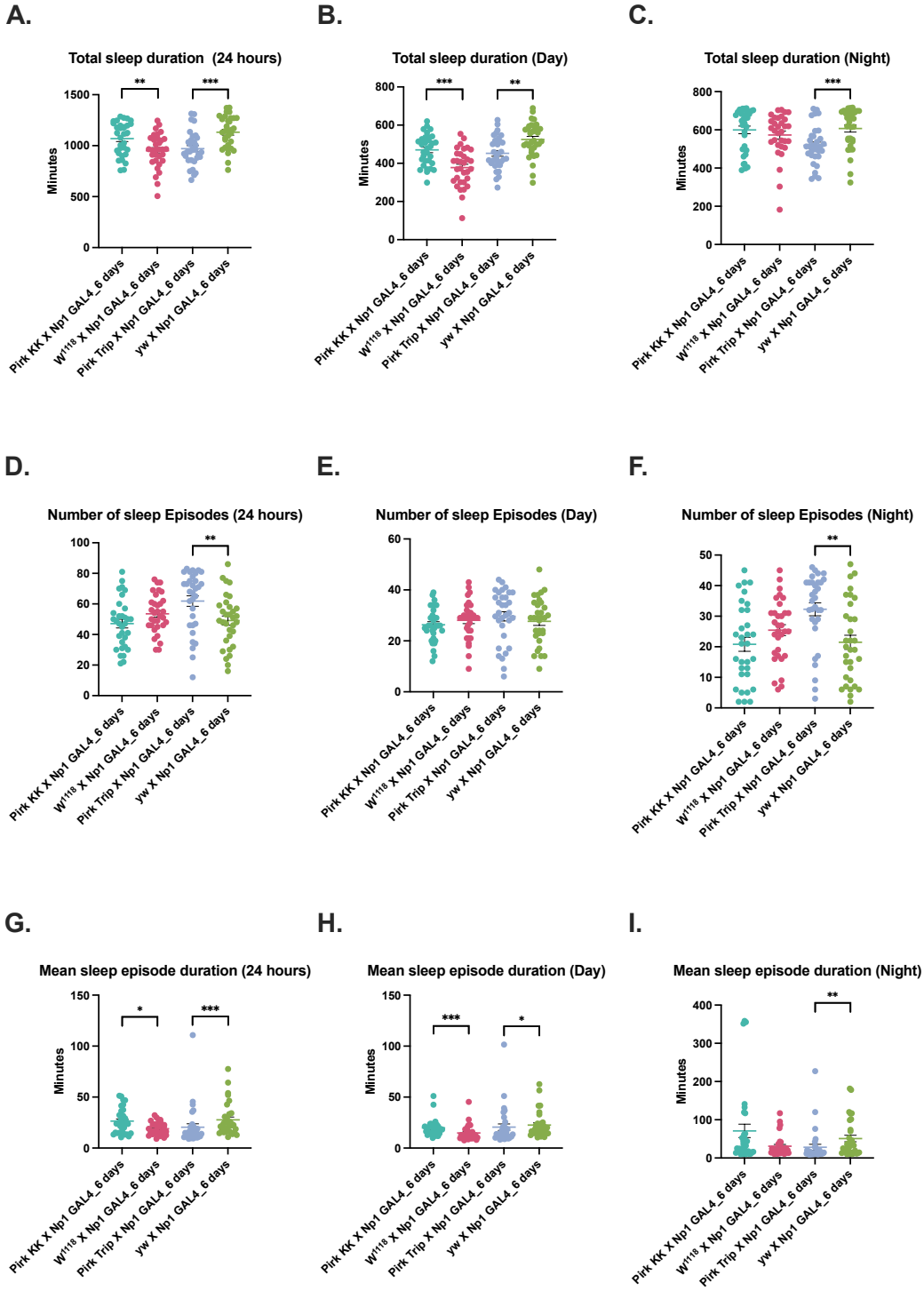

Figure 54: The effect of gut enterocytes knock down of *pirk* on sleep profiles of 6-days old pirk female flies compared to their controls. Three independent repeats were conducted for each genotype, and 32 flies were randomly selected from these repeats, resulting in a total sample size (n) of 32. These 32 flies were then analysed, and a Mann Witney Rank sum test was performed between mutant flies and their respective controls, without consideration of age-dependent analysis. Non-significant results were not marked and p≤ 0.05 (*), ≤ 0.01 (**), ≤ 0.001 (***), ≤ 0.0001 (****).

When observing the total sleep duration in 6-day old *pirk*^{np1} RNAi KK female flies, we see a significant increase in the 24-hour period (p=0.0058, n=32), with a median difference of 122 minutes and during the day (p=0.0002, n=32) with a median difference of 90 minutes. We did not, however, see a significant difference at night (p=0.1976, n=32) **(Figure 54(A-C))**. Conversely, when observing the total sleep duration in 6-day old *pirk* Trip female flies crossed with *np1* flies, we see a decrease in the 24-hour period (p=0.0001, n=32) with a median decline of 178 minutes **(Figure 54A)**, during the day (p=0.00014, n=32) **(Figure 54B)** with a median fall of 77.50 minutes, as well as at night (p=0.0009, n=32) with a median fall of 105.5 minutes **(Figure 54C)**.

We do not see a significant difference in the number of sleep episodes in either of the three time points: the 24-hour period (p=0.0887, n=32) or during the day (p=0.2334, n=32), or at night (p=0.0925, n=32) **(Figure 54(D-F))**. Further, when observing the number of sleep episodes in 6-day old *pirk*^{np1} Trip female flies, we note a significant increase in number of sleep episodes during a 24-hour period (p=0.0054, n=32), as well as at night-time (p=0.0016, n=32). However, we do not see a significant difference during daytime sleep (p=0.2372, n=32) **(Figure 54(D-F))**.

The duration of mean sleep episodes was notably impacted following the reduction of *pirk* protein in the gut enterocytes using *np1* GAL4. We observed a notable median rise of 5.520 minutes in 6-day old *pirk*^{np1} KK female flies (p=0.0177, n=32) and a stark median reduction of 7.076 minutes in *pirk*^{np1} RNAi Trip female flies (p=0.0005, n=32) **(Figure 54G)**. Similarly, we saw a notable increase in 6-day old *pirk* KK RNAi flies during daytime sleep (p=0.0004, n=32) but a decline in *pirk*^{np1} Trip flies (p=0.0350, n=32) **(Figure 54H)**. We did not, however, see a noteworthy change in *pirk*^{np1} KK RNAi flies during night-time sleep (p=0.1127, n=32) but saw

a notable median decline of 13.43 minutes in *pirk*^{np1} Trip RNAi female flies (p=0.0020, n=32) compared to their controls **(Figure 54I)**.

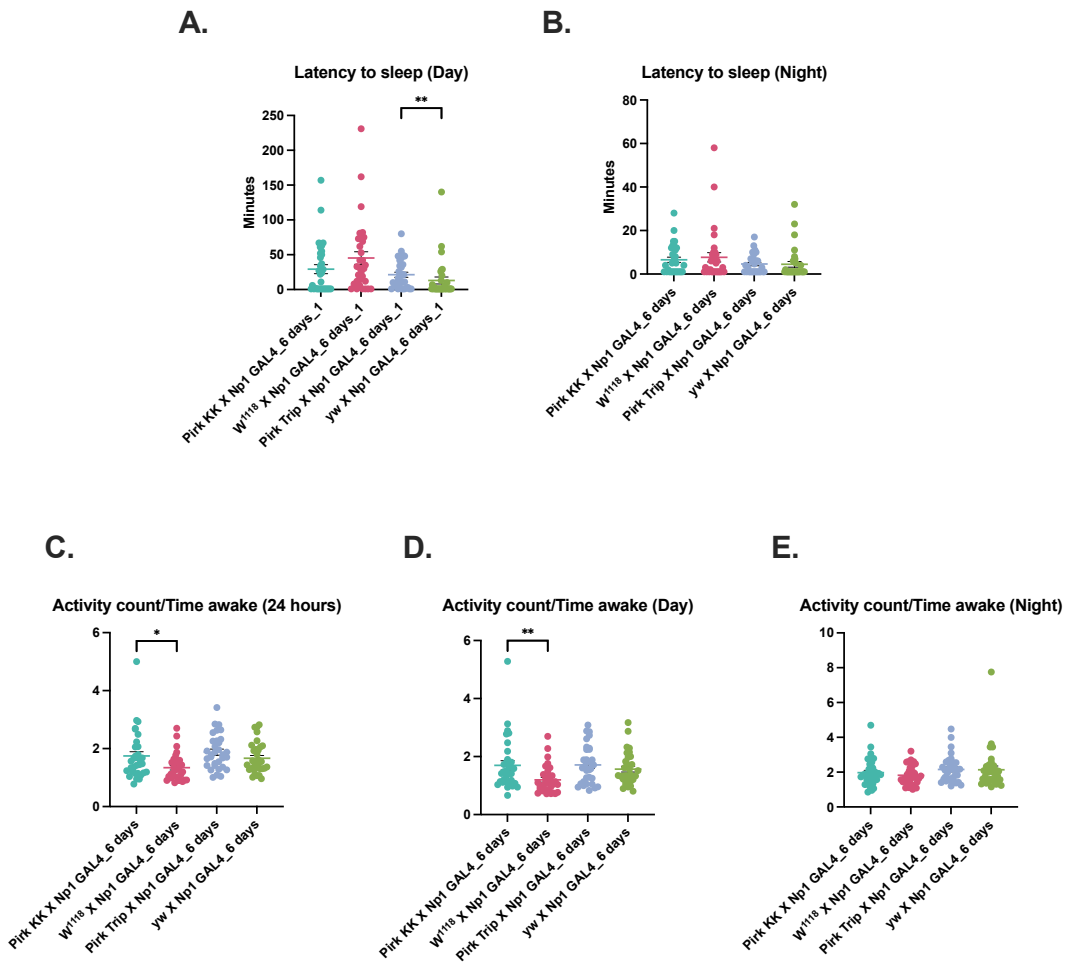

Figure 55: The effect of in gut enterocytes specific knock down of *pirk* on latency to sleep and activity count/time awake of 6-day old *pirk* female flies compared to their controls. Three independent repeats were conducted for each genotype, and 32 flies were randomly selected from these repeats, resulting in a total sample size (n) of 32. These 32 flies were then analysed, and a Mann Witney Rank sum test was performed between mutant flies and their respective controls, without consideration of age-dependent analysis. Non-significant results were not marked and p≤ 0.05 (*), ≤ 0.01 (**), ≤ 0.001 (***), ≤ 0.0001 (****).

When observing the latency to sleep in 6-day old *pirk*^{np1} KK female flies, we do not see a significant difference either during the day (p=0.0859, n=32) or at night (p=0.7742, n=32) **(Figure 55(A-B))**. Further, when observing the latency to sleep in 6-day old *pirk*^{np1} Trip female flies, we see a significant decrease during the day (p=0.0030, n=32) but not during night-time (p=0.2025, n=32) **(Figure 55(A-B))**.

The activity count in 6-day old *pirk*^{np1} KK female flies recorded a significant decrease in rate of activity during the 24-hour period (p=0.0191, n=32) and during the day (p=0.0028, n=32), but no notable change during night-time (p=0.4940, n=32) **(Figure 55(C-E))**.

Similarly, when observing the activity count in 6-day old *pirk*^{np1} Trip female flies, we do not see a significant difference either during the 24-hour period (p=0.1576, n=32), during the day (p=0.5089, n=32), or at night (p=0.2879, n=32) **(Figure 55(C-E))**.

Older

While observing the total sleep duration in 28-day old *pirk*^{np1} RNAi KK female flies, we do not see a significant difference either during the 24-hour period (p=0.6867, n=32) **(Figure 56A)** or at night (p=0.1709, n=32) **(Figure 56C)**. We do however, see a significant median reduction of 67.50 minutes during the daytime sleep (p=0.0119, n=32) **(Figure 56B)**.

Furthermore, while observing the total sleep duration in 28-day old *pirk*^{np1} Trip female flies, we see a median decrease of 95.25 minutes during the 24-hour period (p=0.0010, n=32) **(Figure 56A)**, that of 49.25 minutes during daytime sleep (p=0.0182, n=32) and that of 57.25 minutes during night-time sleep (p=0.0127, n=32), compared to their respective controls **(Figure 56(B-C))**.

The number of sleep episodes of 28-day old *pirk*^{np1} KK female flies showed no notable differences in either of the three time points: the 24-hour period (p=0.0778, n=32), during daytime (p=0.0743, n=32), or at night-time (p=0.3724, n=32) **(Figure 57(D-F))**. Conversely, a strong association between the number of sleep episodes in 28-day old *pirk*^{np1} Trip RNAi crossed to *np1* GAL4 was observed during the course of the day (p=0.0002, n=32), during daytime sleep (p=0.0073, n=32), as well as at night (p=0.0017, n=32) **(Figure 57(D-F))**.

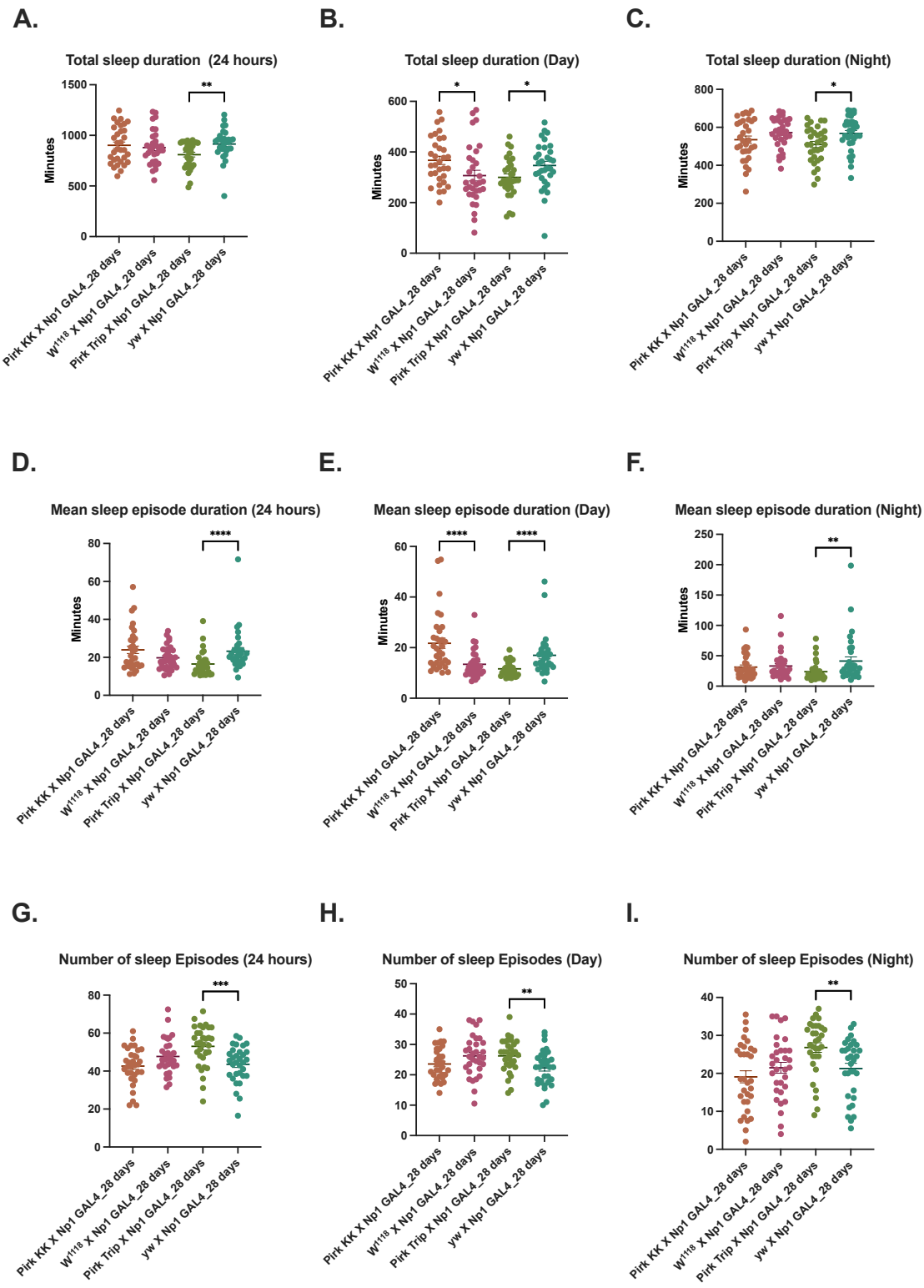

Figure 56: The effect of gut enterocytes knock down of pirk on sleep profiles of 28-days old *pirk* female flies compared to their controls. Three independent repeats were conducted for each genotype, and 32 flies were randomly selected from these repeats, resulting in a total sample size (n) of 32. These 32 flies were then analysed, and a Mann Witney Rank sum test was performed between mutant flies and their respective controls, without consideration of age-dependent analysis. Non-significant results were not marked and p≤ 0.05 (*), ≤ 0.01 (**), ≤ 0.001 (***), ≤ 0.0001 (****).

We saw no notable changes in the mean sleep episode duration during the course of a 24-hour period (p=0.2109, n=32) or during night-time in *pirk*^{np1} RNAi KK flies (p=0.5262, n=32). However, we observe a sharp median increase of 5.870 minutes during daytime sleep p<0.0001, n=32) **(Figure 56(G-I))**. In addition to this, we observed a significant decline in mean sleep episode duration in 28-day old *pirk*^{np1} Trip female flies in all time parameters, with a median change of 5.820 minutes and p<0.0001 (n=32) during a 24-hour period, that of 3.927 and p<0.0001 (n=32) during daytime sleep and finally of 7.527 minutes during night-time sleep (p=0.0029, n=32) **(Figure 56(G-I))**.

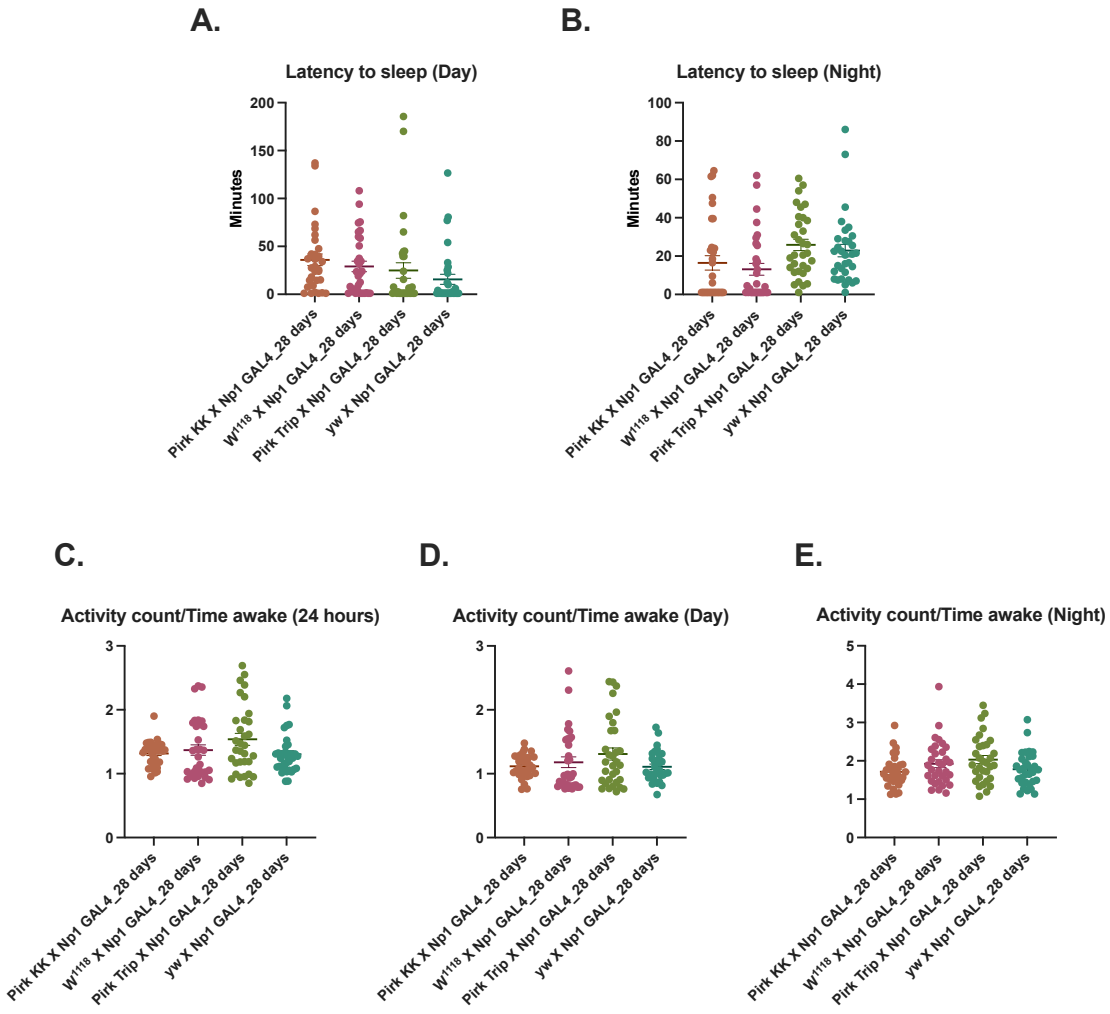

Figure 57: The effect of in gut enterocytes specific knock down of *pirk* on latency to sleep and activity count/time awake of 28-day old *pirk* female flies compared to their controls. Three independent repeats were conducted for each genotype, and 32 flies were randomly selected from these repeats, resulting in a total sample size (n) of 32. These 32 flies were then analysed, and a Mann Witney Rank sum test was performed between mutant flies and their respective controls, without consideration of age-dependent analysis. Non-significant results were not marked and p≤ 0.05 (*), ≤ 0.01 (**), ≤ 0.001 (***), ≤ 0.0001 (****).

When observing the latency to sleep in 28-day old $pirk^{np1}$ KK female flies, we do not see a significant difference either during the day (p=0.2877, n=32) or at night (p=0.9176, n=32) **(Figure 57(A-B))**. Similarly, when observing the latency to sleep in 28-day old $pirk^{np1}$ Trip female flies, we do not see a significant difference either during the day (p=0.3980, n=32) or at night (p=0.4057, n=32) **(Figure 57(A-B))**. Similar to latency to sleep, while observing the activity count in 28-day old $pirk^{np1}$ KK female flies, we do not see a significant difference during the 24-hour period (p=0.4752, n=32), during the day (p=0.3964, n=32), or at night (p=0.1537, n=32) **(Figure 57(D-F))**.

Furthermore, while observing the activity count in 28-day old $pirk^{np1}$ Trip female flies, we do not see a significant difference either of the three time periods: the 24-hour (p=0.1002, n=32), during the day (p=0.4427, n=32), or at night-time (p=0.1002, n=32) **(Figure 57(D-F))**.

Summary

In our study of brain tissue, significant variations were observed in the lifespan and climbing ability of $pirk^{elav}$ and $pirk^{repo}$ flies. While $pirk^{elav}$ KK and $pirk^{repo}$ KK flies exhibited an increase in median lifespan, $pirk^{elav}$ Trip flies showed a notable decline. Climbing ability declined in older KK flies, but remained unchanged in Trip flies. Furthermore, our analysis of sleep and activity in $pirk^{elav}$ flies revealed dynamic changes as they aged. Initially, no significant alterations were noted in young flies, but with age, $pirk^{elav}$ Trip flies experienced a reduction in sleep across all periods, while $pirk^{elav}$ KK flies displayed stable sleep patterns.

In flies with Pirk knockdown in glial cells, distinct sleep phenotypes were observed. Both $pirk^{repo}$ KK and Trip flies exhibited increased total sleep, albeit with differences in sleep episode frequency and duration. However, as these flies aged, the strength of sleep phenotypes weakened, particularly in $pirk^{repo}$ Trip flies, which showed reduced total sleep and increased

sleep episodes. Conversely, *pirk*^{repo} KK flies demonstrated increased sleep duration with age. Our findings suggest complex interactions between Pirk knockdown and age-related changes in sleep patterns.

In gut tissue, we observed a significant increase in median lifespan in *pirk* RNAi KK flies with Pirk protein knocked down in intestinal stem cells (*esg*-GAL4). Among 6-day-old *pirk*^{esg} KK flies, there was an increase in sleep duration across all time periods, while Trip flies showed heightened daytime sleep. At 28-days of age, *pirk*^{esg} KK and Trip flies did not show sleep phenotypes as strongly as earlier in their lifespan. Conversely, when Pirk was expressed solely in gut enterocytes, *pirk*^{np1} KK flies exhibited increased total and daytime sleep, while *pirk*^{np1} Trip flies slept significantly less than controls. As flies aged, *pirk*^{np1} Trip phenotypes persisted, with a decline in total sleep and increased sleep episodes, while *pirk*^{np1} KK line showed increased mean sleep episode duration during daytime sleep.

Lastly, these observed changes may stem from differences in KK lines versus Trip lines or from their individual genetic background. However, intriguingly, we find similarities in young *pirk*^{repo} and *pirk*^{esg} flies. Given that *pirk* is expressed in intestinal stem cells, coupled with our lab's observation of IMD playing a significant role in glial cells, the outcome is not unexpected. We anticipate both the nervous system and the gut to play contributory roles in the neurological phenotypes observed in *pirk* mutant flies

CHAPTER FIVE

Exploring the influence of a constitutive active immune response on drosophila gut microbiota

CHAPTER FIVE:

EXPLORING THE INFLUENCE OF A CONSTITUTIVE ACTIVE IMMUNE RESPONSE ON DROSOPHILA GUT MICROBIOTA

This chapter starts by exploring the composition of the gut microbiome using a culture-independent gut microbiota analysis technique known as 16s rRNA sequencing; to understand the microbial composition of the *pirk* mutant guts. To further examine if there is a direct relationship between the phenotypes observed in **Chapter 2** and the dysbiotic gut microbiome of *pirk* mutant flies, we then co-housed mutant flies with GF *yw* flies and analysed their sleep behaviour patterns.

Section 5.1: We start with an introduction into *Drosophila* gut microbiome, along with a brief explanation of the techniques that we use in this chapter.

Section 5.2 Investigates the effect of constitutively activate immune responseon the gut microbiome of female *pirk* mutant flies using 16s rRNA sequencing.

Section 5.3 Focuses on exploring the influence of local bacterial environment on *Drosophila* sleep and locomotion.

Finally, **section 5.4** provides a brief summary of the results.

5.1 INTRODUCTION

Studies investigating host microbial interactions have primarily focused on pathogens, however, it is worth noting that the immunological cost of interacting with a vast number of commensal microbes is high. A healthy gut needs a carefully balanced immune system that allows the beneficial microbes to thrive while eliminating harmful ones. In previous chapters we have explored the phenotypes of *pirk* mutant flies that are known to have a dysbiotic gut microbiome due to a constitutively active immune response in their guts. However, in this chapter we examine the microbial composition of the guts of *pirk* mutants by using 16s rRNA sequencing and further co-house these flies with germ free controls to investigate a direct role of bacterial families in the sleep phenotype observed.

The experiments in this chapter follow the 16srRNA sequencing experimental protocol outlined by Mistry, Kounatidis and Ligoxygakis (2017), with modifications made in the processing of *Wolbachia* during library prep (Bahuguna *et al.* 2022). Similarly, the co-housing experiment was inspired by work conducted by Mistry (2017) during her doctorate in the laboratory; however, adaptations have been introduced to accommodate any variabilities arising from the maternally transmitted microbiome in wild-type flies.

5.1.1. The Microbiome and its effect on the host

The mammalian gut is an integral yet complex organ responsible for harmonisation of immunometabolism, nutritional signalling and the hormonal network in the host. As mentioned in **Chapter 1**, dysregulation of intestinal epithelium functions significantly impacts host

physiology (Clemente *et al.* 2012; Valdes *et al.* 2018); and leads to devastating and complex diseases in humans, such as inflammatory bowel diseases, diabetes, allergy, intestinal cancers, and obesity (Round and Mazmanian 2009; Levy *et al.* 2017). It also serves as a modulator of several behaviour traits including, memory, learning, social and communicative behaviours, and mood (Vuong et al. 2017).

The animal gut harbours microorganisms, which are generally acquired by maternal vertical transmission, food and their surrounding environment (Wong et al. 2015; Jovel et al. 2017; Bunker et al. 2021). These microbes exist in variable compositions and are influenced by ecological conditions of the gut such as: variation in pH or redox potential of different regions of the gut, digestive enzymes, immune effectors or epithelial cell turnover, excess food flow, and change in production of mucus (Karasov and Douglas 2013). Our understanding of the microbiome and its interaction with the host has been limited. However, with the development of high throughput technology, the last decade has seen a surge in sequencing research that has enabled us to conceptualize the human body as a highly complex ecosystem (O'Hara and Shanahan 2006), proving that the microbiome is not just a bystander but an active influencer of host function.

In mice, several studies have illustrated the role of the gut microbiome in various physiological processes of the host including structural and metabolic maintenance of the gut homeostasis, absorption of nondigestible food residues and iron, IgA secretion and immune system development (Pickard et al. 2017; Hayes et al. 2018). Additionally, dysbiotic microbiome in mice have been shown to cause a number of diseases including gastrointestinal diseases (Nagao-Kitamoto *et al.* 2016a), Huntington's disease (Kong *et al.* 2020), Alzheimer's disease (Chen *et al.* 2020), Parkinson's disease (Wang *et al.* 2021a), IBD (Nagao-Kitamoto *et al.*

2016b) and diabetes (Abdellatif and Sarvetnick 2019). Germ free mice have been shown to be highly susceptible to infections; when challenged with pathogens such as *Shigella flexner* (Maier and Hentges 1972) and *Listeria monocytogenes* (Zachar and Savage 1979), the animals showed decreased immune response and increased mortality compared to their controls, illustrating the importance of a healthy microbiome in animals.

In humans, the microbiome influences disease physiology in a variety of complex ways, one of which is by delivering several biochemical cues that influence host physiology, further regulating homeostasis (O'Hara and Shanahan 2006; Jovel et al. 2017). As mentioned previously, the gut microbiome has been shown to be responsible for many facets of human health (Falony *et al.* 2016), including aspects of the immune system (Hakansson and Molin 2011; Levy *et al.* 2017), metabolic health (Rothschild *et al.* 2018) and neurobehavioral traits (Wiley *et al.* 2017). Hence, it is unsurprising that the gut microbiome plays a pivotal role in the development of complex diseases. The colonic bacteria are responsible to ferment indigestible fibre in human diets and synthesise(Gill *et al.* 2006). These SFA's help modulate the adaptive immune response by regulating cytokine production and expansion of regulatory T cells. Additionally, these SFA's have also been shown to influence brain function via the gut-brain axis (Silva, Bernardi and Frozza 2020; O'Riordan et al. 2022). The gut microbiome is also shown to be responsible for several metabolic disorders such as type 2 diabetes (Qin *et al.* 2012), obesity (Ley *et al.* 2005) and coronary heart disease (Rahman *et al.* 2022). There are several studies that link obesity to a dysbiotic gut, some even at a phylum level (reviewed in Zhao (2013)). Loman and van der Kamp (2016) demonstrated a reduction in the abundance of Bacteroidetes followed by an increase in *Firmicutes* and *Actinobacteria* in obese individuals. It was hypothesised that this dysbiosis is responsible for the activation of inflammatory pathways and likely results in impaired glucose homeostasis (Loman and van der Kamp 2016).

Animal models have been vital in investigating the role of the bacterial microbiome in complex diseases such as obesity (Ley *et al.* 2005; Turnbaugh *et al.* 2006; Bäckhed *et al.* 2007). For instance, studies on mice with either homozygous or heterozygous mutation in the *leptin* gene have shown several variations in microbiome including changes in the abundance of Bacteroidetes and Firmicutes in their gut (Ley *et al.* 2005; Turnbaugh *et al.* 2006). This result was also validated in human studies where obese individuals who were put on either a carbohydrate restrictive or a fat restricted diets show higher abundance of Bacteroidetes and a reduction in Firmicutes (Ruiz *et al.* 2017; Seganfredo *et al.* 2017).

Metagenome-wide association studies (MGWAS) have demonstrated the role of butyrate-producing bacteria and type 2 diabetes (Qin *et al.* 2012), along with a rise in abundance of several opportunistic bacteria such as *Bacteroides caccae*, several species of *Clostridium*, *Eggerthella lenta* and *Escherichia coli*. This was followed by an increase in both *Akkermansia muciniphila* (responsible for mucin degradation) and *Desulfovibrio* (sulfate-reducing bacteria) (Qin *et al.* 2012). Furthermore, this result was also validated in mouse models of type 2 diabetes (Plovier *et al.* 2017). As mentioned in **Chapter 1**, the microbiome has been shown to influence several neurodegenerative disorders (Socała *et al.* 2021). AD patients with amyloidosis show correlation with the abundance of proinflammatory bacteria taxa like *Escherichia/ Shigella* and anti-inflammatory ones like *Eubaterium rectale* (Cattaneo *et al.* 2017).

The microbial diversity of the invertebrate gut is far less than that of mammals, by an order of magnitude or two (Dillon and Dillon 2004; Dunn and Stabb 2005; Lehman, Lundgren and Petzke 2009; Morales-Jiménez *et al.* 2009). Even though there has been a significant effort to investigate the microbial diversity in mammals, these studies are limited by sampling errors caused by the influence of age and physiological conditions of the host (e.g. (Dethlefsen, McFall-Ngai and Relman 2007; Lehman, Lundgren and Petzke 2009). However, *Drosophila*

research allows us to overcome several of these limitations. The fruit fly has a simple gut microbiome composition that enables us to investigate the effects of commensal bacteria on host physiology.

Commensal bacteria play an essential role in the survival of many insects. The composition of the *Drosophila* gut microbiome has been shown to influence complex behaviour such as, rapid genomic adaptation (Rudman *et al.* 2019), reproductive choices (Sharon *et al.* 2010; Leftwich *et al.* 2017), sleep, memory (Silva, Bernardi and Frozza 2020), social behaviour, and mood (Vuong et al. 2017), to name a few (detailed in **Chapter 1**). In many organisms, the microbiome is critical for core physiology and is responsible for the survival of the host (Perlman *et al.* 2022). Axenic / germ free *Drosophila* are viable in laboratory settings but show severe developmental delays, highlighting the importance of these symbionts in early development (Elgart *et al.* 2016). Additionally, the fly possesses an exceptional amenability to experimental manipulations of the microbiome that allows researchers to economically create and maintain axenic, or germ-free animals (Kietz, Pollari and Meinander 2018).

Drosophila has been widely used to study the effect of microbiota on various physiological processes, including ageing, due to its exceptional amenability to experimental manipulations of the microbiome (Kuraishi, Hori and Kurata 2013b; Trinder *et al.* 2017; Gould *et al.* 2018; Ludington and Ja 2020b; Hrdina and Iatsenko 2022). The study of host mechanisms for microbiota management and host factors targeted by commensals is aided by the abundance of genetic, genomic, and molecular resources accessible in the *Drosophila* species. Furthermore, it is simple to get gnotobiotic animals that have a standardised microbiome. Not unexpectedly, *Drosophila* has been widely used to research the effect of microbiota on different physiological

processes, including ageing, because of its outstanding amenability to experimental changes of the microbiome.

5.1.2. Composition of Drosophila microbiome

Unlike humans who have a vast variety of bacterial species colonising their intestines (about 500-1000 species) (Ghosh and Pramanik 2021), the fly gut is relatively less diverse (2-30 species) (Broderick 2016; Arias-Rojas and Iatsenko 2022). However, like humans, where *Firmicutes* and *Bacteroidetes* are the dominant phyla (Johnson *et al.* 2017), the gut of the fruit fly is also dominated by *Firmicutes* along with *Proteobacteria* (also found in the human gut) (Adair *et al.* 2018).

Interestingly, several studies that explore natural populations of *Drosophila* melanogaster in different habitats have observed high variability and restricted bacterial diversity in flies, with microbiomes dominated by three species: *Acetobacteraceae, Enterobacteriaceae and Lactobacillales* (Adair *et al.* 2018). McMullen et al. (2021) analysed 96 isolates from wild flies and found *Enterobacterales, Lactobacillales*, and *Rhodospirillales* to be the dominant bacterial order using culture techniques. Chandler et al. (2011) observed greater diversity in wild caught flies from two geographic locations and found notable *Proteobacteria* in their studies. Additionally, Staubach et al. (2013) identified *Gluconobacter* genus as a core member of the microbiome of natural *Drosophila* species, illustrating the importance of dietary substrate in influencing the microbiome of wild caught flies. It is important to note that in the wild, the host species' identity seems to have a minor influence on the gut microbiome of wild *Drosophila*, and is primarily influenced by its food substrate (Staubach *et al.* 2013)

.

Moreover, laboratory flies are shown to have low bacterial diversity in their guts and are further dominated by two species that influence each other: *Acetobacter* and *Lactobacillus* (Wong, Chaston and Douglas 2013; Newell and Douglas 2014). Several studies have observed variation in the composition of the microbiome among different lines in the lab that are raised in uniform conditions, indicating that although the microbiome is acquired from the surroundings, it is filtered by the host (Sharon *et al.* 2010; Broderick and Lemaitre 2012). Obadia et al.'s (2017) study elucidated the establishment of stable associations between a diverse array of species and the *Drosophila* gut. This process, although fundamentally stochastic, is instrumental in the formation of the microbiome and contributes significantly to the organism's ability to combat infections (Obadia *et al.* 2017).

However, studies such as Broderick and Lemaitre (2012) and Blum et al. (2013) have suggested that the microbiome is extremely dynamic, and flies need to be constantly exposed to bacteria to retain the beneficial microbes in their guts (Broderick and Lemaitre 2012; Blum *et al.* 2013; Storelli *et al.* 2018). Interestingly, Blum et al. (2013) and Pais et al. (2018) showed that flies frequently transferred into sterile food eventually lose their microbiome and become germ free. Therefore, *Drosophila* is dependent on the substrate in establishing and maintaining its gut microbiome.

IMD/Relish signalling pathway has been shown to regulate microbiome / pathogen dependent changes in the midgut transcriptome that lead to regulation of host digestion and metabolism (Erkosar and Leulier 2014). Moreover, previous studies in our lab have shown that the microbiome composition of flies with a constitutively active immune system in the gut (*pirk;trbd*) had distinct diversity patterns and densities across their lifespan compared to their *yw* controls (Mistry, Kounatidis and Ligoxygakis 2017). The study illustrated the significance

of investigating constitutively active immunity, as opposed to relying solely on immune-deficiency models, to gain insights into the complexities of inflammation. It achieves this by demonstrating the impact of the dysbiotic microbiome in *pirk;trbd* flies, emphasising a notable increase in gut cell death in contrast to their controls (Mistry, Kounatidis and Ligoxygakis 2017). This observation not only emphasises on the critical role of constitutive immune activation but also highlights the importance of considering gut dysbiosis when investigating the intricate interactions between the immune system and the microbiome.

5.1.3 Wolbachia

40%-70% of all arthropods (including *Drosophila*) are estimated to be infected with an intra-cellular facultative endosymbiont known as *Wolbachia* (Hilgenboecker *et al.* 2008; Zug and Hammerstein 2012). *Wolbachia* infects the germ line and are generally vertically transmitted between generations (Werren, Baldo and Clark 2008). The reason for its success has been thought to be due to its ability to manipulate the host's reproductive processes and enhance the selection of infected females and further its transmission (Werren, Baldo and Clark 2008). *Wolbachia* is known to cause reproductive distortion and further cause impaired reproductive behaviours such as: sperm-egg cytoplasmic incompatibility (CI) (Holden, Jones and Brookfield 1993; Hedges *et al.* 2008; Werren, Baldo and Clark 2008), parthenogenesis induction, feminization, and male killing / aggression (Rohrscheib *et al.* 2015; Vale and Jardine 2015)

Additionally, *Wolbachia* has been shown to affect host physiology in a number of ways including protection of the host from positive strand RNA viruses (Hedges *et al.* 2008; Teixeira, Ferreira and Ashburner 2008; Osborne *et al.* 2012; Martinez *et al.* 2014), immunity (Moreira *et al.* 2009; Bian *et al.* 2010; Kambris *et al.* 2010; Wong *et al.* 2011) lifespan (Kambris *et al.* 2010; Chrostek and Teixeira 2015), fecundity (Fast *et al.* 2011; Zhao *et al.*

2013; Caragata *et al.* 2014) stem cell activity (Fast *et al.* 2011), apoptosis, insulin signalling, sleep (Bi *et al.* 2018) and metabolism (Nikoh *et al.* 2014; Moriyama *et al.* 2015; Molloy *et al.* 2016). Despite being absent from gut lumen, *Wolbachia* has also been shown to affect host gut microbiome composition (Simhadri *et al.* 2017). This study demonstrated that the *Wolbachia* infected flies have a decreased abundance of *Acetobacter*. Furthermore, the study highlighted the importance of *Wolbachia* in gut microbiome composition throughout the developmental stages of the fly (Simhadri *et al.* 2017).

Due to its abundance in *Drosophila* cells, the read out of 16srRNA analysis of *Drosophila* gut is challenged by the presence of *Wolbachia* sequences (Wong, Chaston and Douglas 2013; Wilches, Coghlin and Floate 2021). Even though, *Wolbachia* is absent from the gut lumen (O'Neill *et al.* 1997; Jaenike *et al.* 2010), it has been shown to have a significant effect on the *Drosophila* microbiome (Early *et al.* 2017; Simhadri *et al.* 2017). Our study is therefore modified to try and remove / reduce this effect by digesting the 16s sequence of *Wolbachia* by treating the genomic DNA with restriction enzyme BstZ17I (R3594S, NEB, UK). This creates incisions at unique restriction sites only present in the 16s region of *Wolbachia* RNA (Bahuguna *et al.* 2022).

5.1.4 Age related changes in the gut composition of Drosophila

The composition of the fruit fly microbiome is dynamic and has been shown to vary with genetics, age and environmental changes (Nicholson *et al.* 2012). Female flies transfer their microbiome to their offspring by covering the egg with a sticky layer called the "chorion". The chorion becomes the first meal of the larvae, and the transferred microbiome develop into the first colonies of the gut microbiota (Broderick and Lemaitre 2012; Blum *et al.* 2013; Broderick,

Buchon and Lemaitre 2014). The larvae then spend the next four days ingesting bacteria and increasing their bacterial load from its surroundings till it is eventually replaced by the adult gut. The newly eclosed fly contains a small number of highly diverse bacteria in its gut and continue to ingest and acquire more bacteria from its surroundings that is contaminated by the excreta of the previous generations (Broderick and Lemaitre 2012; Blum *et al.* 2013).

Wong, Ng and Douglas (2011) demonstrated the microbiome composition of the Drosophila gut in different stages in its lifecycle (egg, larvae, pupae and adults). They showed that the fly gut is dominated by 5 major phyla; Firmicutes, Proteobacteria, Actinobacteria, Bacteroidetes, and Cyanobacteria. Additionally, greater than 60% of reads in early instar-larvae and young adults (3-7 days) were *Lactobacillus fructivorans* in both sexes with *L. plantarum* dominating the later larval stages (third-instar larvae). As the fly ages (3 to 5 weeks old), the representation of Acetobacteriace family increases, with *A. tropicalis* and *A. pomorum* dominating the gut. Interestingly, all these species were observed in the chorion with varying densities (Wong, Ng and Douglas 2011).

Although the microbiome has several beneficial effects on the host, the production of AMPs and ROS are result of the trade-off of harbouring microbes (Sannino *et al.* 2018). The host has a basal AMP and ROS production to regulate the microbiome and fight any potential pathogens. Nevertheless, this basal expression causes epithelial damage causing an increase in epithelial cell turnover (Li, Qi and Jasper 2016). As the fly ages, the bacterial load accelerates a decline in the ability for the gut barrier to renew itself, which then leads to compromised gut integrity. This gradual loss of barrier function coincides with a reduction of *Firmicutes* in the gut along with an increase with *Gammaproteobacteria* (Clark *et al.* 2015). Furthermore, this barrier malfunction has been shown to increase in Acetobacter composition in the gut along with a rise in immunological response and eventually host mortality (Clark *et al.* 2015).

5.1.5 Identification of the microbiome

Traditional approaches for identifying and characterising gut bacteria typically entail dilution plating on selective media, including but not limited to MRS, BHI, and bile esculin azide agar; followed by the examination of bacterial colonies (Cox and Gilmore 2007; Broderick, Buchon and Lemaitre 2014; Wong et al. 2015). However, standard culture techniques have several limitations; neither do they account for all the diversity in the environment (Donachie, Foster and Brown 2007), nor for the influence of physiochemical changes in the gut environment; like availability of oxygen, pH, variability of nutrients such as sugar etc (Riesenfeld, Schloss and Handelsman 2004). Additionally, it is difficult to identify the dominant families and how they influence the diversity (Riesenfeld, Schloss and Handelsman 2004). for development. Culture-independent techniques such as gel electrophoresis, qPCR (quantitative polymerase chain reaction)Finally, plating methods do not account for symbiotic or rival species that depend on one another's metabolic activities , FISH (fluorescence in situ hybridization) and NGS (next-generation sequencing) can be used to not only overcome the limitations of conventional plating techniques but also provide sensitive assays that can detect uncultivable (Zengler *et al.* 2002; Ingham *et al.* 2007) and low abundance bacterial families. Sequencing is a sophisticated technique that is commonly used in the identification of the gut microbiome. More specifically, amplifying the 16srRNA region of bacteria and aligning the sequences using BLAST (basic local alignment search tool) is used to identify different bacterial species.

The 16S rRNA, or 16S ribosomal RNA, codes for the small subunit of the bacterial and archaeal ribosome. We know that ribosomes are found in all living cells and are an integral part of the translational machinery of the cell. They consist of two subunits made of protein and RNA; in prokaryotes these are the 50s (large subunit) and 30s (small subunit), which

together form 70s ribosome. The smaller subunit is composed of 16s rRNA and 21 polynucleotide chains. Furthermore, the 16S sequence is made up of nine hypervariable regions known as V1–V9. Variation in these regions is species-specific and is used to identify bacterial families. Therefore, NGS offers a way to quickly and precisely identify the composition of the microbiome (Mistry, Kounatidis and Ligoxygakis 2017).

In this chapter, we aim to explore the bacterial communities associated with the midgut of Pirk mutant flies and to identify where the factors causing the neurological phenotypes observed in the previous chapters are microbiota driven. We conducted this by using NGS with the Ion ProtonTM platform. This was succeeded by thorough bioinformatic analysis using Ion ReporterTM software, wherein sequences were aligned against the curated microSEQ® 16S reference library v2013.1, and various parameters were fine-tuned (including the number of valid reads, genus percentage identity, etc.). Operational taxonomic units (OTUs) were employed to construct relative abundance graphs (refer to **Chapter 7**: Materials and Methods). Additionally, we used controls raised in the same batches of food as the mutant and performed all experiments simultaneously for both phenotypes to minimise any variability caused by human error.

Furthermore, while we recognise that the microbiome includes non-bacterial symbionts such as yeasts and archaea, our research concentrates on the bacterial microbiome due to its proven role in animal and Drosophila biology.

Our analysis builds on previous research done in that lab that identified age related changes in the composition of the bacterial microbiome and how it differs in flies with a constitutively active immune response (Mistry, Kounatidis and Ligoxygakis 2017). However, the study was performed in *trabid;pirk* flies and was not *pirk* specific. This study aims to overcome the

limitation of previous studies by digesting the *Wolbachia* sequences using restrictive digestion, prior to library prep, instead of removing it in silico after (Bahuguna *et al.* 2022).
Here, we use the term microbiome to refer to the bacterial microbiome present in the gut for simplicity.

5.1.6 Aims of the chapter

This chapter focuses on examining the role of a constitutively active immune response on the composition of the gut microbiome using culture-independent gut microbiota analysis. Furthermore, it aims to answer the complicated question of whether microbiomes acquired from the environment are capable of influencing neurological behaviour.

We chose to investigate the composition at 6-days and 30-days of age, rather than 28-days, due to the concurrent nature of most experiments and the extensive time needed for dissections and library preparations. However, the co-housed flies were still analysed at 28-days to maintain consistency in sleep assays

5.2 RESULTS

5.2.1 Culture-independent gut microbiota analysis

The aim of this section is to analyse the microbial composition of Drosophila gut using next-generation sequencing (NGS) with the Ion Proton™ platform. We raised conventionally reared *pirk* flies along with their controls. We dissected 40 mid guts of flies of both male and female *pirk* mutant flies at 6 and 28-days of age along with their respective controls to help provide an accurate representation of the composition of the gut microbiota in a specific strain at a particular period and ascertain the contribution of immune status on the result.

After isolating the genomic DNA, 16sRNA regions were amplified and treated with BstZ17I (R3594S, NEB, UK), to remove *Wolbachia* reads from the sample. We then multiplexed our sequencing chips with 16 samples per chip. Following quality filtering, all rarefaction curves tended to saturation; we got an average of 93348.5 reads in female flies and that of 73305.75 reads in male in the first repeat. However, when we analysed other biological repeats, we could not satisfy the cut-off of the minimum number of repeats to accurately represent the microbial population. Nevertheless, the following section contains the results of the first repeat of the analysis that can be used as a foundation to understand the influence immune status has on microbiome composition (See **Covid** statement on page 2 for detail).

The data analysis was performed using Ion Reporter™ software. Each read was examined for single-end primers and reads less than 125 bp were disregarded, and an alignment coverage of 90% was enforced. Given the technical limitations of the Ion Proton, Operational Taxonomic Units (OTUs) were only counted if they had at least three readings. Graphs were

generated using GraphPad Prism, while examination of alpha diversity indexes (Simpson 1-D, Shannon H, and Sobs) was conducted using PAST3 software.

5.2.1.1 The effect of constitutively activate immune responseon the gut microbiome of female *pirk* mutant flies using 16s rRNA sequencing

We performed 16s rRNA high-throughput DNA sequencing to investigate the role of Pirk protein on the bacterial composition in the Drosophila midgut. For this, we first analysed the relative abundances of the bacterial families detected in the guts of both 6-day and 30-day old female and male *pirk* flies compared to their w^{1118} controls (n=40 guts/strain). Then we looked at the sequencing analysis of 16S rRNA gene amplicons from the dissected female guts of *D. melanogaster pirk* strain. It produced 88991 reads in 6-day old w^{1118} female flies and 119769 in 6-day old *pirk* flies. Additionally, the analysis produced 136479 reads in 30-day old w^{1118} female flies and 81607 in 30-day old *pirk* flies after quality filtering and removal of chimaeric sequences an including the multiplex identifier 'MID' and primer sequences. However, the sequences were then processed to remove reads from the Rickettsiales family (*Wolbachia*) that does not colonise the gut but is present intracellularly. After this, we had 51701 reads in 6-day old w^{1118} female flies and 102032 in *pirk* 6-day old female flies, along with 71301 in w^{1118} 30-day old female flies and 81353 reads in older *pirk* flies.

flies, along with 71301 in w^{1118} 30-day old female flies and 81353 reads in older *pirk* flies.

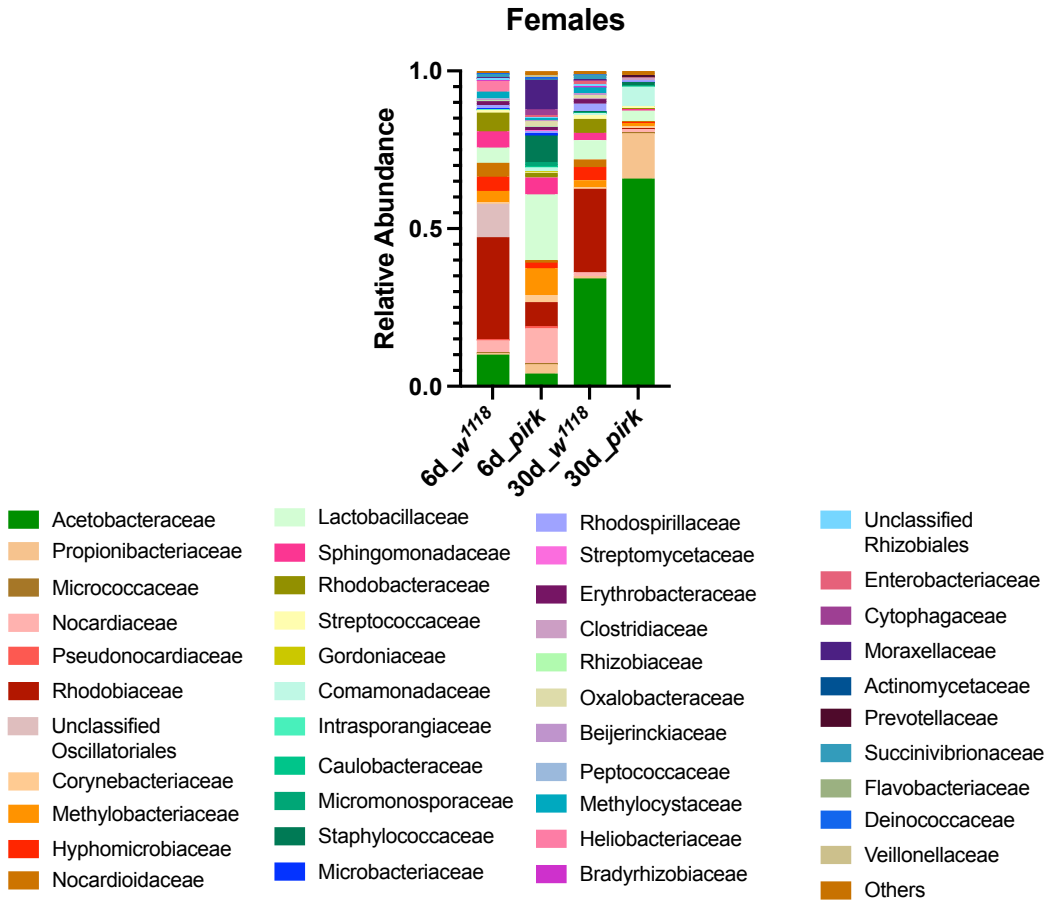

Figure 58: Relative abundance of the various bacterial families observed in 6 and 30-day old *pirk* female flies compared to their controls (n=40/strain). Forty flies were dissected for each genotype and sex. *Wolbachia* reads were removed via BstZ17I digestion and libraries were prepped simultaneously.

Relative Abundance

The midgut of 6-day old w^{1118} female flies were dominated with Rhodobiaceae (~ 32.5%), Acetobacteraceae (~10%) and unclassified Oscillatoriales (~10.5%). However, this dominance is not observed in *pirk* 6-day old female flies, where we observe Lactobacillaceae (~21%) as the dominant specie, along with Nocardiaceae (~11%) and Moraxellaceae (~9.2%) **(Figure 58)**. The relative abundance of Acetobacteraceae was shown to have severely declined in the absence of Pirk, from 10% in controls to 4% in young female *pirk* flies. This reduction in Acetobacteraceae corelates to an increase in Lactobacillaceae from 4% in control flies to 21% in 6-day old Pirk female flies.

In contrast to the 6-day old flies, the 30-day old flies were dominated by Acetobacteraceae, with 34% in w^{1118} females to 68% in *pirk* flies. The guts of older w^{1118} flies also contained 26% Rhodobiaceae and 6% Lactobacillaceae. However, only two families made up approximately 83% of the total bacterial population of the mid gut in 30-day old *pirk* female flies: Acetobacteraceae (68%) and Lactobacillaceae (14%) **(Figure 58)**. Interestingly, we observed a 17-fold age dependent increase in the relative abundance of the Acetobacteraceae family in *pirk* female flies in comparison with a 3.4 fold increase in w^{1118} female flies.

Alpha Indices

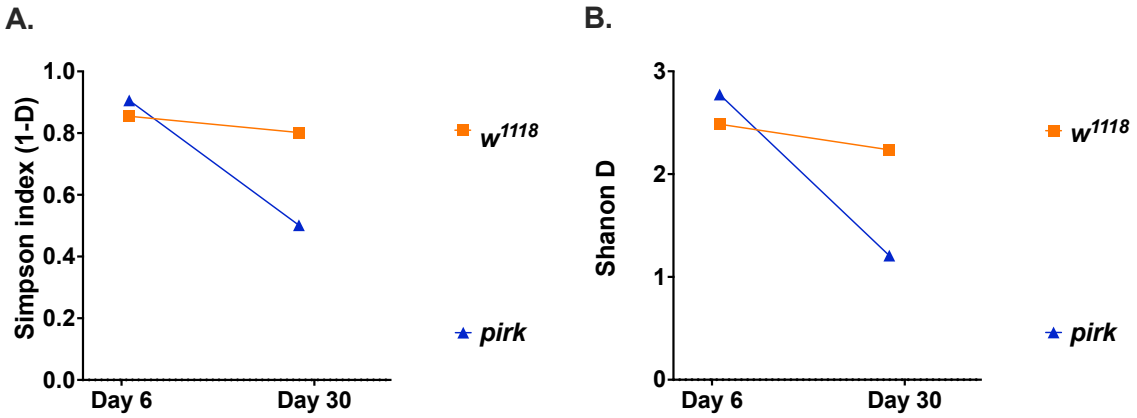

Figure 59: Simpson (1-D) and Shanon D index of female *pirk* mutant flies compared to their controls at 6 and 30-day of age (n=40/strain)

To understand diversity further we measured the alpha index of the samples. This analysis revealed that even though 6-day old *pirk* mutant flies (Simpson 1-D = 0.9135, Shannon H =2.897) displayed similar diversity than that on 6-day old w^{1118} flies(Simpson 1-D = 0.8617, Shannon H =2.629), this drastically changed in 30-day old flies with w^{1118} 30-day old flies (Simpson 1-D = 0.8067, Shannon H = 2.373) were considerably more diverse than *pirk* flies (Simpson 1-D = 0.5048, Shannon H = 1.353) **(Figure 59(A-B))**. Furthermore, it is worth noting that we observed few age dependent changes in diversity of w^{1118} flies but a significant reduction in diversity in *pirk* mutant flies.

5.2.1.2 The effect of constitutively activate immune response on the gut microbiome of male *pirk* mutant flies using 16s rRNA sequencing

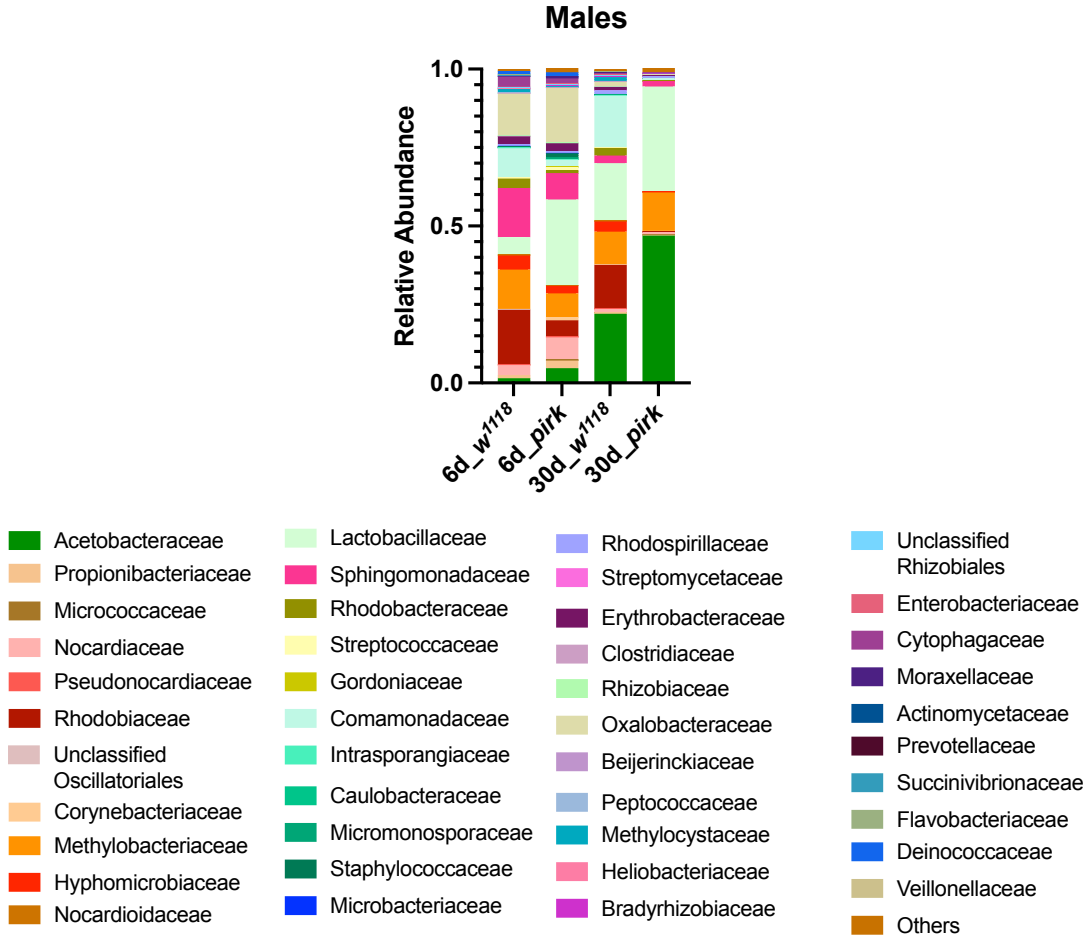

Figure 60: Relative abundance of the various bacterial families observed in 6 and 30-day old *pirk* male flies compared to their controls (n=40/strain). Forty flies were dissected for each genotype and sex. *Wolbachia* reads were removed via BstZ17I digestion and libraries were prepped simultaneously.

Relative Abundance

Like the female, the midgut of male 6-day old w^{1118} was dominated by Rhodobiaceae (~ 17.5%). However, other families such as Sphingomonadaceae (~ 15.6%) and Oxalobacteraceae (~ 13.7%) were also observed. We found that the w^{1118} male gut microbiome only contained about 5.4% Lactobacillaceae and 1.4% Acetobacteraceae. Interestingly, the *pirk* male flies, harboured approximately ~ 27% Lactobacillaceae and ~ 4.6% Acetobacteraceae. The *pirk*

mutants were dominated by Lactobacillaceae (~ 27%), Oxalobacteraceae (~ 17.5%) and Sphingomonadaceae (~ 8.3%) **(Figure 60)**.

As the fly aged, at 30-days w^{1118} gut composition was mainly dominated by Lactobacillaceae (~ 22%) and Acetobacteraceae (~ 18%), along with Comamonadaceae (~ 16.6%) and Rhodobiaceae (~ 14%). In contrast to this, the *pirk* microbiome harboured ~46% Acetobacteraceae and ~33% Lactobacillaceae. The relative abundance of Lactobacillaceae was shown to considerably increase in an age dependent manner in both w^{1118} and *pirk* mutant flies **(Figure 60)**. However, we observed a 10-fold increase in Acetobacteraceae composition in *pirk* mutant flies (from 4.6% to 46%) and a slight decrease in Lactobacillaceae (from 27% to 22%) composition. Similarly, we noted a 12-fold increase in Acetobacteraceae composition in w^{1118} control flies (from 1.4% to 18%) along with a 4 fold increase in Lactobacillaceae abundance (5.4% to 22%) **(Figure 60)**.

Alpha Indices

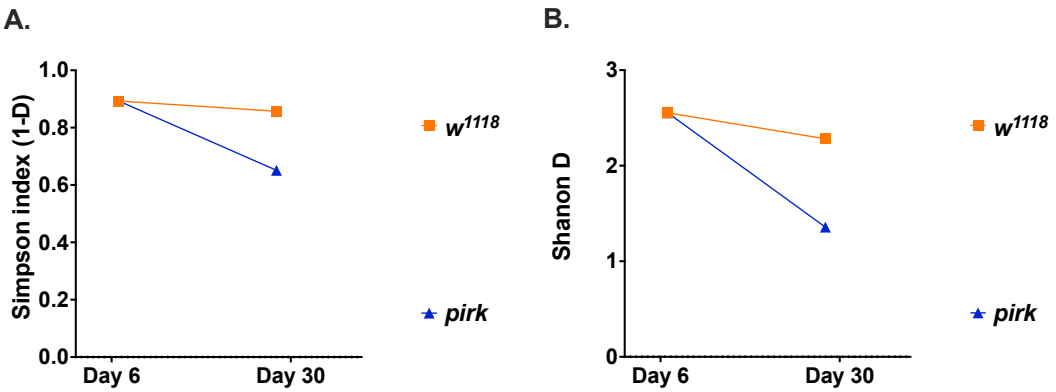

Figure 61: Simpson (1-D) and Shanon D index of male *pirk* mutant flies compared to their controls at 6 and 30-day of age (n=40/strain)

We then analysed the alpha indices to assess diversity further. Like female flies, 6-day old male *pirk* mutant (Simpson 1-D = 0.8746, Shannon H =2.655) and w^{1118} flies (Simpson 1-D = 0.9008, Shannon H =2.691) displayed similar diversity. However, we observed a significant

drop in diversity in 30-day old male *pirk* mutant flies (Simpson 1-D = 0.6532, Shannon H = 1.489) but not in 30-day old male w^{1118} flies (Simpson 1-D = 0.864, Shannon H = 2.424) **(Figure 61 (A-B))**.

5.2.2 Co-housing

Previous studies from our lab have demonstrated co-housing as a method to study the impact of the microbiome has on its surrounding environment. Mistry, Kounatidis and Ligoxygakis (2017), co-housed *pirk;trabid* (flies with constitutively active immune response) with *yw* (control) flies and observed that despite having different microbiome composition (at 2 daytime point), these flies start showing similar composition as early as 14 days; as a result, illustrating the possibility of a "microbiome transfer" from one strain to another. In the second half of this chapter, we co-housed *pirk* mutant flies (with a constitutively active immune response) with dechlorinated or germ-free wild type control flies (*yw*) in conventional food, to further examine if the sleep phenotype observed in **Chapter 2** could potentially be caused by the gut microbiome itself.

5.2.3. Effects on Sleep and Locomotion on Drosophila co-housed with Pirk Mutant

Next, we aimed to observe the effects of co-housing GF wild type flies with *pirk* mutant flies on sleep and activity behaviour of flies, and whether the phenotype observed in **Chapter 2** is microbiome dependent or not. Like previous chapters, we assessed the sleep behaviour using the Drosophila Activity monitor or DAM system. For this chapter, we opted to evaluate only those sleep parameters wherein notable alterations were observed in **Chapter 2**.

2.2.3.1 Effects on Females

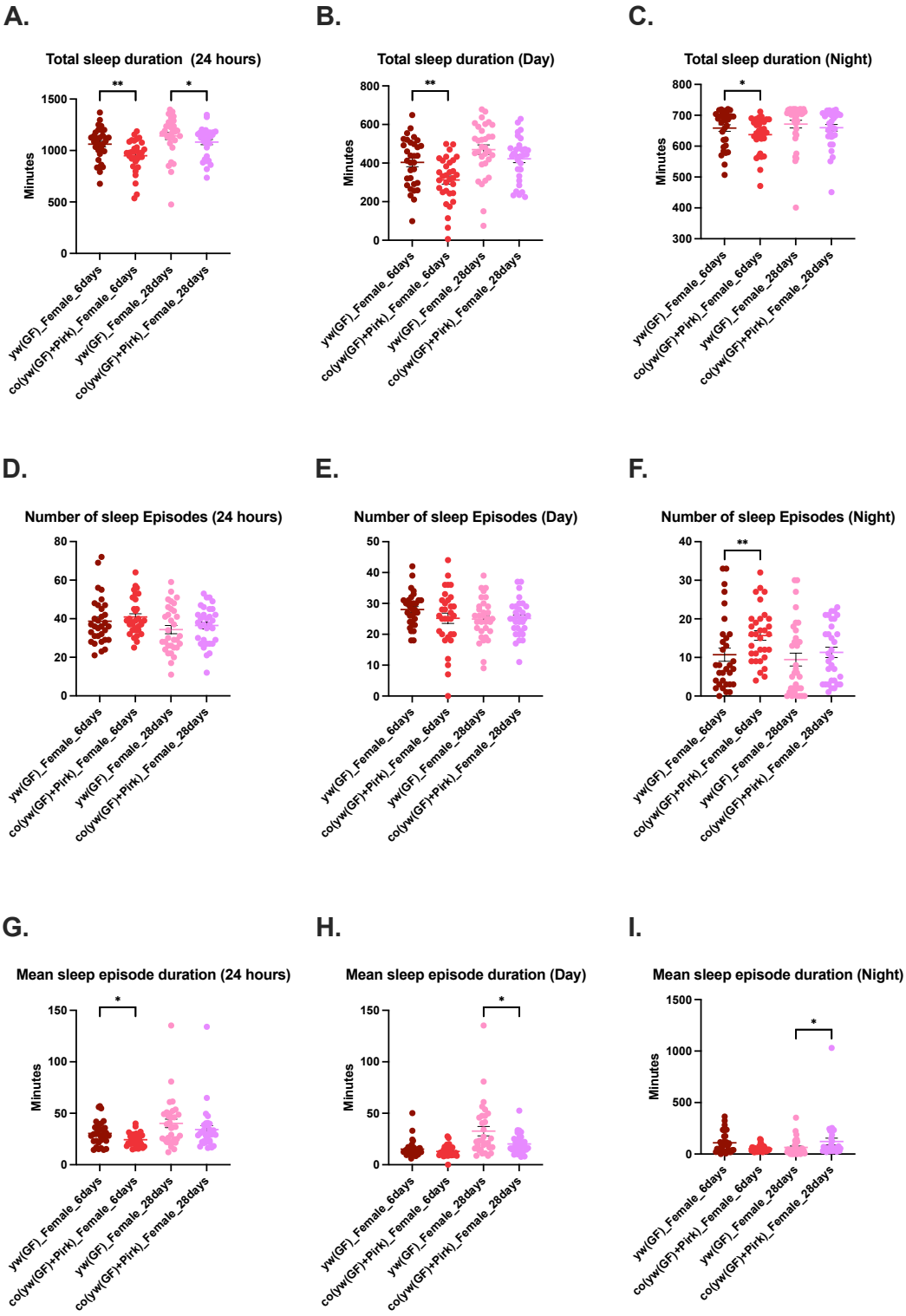

Figure 62: Sleep parameters of 6 and 28-day old female germ free control and germ free *yw* flies co-housed with *pirk* flies. Three independent repeats were conducted for each genotype, and 32 flies were randomly selected from these repeats, resulting in a total sample size (n) of 32. These 32 flies were then analysed, and a Mann Witney Rank sum test was performed between mutant flies and their respective controls, without consideration of age-dependent analysis. Non-significant results were not marked and $p \leq 0.05$ (*), ≤ 0.01 (**), ≤ 0.001 (***), ≤ 0.0001 (****).

Total sleep is measured by counting total minutes of sleep in a given time period. Like in previous chapters, we have divided all parameters into daytime and night-time (or light and dark periods).

We observed a significant decline in the total sleep duration in both 6-day and 28-day co-housed female flies with respect to their germ free controls, with p=0.0032 (n=32) when flies were co-housed for 6-days, and p=0.0302 (n=32) when co-housed for 28-days **(Figure 62A)**. However, in 6-day old flies, this reduction is predominantly affected by daytime sleep, with p=0.0054 (n=32) but not in 28-day old flies with p=0.0745 (n=32) **(Figure 62B)**. Furthermore, a similar effect is observed in night-time sleep with a median decline of 25 minutes in sleep in 6-day old flies (p = 0.0313, n=32) and p=0.0620 (n=32) in 28-day old flies **(Figure 62C)**.

To further examine if the decrease in total sleep is due to disturbed sleep quality or quantity, we explore the total number of sleep episodes, along with latency, mean and max sleep episode durations. There was no notable difference in the total number of sleep episodes observed in either 6-day or 28-day old flies co-housed with *pirk* mutant versus their germ free counter parts (p = 0.2348 (n=32) and p = 0.3979 (n=32) respectively) **(Figure 62D)**. A similar effect was also observed in daytime sleep with p=0.2620 (n=32) in 6-day old and p = 0.9441 (n=32) in 28-day old flies **(Figure 62E)**. However, a slight but significant increase of 6 episodes was observed during night-time sleep in 6-day old co-housed flies, but no significant change in 28-days (p=0.1250, n=32) was observed **(Figure 62F)**.

A notable decline in mean sleep episode duration of approximately 5 minutes was observed in 6-day old co-housed flies (p=0.00274, n=32) but no significant interactions was noted in 28-day old flies through the day (p=0.1784, n=32) **(Figure 62G)**. In contrast of this, we found a significant change in the mean sleep episode duration 28-day old flies in both daytime and

night-time sleep with a median reduction of 5.6 minutes during the day (p = 0.0453, n=32) **(Figure 62H),** and a median increase of 26 minutes at night (p =0.0150, n=32) **(Figure 62I)**. No observable change in 6-day old flies in either day (p =0.1965, n=32) **(Figure 62H)** or night (p=0.0503, n=32) **(Figure 62I)** time sleep with respect to their controls was observed. We found that max sleep episode duration per day was statistically affected by co-housing GF wild type flies with Pirk at both 6-days (p=0.0102, n=32) and at 28-days (p=0.0377, n=32) **(Figure 62A)**. However, this effect was lost when we analysed day and night-time sleep separately, except a median decline of 115 (p=0.0157, n=32) that was observed in 28-day old co-housed flies during daytime sleep **(Figure 62(B-C))**.

We observed a significant increase in the latency to sleep during the day in 6-day old co-housed flies versus their non cohoused controls (p=0.0378, n=32), but no significant observations in 28-day old flies (p=0.9137, n=32) **(Figure 63D)**. In contrast to this, during night-time we observed a significant median decline of 2 minutes in 28-day old co-housed flies (p<0.0001, n=32) but no notable difference was seen in 6-day old flies (p=0.5983, n=32) **(Figure 63E)**.

Finally, to account for any neuromuscular damages, we also examined the activity count per minute of wakefulness or activity count / time awake. We observed no significant differences in this parameter in either 6-day or 28-day old co-housed flies through the course of the day (p=0.4752, n=32 and p=0.4447, n=32 respectively) **(Figure 63F)** or during daytime sleep (p=0.0975, n=32 and p=0.3066, n=32 respectively) **(Figure 63G)**. However, significant rise in activity per time awake was observed in 28-day old co-housed flies (p=0.0070, n=32) but no notable change was observed in 6-day old flies (p=0.9018, n=32), with respect to their non-co-housed counterparts **(Figure 63H)**.

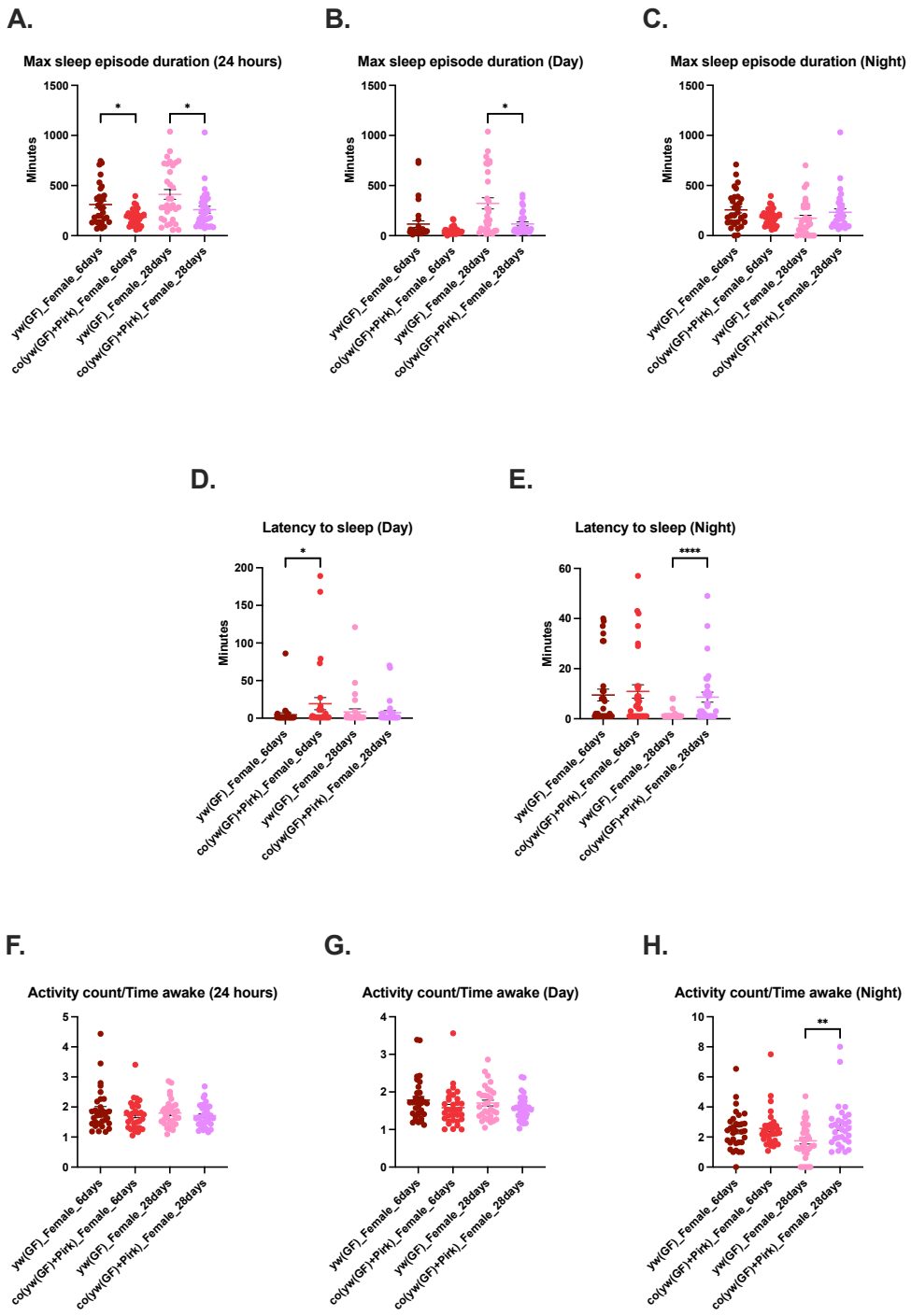

Figure 63: Additional sleep parameters of 6 and 28-day old female germ free control and germ free *yw* flies co-housed with *pirk* flies. Three independent repeats were conducted for each genotype, and 32 flies were randomly selected from these repeats, resulting in a total sample size (n) of 32. These 32 flies were then analysed, and a Mann Witney Rank sum test was performed between mutant flies and their respective controls, without consideration of age-dependent analysis. Non-significant results were not marked and $p \leq 0.05$ (*), ≤ 0.01 (**), ≤ 0.001 (***), ≤ 0.0001 (****).

2.2.3.1 Effects on Males

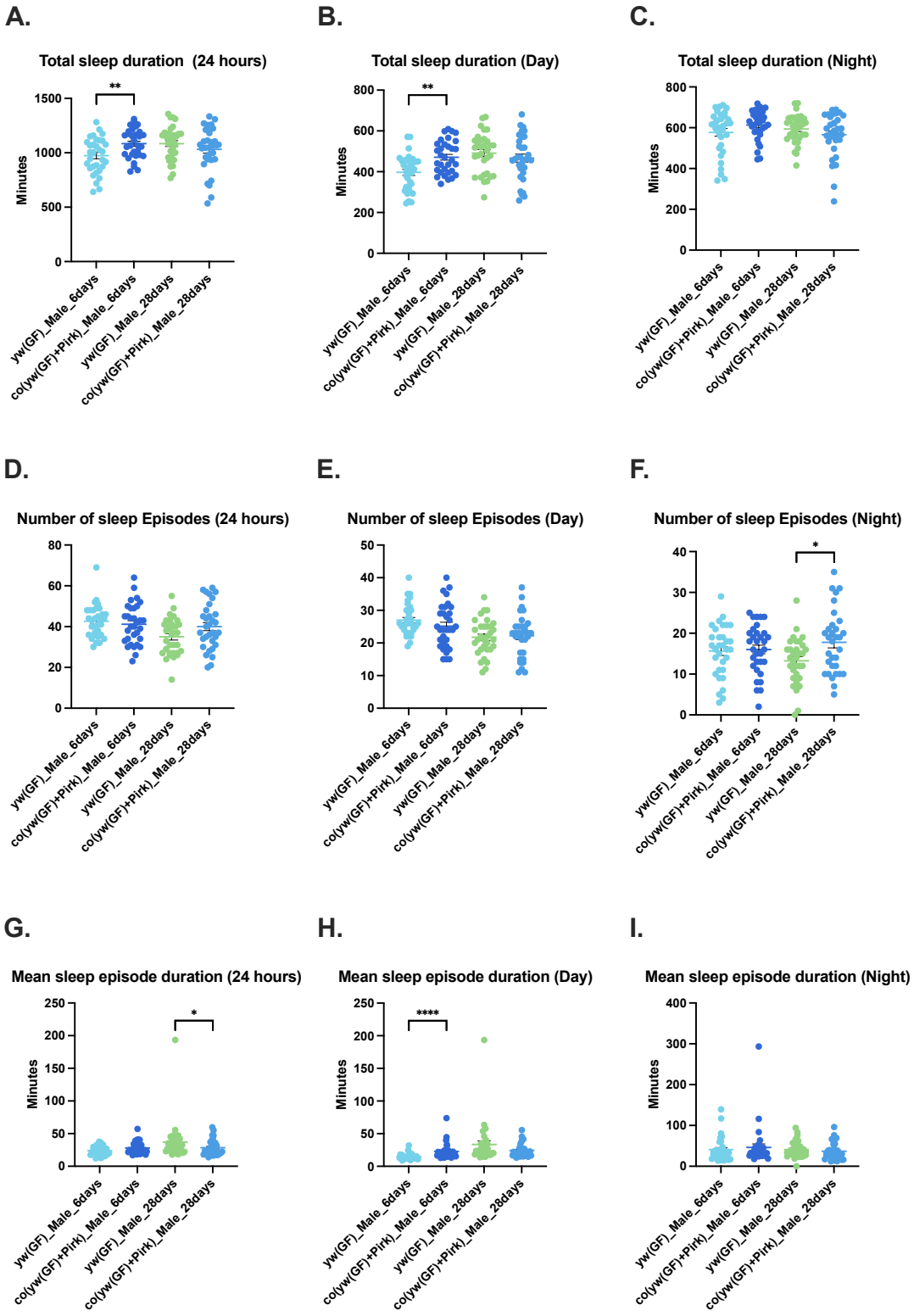

Figure 64 Sleep parameters of 6 and 28-day old male germ free control and germ free *yw* flies co-housed with *pirk* flies. Three independent repeats were conducted for each genotype, and 32 flies were randomly selected from these repeats, resulting in a total sample size (n) of 32. These 32 flies were then analysed, and a Mann Witney Rank sum test was performed between mutant flies and their respective controls, without consideration of age-dependent analysis. Non-significant results were not marked and p≤ 0.05 (*), ≤ 0.01 (**), ≤ 0.001 (***), ≤ 0.0001 (****).

We found a stark median increase of 106 minutes in the total duration of sleep in 6-day old male co-housed flies when compared to their wild type counterpart (p=0.0094, n=32), but no notable change in 28-day old co-housed flies (p=0.4096, n=32) **(Figure 64A)**. This change is likely due to an increase in daytime sleep in 6-day old flies (p=0.0029, n=32). This effect was not observed in daytime sleep of 28-day old co-housed flies with respect to their non-co-housed wild type controls (p=0.3277, n=32) **(Figure 65B)**. Additionally, no significant changes were observed in night-time sleep in either 6-day or 28-day old male co-housed flies (p=0.2774, n=32 and p=0.5820, n=32 respectively) **(Figure 66C)**.

We subsequently looked deeply into the sleep episodes during a 24-hour period, and then day and night-time. We did not observe any solitary effect of co-housing flies with the number of sleep episode duration during the course of the day in either 6-day or 28-day old male mutant flies (p=0.5323, n=32 and p=0.0848, n=32 respectively) **(Figure 67D)**. An analogous result was seen during daytime sleep with p=0.1921 (n=32) in 6-day old and p =0.7256 (n=32) in 28-day old male co-housed flies **(Figure 67E)**. Even though we did not observe any stark differences during night-time sleep in 6-day old male flies (p=0.7510, n=32), we noted a median increase of 4 episodes in 28-day old male co-housed flies (p=0.0205, n=32) **(Figure 67F)**. The mean sleep episode duration or average duration of a sleep episode was not affected by co-housing in 6-day old male flies. However, a slight median decrease of 4.8 minutes was observed in 28-day old male co-housed flies (p=0.0483, n=32) with respect to their non-co-housed controls **(Figure 67G)**. However, this effect was not observed during daytime sleep with an observable median increase of 5.4 minutes in average sleep episode durations in 6-day old male co-housed flies (p>0.0001, n=32), and no observable changes in 28-day old flies (p=0.0981, n=32) **(Figure 67H)**. Furthermore, no significant change was observed during

night-time sleep in either 6-day (p=0.6169, n=32) or 28-day (p=0.1752, n=32) old male co-housed flies versus their respective controls **(Figure 67I)**.

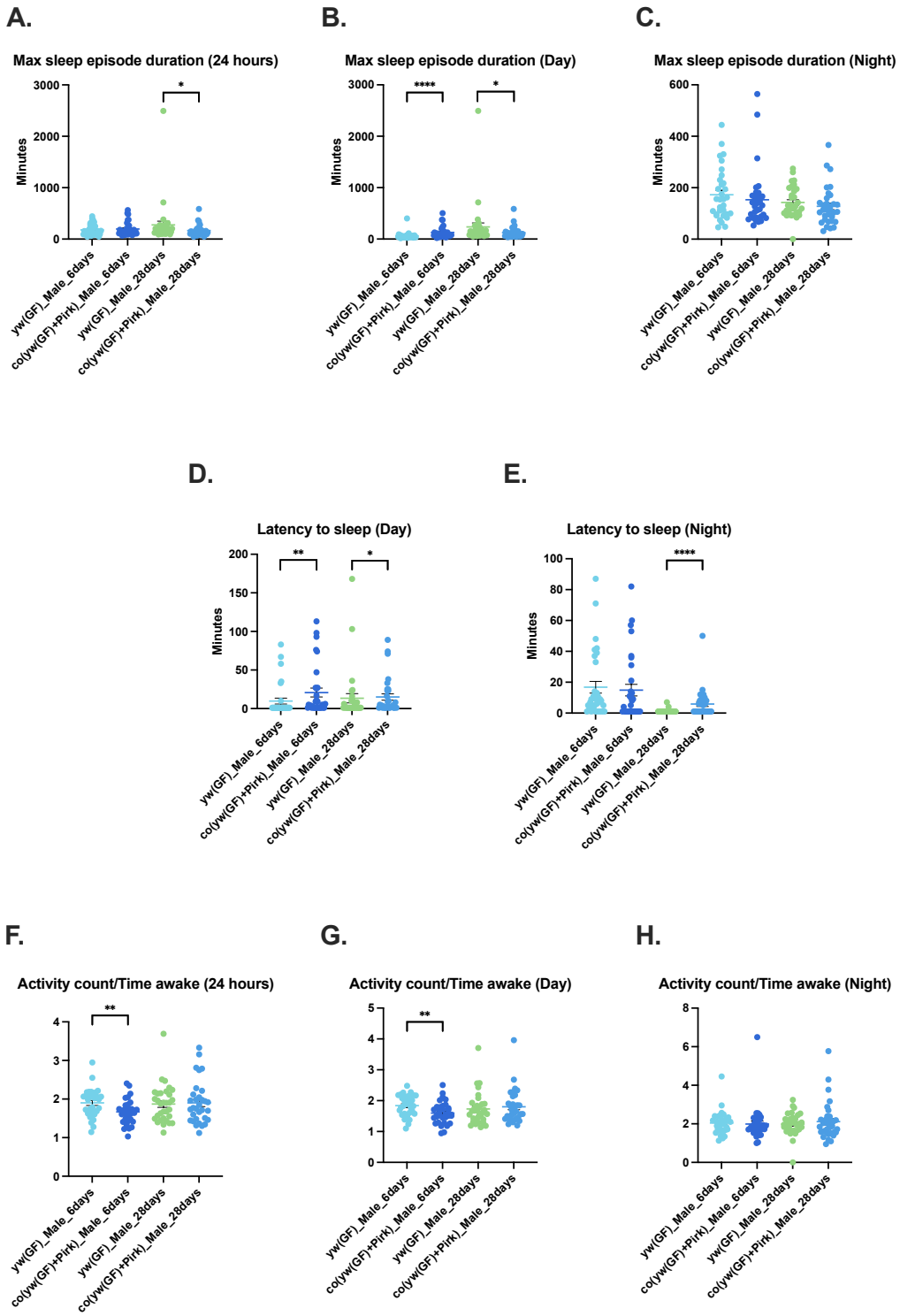

Figure 65: Additional sleep parameters of 6 and 28-day old male germ free control and germ free *yw* flies co-housed with *pirk* flies. Three independent repeats were conducted for each genotype, and 32 flies were randomly selected from these repeats, resulting in a total sample size (n) of 32. These 32 flies were then analysed, and a Mann Witney Rank sum test was performed between mutant flies and their respective controls, without consideration of age-dependent analysis. Non-significant results were not marked and p≤ 0.05 (*), ≤ 0.01 (**), ≤ 0.001 (***), ≤ 0.0001 (****).

A similar observation was made in the max sleep episode duration over the course of a 24-hour period, with no stark changes in 6-day old flies (p=0.6817, n=32) but a notable median rise of 46 minutes in the maximum sleep episode duration of 28-day old co-housed flies (p=0.0244, n=32) **(Figure 65A)**. The maximum sleep episode during the day was significantly affected by co-housing male flies, with an increase of 42 minutes in 6-day old flies (p<0.0001, n=32) along with a significant decrease of 33.5 minutes in 28-day old co-housed male flies (p=0.0244, n=32) **(Figure 65B)**. However, no notable change was observed at night-time in either 6 or 28-day old male co-housed flies (p=0.2432, n=32 and p=0.1730, n=32 respectively) **(Figure 66C)**.

We observed a significant association between latency of sleep and co-housing with *pirk* flies during the day in both 6-day (p=0.0022, n=32) and 28-day (p=0.0495, n=32) old male flies with respect to their controls **(Figure 67D)**. However, this was not the case at night-time, with no notable change in the latency of 6-day old flies (p=0.2851, n=32), but a significant increase in latency to sleep at night in 28-day old male co-housed flies (p<0.0001, n=32) **(Figure 67E)**. We finally assessed the activity count / time awake of male co-housed flies with respect to their controls to account for any sleep phenotypes that could be a result of potential neuromuscular damage. Although we found a significant reduction in 6-day old male flies throughout the course of the day (p=0.0074, n=32), but no significant fluctuations in 28-day old male co-housed flies (p=0.9415, n=32) **(Figure 67F)**. A similar observation was seen during daytime assessment, where a decline of 0.26 was observed in 6-day old flies (p=0.0060, n=32) but no change in 28-day old (p=0.5262, n=32) flies **(Figure 67G)**. Additionally, we saw no notable changes in night-time activity / time awake in either 6 or 28-day old male co-housed flies versus their controls (p=0.2930, n=32 and p=0.4914, n=32 respectively) **(Figure 67H)**.

Summary

This chapter focused on establishing the role of the microbiome in the previously observed sleep defects in flies with constitutively active immune response in their gut. From 16srRNA sequencing analysis of *pirk* mutant flies, we deduce that young *pirk* flies have a diverse microbiome, which is as diverse if not slightly more as that of young control (w^{1118}) in both male and female flies. Of particular note, our investigation unveils an expected but notable correlation between elevated levels of *Acetobacter* and advancing age, with 30-day-old *pirk* flies representing a cohort akin to more mature control flies. However, as the flies age, we observed a stark reduction in alpha diversity in both sexes compared to their controls.

We then investigated if the "dysbiotic" bacteria present in the *pirk* mutants could transfer to control flies when co-housed and cause similar sleep defects or not. Unsurprisingly, we observed sleep defects in co-housed control flies compared to their non cohoused siblings.
Noteworthy observations also include a decline in the quality of sleep, as evidenced by significantly reduced maximum and average sleep episode durations in young flies throughout the diurnal cycle, alongside reduced maximum sleep durations in aged counterparts relative to controls.
In young male co-housed flies, we noted a significant rise in total sleep among young flies over a 24-hour period, but this trend was not apparent in co-housed flies aged 28-days. This increase in sleep was likely attributable to heightened daytime sleep among co-housed male flies. However, despite our observations of multiple sleep phenotypes, it is essential to acknowledge that sleep is influenced by various factors, such as social interaction and aggression, which could potentially act as confounding variables when analysing males.

In summary, the key takeaway from this chapter is that while we didn't find statistical significance, there's a notable variance in bacterial diversity between *pirk* flies and their controls. Intriguingly, the bacterial diversity in the 30-day time point mirrors that of control flies much older than them (Mistry, Kounatidis and Ligoxygakis 2017). Regarding co-housing, although we didn't consistently observe similar sleep phenotypes to those of the *pirk* mutant, the mere presence of a discernible phenotype suggests the potential for finetuning the co-housing protocol to enhance sensitivity. This could prove invaluable in further investigating the gut-brain axis.

CHAPTER SIX

Discussion

DISCUSSION

Predisposing flies to chronic immune activation by knockouts of IMD negative regulators, overexpressing AMPs in the brain, or dysregulating autophagy (leading to induction of AMP genes) resulted in age-dependent neurodegeneration (Cao *et al.* 2013; Kounatidis *et al.* 2017; Shukla *et al.* 2019). Distinct from all other IMD intracellular negative regulators, *pirk* expression is dependent on the presence of gut bacteria (Lhocine *et al.* 2008). This opens up the possibility that the *pirk*-induced neurodegeneration (Kounatidis *et al.* 2017) was microbiota-dependent.

Our investigation delved into the intricate relationship between immunity and the neurological phenotypes linked to neurodegeneration, building on previous work by Kounatidis et al. (2017). The study illustrated the role of *pirk* in early neurodegeneration and reduced longevity. Both Paredes et al. (2011) and Kounatidis et al. (2017) have observed that lifespan of these mutant flies was restored in axenic conditions. The question then was to determine the relative contribution of the microbiota and *pirk* in the brain in relation to the neurological decline connected to neurodegeneration. Implicating gut bacteria would be consistent with findings linking crucial bacterial products, such as peptidoglycan, to the reciprocal interaction between the microbiome and gut in the initiation of neurodegeneration in humans. (reviewed in Sarubbo, Cavallucci and Pani 2022) and flies (Wu *et al.* 2017).

The primary aim of the study was to characterise the cognitive decline observed in previous studies and explore the potential contributions of gut and brain immunity in age-dependent neurodegeneration in the context of Pirk loss or reduction of function.

Contributions of the Immune System and Age-Related Differences

In the absence of Pirk, the IMD pathway is de-repressed, as demonstrated by the elevated expression of AMP genes that are direct transcriptional targets of Relish (Aggarwal and Silverman 2008; Kleino *et al.* 2008; Lhocine *et al.* 2008). We corroborated and extended previous established climbing phenotype (Kounatidis *et al.* 2017) by examining sex-specific differences in the neurology of *pirk* mutants. We observed a significant decrease in the climbing ability of young (6-day old) female *pirk* flies, along with a notable reduction in the climbing ability of both male and female *pirk* flies at day 28.

Next, we investigated sleep as a means to explore the extent of neurological phenotypes linked to neurodegeneration. Impaired sleep is associated with various neurodegenerative diseases and serves as a biomarker for allostatic load, given that disturbances in sleep manifest long before any cognitive decline becomes apparent (Sabia *et al.* 2021). Furthermore, individuals with impaired sleep have been shown to have a 3.7 times higher likelihood of developing AD (Zhang *et al.* 2022). The debate over whether sleep defects drive neurodegeneration or results from the loss of neural regionsinvolved in sleep regulation in patients with the onset of neurodegenerative diseases is still ongoing (reviewed in Vidal and Pacheco 2020). Sleep is intricately intertwined with immunity in both mammals (reviewed in Ingiosi, Opp and Krueger (2013)) and *Drosophila* (Williams *et al.* 2007; Kuo *et al.* 2010b). Therefore, to assess the degree of cognitive decline in flies with consecutively active immunity, we measured sleep in 6 and 28-day old pirk mutant flies.

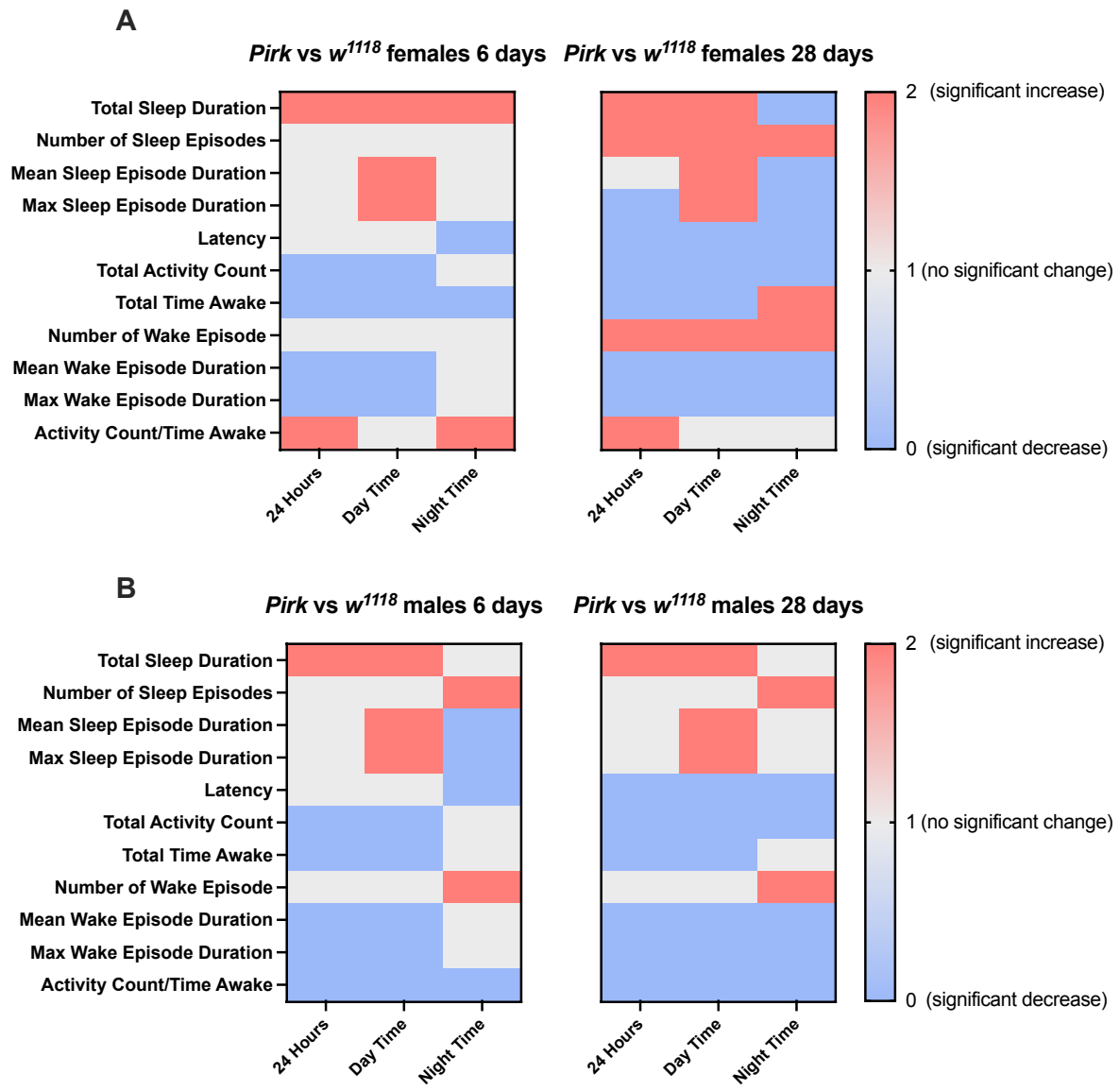

Figure 66: A heatmap summarising the sleep phenotype findings observed in Chapter 2 (*pirk* vs *yw*). The red colour indicates significant increase, grey representing no significant change, and blue denotes a significant reduction in the parameter. The data is divided into three time points (24h, day and night).

Compared to their w^{1118} genetic background, *pirk* mutant female flies exhibited deregulation in their 24-hour sleep profile. When analysing patterns of daytime and night-time sleep separately, we observed that a *pirk*-dependent hyperactive immune response caused both male and female flies to experience increased daytime sleep and sleep fragmentation (**Figure 66(A-B)**). Furthermore, this effect of impaired sleep was more pronounced in females than males and exacerbated with age.

In young flies, only daytime sleep was impaired, whereas in relatively older flies, both daytime and night-time sleep were affected. Regarding sleep quality, evidence of night-time sleep fragmentation was observed in 6-day old, but not 28-day old, *pirk* flies (**Figure 66**). Sleep defects manifested in younger flies with an overall increase in mean sleep episode duration. While age-dependent neurological decline is expected in the context of healthy ageing

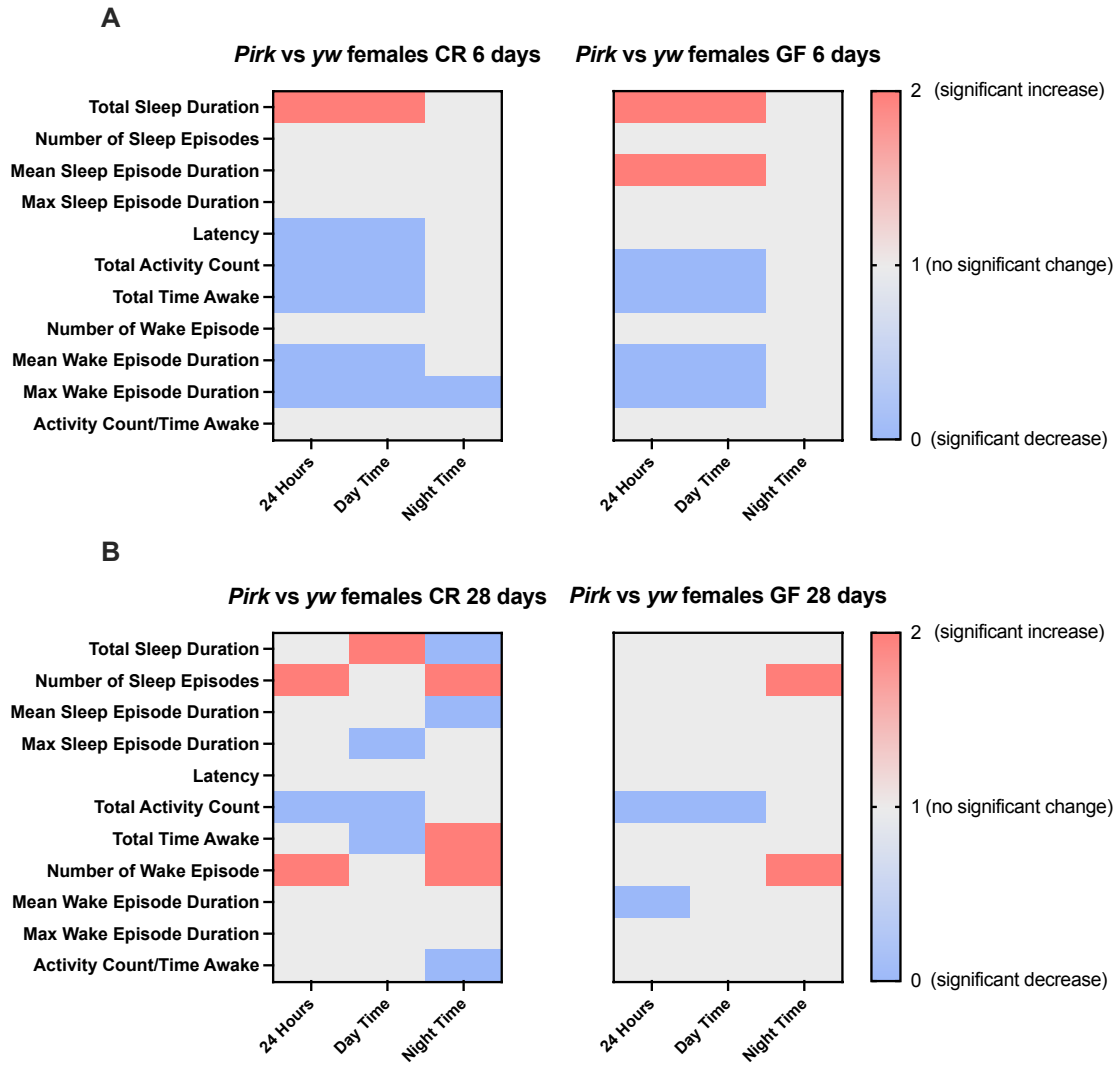

Figure 67: A heatmap summarising the sleep phenotype findings observed in female *pirk* vs *yw* flies in both GF and CR conditions (Chapter 3). The red colour indicates significant increase, grey representing no significant change, and blue denotes a significant reduction in the parameter. The data is divided into three time points (24h, day and night).

As indicated in the COVID statement, the pandemic resulted in the loss of our *pirk* mutant stock which was backcrossed with the w^{1118} flies. Consequently, we opted to proceed with *yw* controls for our experiments. Notably, Germ-free (GF) pirk female flies exerted only a

marginal influence on sleep patterns, closely resembling those of conventionally reared (CR) *pirk* flies in terms of both daytime and night-time sleep, as well as the frequency and duration of sleep episodes at 6-days of age. **Figure 67(B)** illustrates significant sleep fragmentation in *pirk* CR flies, contrasting with the absence of such fragmentation in GF flies aged 28-days. However, it is important to acknowledge that while the heatmap does not demonstrate statistical significance, the data still indicates a tendency towards the CR phenotype (**Figure 67**).

Taken together, these results reveal that gut dysbiosis, occurring in the *pirk* mutant context, only partly contributed to the neurological decline of *pirk* flies. Moreover, gut dysbiosis influenced early rather than late adulthood, as raising *pirk* germ-free delayed but did not prevent sleep phenotype brain lesions from forming later in life (**S2**) in female flies, indicating a microbiota-independent role for brain immunity in the process.

What is surprising is the apparent disparity between the sleep phenotypes between the CR flies of Chapters 2 and 3. This finding was unexpected. It is likely attributable to the fact that w1118 flies are typically employed in sleep studies due to their more predictable sleep cycles (laboratory observation). However, it could also be influenced by the egg collection protocol. Nonetheless, we did not observe any rescue in the observed sleep phenotype in GF conditions.

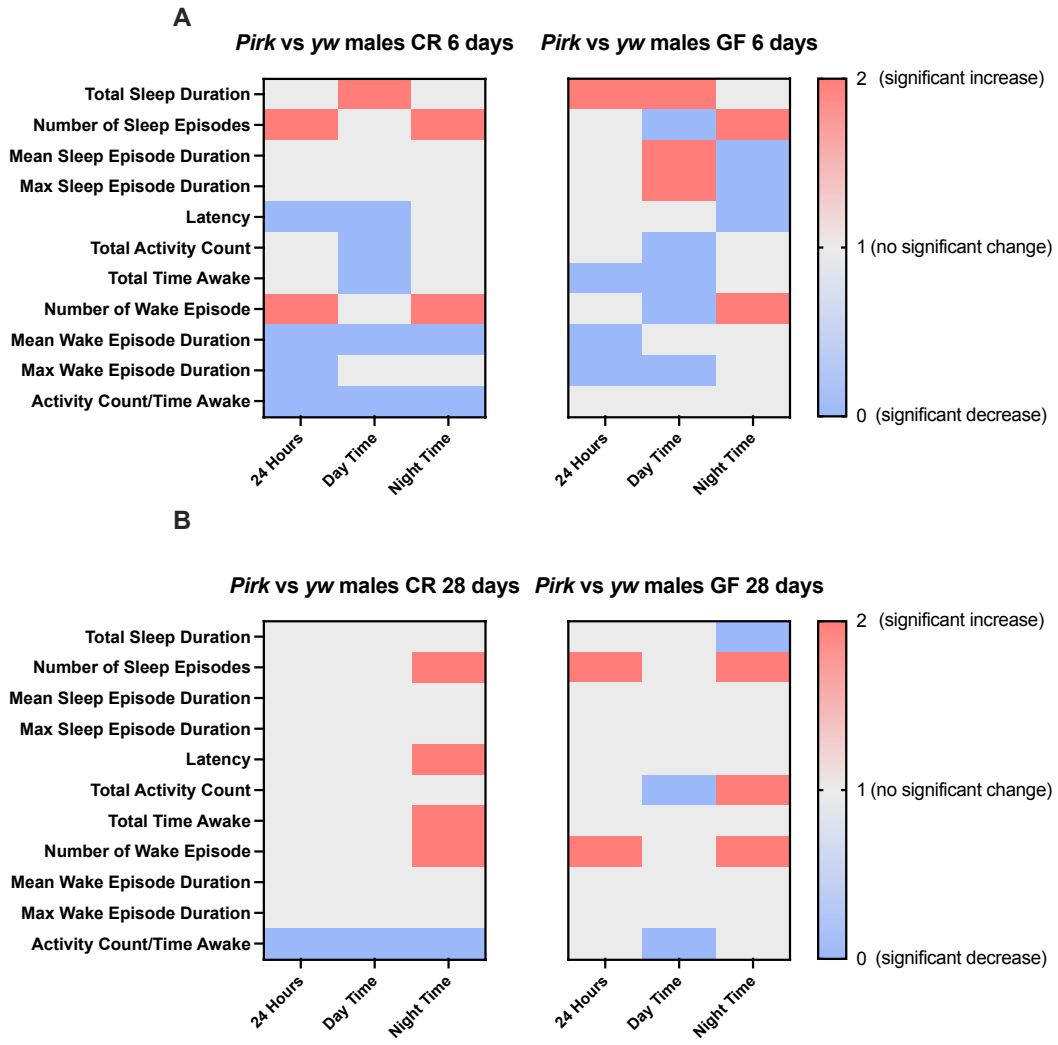

Figure 68: A heatmap summarising the sleep phenotype findings observed in male *pirk* vs *yw* flies in both GF and CR conditions (Chapter 3). The red colour indicates significant increase, grey representing no significant change, and blue denotes a significant reduction in the parameter. The data is divided into three time points (24h, day and night).

Lastly, it is well-documented that flies exhibiting early signs of ageing often display compromised gut barriers (Rera, Clark, & Walker, 2012). However, it is interesting to note that we did not observe any gut barrier impairments via the "smurf assay" in *pirk* flies. Several factors may account for this observation. In the original 2012 paper by Rera, Clark and Walker (2012a), smurfness was described as binary, wherein flies were classified as either smurfs or non-smurfs. However, Martins et al. (2018) (a study from the same laboratory) demonstrated that, like most phenotypes, smurfness exists on a continuum. During my experiments, I noticed

that intermediary phenotypes could lead to misidentification. Light smurfs were not counted unless blue dye diffused throughout the abdomen (as indicated in the original paper), indicating a stage between light smurfs and full smurfs. Alternatively, it is plausible that *pirk* mutants lack intestinal permeability. This hypothesis is not unfounded, considering the notion that a constitutively active immunity in the gut, along with NF-κB-dependent AMPs, might induce a heightened oxidative state that impairs sleep, as recently evidenced (Vaccaro et al., 2020). This could be rescued by reducing oxidative stress in the gut (as discussed in future experiments). Additionally, despite the absence of significant alterations, the data suggests a trend towards an increased number of smurfs in 28-day old *pirk* flies. Whether this is attributable to impaired intestinal permeability induced by a hyperactive immune response, or due to *pirk* flies ageing faster, warrants further investigation.

Pirk's Expression in the brain: elav and repo

We then knocked down Pirk protein in brain tissues, the neurons and glial cells. We found a significant rise in the median lifespans of $pirk^{elav}$ and $pirk^{repo}$ KK flies, and of $pirk^{elav}$ Trip RNAi flies, along with increase in climbing ability in 6-day-old $pirk^{repo}$ KK flies and climbing defects in 28-day-old $pirk^{elav}$ KK flies and 28-day-old $pirk^{repo}$ Trip flies.

In terms of sleep behaviour, both KK and Trip 6-day-old $pirk^{elav}$ flies hardly showed any strong sleep phenotypes. However, as the flies age, we begin to see more prominent phenotypes in Trip lines, including a significant decline in total sleep at all three time points (24h, daytime, and night-time) (**Figure 69**). This loss of sleep is likely due to fragmented sleep or reduced sleep quality, marked by an increase in the number of sleep episodes and a reduction in mean sleep episode duration. In contrast, sleep exhibited a significant increase in both 6-day-old

pirk^{repo} KK and Trip flies, with a notable rise in total sleep observed across all three time points(24-hours, daytime, and night-time) (**Figure 70(A)**).

As the *pirk*^{repo} flies age, KK flies displayed an elevation in total sleep duration at all time points, likely due to sleep fragmentation (**Figure 70 (B)**). In Trip flies, we observed an increase in the number of sleep episodes throughout the day, and a change in latency to sleep during daytime sleep in 28-day-old *pirk*^{repo} flies. When compared to *pirk* mutant flies, young *pirk*^{repo} is able to reproduce the increased total and daytime sleep in both RNAi-type fly lines but not in 28-day old flies (**Figure 70**). We speculate that this could indicate that neuronal damage may have occurred prior to the flies reaching adulthood, or that the Trip RNAi may be leaky and ineffective at knocking down pirk by 28-days of age. To address this, we propose employing qPCR to measure the expression levels more accurately.

Assessing gene expression levels using qPCR is critical for validating the efficacy, specificity of RNAi-mediated gene knockdowns; as it provides quantitative data essential for understanding the biological consequences of gene silencing, and ensures the results observed are not due to any off-target effects. Despite our diligent efforts to conduct qPCR assays and collect samples on two separate occasions, we were unable to present the results as planned. Unfortunately, we encountered technical errors with the machine, rendering our data acquisition and analysis unfeasible.

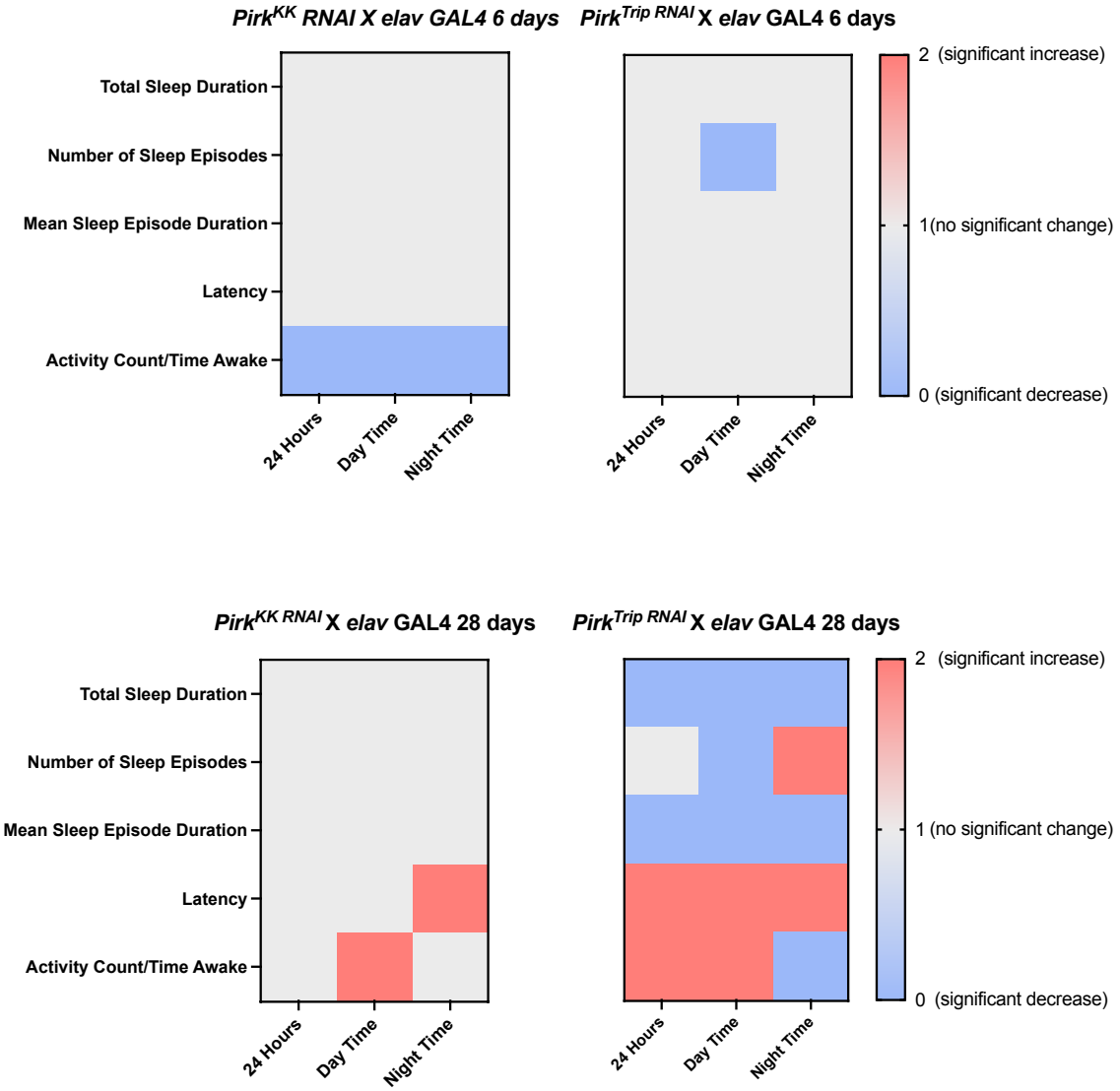

Figure 69: A heatmap summarising the sleep phenotype findings observed in female flies with *pirk* knocked down in the pan neuronal network (via *elav* GAL4). The red colour indicates significant increase, grey representing no significant change, and blue denotes a significant reduction in the parameter. The data is divided into three time points (24h, day and night).

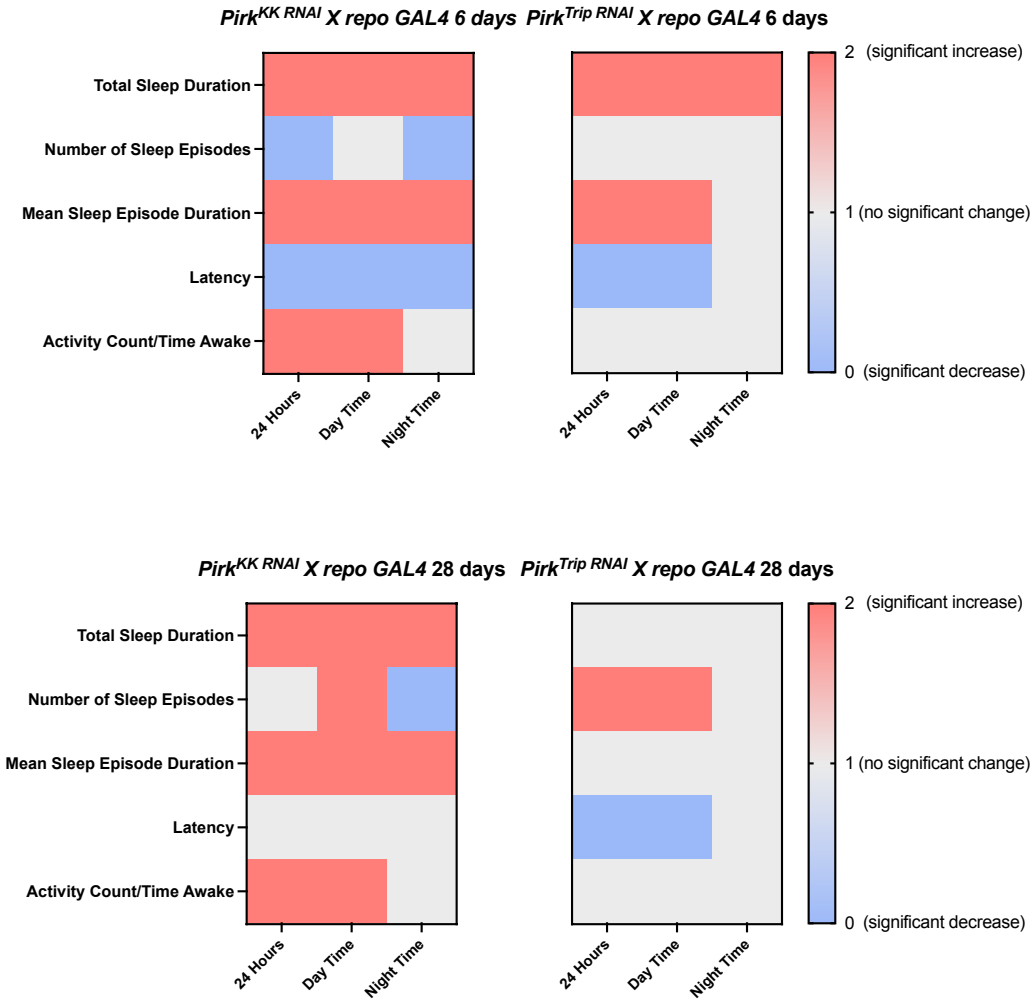

Figure 70: A heatmap summarising the sleep phenotype findings observed in female flies with *pirk* knocked down in glial cells (via *repo* GAL4). The red colour indicates significant increase, grey representing no significant change, and blue denotes a significant reduction in the parameter. The data is divided into three time points (24h, day and night).

Immune Competent Tissue: np1 and esg

The RNAi-mediated knockdown of pirk in various tissues replicated the *pirk* neurological phenotype to different extents. It is important to highlight that different RNAi lines are generated using different methodologies. Hence, we used two distinct lines (KK and Trip) to mitigate potential off-target effects (refer to **Chapter 4** for details).

We analysed the role of the gut by silencing *pirk* in gut enterocytes (via *np1* GAL4) and the gut stem cells (via *esg* GAL4). This approach aimed to elucidate on whether the neurological phenotype we observed was associated with intestinal tissue.

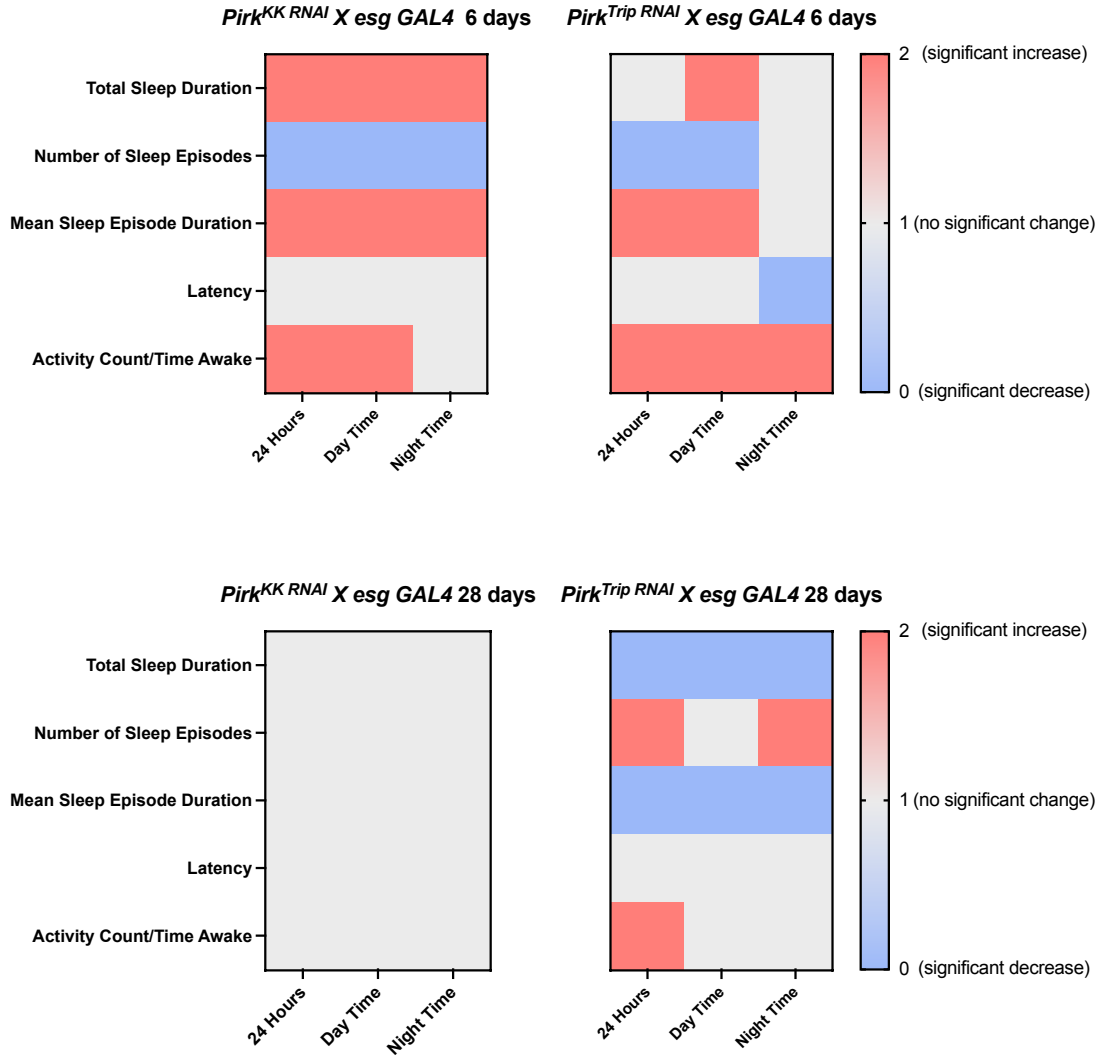

Figure 71: A heatmap summarising the sleep phenotype findings observed in female flies with *pirk* knocked down in gut stem cells (via *esg* GAL4). The red colour indicates significant increase, grey representing no significant change, and blue denotes a significant reduction in the parameter. The data is divided into three time points (24h, day and night).

The *pirk*^{esg} KK exhibited a surprising increase in median lifespan compared to its control. Regarding sleep patterns, *pirk*^{esg} KK and Trip females displayed notable sleep defects at 6-days of age, including an increase in total sleep during all three time points (24hr, daytime, night-time) in KK flies and increased daytime sleep in *pirk*^{esg} KK and Trip flies. Interestingly, despite

not observing all sleep phenotypes in both KK and Trip lines, they demonstrated similar data trends (**Figure 71(A)**). However, by the age of 28-days, *pirk*^{esg} KK and Trip flies did not exhibit sleep phenotypes as prominently as they did earlier in their lifespan. Remarkably, no sleep phenotype was discernible in *pirk*^{esg} KK female flies but *pirk*^{esg} Trip flies demonstrated sleep fragmentation (**Figure 71(B)**). Therefore, based on our own selection criteria, we cannot assert with certainty that the ISC's are responsible for the sleep phenotype.

When *pirk* was exclusively expressed in gut enterocytes, we noted divergent sleep phenotypes in KK and Trip fly lines. Consequently, these observed sleep phenotypes are unlikely to be attributed to heightened immune reactions in the EE cells of the gut (**Figure 72**).

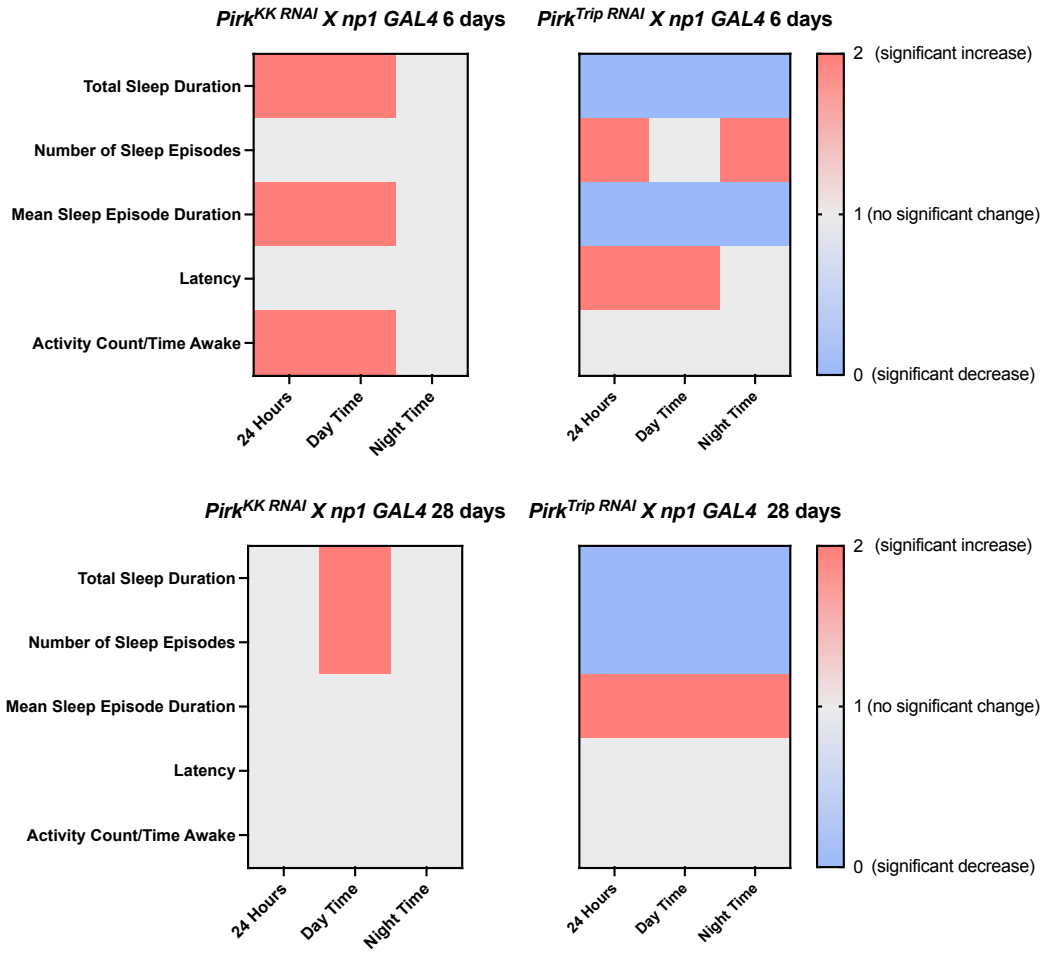

Figure 72: A heatmap summarising the sleep phenotype findings observed in female flies with *pirk* knocked down in gut enterocytes (via *np1* GAL4). The red colour indicates significant increase, grey representing no significant change, and blue denotes a significant reduction in the parameter. The data is divided into three time points (24h, day and night).

Exploring the Microbiome and its influence on sleep and activity

Since *pirk* expression in the gut is microbiota-dependent (Lhocine *et al.* 2008), we sought to examine how a constitutively active immune system influences the density and diversity of gut bacteria in *pirk* mutants. This exploration aimed to enhance our comprehension of the *pirk* mutant fly environment, with the goal of identifying potential factors contributing to the observed phenotypes. Studies conducted in our lab showed that *pirk* flies had significantly more bacterial colonies in their gut than w^{1118} controls on MRS agar at day 28 but not day 6 **(S3)**. To confirm whether this result was consistent across various cultivable bacterial strains, the experiment was repeated using LB agar. This facilitated the growth of a different composition of gut-derived bacteria and resulted in a significant increase in bacterial colonies again at day 28 but not day 6. These results indicated an age-dependent increase in gut bacteria density in *pirk* mutants **(S3).**

To investigate the impact of pirk on the bacterial composition of the gut, we conducted high-throughput DNA sequencing of 16S rRNA libraries. Our analysis focused on determining the relative abundance of bacterial families present in the guts of both 6-day and 30-day old female and male *pirk* flies in comparison to their w^{1118} controls.

We infer that young *pirk* flies possess a diverse microbiome, comparable if not slightly more diverse than that of young controls (w^{1118}) in both male and female flies. Consistent with previous studies (Wong, Ng and Douglas 2011; Mistry, Kounatidis and Ligoxygakis 2017), we observed an age-dependent increase in Acetobacteraceae in both control and *pirk* male flies. Analysis using alpha indices revealed that in both females and males, the diversity in w^{1118} remained relatively stable over the time course, even though the relative abundance changed from young to older flies. In contrast, diversity was diminished in *pirk* mutants for both females

and males, with older flies carrying a less diverse intestinal bacteriome. In conclusion, our data indicate that as *pirk* flies exhibited an age-dependent increase in the density of gut bacteria, there was a concurrent loss of diversity.

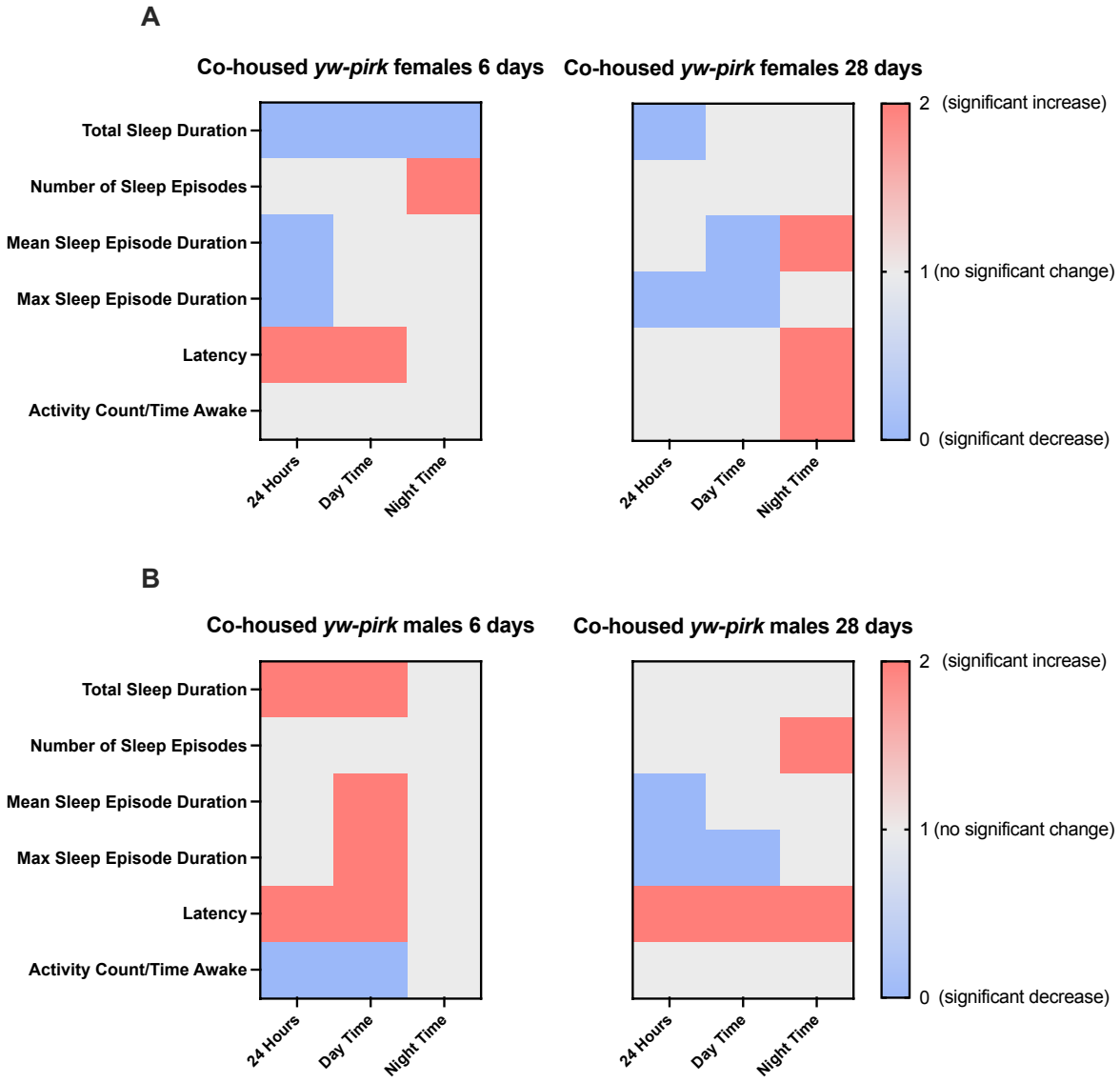

Figure 73: A heatmap summarising the sleep phenotype findings observed in GF male and female *yw* flies co-housed with *pirk* flies vs non cohoused GF *yw* flies. The red colour indicates significant increase, grey representing no significant change, and blue denotes a significant reduction in the parameter. The data is divided into three time points (24h, day and night).

We then investigated whether transferring *pirk* microbiota could modify behaviour in control GF non-co-housed flies. As discussed in **Chapter 3**, the process of generating GF flies has limited influence on sleep behaviour (as also observed by Selkrig et al. (2018)). We employed

a modified version of a previous method for transferring a fly genotype's microbiome to another fly genotype (Mistry, Kounatidis and Ligoxygakis 2017). In this thesis, we co-housed GF *yw* control flies with *pirk* mutant flies: 2-day old GF *yw*, along with *pirk* mutant flies of variable ages, cultured in standard food. GF *yw* controls not co-housed were used as controls, and the food was changed three times a week. Unsurprisingly, we observed sleep defects in co-housed control flies compared to their non-cohoused siblings in both male and female flies as illustrated in **Figure 73**.

Female co-housed flies exhibited a reduction in their sleep duration over the course of the day in both 6-days and 28-days of age. This decline in total sleep was also observed during daytime and night-time sleep in young flies, and is likely due to a reduction in sleep quality. In support of this, we observed a significant reduction in the maximum and average sleep episode duration in young flies over the course of the day, as well as a decline in maximum sleep in 28-day-old flies, compared to their controls **(Figure 73(A))**. A contrasting effect was observed in total sleep in young male co-housed flies during the course of the day and during daytime sleep. This increase in sleep resulted in an increase of both the maximum and average sleep episode duration in young males during daytime sleep. However, this change might be compensated for during night-time, as no observable change was noted in young flies throughout the day (**Figure 73(B)**).

Taken together, results on the diversity and density of gut bacteria argue for intestinal dysbiosis in the absence of *pirk* and suggest a causative role for the microbiome in parts of the neurological phenotypes observed related to sleep patterns.

While we could not replicate the exact symptoms outlined in Chapter 2, the mere observation of any sleep phenotype being transferred is fascinating. This underscores the potential of co-

housing as a method to investigate the role of environmental bacteria on age-dependent neurodegeneration in flies predisposed to heightened immunity.

Conclusions of the Study

Our primary hypothesis posits that dysbiosis, caused from the absence of Pirk in the gut, exerts a notable influence on *pirk* neurology during the early stages of adulthood, while chronic immune activity in glial cells ($pirk^{repo}$) contributes to neurodegeneration throughout the lifespan. This aligns with previous research, highlighting the suppression of neurodegeneration when NF-κB signalling is blocked in glia within the context of chronic Imd activation (Kounatidis *et al.* 2017). Noteworthy findings from studies in axenic conditions demonstrate the rescue of *pirk* lifespan (Paredes *et al.* 2011; Kounatidis *et al.* 2017). However, our results suggest that health span is not fully restored, evident from the persistent neurological defects in later life. Interestingly, germ-free *pirk* flies appear to manifest a delayed onset of neurological phenotypes, as indicated by brain histology **(Supplementary Figure 2)** and locomotion assays conducted by other members of the lab. However, in the context of sleep, we observed an increase in sleep duration in both GF and CR flies at 6-days of age but not in GF 28-day old flies in both males and female flies. This indicates that the sleep phenotype remained unaltered under germ-free conditions.

The potential involvement of bacteria in the onset of neurodegeneration presents a plausible explanation for the observed earlier onset of neurological decline in cases of immune dysregulation in ISC cells ($pirk^{esg}$). This may occur through two non-mutually exclusive pathways: the passage of metabolites derived from commensal gut bacteria through the blood-brain barrier (BBB)(Emery *et al.* 2017). Furthermore, studies in *Drosophila* neurodegeneration models have already uncovered a correlation between dysbiotic gut flora and exacerbated brain

cell death (Wu *et al.* 2021). An alternative explanation involves the role of reactive oxygen species (ROS), as ROS accumulation in the gut has been linked to chronic sleep deprivation in *Drosophila*, leading to premature death (Vaccaro *et al.* 2020).

Limitations of the Study

Needless to say, no model system is without limitations. It is important to note that like most invertebrate organisms, the fruit fly is evolutionarily distant from humans and does not accurately mimic all the neurodegenerative phenotypes observed in human diseases such as tau aggregates and plaques (Jeibmann and Paulus 2009). *Drosophila* making it difficult to recapitulate the complex changes in the immune response that might take place during ageing. lacks an adaptive immune response. Additionally, the hemolymph of the fly contains primitive hemocytes, which cannot undergo DNA rearrangement and somatic hypermutation, like mammalian lymphocytes. Unlike mammals, flies do not possess microglia, rather, all glial cells can perform microglial tasks such as engulfing neuronal corpses during development (Freeman and Doherty 2006). However, this restricts studies that attempt to understand the complicated relationship between the immune system and the relation between neuroprotection and neurodegeneration.

Nevertheless, this thesis highlights evidence suggesting that the immune system plays an important role in neurodegenerative disorder in *Drosophila*. Two key contributors to lifespan reduction and neuropathy are overproduction of AMPs and impaired phagocytosis.

Even though animal models do not represent the diseases completely (for example in the lack of direct orthologs for the human proteins prone to aggregation in AD or PD), comparative studies of brain development and the innate immune response have demonstrated significant evolutionary conserved mechanisms between vertebrates and invertebrates. Moreover, the

deregulation of innate immunity as aetiology for neurodegeneration stands in *Drosophila.* There is great therapeutic potential in immunomodulation and therapeutic immunisation (Benner et al. 2004) to help combat the development of such diseases, aided by rapid screening in whole-animal models such as the fruit fly even in the absence of tau or Aβ. Moreover, since the role of immune activity in microglia and astrocytes in neurodegeneration is well-documented, we could envisage that negative regulators of immunity could be potential candidates for early interventions.

While our experiments have provided valuable insights, it is important to acknowledge its inherent limitations in the experimental design. Even though there are evolutionary conserved mechanisms between vertebrates and invertebrates, Pirk is *Drosophila*-specific and not present in mammals (Kleino *et al.* 2008). One notable constraint lies in the leaky and unpredictable nature of the UAS / GAL4 and RNAi systems. Furthermore, the effectiveness of the gene knockdown is assessed through qRT-PCR, which detects mRNA levels of the gene but not its protein levels. This is crucial, since, in nature the expression of a protein can also be inhibited via post-transcriptional silencing, such as microRNA. Moreover, the DAM system requires a single fly in one tube, potentially leading to inactivity caused by a lack of social stimulation. Finally, there is room for improvement in the co-housing protocol by using pirk flies of a specific age and accounting for any social aggression caused by housing non-sibling male flies.

Future Directions

Continuous refinement is intrinsic to the process of research. Within the scope of this study, there is potential for further investigation through the implementation of the following experiments that can further enhance our understanding of the intricate relationship between immunity, gut microbiota, and neurodegeneration in *Drosophila*.

Firstly, accumulation of ROS in the gut has been shown to chronic sleep deprivation in *Drosophila*, that leads to premature death (Xie *et al.* 2013; Vaccaro *et al.* 2020). Investigating the potential concentration of ROS in the context of *pirk* mutants represent a promising direction in understanding the way the gut causes the observed sleep phenotypes and potentially aid in developing therapeutics for humans. Additionally, Zhang et al. (2018) illustrated that the BBB is governed by the circadian rhythm. A comprehensive study examining the integrity and function of the BBB in *pirk* mutants could elucidate whether gut dysbiosis influences neurodegeneration by impacting the passage of metabolites or bacteria into the brain. Exploring the effects of non-*Wolbachia* flies further add depth to our investigations, allowing us to discern the specific influence of *pirk* on neurological phenotypes without the confounding factor of *Wolbachia*.

Lastly, completing the 16s rRNA analysis will be crucial, providing a comprehensive understanding of the gut bacterial composition in *pirk* mutants at different ages, and aiding in correlating specific bacterial strains with observed phenotypic variations. Additionally, 16S rRNA sequencing could also be performed in co-housed flies to identify bacterial families potentially responsible for sleep phenotypes. These future experiments collectively aim to refine our knowledge and contribute to unravelling the complex mechanisms underlying neurodegeneration in *Drosophila*.

CHAPTER SEVEN

Materials and Methods

7.1 MATERIAL AND METHODS

7.1.1 Fly Food Preparation

General

Standard food was prepared using soy flour, molasses, and yeast powder **(Table 2)**. However, amid the COVID-19 pandemic, due to the unavailability of soya, it was substituted with cornmeal. All experiments, with the exception of conventionally reared sleep, climbing, and the smurf assay **(Chapter 2)**, as well as 16srRNA sequencing **(Chapter 5)**, were conducted using the revised cornmeal recipe **(Table 3)**.

Reagent	Mass/Volume
95% propionic acid (Sigma-Aldrich P5561), 5% phosphoric acid (Sigma-Aldrich P5811) solution	140mL
Agar (Fisher Scientific, BPE2641-1)	169g
Ethanol (VWR)	703 mL
Maize Flour (Brian Drewitt)	1.8kg
Malt Extract (Brian Drewitt)	1.8kg
Methyl 4-hydroxybenzoate (Nipagin, Sigma- Aldrich W271004)	74g
Molasses (Rayners, Brian Drewitt)	500g
Soya Flour (Brian Drewitt)	216g
Water	28L
Yeast Powder (Brian Drewitt)	366g

Table 2 Fly food component list (Soya Flour Food)

Reagent	Mass/Volume
95% propionic acid (Sigma-Aldrich P5561), 5% phosphoric acid (Sigma-Aldrich P5811) solution	140mL
Agar (Fisher Scientific, BPE2641-1)	169g
Ethanol (VWR)	703 mL
Cornmeal	1.8kg
Methyl 4-hydroxybenzoate (Nipagin, Sigma- Aldrich W271004)	74g
Molasses (Rayners, Brian Drewitt)	500g
Distilled Water	28L
Yeast Powder (Brian Drewitt)	366g

Table 3: Fly food component list (Cornmeal Molasses Flour Food)

Sleep

Freshly prepared food was stored in 1L bottles for later use. Subsequently, it was gently warmed while avoiding bubbling and then poured into standard-size petri dishes.

Germ Free Experiments

Food poured into 1L bottles was gently warmed, taking care to prevent bubbling, and then cooled to approximately 60°C. The cocktail of antibiotics or MeOH (for controls) were added in the desired concentration (see **Table 4**), and the food was stirred before being poured into vials or petri dishes.

Antibiotic	Concentration	Stock Solution
Tetracycline (MP Bio)	50 µg/mL	5mg/mL in MeOH
Rifampicin	200 µg/mL	10mg/mL in MeOH
Streptomycin (Merk)	100 µg/mL	10 mg/mL in dH_2O

Table 4 List of Antibiotics used in GF food (Sharon *et al.* 2010)

7.1.2 Fly Stocks

Information on the *Drosophila melanogaster* lines used in this thesis is detailed in **Table 5**. Inbred yw^{67c23} and w^{1118} flies were maintained in bottles by the Ligoxygakis lab and served as the genetic background for all experiments. The experimental flies were kept under standard conditions: 25°C, 33% humidity, with a 12-hour light / 12-hour dark cycle. 'Backup' stocks for each line were maintained 18°C with 57% humidity on a 12-hour light / 12-hour dark cycle on standard soya flour-molasses or cornmeal-molasses medium and were transferred to a new medium every 14-21 days.

Fly Line	Flybase ID/ Stock Reference Number
w^{1118}	Inbred lab stock BL #6326
yw^{67c23}	Inbred lab stock BL #6599
$pirk^{EY}$	Neal Silverman (w^{1118} background) Mika Ramet (*yw* background)
Pirk RNAi KK	v105790
Pirk RNAi Trip	BL#67011
Repo Gal4	BL#7415
Elav Gal4	BL#8765
Esg Gal4	BL#84324
NP1-GAL4/Cyo; drsGFP/TM3	BL#84307
w^{1118}*; T(2;3)/Cyo; Δ(2-3)sb*	BL#639

Table 5 Fly Stocks used in this study

7.1.3 Fly Husbandry

Flies were housed in plastic vials (diameter 29.21 mm X Height 3.74 in, K-Resin Fisherbrand™ Drosophila Vials) or stock bottles (Fisherbrand™ Drosophila Bottles), filled with standard medium (**Section: 7.1.1**: General food preparation) and sealed with cotton plugs (also known as flugs). During the experiments, flies were reared at 25°C, 35% humidity under a 12hr:12hr light / dark (LD) cycle in an environmentally controlled incubator.

Experimental flies were allowed to mate for 48 hours in bottles / vials (depending on their densities) and collected under light CO_2-induced anaesthesia, segregated based on sex and housed at a density of 10–16 flies per vial. The food was changed every 2–3 days throughout adult life or until the desired time point.

Virgin Collection

Adults from bottles with dark pupae were discarded the night before and female flies with a pale appearance with a dark meconium on the stomach (characteristic of virgins) were collected every 4 hours. This is because freshly enclosed males remain sterile for 4-6 hours at 25°C.

Setting Crosses

The required number of female (virgins) and males were collected over a span of 3 days. Crosses were established either in bottles (where eggs did not necessitate bleaching/washing) or in cages with apple juice plates.

Apple juice plates for egg collection

Apple juice plates were prepared by combining 22g of agar with 750 mL of water in a 1-litre bottle, which was autoclaved with a stirrer. Then, 25g of sucrose was dissolved in 250 mL of

apple juice and incorporated into the mixture. After cooling to approximately 37°C, the solution was poured into petri dishes and stored. For setting cages, a small portion of ready-to-use yeast paste (consisting of equal parts commercially available baker's yeast and water) was added to the sealed end of apple juice plates.

7.1.4 Fly Mating Scheme

For this study, we used flies that were prepared containing the UAS- GAL4 system, a transcription system co-opted from yeast responsible for tissue-specific activation / silencing of genes. A site specific GAL4 transcription factor binds to an up-stream activating sequence (UAS) tagged with a RNAi sequence, resulting in gene knockdowns.

After expanding and preparing the flies, virgins were collected from the UAS *pirk* flies and subsequently crossed with various GAL4 drivers. The resulting progeny provided us with the desired flies for the experiments, carrying one copy of the UAS-Pirk RNAi and one copy of the GAL4 driver of interest. The crosses set for **Chapter 4** are detailed in the following table:

A.

	Pirk RNAi KK X Gal4 Line	*Control Line used*
1.	*Pirk RNAi KK X elav GAL4*	w^{1118} *KK X elav GAL4*
2.	*Pirk RNAi KK X repo GAL4*	w^{1118} *KK X repo GAL4*
3.	*Pirk RNAi KK X np1 GAL4*	w^{1118} *KK X np1 GAL4*
4.	*Pirk RNAi KK X esg GAL4*	w^{1118} *KK X esg GAL4*

B.

	Pirk RNAi Trip X Gal4 Line	*Control Line used*
1.	*Pirk RNAi Trip X elav GAL4*	*yw X elav GAL4*
2.	*Pirk RNAi Trip X repo GAL4*	*yw X repo GAL4*
3.	*Pirk RNAi Trip X np1 GAL4*	*yw X np1 GAL4*
4.	*Pirk RNAi Trip X esg GAL4*	*yw X esg GAL4*

Table 6:Pirk RNAi/GAL4 mating scheme for Chapter 4

7.1.6 Behavioural Studies

Lifespan Analysis

Once the adult flies emerged from pupae (approximately 10 days later), they were transferred to fresh food and allowed to mate for 48 hours. Following this, they were anaesthetized and sorted by sex. Flies were then randomly transferred to vials at a density of 15 flies per vial. Mortality was recorded on scoring sheets during the thrice-weekly transfers to fresh food.

Sleep analysis

Glass tubes with a diameter of 10 mm were pre-prepared with food on one side and sealed with wax. Flies were aged until the desired time points (6-days and 28-days) on standard food and were then transferred into the tubes, which were finally sealed with a cotton plug. A monitor, consisting of 32 tubes, was prepared for each condition and placed in a separate incubator with a 12:12 light-dark (LD) cycle

For the *pirk* mutant experiments, flies were initially mouth-pipetted into individual glass vials. However, later, due to COVID-19 mask restrictions, the flies were anesthetised using ice and placed with the help of a brush.

Climbing Assay

Two autoclavable fly vials were combined to create a climbing assay tube. Each tube was divided into three sections: top, middle, and bottom, marked at 3 cm and another at 10 cm from the bottom of the tube.Flies were transferred into climbing tubes and left in the incubator for 20 minutes to acclimatise before the experiments. The climbing tubes were tapped down using

identical pressure, allowing the flies to fall into the lowest compartment of the tubes. From here, they were permitted to climb for 30 seconds, after which the number of flies in each compartment was noted. To minimise trial errors, the process was repeated four times, with the first one not recorded, and the average of the three repeats was taken. Finally, the total number of flies was counted, and the performance index of flies was calculated using the following formula.

$$Performance\ Index\ PI = 0.5 * (nTotal + nTop - nBottom)\ /nTotal$$

Where nTop is equal to the number of flies on top, nMiddle is equal to the number of flies in the middle, nBottom is equal to the number of flies at the bottom and nTotal is equal to the total number of flies in a tube.

Intestinal permeability assay

The intestinal permeability assay, also known as the Smurf Assay, was developed by Rera et al., 2012. Flies were aged until the desired time point on standard medium until the morning of the assay. The Smurf dye was freshly prepared on the day, using Blue dye no. 1 (purchased from Sigma-Aldrich) at a 2.5% (wt/vol) concentration in 10% sucrose. The solution was then added to a 2mm filter paper disc (Whatman™) and carefully inserted into a vial containing food. The flies were left on the dye for 9 hours. Flies with food dispersed throughout their body (outside the digestive tract) were marked as Smurfs.

Drosophila co-housing assay

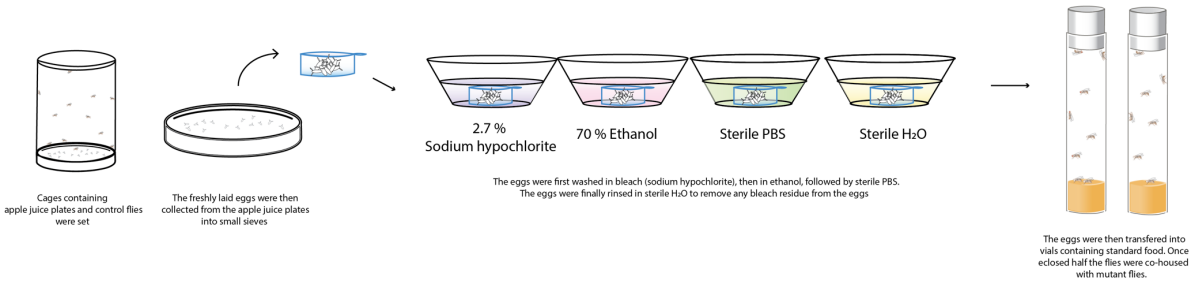

Figure 74: An illustration describing the generation of flies that are used in the cohousing experiment.

The co-housing assay is a modification of a previous method for transferring a fly genotype's microbiome to another (Mistry, Kounatidis and Ligoxygakis 2017). Co-housed flies were prepared by housing each strain separately in cages on apple juice plates to collect embryos, which were then dechorionated using bleach and ethanol, as described above. Once germ-free, the eggs were transferred into antibiotic vials where they matured in axenic conditions. Once eclosed, the adult germ-free flies were transferred onto fresh food, where they were allowed to mate for 48 hours before being separated based on their sex. Seven germ-free control flies were then carefully placed along with 6-7 mutant flies of the same sex in a fresh standard food vial that was changed every alternate day.

7.1.7 Drosophila Gut Dissections

The flies were first anesthetised by putting them on a cold pad. Each fly was fastened under a dissection microscope, and the abdomen was revealed by delicately removing the wings and legs with tiny forceps and scissors. After the fly was cleaned and placed in a sanitised dissection dish, external impurities were aided to disappear with a rinse using 1x PBS. Using tiny forceps, the cuticle around the back of the abdomen was carefully split to reveal the internal organs,

with particular attention paid to identifying the gut, a tubular structure that runs down the dorsal side of the abdomen. To reduce harm, the stomach was carefully isolated from the surrounding tissues. The separated gut was then moved to a microcentrifuge tube containing PBS. To guarantee accuracy, every process was carried out under a dissecting microscope, and sterility was upheld the whole time to avoid contamination.

7.1.8 Characterisation of the Drosophila gut microbiota

Germ Free Flies/ Axenic Flies

Several techniques can be employed to generate axenic (GF) flies, including dechorionation: removing the chorion from freshly deposited eggs, as well as autoclaved, germ-free food, and antibiotic cocktail rearing. Eggs are collected using cages and plates during the dechorionation process. With a sterile paintbrush, the eggs are gathered and then treated with a hypochlorite solution, ethanol, MilliQ water, and PBS washes **(Figure 67)**. Subsequently, chorion-free eggs are carefully placed in food that has either been autoclaved or contains antibiotics (Kounatidis et al. 2017). Broad-spectrum antibiotics, such as tetracycline, penicillin, streptomycin, and rifamycin, can be used individually or in combination (Sharon *et al.* 2010; Heys *et al.* 2018). These flies can remain GF for several generations.

After being rinsed with PBS and cleaned in sterile water, the control group is given standard fly food. The same process is applied to produce gnotobiotic flies, which are used to investigate host-microbe interactions unique to a species and whose axenic meal comprises a single or a mix of bacterial species. Ultimately, PCR amplification of the 16S rRNA gene region or conventional culture methods on selective media like MRS (de Man, Rogosa, and Sharpe), BHI (Brain Heart Infusion agar), and LB (Luria Broth agar) are used to confirm that eggs and flies

are germ-free (Sabat and Johnson 2015; Kounatidis *et al.* 2017; Mistry, Kounatidis and Ligoxygakis 2017).

Creating Germ Free flies

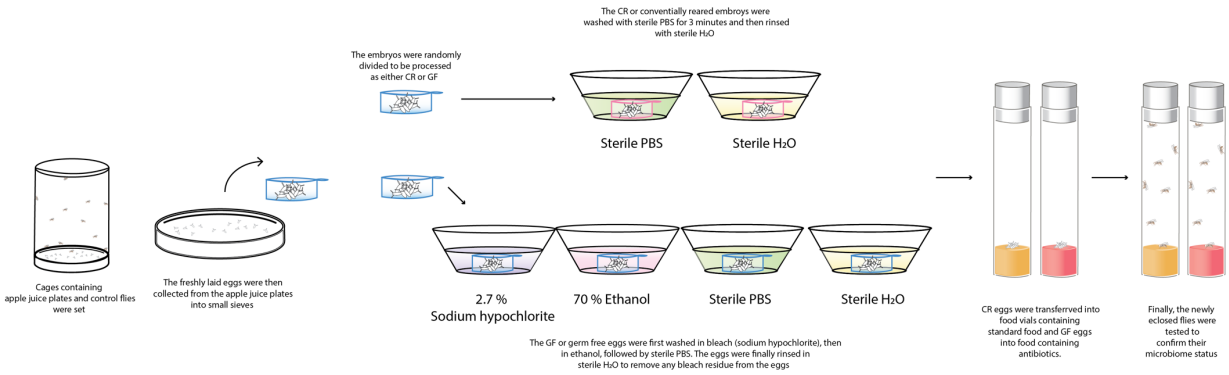

Figure 75: An illustration demonstrating the process of generating germ free flies.

The cages were set with approximately 70 virgins females and 30 males on apple juice plates. Every 24-hours, the flies were anesthetised, and the apple juice plate was removed. Eggs from the first day were discarded. Subsequently, eggs were collected after 24-hours by pouring PBS and collecting them with the help of a paintbrush and pipette. These were then transferred into a 15ml Falcon tube and washed with PBS until the solution was clear. After the final wash, the tubes were filled with PBS and shaken. Once the eggs were dispersed, the solution was poured onto a mini sieve. The sieve was then transferred into a petri dish containing 50% bleach (or 2.5% sodium hypochlorite) and washed for 30 seconds using a pipette. This process was repeated for 30 seconds with 70% EtOH, for 2 minutes with MilliQ H2O, and then for 2 minutes with PBS **(Figure 67)**. The eggs were then examined under the microscope to check for the loss of chorion and were transferred into bottles containing antibiotic food or MeOH food.

Testing for Germ Free flies

Once enclosed, the flies were allowed to mate for 48 hours in vials containing their respective food. Afterward, they were anaesthetised with CO2 and transferred into food containing antibiotic or MeOH. Guts were extracted weekly and plated on MRS plates. Once plated, the MRS plates were incubated at 30°C for 48 hours and checked for colonies.

7.1.9 Culture-independent gut microbiota identification

The 16s rRNA sequencing process was divided in various parts:

Sample Collection

Midgut of forty flies were dissected from 6-day and 28-day old male and female flies at selected time points. The dissections were performed in sterile PBS and their genomic DNA (gDNA) was extracted using QIAamp DNA Mini Kit (51304, Qiagen, Germany), according to manufactures instruction along with a reagent control to exclude any contaminants.

DNA isolation and processing

One of the major drawbacks of identifying the microbial families using sequencing is caused by the read outs of *Wolbachia*. To try and eliminate the read out of *Wolbachia* from the extracted DNA, it was first digested with the restriction enzyme BstZ17I (R3594S, NEB, UK) that fragments the 16s region of Wolbachia RNA reads only, hindering its amplification in the next steps.

Approximately 500 ng of DNA was incubated with BstZ17I, followed by the heat inactivation of the enzyme for 2 hours (manufactures instructions). The digested gDNA was then used to amplify the 16S hypervariable regions V1-V3 using primers given in **Table 8** using Phusion HF DNA polymerase (MO530L, NEB, UK) (PCR conditions **Table 7**). The PCR product was then purified by using the Qiagen PCR Purification Kit (27106, Qiagen, Germany), which was further used to amplify the V3 hypervariable region, using Phusion HF polymerase (MO530L, NEB, UK)**.** Finally, the V3 product was run on a 1.2% agarose gel, and a 200bp V3 band was excised and purified using the QIAquick Gel Extraction Kit (28706, Qiagen, Germany).

V3 Library Prep

The DNA purified from the agarose gel was then measured and approximately 100ng of V3 DNA samples (measured using Picogreen assay (P11496, Thermo Fisher, USA), according to manufacturer's instructions was used for library preparation using NEBNext® Fast DNA Library Prep Set for Ion TorrentTM (E6270, NEB, UK) and Ion XpressTM Barcode Adaptors (4471250, ThermoFisher Scientific, USA). The libraries were further purified using Agencourt AMPure XP DNA purification beads (A63881, Beckman Coulter, Germany) to eliminate any contaminants and primer dimers. Samples were further size selected at 300bp using a 2% E-gel (G501802, ThermoFisher Scientific, USA), and further quantified using quantitative PCR using KAPA library quantification kits for Ion TorrentTM platform against Ion TorrentTM DNA Standards (KK4812, KAPA Biosystems, USA). Samples that were too low in concentration were re-amplified using the NEBNext® Fast DNA Library Prep Set for Ion TorrentTM (E6270, NEB, UK) protocol and re-quantified.

Temperatures	Duration	Number of Cycles
98°C	30 seconds	1 cycle
95°C	30 seconds	35 cycles
65°C	30 seconds	
72°C	1 minute	
72°C	5 minutes	1 cycle

Table 7: PCR cycling conditions used to amplify hypervariable regions 1-3 (V1-V3) from BSTZ17I (R3594S, NEB, UK) digested Drosophila gut gDNA. Amplification was performed using phusion polymerase (MO530L, NEB, UK).

Primer ID	Sequence	Template
16S 27Fw	5'-AGAGTTTGATCCTGGCTCAG-3'	V1-V3
V3 Fw	5'-CCAGACTCCTACGGGAGGCAG-3'	V3
V3 Rv	5'-CGTATTACCGCGGCTGCTG-3'	V1-V3, V3
IT A	5'-CCATCTCATCCCTGCGTGTC-3'	V3 library
IT tr P1	5'-CCACTACGCCTCCGCTTTCCTCTCTATG-3'	V3 library

Table 8: Primers used to amplify 16S hypervariable regions V1-3 (16S 27Fw, V3 Rv), V3 (V3 Fw, V3 Rv) and quantify V3 DNA libraries (IT A,IT tr P1).

Sequencing

Samples were loaded onto an Ion 314TM Chip v2 (multiplexing 16 samples per chip) using the Ion Chef System, and sequenced using the Ion ProtonTM system, (ThermoFisher Scientific, USA) according to manufacturer's instructions (Mistry, Kounatidis and Ligoxygakis 2017; Bahuguna *et al.* 2022).

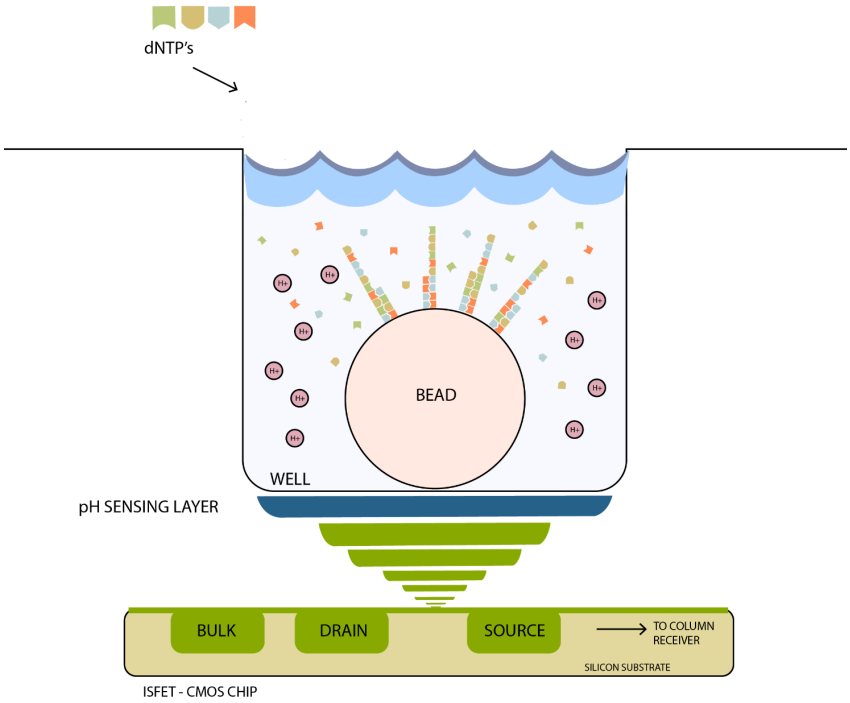

Figure 76: Principle of ion torrent sequencing. Single nucleotides are introduced to the Ion 314T M Chip V2, housing DNA libraries ligated to beads. These nucleotides adhere to the DNA strand through nucleotide complementarity, causing the release of hydrogen ions. The liberation of protons induces a pH alteration in the well. The sensor plates detect this change, which is subsequently converted into a digital signal by ISFET detectors. The digital signals are then transmitted through the silicon chip, presenting the nucleotide readouts.

Ion Torrent's systems are based on standard pyrosequencing chemistry where sequencing is done by synthesis. Here, each base is introduced separately and includes DNA polymerase. This sets the sequencing technology apart. Further, this technology measures the direct release of H+ protons from the reaction, whereas sequencing technologies based on pyrosequencing measure light released from chemiluminescent reagents. The Ion Torrent sequencing technology can be more cost effective as the instruments don't require optics and it has disposable chips which can be compared to a pH meter. Further, it has comparatively faster sequencing reactions due to the lack of optics and doesn't have to deal with slow image scans. This means that 200b reads can be taken in 2 hours. Additionally, the system uses unmodified nucleotides which are tolerated better by DNA polymerase and are comparatively inexpensive. They are able to use this because of the lack of fluorescence or chemiluminescence. long homopolymers (stretches of the same base, e.g., AAAAAA) are challenging for

pyrosequencing chemistry, even though the error rates are not that bad (~1%). Stretches of the same base result in a single, strong signal as the chemistry doesn't pause at the end of each base incorporation. This makes it difficult with long stretches although short stretches can be differentiated.

Statistical analysis of 16s rRNA libraries

ThermoFisher Scientific, USA, provided the Ion ReporterTM software, which was utilised for data analysis. Using V3 primers and a customised metagenomics workflow version 5, the analysis was measured against the microSEQ® 16S reference library v2013.1.

Each read was examined for single-end primers, and reads that were less than 125 bp (after primer trimming) were disregarded. A minimum alignment coverage of 90% was also applied. Considering the technical inaccuracy of the Ion Proton, Operational Taxonomic Units (OTUs) were only kept if they had a minimum of three readings, and the species percentage identification was fixed at 99%. It was determined that there was a 0.8% percentage difference between the top hit and the subsequent hit.

The diversity of microbiota within and between each sample was measured by plotting alpha (Simpson's 1-D, and Shannon H) using PAST3 software. Simpson's index (D) measures the probability of selecting two individuals from a population belonging to the same species, while Shannon's diversity index (H) measures the species richness and evenness in terms of uncertainty of predicting species in a sample (ie. entropy).

Graphs were designed using GraphPad Prism version 8. Analytic Rarefaction v1.3 (http://www.uga.edu/~strata/software/index.html) was used to create rarefaction curves showing sample saturation. PAST3 software (Hammer and Harper 2001; Morris *et al.* 2014)

was utilised for the examination of beta diversity (principal component analysis, PCA) and alpha diversity (Simpson 1-D, Shannon H, and Sobs) statistics.

7.1.10 Molecular Work

DNA isolation

DNA was isolated sing the SuperScriptTM VILOTM cDNA Synthesis Kit (11754050, Thermo Fisher, USA) and the manufacturer's instructions, total RNA was used as the starting material for the synthesis of cDNA.

RNA Isolation

Norgen total RNA purification plus kit (48400, Norgen-Biotek, Canada) was used to extract total RNA. For each RNA sample, a pool of ten guts was used, and three biological replicates were isolated per genotype. Nanodrop was used to evaluate the RNA content and purity, which ranged from 50 to 500 ng/µl and were indicated by the 260nm/280nm absorbance ratio. The purity of the RNA in the sample is determined by measuring the absorbance ratio of proteins at 280 nm to RNA at 260 nm.

7.1.11 Statistical Analysis

Statistical analyses were conducted using various tests depending on the nature of the data. A two-tailed, unpaired Student’s t-test was used for all parametric analysis, whereas a Mann-Whitney rank sum test was performed for all data sets that did not show a normal distribution. A two-way ANNOVA test was performed for all GF sleep and activity analysis and the recommended Šídák's corrections was used to correct for multiple comparisons. Bacterial

density was evaluated by Log10CFU values, and compared between mutants and controls using an unpaired Student's t-test. RT-qPCR data underwent statistical scrutiny through unpaired student's t-tests with Bonferroni correction for multiple comparisons. Lifespan analysis was depicted as survival curves and subjected to a Log-Rank test.

Significance was established at a p-value less than 0.05 (alpha value). Graphs and statistical analyses were generated using GraphPad Prism, version 9.5 and all the data was presented mean ± SEM (unless stated otherwise).

CHAPTER EIGHT

APPENDIX

8.1 Supplementary data

Supplementary Figure 1 (S1)

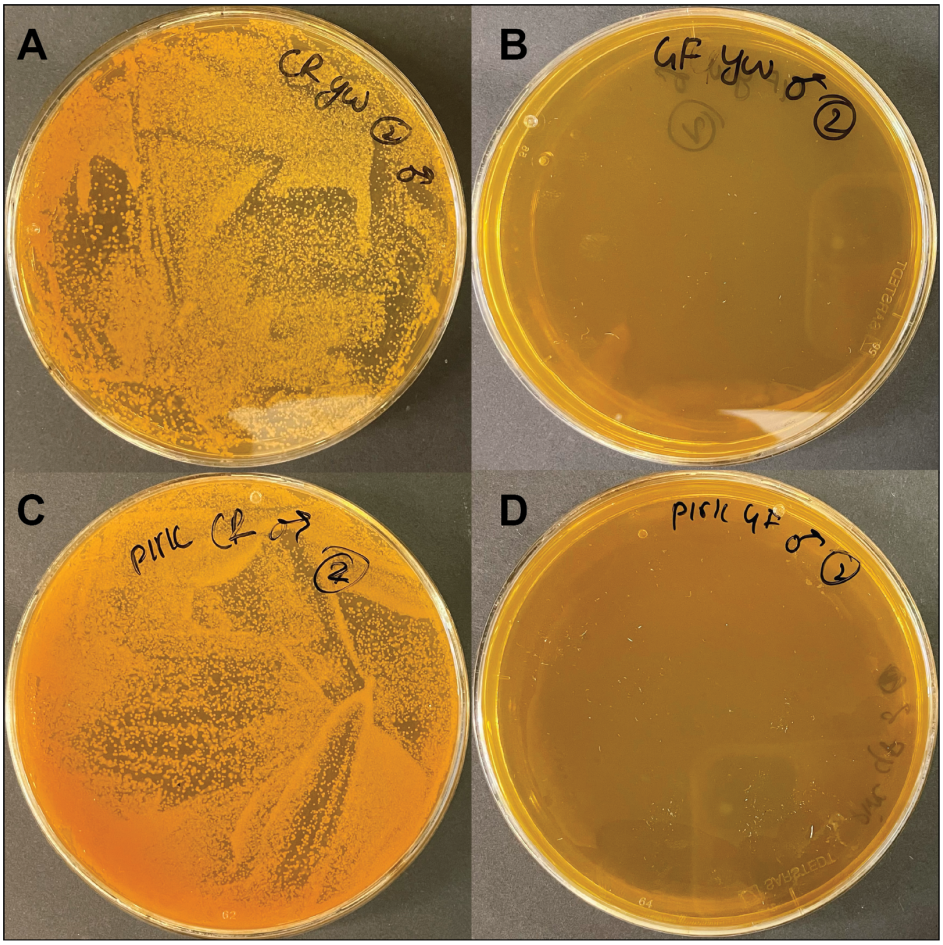

Figure S1: MRS plates to confirm the germ free status of flies. Individual Drosophila midguts were dissected in Phosphate-buffered saline (PBS) solution and then homogenized in De Man, Rogosa and Sharpe (MRS) broth (CM0359, Oxoid,Thermo Fisher, USA using a sterile needle. The resulting suspension was then plated on MRS agar (CM0361, Oxoid,Thermo Fisher, USA), and incubated at 30◦C for 48 hours.

The germ-free status of the flies was confirmed using conventional culture methods on MRS media, weekly from Day 1 to Day 30, and validated on the day of the experiment.

Supplementary Figure 2 (S2)

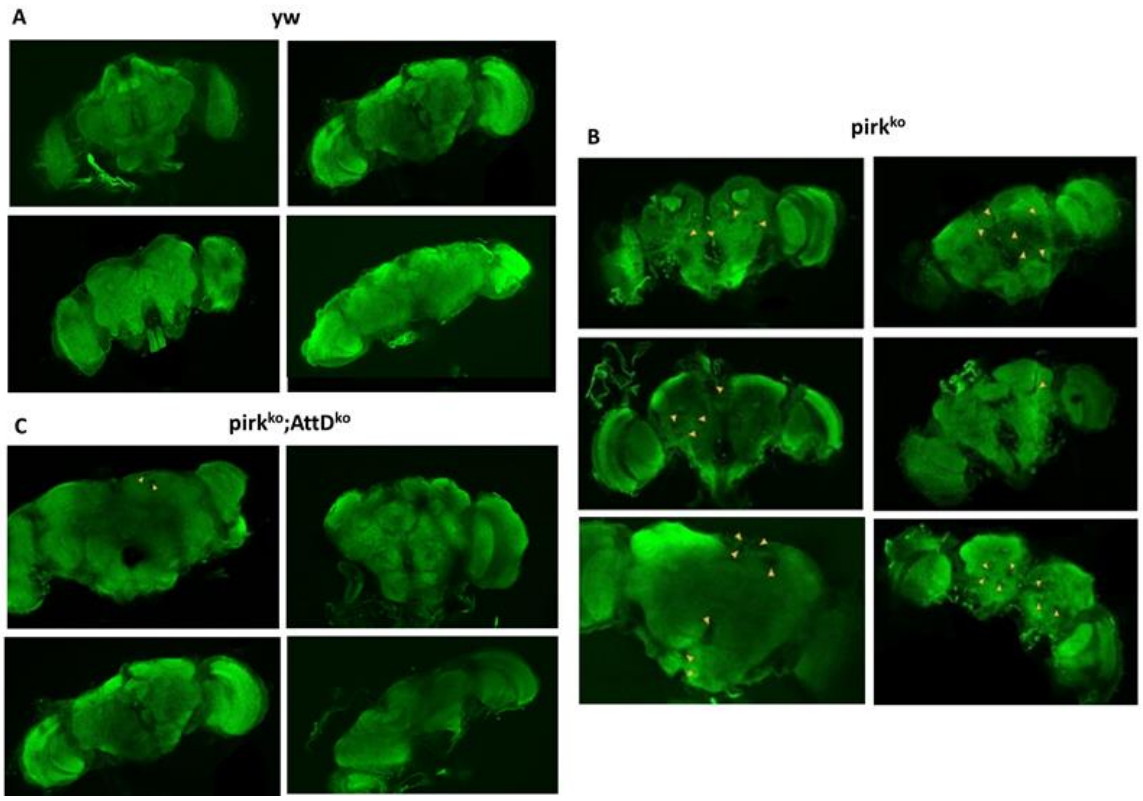

D

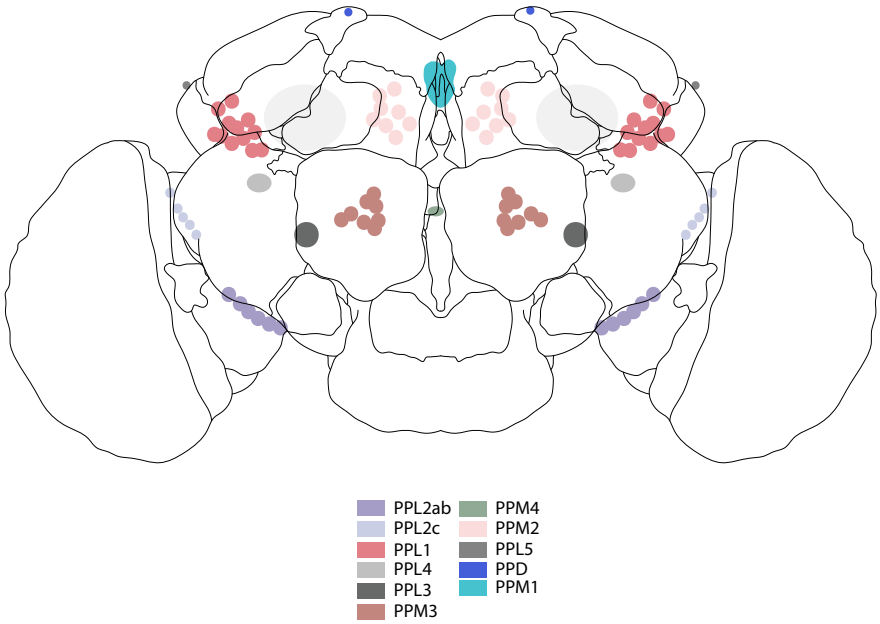

FigureS2: Neurodegeneration suppression in *pirk*;AttD double knockout. (A) Brains of *yw* controls (B) Brains of *pirk* mutants(C) Brains of *pirk*;AttD double mutants (lesions are shown with white arrowheads) (D) Posterior neuronal clusters shown in false colour

According to the initial experimental design, counting of DA neurons was intended to investigate the extent of neurodegeneration observed in *pirk* mutant flies. Despite the development and refinement of a protocol (**SM2**), the execution of the experiment remained incomplete. Successively, following my tenure in the laboratory, a subsequent researcher, Grace Critchley (a Part II student), endeavoured to employ the aforementioned protocol. Regrettably, despite her efforts, the visualisation of dopaminergic neurons proved unattainable. Nevertheless, she utilised*pirk* mutant flies. Notably, she demonstrated the successful rescue of these lesions by generating pirkko;AttD double knockout flies.

Supplementary Figure 3 (S3)

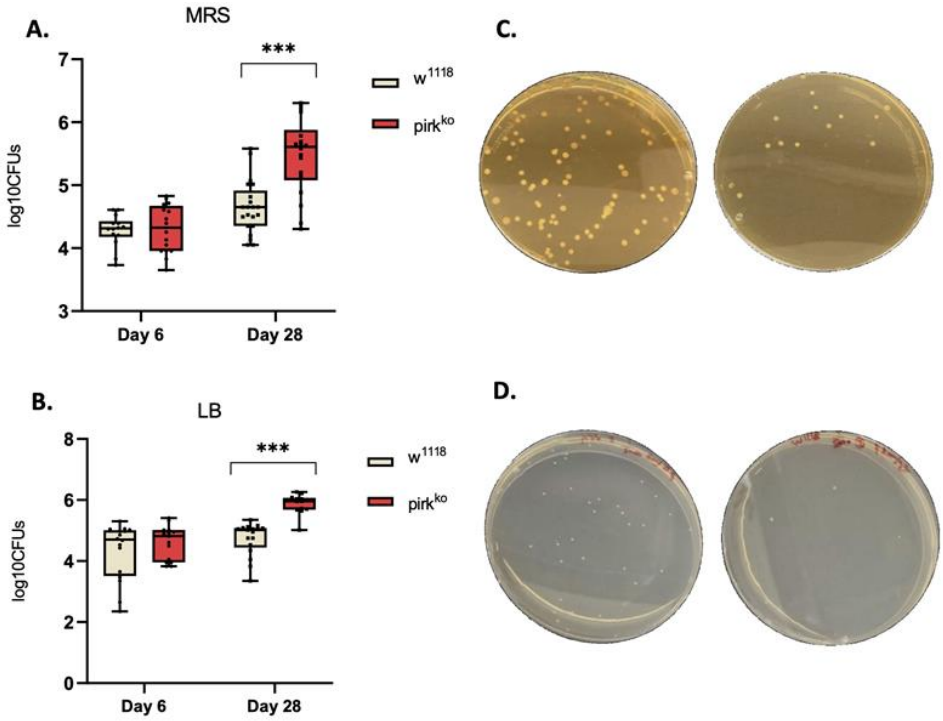

Figure S3: *Pirk* mutants displayed higher gut bacterial density when plated onto two different agar mediums. Boxplots of Log10CFU's of single guts; each point represents a single gut (n=20+/-5, over 3 biological replicates), which were taken from both wt controls and *pirk* flies at day 6 and day 28 on **(A)** MRS plates and **(B)** LB plates. Values shown are mean ± SEM. p <0.001, *** **(C)** MRS plates containing bacterial colonies from a single *pirk* fly (left) and single wt control fly (right) at day 28, diluted to 1/5000. **(D)** LB plates containing bacterial colonies from a single *pirk* fly (left) and wt control fly (right) at day 28, diluted to 1/5000.

The bacterial density of *pirk* mutant guts was measured by Grace Critchley. She analysed the cultivable gut microbial load of pirk flies at 6-days and 28-days of age using both LB and MRS

medium. Since *pirk* expression in the gut is microbiota dependent (Lhocine *et al*., 2008). *Pirk* flies had significantly more bacterial colonies in their gut than w^{1118} controls on MRS agar at day 28 but not day 6 (**Figure S3(A)**). To confirm whether this result was consistent across various cultivable bacterial strains, the experiment was repeated using LB agar. This facilitated growth of a different composition of gut-derived bacteria and resulted in a significant increase of bacterial colonies again at day 28 but not day 6 (**Figure S3(B)**). These results indicated an age-dependent increase of gut bacteria density in *pirk* mutants.

Supplementary Methodology 1 (SM1): Genomic Rescue

I formulated the protocol and initiated the primary crosses aimed at mitigating the sleep phenotype manifested in pirk flies through the excision of the p-element. Following is the initial protocol designed for this purpose:

Crossing $pirk^{EY00723}$ flies with the transposase stock w^{1118}; T(2;3)/Cyo; Δ(2-3),sb was necessary for the excision of $pirk^{EY00723}$. An F1 Cyo/$pirk^{EY00723}$; Δ(2-3),sb progeny was therefore produced, and it was crossed with a Cyo/Gla stock. Following this, individual F1 offspring from this cross that were non-Gla, non-sb, and Cyo were established as single fly crosses and subsequently backcrossed with Cyo/Gla.

To find out if the pirk gene contains a transposable element or not, genomic DNA was taken from the whole bodies of fifteen to twenty homozygous (non-Cyo) F1 offspring from these single fly crossings. In β-mercaptoethanol (β-ME), homogenisation was carried out using a mechanical rotor and fine needle, and QIAamp DSP DNA Kit (Qiagen) was used for DNA extraction.

We evaluated the extracted DNA's concentration and purity using Thermo Fisher Scientific's Nanodrop1000. The T100 Thermal Cycler (Bio-Rad) was used to perform polymerase chain reaction (PCR)

The final products were subjected to gel electrophoresis on a 1.5% agarose gel at 120V, 400mA, and for 45 minutes. The band DNA base pair (bp) size was measured using a Hyperladder (Bioline).

Primers complementary to the P{EPgy2} element's Long Terminal Repeat (LTR) regions were used in the PCR. Since LTR sections make up the majority of transposable elements, excision that was unsuccessful was indicated by successful PCR reactions and subsequent amplification of the DNA product. We also used additional primers that bound within 100 bp of the insertion site of the transposable element. Only in the absence of a major transposable element can binding occur, providing an extra way to gauge the effectiveness of excision.

Supplementary Methodology 2 (SM2): Drosophila Brain Dissections

The immunostaining and brain dissection techniques used in this work were modified from the Wu and Luo (2006) procedure. PBS+ (0.3% Triton-X), 4% PFA in PBS+, and 10% BSA in PBS+ were the necessary reagents. The 4% PFA in PBS+ was purchased from Santa Cruz, and 150 uL of Triton-X100 was added per 50 mL to create the PBS+ solution, which was made by dissolving 1.5 mL of Triton-X100 in 500 mL of 1x PBS. After 0.5 g of BSA was dissolved in PBS+ and the container was filled to the brim, 10% BSA in PBS+ was produced.

Brains were dissected in PBS+ at room temperature (RT) and then placed in 4% PFA solution on ice as part of the dissection technique. Following the dissection of every brain, the 4% PFA tube was shaken at room temperature for fifteen minutes. The PFA was then removed, and

PBS+ washes were then performed three times. Washing in between phases, primary and secondary antibody incubation, and blocking with 10% BSA were the next procedures. The brains were then mounted on a slide using mounting medium containing DAPI, and kept at 4C in the dark. The goal of the entire procedure was to protect the brain tissues' integrity and make immunostaining easier for later examination.

Supplementary Methodology 3 (SM3): Culture-dependent gut microbiota identification

This protocol was developed by me to analyse the bacterial density the gut microbiome in Drosophila and was used in Bahuguna et al. (2022a)

The methodology developed from techniques used in previous investigations (Dantoft et al. 2013; Bahuguna et al. 2022a) was used to assess the bacterial density. A single fly was first sterilised by dipping it in ethanol and rinsing with PBS, it was then dissected in sterile PBS and its gut isolated and homogenised using a sterile needle in autoclaved PBS. Serial dilutions were prepared and plated on De Man, Rogosa and Sharpe (MRS) broth (CM0359, Oxoid, Thermo Fisher, USA). After that, 200µl of the homogenised guts were separately plated onto MRS and LB plates while maintaining sterility. The plating were performed using a flame treated glass rod that was sterilised in between plates. After 72 hours of incubation at 38°C, the plates were counted for bacterial colonies using ImageJ, with the Colony Counter plug-in used as needed. The formula used to calculate CFUs was:

*Total CFU's counted on plate = (dilution factor * amount plated)/ total starting volume*

CFU values were computed for several concentrations of homogenised guts in order to verify the appropriateness of the procedure and the representativeness of dilutions with respect to real CFU values. The Log10 values were of mutants and controls were statistically compared using student's t-test, and graphs were plotted in Graphpad Prism version 10.0.3 (217).

CHAPTER NINE

Bibliography

9.1 BIBLIOGRAPHY

Abdellatif AM, Sarvetnick NE. Current understanding of the role of gut dysbiosis in type 1 diabetes. *J Diabetes* 2019;**11**:632–44.

Adair KL, Wilson M, Bost A *et al.* Microbial community assembly in wild populations of the fruit fly Drosophila melanogaster. *ISME J* 2018;**12**:959–72.

Adam K. Sleep as a Restorative Process and a Theory to Explain Why. *Prog Brain Res* 1980;**53**:289–305.

Aggarwal K, Rus F, Vriesema-Magnuson C *et al.* Rudra interrupts receptor signaling complexes to negatively regulate the IMD pathway. *PLoS Pathog* 2008;**4**, DOI: 10.1371/journal.ppat.1000120.

Aggarwal K, Silverman N. Positive and negative regulation of the Drosophila immune response. *BMB Rep* 2008:267–77.

Ahluwalia B, Magnusson MK, Öhman L. Mucosal immune system of the gastrointestinal tract: maintaining balance between the good and the bad. *Scand J Gastroenterol* 2017;**52**:1185–93.

Ahmadian N, Hejazi S, Mahmoudi J *et al.* Tau pathology of Alzheimer disease:Possible role of sleep deprivation. *Basic Clin Neurosci* 2018;**9**:307–16.

Aidman E, Jackson SA, Kleitman S. Effects of sleep deprivation on executive functioning, cognitive abilities, metacognitive confidence, and decision making. *Appl Cogn Psychol* 2019;**33**:188–200.

Aidy S El, Dinan TG, Cryan JF. Immune modulation of the brain-gut-microbe axis. *Front Microbiol* 2014;**5**:3–6.

Al-Asmakh M, Zadjali F. Use of germ-free animal models in microbiota-related research. *J Microbiol Biotechnol* 2015;**25**:1583–8.

Aldabal L, Bahammam AS. Metabolic, Endocrine, and Immune Consequences of Sleep Deprivation. *Open Respir Med J* 2011;**5**:31–43.

Alvarez-Erviti L, Couch Y, Richardson J *et al.* Alpha-synuclein release by neurons activates the inflammatory response in a microglial cell line. *Neurosci Res* 2011;**69**:337–42.

Alves L de F, Westmann CA, Lovate GL *et al.* Metagenomic approaches for understanding new concepts in microbial science. *Int J Genomics* 2018;**2018**.

Ameres SL, Zamore PD. Diversifying microRNA sequence and function. *Nat Rev Mol Cell Biol* 2013;**14**:475–88.

Anderson G, Maes M. Gut dysbiosis dysregulates central and systemic homeostasis via suboptimal mitochondrial function: assessment, treatment and classification implications. *Curr Top Med Chem* 2020;**20**:524–39.

Anderson K V, Bokla L, Niisslein-Volhard C. *Establishment of Dorsal-Ventral Polarity in the Drosophila Embryo: The Induction of Polarity by the To// Gene Product*., 1985.

Andretic R, Van Swinderen B, Greenspan RJ. Dopaminergic modulation of arousal in Drosophila. *Current Biology* 2005;**15**:1165–75.

Apidianakis Y, Rahme LG. Drosophila melanogaster as a model for human intestinal infection and pathology. *DMM Disease Models and Mechanisms* 2011;**4**:21–30.

Arias-Rojas A, Iatsenko I. The role of microbiota in Drosophila melanogaster Aging. *Frontiers in Aging* 2022;**3**:909509.

Arnot CJ, Gay NJ, Gangloff M. Molecular mechanism that induces activation of Spätzle, the ligand for the Drosophila toll receptor. *Journal of Biological Chemistry* 2010;**285**:19502–9.

Arora S, Ligoxygakis P. Beyond Host Defense: Deregulation of Drosophila Immunity and Age-Dependent Neurodegeneration. *Front Immunol* 2020;**11**, DOI: 10.3389/fimmu.2020.01574.
Arumugam M, Raes J, Pelletier E *et al.* Enterotypes of the human gut microbiome. *Nature* 2011;**473**:174–80.
Ayres JS, Schneider DS. A Signaling Protease Required for Melanization in Drosophila Affects Resistance and Tolerance of Infections. *PLoS Biol* 2008;**6**:2764–73.
Bäckhed F, Manchester JK, Semenkovich CF *et al.* Mechanisms underlying the resistance to diet-induced obesity in germ-free mice. *Proc Natl Acad Sci U S A* 2007;**104**:979–84.
Bahuguna S, Atilano M, Glittenberg M *et al.* Bacterial recognition by PGRP-SA and downstream signalling by Toll/DIF sustain commensal gut bacteria in Drosophila. *PLoS Genet* 2022;**18**, DOI: 10.1371/journal.pgen.1009992.
Bakula M. The persistence of a microbial flora during postembryogenesis of Drosophila melanogaster. *J Invertebr Pathol* 1969;**14**:365–74.
Barbara G, Barbaro MR, Fuschi D *et al.* Inflammatory and microbiota-related regulation of the intestinal epithelial barrier. *Front Nutr* 2021;**8**:718356.
Barnes RD, Fairweather DVI, Holliday J *et al.* A germfree infant. *The Lancet* 1969;**293**:168–71.
Barnes RD, Tuffrey M, Cook R. A" germfree" human isolator. *The Lancet* 1968;**291**:622–3.
Basbous N, Coste F, Leone P *et al.* The Drosophila peptidoglycan-recognition protein LF interacts with peptidoglycan-recognition protein LC to downregulate the Imd pathway. *EMBO Rep* 2011;**12**:327–33.
Basic M, Bleich A. Gnotobiotics: Past, present and future. *Lab Anim* 2019;**53**:232–43.
Beaver LM, Gvakharia BO, Vollintine TS *et al. Loss of Circadian Clock Function Decreases Reproductive Fitness in Males of Drosophila Melanogaster*., 2002.
Beccutia G, Pannain S. Sleep and Obesity. *Curr Opin Clin Nutr Metab Care* 2011:402–12.
Belkaid Y, Hand TW. Role of the microbiota in immunity and inflammation. *Cell* 2014;**157**:121–41.
Bellen HJ, Levis RW, Liao G *et al.* The BDGP Gene Disruption Project : Single Transposon Insertions Associated With 40 % of Drosophila Genes. 2004;**781**:761–81.
Benner EJ, Mosley RL, Destache CJ *et al.* Therapeutic immunization protects dopaminergic neurons in a mouse model of Parkinson's disease. *Proc Natl Acad Sci U S A* 2004;**101**:9435–40.
Bernert RA, Joiner TE. Sleep disturbances and suicide risk: A review of the literature. *Neuropsychiatr Dis Treat* 2007;**3**:735–43.
Bi J, Sehgal A, Williams JA *et al.* Wolbachia affects sleep behavior in Drosophila melanogaster. *J Insect Physiol* 2018;**107**:81–8.
Bian G, Xu Y, Lu P *et al.* The endosymbiotic bacterium Wolbachia induces resistance to dengue virus in Aedes aegypti. *PLoS Pathog* 2010;**6**:e1000833.
Bibiloni R. Rodent models to study the relationships between mammals and their bacterial inhabitants. *Gut Microbes* 2012;**3**:536–43.
Birmingham A, Selfors LM, Forster T *et al.* Statistical methods for analysis of high-throughput RNA interference screens. *Nat Methods* 2009;**6**:569–75.
Bischof J, Maeda RK, Hediger M *et al.* An optimized transgenesis system for Drosophila using germ-line-specific C31 integrases. *PNAS* 2007;**104**:3312–7.
Bischoff V, Vignal C, Boneca IG *et al.* Function of the drosophila pattern-recognition receptor PGRP-SD in the detection of Gram-positive bacteria. *Nat Immunol* 2004;**5**:1175–80.
Bischoff V, Vignal C, Duvic B *et al.* Downregulation of the Drosophila immune response by peptidoglycan- recognition proteins SC1 and SC2. *PLoS Pathog* 2006;**2**:0139–47.

Bishir M, Bhat A, Essa MM *et al.* Sleep Deprivation and Neurological Disorders. *Biomed Res Int* 2020;**2020**, DOI: 10.1155/2020/5764017.
Biteau B, Hochmuth CE, Jasper H. JNK Activity in Somatic Stem Cells Causes Loss of Tissue Homeostasis in the Aging Drosophila Gut. *Cell Stem Cell* 2008;**3**:442–55.
Björkqvist M, Wild EJ, Thiele J *et al.* A novel pathogenic pathway of immune activation detectable before clinical onset in Huntington's disease. *Journal of Experimental Medicine* 2008;**205**:1869–77.
Blackmer-Raynolds LD, Sampson TR. The gut-brain axis goes viral. *Cell Host Microbe* 2022;**30**:283–5.
Bland ML. Regulating metabolism to shape immune function: Lessons from Drosophila. *Semin Cell Dev Biol* 2023;**138**:128–41.
Blum JE, Fischer CN, Miles J *et al.* Frequent replenishment sustains the beneficial microbiome of Drosophila melanogaster. *mBio* 2013;**4**, DOI: 10.1128/mBio.00860-13.
Borbély AA. A two process model of sleep regulation. *Hum Neurobiol* 1982;**1**:195–204.
Borbély AA, Achermann P. Sleep Homeostasis and Models of Sleep Regulation. *J Biol Rhythms* 1999;**14**:559–70.
Bosco N, Noti M. The aging gut microbiome and its impact on host immunity. *Genes Immun* 2021;**22**:289–303.
Le Bourg E, Lints FA. Hypergravity and Aging in Drosophila melanogaster. 4. Climbing Activity: 4. Climbing Activity. *Gerontology* 1992;**38**:59–64.
Braley TJ, Boudreau EA. Sleep disorders in multiple sclerosis. *Curr Neurol Neurosci Rep* 2016;**16**, DOI: 10.1007/s11910-016-0649-2.
Brand H, Perrimon N. Targeted gene expression as a means of altering cell fates and generating dominant phenotypes. *Development* 1993a;**118**:401–15.
Brand H, Perrimon N. Targeted gene expression as a means of altering cell fates and generating dominant phenotypes. *Development* 1993b;**118**:401–15.
Broderick NA. Friend, foe or food? Recognition and the role of antimicrobial peptides in gut immunity and Drosophila–microbe interactions. *Philosophical Transactions of the Royal Society B: Biological Sciences* 2016;**371**:20150295.
Broderick NA, Buchon N, Lemaitre B. Microbiota-induced changes in Drosophila melanogaster host gene expression and gut morphology. *mBio* 2014;**5**:1–13.
Broderick NA, Lemaitre B. Gut-associated microbes of Drosophila melanogaster. *Gut Microbes* 2012;**3**, DOI: 10.4161/gmic.19896.
Buchon N, Broderick NA, Chakrabarti S *et al.* Invasive and indigenous microbiota impact intestinal stem cell activity through multiple pathways in Drosophila. *Genes Dev* 2009;**23**:2333–44.
Buchon N, Osman D, David FPA *et al.* Morphological and Molecular Characterization of Adult Midgut Compartmentalization in Drosophila. *CellReports* 2013;**3**:1725–38.
Bunker ME, Elliott G, Heyer-Gray H *et al.* Vertically transmitted microbiome protects eggs from fungal infection and egg failure. *Anim Microbiome* 2021;**3**, DOI: 10.1186/s42523-021-00104-5.
Burokas A, Moloney RD, Dinan TG *et al.* Microbiota regulation of the mammalian gut–brain axis. *Adv Appl Microbiol* 2015;**91**:1–62.
Bushey D, Tononi G, Cirelli C. Sleep and synaptic homeostasis: Structural evidence in Drosophila. *Science (1979)* 2011;**332**:1576–81.
Buxton OM, Marcelli E. Short and long sleep are positively associated with obesity, diabetes, hypertension, and cardiovascular disease among adults in the United States. *Soc Sci Med* 2010;**71**:1027–36.
Cahenzli J, Balmer ML, McCoy KD. Microbial–immune cross-talk and regulation of the immune system. *Immunology* 2013;**138**:12–22.

Cao Y, Chtarbanova S, Petersen AJ *et al.* Dnr1 mutations cause neurodegeneration in Drosophila by activating the innate immune response in the brain. *PNAS* 2013;**110**:1752–60.
Capo F, Wilson A, Di Cara F. The intestine of Drosophila melanogaster: An emerging versatile model system to study intestinal epithelial homeostasis and host-microbial interactions in humans. *Microorganisms* 2019;**7**, DOI: 10.3390/microorganisms7090336.
Cappuccio FP, Miller MA. Sleep and Cardio-Metabolic Disease. *Curr Cardiol Rep* 2017;**19**:1–9.
Carabottia M, Sciroccoa A, Masellib MA *et al.* The gut-brain axis: interactions between enteric microbiota, central and enteric nervous systems. *Ann Gastroenterol* 2015;**28**:1–7.
Caragata EP, Rancès E, O'Neill SL *et al.* Competition for amino acids between Wolbachia and the mosquito host, Aedes aegypti. *Microb Ecol* 2014;**67**:205–18.
Carding S, Verbeke K, Vipond DT *et al.* Dysbiosis of the gut microbiota in disease. *Microb Ecol Health Dis* 2015;**26**:1–9.
Carthew RW, Sontheimer EJ. Origins and Mechanisms of miRNAs and siRNAs. *Cell* 2009;**136**:642–55.
Carvalho L, Jacinto A, Matova N. The Toll/NF-κB signaling pathway is required for epidermal wound repair in Drosophila. *Proc Natl Acad Sci U S A* 2014;**111**:E5373–82.
Cattaneo A, Cattane N, Galluzzi S *et al.* Association of brain amyloidosis with pro-inflammatory gut bacterial taxa and peripheral inflammation markers in cognitively impaired elderly. *Neurobiol Aging* 2017;**49**:60–8.
Chamilos G, Samonis G, P Kontoyiannis D. Drosophila melanogaster as a model host for the study of microbial pathogenicity and the discovery of novel antimicrobial compounds. *Curr Pharm Des* 2011;**17**:1246–53.
Chamy L el, Leclerc V, Caldelari I *et al.* Sensing of "danger signals" and pathogen-associated molecular patterns defines binary signaling pathways "upstream" of Toll. *Nat Immunol* 2008;**9**:1165–70.
Chandler JA, Lang J, Bhatnagar S *et al.* Bacterial communities of diverse Drosophila species: Ecological context of a host-microbe model system. *PLoS Genet* 2011;**7**, DOI: 10.1371/journal.pgen.1002272.
Charroux B, Capo F, Kurz CL *et al.* Cytosolic and Secreted Peptidoglycan-Degrading Enzymes in Drosophila Respectively Control Local and Systemic Immune Responses to Microbiota. *Cell Host Microbe* 2018;**23**:215-228.e4.
Charroux B, Rival T, Narbonne-Reveau K *et al.* Bacterial detection by Drosophila peptidoglycan recognition proteins. *Microbes Infect* 2009;**11**:631–6.
Charroux B, Royet J. Gut-microbiota interactions in non-mammals: What can we learn from Drosophila? *Semin Immunol* 2012;**24**:17–24.
Chasan RT, Jin Y, Anderson K V. *Activation of the Easter Zymogen Is Regulated by Five Other Genes to Define Dorsal-Ventral Polarity in the Drosophila Embryo*., 1992.
Chen C, Ahn EH, Kang SS *et al.* Gut dysbiosis contributes to amyloid pathology, associated with C/EBPB/AEP signaling activation in Alzheimer's disease mouse model. *Sci Adv* 2020;**6**:1–16.
Chen J, Chen ZJ. Regulation of NF-κB by ubiquitination. *Curr Opin Immunol* 2013;**25**:4–12.
Chiang MH, Ho SM, Wu HY *et al.* Drosophila Model for Studying Gut Microbiota in Behaviors and Neurodegenerative Diseases. *Biomedicines* 2022;**10**, DOI: 10.3390/biomedicines10030596.
Chiara Cirelli. The genetic and molecular regulation of sleep: from fruit flies to humans. *Nat Rev Neurosci* 2009.

Chinchore Y, Gerber GF, Dolph PJ. Alternative pathway of cell death in Drosophila mediated by NF-κB transcription factor Relish. *Proc Natl Acad Sci U S A* 2012;**109**:E605-12.
Chintapalli VR, Wang J, Dow JAT. Using FlyAtlas to identify better Drosophila melanogaster models of human disease. *Nat Genet* 2007;**39**:715–20.
Cho I, Blaser MJ. The human microbiome: At the interface of health and disease. *Nat Rev Genet* 2012;**13**:260–70.
Cho YS, Stevens LM, Stein D. Pipe-dependent ventral processing of easter by snake is the defining step in drosophila embryo DV axis formation. *Current Biology* 2010;**20**:1133–7.
Choe K-M, Werner T, Stöven S *et al.* Requirement for a Peptidoglycan Recognition Protein (PGRP) in Relish activation and antimicrobial immune responses in Drosophila. *Science (1979)* 2002;**296**:359–62.
Choi NH, Kim JG, Yang DJ *et al.* Age-related changes in Drosophila midgut are associated with PVF2, a PDGF/VEGF-like growth factor. *Aging Cell* 2008;**7**:318–34.
Chrostek E, Teixeira L. Mutualism breakdown by amplification of Wolbachia genes. *PLoS Biol* 2015;**13**:e1002065.
Churchill L, Rector DM, Yasuda K *et al.* Tumor necrosis factor α: Activity dependent expression and promotion of cortical column sleep in rats. *Neuroscience* 2008;**156**:71–80.
Cirelli C. Searching for sleep mutants of Drosophila melanogaster. *BioEssays* 2003;**25**:940–9.
Cirelli C. The genetic and molecular regulation of sleep: from fruit flies to humans. *Nat Rev Neurosci* 2009;**10**:549–60.
Cirelli C, Bushey D. Sleep and wakefulness in Drosophila melanogaster. *Annals of the New York Academy of Sciences*. Vol 1129. Blackwell Publishing Inc., 2008, 323–9.
Cirelli C, Tononi G. Is sleep essential? *PLoS Biol* 2008;**6**:1605–11.
Clark ME, Anderson CL, Cande J *et al.* Widespread prevalence of Wolbachia in laboratory stocks and the implications for Drosophila research. *Genetics* 2005;**170**:1667–75.
Clark RI, Salazar A, Yamada R *et al.* Distinct Shifts in Microbiota Composition during Drosophila Aging Impair Intestinal Function and Drive Mortality. *Cell Rep* 2015;**12**:1656–67.
Clark RI, Walker DW. Role of gut microbiota in aging-related health decline: insights from invertebrate models. *Cellular and Molecular Life Sciences* 2018;**75**:93–101.
Clemente JC, Ursell LK, Parfrey LW *et al.* Review The Impact of the Gut Microbiota on Human Health : An Integrative View. *Cell* 2012;**148**:1258–70.
Coates ME. The germ-free animal in research. *The germ-free animal in research* 1968.
Coats SR, Do CT, Karimi-Naser LM *et al.* Antagonistic lipopolysaccharides block E. coli lipopolysaccharide function at human TLR4 via interaction with the human MD-2 lipopolysaccharide binding site. *Cell Microbiol* 2007;**9**:1191–202.
Cognigni P, Bailey AP, Miguel-Aliaga I. Enteric neurons and systemic signals couple nutritional and reproductive status with intestinal homeostasis. *Cell Metab* 2011;**13**:92–104.
Collier-Hyams LS, Neish AS. Intestinal epithelial barrier and mucosal immunity: Innate immune relationship between commensal flora and the mammalian intestinal epithelium. *Cellular and molecular life sciences* 2005;**62**:1339–48.
Colombani J, Andersen DS. The Drosophila gut: A gatekeeper and coordinator of organism fitness and physiology. *Wiley Interdiscip Rev Dev Biol* 2020;**9**:1–19.
Consortium HMP. Structure, function and diversity of the healthy human microbiome. *Nature* 2012;**486**:207–14.

Cox CR, Gilmore MS. Native microbial colonization of Drosophila melanogaster and its use as a model of Enterococcus faecalis pathogenesis. *Infect Immun* 2007;**75**:1565–76.
Croisier E, Moran LB, Dexter DT *et al.* Microglial inflammation in the parkinsonian substantia nigra: Relationship to alpha-synuclein deposition. *J Neuroinflammation* 2005;**2**:1–8.
Cryan JF, Dinan TG. Mind-altering microorganisms: The impact of the gut microbiota on brain and behaviour. *Nat Rev Neurosci* 2012, DOI: 10.1038/nrn3346.
Cryan JF, O KJ, M Cowan CS *et al.* The Microbiota-Gut-Brain Axis. *Physiol Rev* 2019;**99**:1877–2013.
Dalmasso MC, Brusco LI, Olivar N *et al.* Transethnic meta-analysis of rare coding variants in PLCG2, ABI3, and TREM2 supports their general contribution to Alzheimer's disease. *Transl Psychiatry* 2019;**9**, DOI: 10.1038/s41398-019-0394-9.
Dantoft W, Davis MM, Lindvall JM *et al.* The Oct1 homolog Nubbin is a repressor of NF-κB-dependent immune gene expression that increases the tolerance to gut microbiota. *BMC Biol* 2013;**11**:1–18.
Dauer W, Przedborski S. Parkinson's Disease: Mechanisms and models. *The Cambridge Companion to the Philosophy of Biology* 2007;**39**:139–59.
David LA, Maurice CF, Carmody RN *et al.* Diet rapidly and reproducibly alters the human gut microbiome. *Nature* 2014;**505**:559–63.
Davies G, Haddock G, Yung AR *et al.* A systematic review of the nature and correlates of sleep disturbance in early psychosis. *Sleep Med Rev* 2017;**31**:25–38.
Delgado S, Cabrera-Rubio R, Mira A *et al.* Microbiological survey of the human gastric ecosystem using culturing and pyrosequencing methods. *Microb Ecol* 2013;**65**:763–72.
Demerec M. *Biology of Drosophila*., 1950.
Dempsey PW, Vaidya SA, Cheng G. The Art of War: Innate and adaptive immune responses. *Cellular and Molecular Life Sciences* 2003;**60**:2604–21.
Dethlefsen L, McFall-Ngai M, Relman DA. An ecological and evolutionary perspective on human–microbe mutualism and disease. *Nature* 2007;**449**:811–8.
Dew MA, Hoch C, Buysse DJ *et al.* No TitlHealthy Older Adults' Sleep Predicts All-Cause Mortality at 4 to 19 Years of Follow-Upe. *Psychosom Med* 2003;**65**:63–73.
Dharne M, Patole M, Shouche YS. Microbiology of the insect gut: tales from mosquitoes and bees. *J Biosci* 2006;**31**:293–5.
Dicks LMT. Gut bacteria and neurotransmitters. *Microorganisms* 2022;**10**:1838.
Dicksved J, Lindberg M, Rosenquist M *et al.* Molecular characterization of the stomach microbiota in patients with gastric cancer and in controls. *J Med Microbiol* 2009;**58**:509–16.
Dietzl G, Chen D, Schnorrer F *et al.* A genome-wide transgenic RNAi library for conditional gene inactivation in Drosophila. *Nature* 2007;**448**:151–6.
Dillon RJ, Dillon VM. The Gut Bacteria of Insects: Nonpathogenic Interactions. *Annu Rev Entomol* 2004;**49**:71–92.
Dmitrieva AS, Maksimova IA, Kachalkin A V. *et al.* Age-Related Changes in the Yeast Component of the Drosophila melanogaster Microbiome. *Microbiology (Russian Federation)* 2021;**90**:229–36.
Doifode T, Giridharan V V., Generoso JS *et al.* The impact of the microbiota-gut-brain axis on Alzheimer's disease pathophysiology. *Pharmacol Res* 2021;**164**:105314.
Donachie SP, Foster JS, Brown M V. Culture clash: challenging the dogma of microbial diversity. *ISME J* 2007;**1**:97–9.
Douglas AE. Multiorganismal insects: diversity and function of resident microorganisms. *Annu Rev Entomol* 2015;**60**:17–34.

Douglas AE. The Drosophila model for microbiome research. *Lab Anim (NY)* 2018;**47**:157–64.
Douglas AE. Simple animal models for microbiome research. *Nat Rev Microbiol* 2019;**17**:764–75.
Drier EA, Huang LH, Steward R. *Nuclear Import of the Drosophila Rel Protein Dorsal Is Regulated by Phosphorylation*., 1999.
Dubey SK, Tapadia MG. Yorkie Regulates Neurodegeneration Through Canonical Pathway and Innate Immune Response. *Mol Neurobiol* 2018;**55**:1193–207.
Duffy JB. GAL4 system in Drosophila: A fly geneticist's Swiss army knife. *Genesis (United States)* 2002;**34**:1–15.
Dunn AK, Stabb E V. Culture-Independent Characterization of the Microbiota of the Ant Lion. *Society* 2005;**71**:8784–94.
Dworkin J. The medium is the message: Interspecies and interkingdom signaling by peptidoglycan and related bacterial glycans. *Annu Rev Microbiol* 2014;**68**:137–54.
Early AM, Shanmugarajah N, Buchon N *et al.* Drosophila genotype influences commensal bacterial levels. *PLoS One* 2017;**12**:e0170332.
Eisemann C, Wijffels G, Tellam RL. Secretion of the type 2 peritrophic matrix protein, peritrophin-15, from the cardia. *Archives of Insect Biochemistry and Physiology: Published in Collaboration with the Entomological Society of America* 2001;**47**:76–85.
Eldon E, Kooyer S, D'Evelyn D *et al.* The Drosophila18 wheeler is required for morphogenesis and has striking similarities to Toll. *Development* 1994;**120**:885–99.
Elgart M, Stern S, Salton O *et al.* Impact of gut microbiota on the fly's germ line. *Nat Commun* 2016;**7**:11280.
Elrod-Erickson M, Mishra S, Schneider D. *Interactions between the Cellular and Humoral Immune Responses in Drosophila*., 2000.
Emery DC, Shoemark DK, Batstone TE *et al.* 16S rRNA next generation sequencing analysis shows bacteria in Alzheimer's post-mortem brain. *Front Aging Neurosci* 2017;**9**:195.
Erkosar B, Leulier F. Transient adult microbiota, gut homeostasis and longevity: novel insights from the Drosophila model. *FEBS Lett* 2014;**588**:4250–7.
Falony G, Joossens M, Vieira-Silva S *et al.* Population-level analysis of gut microbiome variation. *Science (1979)* 2016;**352**:560–4.
Fast EM, Toomey ME, Panaram K *et al.* Wolbachia enhance Drosophila stem cell proliferation and target the germline stem cell niche. *Science (1979)* 2011;**334**:990–2.
Fernando MDA, Kounatidis I, Ligoxygakis P. Loss of Trabid, a New Negative Regulator of the Drosophila Immune-Deficiency Pathway at the Level of TAK1, Reduces Life Span. *PLoS Genet* 2014;**10**:1–13.
Ferrandon D, Imler JL, Hetru C *et al.* The Drosophila systemic immune response: Sensing and signalling during bacterial and fungal infections. *Nat Rev Immunol* 2007;**7**:862–74.
Ferrandon D, Jung AC, Criqui MC *et al.* A drosomycin-GFP reporter transgene reveals a local immune response in Drosophila that is not dependent on the Toll pathway. *EMBO Journal* 1998, DOI: 10.1093/emboj/17.5.1217.
Ferrucci L, Fabbri E. Inflammageing: chronic inflammation in ageing, cardiovascular disease, and frailty. *Nat Rev Cardiol* 2018;**15**:505–22.
Fire A, Xu S, Montgomery MK *et al.* Potent and specific genetic interference by double-stranded RNA in Caenorhabditis elegans. *Nature* 1998;**391**:806–11.
Fischer JA, Giniger E, Maniatis T *et al.* GAL4 activates transcription in Drosophila. *Nature* 1988;**332**:853–6.
Foley D, Ancoli-Israel S, Britz P *et al.* Sleep disturbances and chronic disease in older adults: Results of the 2003 National Sleep Foundation Sleep in America Survey. *J Psychosom Res* 2004;**56**:497–502.

Forsythe P, Bienenstock J, Kunze WA. Vagal pathways for microbiome-brain-gut axis communication. *Microbial endocrinology: the microbiota-gut-brain axis in health and disease* 2014:115–33.
Forsythe P, Kunze W, Bienenstock J. Moody microbes or fecal phrenology: what do we know about the microbiota-gut-brain axis? *BMC Med* 2016;**14**:1–14.
Foster JA, McVey Neufeld KA. Gut-brain axis: How the microbiome influences anxiety and depression. *Trends Neurosci* 2013, DOI: 10.1016/j.tins.2013.01.005.
Fox DT, Spradling AC. The Drosophila hindgut lacks constitutively active adult stem cells but proliferates in response to tissue damage. *Cell Stem Cell* 2009;**5**:290–7.
Franceschi C, Capri M, Garagnani P *et al.* Inflammaging. *Handbook of Immunosenescence*. Springer International Publishing, 2019, 1599–629.
Franceschi C, Capri M, Monti D *et al.* Inflammaging and anti-inflammaging: A systemic perspective on aging and longevity emerged from studies in humans. *Mech Ageing Dev* 2007;**128**:92–105.
Franceschi C, Garagnani P, Parini P *et al.* Inflammaging: a new immune–metabolic viewpoint for age-related diseases. *Nat Rev Endocrinol* 2018;**14**:576–90.
Frank DN, Pace NR. Gastrointestinal microbiology enters the metagenomics era. *Curr Opin Gastroenterol* 2008;**24**:4–10.
Frank MO, Caceres BA. Inflammaging: A Concept Analysis. *Journal for Nurse Practitioners* 2015;**11**:258–61.
Fraune S, Bosch TCG. Why bacteria matter in animal development and evolution. *BioEssays* 2010;**32**:571–80.
Freeman MR, Doherty J. Glial cell biology in Drosophila and vertebrates. *Trends Neurosci* 2006;**29**:82–90.
Frey DJ, Fleshner M, Wright KP. The effects of 40 hours of total sleep deprivation on inflammatory markers in healthy young adults. *Brain Behav Immun* 2007;**21**:1050–7.
Fulop T, Larbi A, Dupuis G *et al.* Immunosenescence and inflamm-aging as two sides of the same coin: Friends or Foes? *Front Immunol* 2018;**8**, DOI: 10.3389/fimmu.2017.01960.
Gáliková M, Klepsatel P. Obesity and aging in the Drosophila model. *Int J Mol Sci* 2018;**19**:1896.
Ganguly-Fitzgerald I, Donlea J, Shaw PJ. Waking Experience Affects Sleep Need in Drosophila. *Science (1979)* 2006;**313**:1775–81.
Garbarino S, Lanteri P, Bragazzi NL *et al.* Role of sleep deprivation in immune-related disease risk and outcomes. *Commun Biol* 2021;**4**, DOI: 10.1038/s42003-021-02825-4.
Gargano JW, Martin I, Bhandari P *et al.* Rapid iterative negative geotaxis (RING): A new method for assessing age-related locomotor decline in Drosophila. *Exp Gerontol* 2005;**40**:386–95.
Garrett WS, Gallini CA, Yatsunenko T *et al.* Enterobacteriaceae Act in concert with the gut microbiota to induce spontaneous and maternally transmitted colitis. *Cell Host Microbe* 2010;**8**:292–300.
Gartner LP. The fine structural morphology of the midgut of adult Drosophila: a morphometric analysis. *Tissue Cell* 1985;**17**:883–8.
Georgel P, Kappler C, Langley E *et al.* Drosophila immunity. A. 1995;**23**:1140–5.
Georgel P, Naitza S, Kappler C *et al. Drosophila Immune Deficiency (IMD) Is a Death Domain Protein That Activates Antibacterial Defense and Can Promote Apoptosis*., 2001.
Ghosh S, Pramanik S. Structural diversity, functional aspects and future therapeutic applications of human gut microbiome. *Arch Microbiol* 2021;**203**:5281–308.
Gilbert JA, Blaser MJ, Caporaso JG *et al.* Current understanding of the human microbiome. *Nat Med* 2018a;**24**:392–400.

Gilbert JA, Blaser MJ, Caporaso JG *et al.* Current understanding of the human microbiome. *Nat Med* 2018b;**24**:392–400.
Gill SR, Pop M, DeBoy RT *et al.* Metagenomic analysis of the human distal gut microbiome. *Science (1979)* 2006;**312**:1355–9.
Glass CK, Saijo K, Winner B *et al.* Mechanisms Underlying Inflammation in Neurodegeneration. *Cell* 2010;**140**:918–34.
Gobert V, Gottar M, Matskevich AA *et al.* Dual Detection of Fungal Infections in Drosophila via Recognition of Glucans and Sensing of Virulence Factors. *Cell* 2006;**127**:1425–37.
Goldschmied JR, Kuna ST, Maislin G *et al.* The Sleep Homeostatic Response to Sleep Deprivation in Humans is Heritable. *Sleep* 2022:1–10.
Gonçalves P, Araújo JR, Di Santo JP. A cross-talk between microbiota-derived short-chain fatty acids and the host mucosal immune system regulates intestinal homeostasis and inflammatory bowel disease. *Inflamm Bowel Dis* 2018;**24**:558–72.
Gordon HA. The germ-free animal: its use in the study of "physiologic" effects of the normal microbial flora on the animal host. *Am J Dig Dis* 1960;**5**:841–67.
Gordon MD, Dionne MS, Schneider DS *et al.* WntD is a feedback inhibitor of Dorsal/NF-κB in Drosophila development and immunity. *Nature* 2005;**437**:746–9.
Gordon S. Elie Metchnikoff, the man and the myth. *J Innate Immun* 2016;**8**:223–7.
Goto Y, Kiyono H. Epithelial barrier: an interface for the cross-communication between gut flora and immune system. *Immunol Rev* 2012;**245**:147–63.
Gottar M, Gobert V, Michel T *et al.* The Drosophila immune response against Gram-negative bacteria is mediated by a peptidoglycan recognition protein. *Letters to Nature* 2002;**416**:640–4.
Gould AL, Zhang V, Lamberti L *et al.* Microbiome interactions shape host fitness. *Proceedings of the National Academy of Sciences* 2018;**115**:E11951–60.
Grandner MA, Hale L, Moore M *et al.* Mortality associated with short sleep duration: The evidence, the possible mechanisms, and the future. *Sleep Med Rev* 2010;**14**:191–203.
Grandner MA, Jackson NJ, Pak VM *et al.* Sleep disturbance is associated with cardiovascular and metabolic disorders. *J Sleep Res* 2012;**21**:427–33.
Green EW, Fedele G, Giorgini F *et al.* A Drosophila RNAi collection is subject to dominant phenotypic effects. *Nat Methods* 2014;**11**:222–3.
Griffith LC. Identifying behavioral circuits in Drosophila melanogaster: Moving targets in a flying insect. *Curr Opin Neurobiol* 2012;**22**:609–14.
Guo L, Karpac J, Tran SL *et al.* PGRP-SC2 promotes gut immune homeostasis to limit commensal dysbiosis and extend lifespan. *Cell* 2014;**156**:109–22.
Gustafsson BE, Maunsbach AB. Ultrastructure of the enlarged cecum in germfree rats. *Zeitschrift für Zellforschung und Mikroskopische Anatomie* 1971;**120**:555–78.
Ha E-M, Oh C-T, Bae YS *et al.* A direct role for dual oxidase in Drosophila gut immunity. *Science (1979)* 2005;**310**:847–50.
Haghayeghi A, Sarac A, Czerniecki S *et al.* Pellino enhances innate immunity in Drosophila. *Mech Dev* 2010;**127**:301–7.
Hakansson A, Molin G. Gut microbiota and inflammation. *Nutrients* 2011;**3**:637–87.
Hakim RS, Baldwin K, Smagghe G. Regulation of midgut growth, development, and metamorphosis. *Annu Rev Entomol* 2010;**55**:593–608.
Halász P. How Sleep Activates Epileptic Networks? *Epilepsy Res Treat* 2013;**2013**:1–19.
Hammer Ø, Harper DAT. Past: paleontological statistics software package for educaton and data anlysis. *Palaeontologia electronica* 2001;**4**:1.
Haselkorn TS, Markow TA, Moran NA. Multiple introductions of the Spiroplasma bacterial endosymbiont into Drosophila. *Mol Ecol* 2009;**18**:1294–305.

Hashimoto C, Gerttula S, Anderson K v. *Plasma Membrane Localization of the Toll Protein in the Syncytial Drosophila Embryo: Importance of Transmembrane Signaling for Dorsal-Ventral Pattern Formation*., 1991.
Hauglund NL, Pavan C, Nedergaard M. Cleaning the sleeping brain – the potential restorative function of the glymphatic system. *Curr Opin Physiol* 2020;**15**:1–6.
Hayes CL, Dong J, Galipeau HJ *et al.* Commensal microbiota induces colonic barrier structure and functions that contribute to homeostasis. *Sci Rep* 2018;**8**:1–14.
Hedges LM, Brownlie JC, O'Neill SL *et al.* Wolbachia and virus protection in insects. *Science (1979)* 2008;**322**:702.
Heier C, Klishch S, Stilbytska O *et al.* The Drosophila model to interrogate triacylglycerol biology. *Biochimica et Biophysica Acta (BBA)-Molecular and Cell Biology of Lipids* 2021;**1866**:158924.
Hendricks JC, Finn SM, Panckeri KA *et al.* Rest in Drosophila is a sleep-like state. *Neuron* 2000;**25**:129–38.
Hendricks JC, Kirk D, Panckeri K *et al.* Modafinil maintains waking in the Fruit fly Drosophila Melanogaster. *Pharmacology* 2003;**26**.
Heneka MT, Carson MJ, Khoury J el *et al.* Neuroinflammation in Alzheimer's disease. *Lancet Neurol* 2015;**14**:388–405.
Herrera AJ, Tomás-Camardiel M, Venero JL *et al.* Inflammatory process as a determinant factor for the degeneration of substantia nigra dopaminergic neurons. *Journal of Neural Transmission*. Vol 112. 2005, 111–9.
Heys C, Lizé A, Blow F *et al.* The effect of gut microbiota elimination in Drosophila melanogaster : A how- to guide for host – microbiota studies. 2018:4150–61.
Hilgenboecker K, Hammerstein P, Schlattmann P *et al.* How many species are infected with Wolbachia?–a statistical analysis of current data. *FEMS Microbiol Lett* 2008;**281**:215–20.
Hochmuth CE, Biteau B, Bohmann D *et al.* Redox regulation by Keap1 and Nrf2 controls intestinal stem cell proliferation in Drosophila. *Cell Stem Cell* 2011;**8**:188–99.
Hoesel B, Schmid JA. The complexity of NF-κB signaling in inflammation and cancer. *Mol Cancer* 2013;**12**:1.
Holden PR, Jones P, Brookfield JFY. Evidence for a Wolbachia symbiont in Drosophila melanogaster. *Genet Res (Camb)* 1993;**62**:23–9.
Hornef MW, Wick MJ, Rhen M *et al.* Bacterial strategies for overcoming host innate and adaptive immune responses. *Nat Immunol* 2002;**3**:1033–40.
Houlden A, Goldrick M, Brough D *et al.* Brain injury induces specific changes in the caecal microbiota of mice via altered autonomic activity and mucoprotein production. *Brain Behav Immun* 2016;**57**:10–20.
Hrdina A, Iatsenko I. The roles of metals in insect–microbe interactions and immunity. *Curr Opin Insect Sci* 2022;**49**:71–7.
Hu J, Chen Z, Gorczynski CP *et al.* Sleep-deprived mice show altered cytokine production manifest by perturbations in serum IL-1ra, TNFa, and IL-6 levels. *Brain Behav Immun* 2003;**17**:498–504.
Hu Y, Sopko R, Foos M *et al.* FlyPrimerBank: an online database for Drosophila melanogaster gene expression analysis and knockdown evaluation of RNAi reagents. *G3 (Bethesda)* 2013;**3**:1607–16.
Hudson AN, Van Dongen HPA, Honn KA. Sleep deprivation, vigilant attention, and brain function: a review. *Neuropsychopharmacology* 2020;**45**:21–30.
Hultmark D. Drosophila immunity : paths and patterns. *Curr Opin Immunol* 2003;**15**:12–9.
Humann J, Lenz LL. Bacterial peptidoglycan-degrading enzymes and their impact on host muropeptide detection. *J Innate Immun* 2009;**1**:88–97.

Hussain R, Zubair H, Pursell S *et al.* Neurodegenerative diseases: Regenerative mechanisms and novel therapeutic approaches. *Brain Sci* 2018;**8**:177.
Imler J-L, Hoffmann JA. Toll receptors in innate immunity. *Trends Cell Biol* 2001;**11**.
Ingham CJ, Sprenkels A, Bomer J *et al.* The micro-Petri dish, a million-well growth chip for the culture and high-throughput screening of microorganisms. *Proceedings of the National Academy of Sciences* 2007;**104**:18217–22.
Ingiosi AM, Opp MR, Krueger JM. Sleep and immune function: glial contributions and consequences of aging. *Curr Opin Neurobiol* 2013;**23**:806–11.
Isaac RE, Li C, Leedale AE *et al.* Drosophila male sex peptide inhibits siesta sleep and promotes locomotor activity in the post-mated female. *Proceedings of the Royal Society B: Biological Sciences* 2010;**277**:65–70.
Jacqueline AC, Parvy J, Faugère D. Infection triggers tumor regression through activation of innate immunity in Drosophila Affiliations : 2019.
Jaenike J, Stahlhut JK, Boelio LM *et al.* Association between Wolbachia and Spiroplasma within Drosophila neotestacea: an emerging symbiotic mutualism? *Mol Ecol* 2010;**19**:414–25.
Jang IH, Chosa N, Kim SH *et al.* A Spätzle-processing enzyme required for toll signaling activation in drosophila innate immunity. *Dev Cell* 2006;**10**:45–55.
Jarchum I, Pamer EG. Regulation of innate and adaptive immunity by the commensal microbiota. *Curr Opin Immunol* 2011;**23**:353–60.
Jeck WR, Siebold AP, Sharpless NE. Review: A meta-analysis of GWAS and age-associated diseases. *Aging Cell* 2012;**11**:727–31.
Jeibmann A, Paulus W. Drosophila melanogaster as a Model Organism of Brain Diseases. 2009:407–40.
Jewett KA, Taishi P, Sengupta P *et al.* Tumor necrosis factor enhances the sleep-like state and electrical stimulation induces a wake-like state in co-cultures of neurons and glia. *European Journal of Neuroscience* 2015;**42**:2078–90.
Jia Y, Jin S, Hu K *et al.* Gut microbiome modulates Drosophila aggression through octopamine signaling. *Nat Commun* 2021;**12**:2698.
Jiang H, Edgar BA. Intestinal stem cells in the adult Drosophila midgut. *Exp Cell Res* 2011;**317**:2780–8.
Johnson EL, Heaver SL, Walters WA *et al.* Microbiome and metabolic disease: revisiting the bacterial phylum Bacteroidetes. *J Mol Med* 2017;**95**:1–8.
Johnson KV-A, Foster KR. Why does the microbiome affect behaviour? *Nat Rev Microbiol* 2018;**16**:647–55.
Jones MA, Grotewiel M. Drosophila as a model for age-related impairment in locomotor and other behaviors. *Exp Gerontol* 2011;**46**:320–5.
Jones RM, Luo L, Ardita CS *et al.* Symbiotic lactobacilli stimulate gut epithelial proliferation via Nox-mediated generation of reactive oxygen species. *EMBO Journal* 2013;**32**:3017–28.
Jovel J, Dieleman LA, Kao D *et al. The Human Gut Microbiome in Health and Disease*. Elsevier Inc., 2017a.
Jovel J, Dieleman LA, Kao D *et al. The Human Gut Microbiome in Health and Disease*. Elsevier Inc., 2017b.
Kahn MS, Kranjac D, Alonzo CA *et al.* Prolonged elevation in hippocampal Aβ and cognitive deficits following repeated endotoxin exposure in the mouse. *Behavioural brain research* 2012;**229**:176–84.
Kajava A V., Klopffleisch K, Chen S *et al.* Evolutionary link between metazoan RHIM motif and prion-forming domain of fungal heterokaryon incompatibility factor HET-s/HET-s. *Sci Rep* 2014;**4**:1–6.

Kakizaki M, Kuriyama S, Sone T *et al.* Sleep duration and the risk of breast cancer: The Ohsaki Cohort Study. *Br J Cancer* 2008;**99**:1502–5.
Kallio J, Leinonen A, Ulvila J *et al.* Functional analysis of immune response genes in Drosophila identifies JNK pathway as a regulator of antimicrobial peptide gene expression in S2 cells. *Microbes Infect* 2005;**7**:811–9.
Kambris Z, Blagborough AM, Pinto SB *et al.* Wolbachia stimulates immune gene expression and inhibits Plasmodium development in Anopheles gambiae. *PLoS Pathog* 2010;**6**:e1001143.
Kaneko T, Goldman WE, Mellroth P *et al.* Monomeric and polymeric gram-negative peptidoglycan but not purified LPS stimulate the Drosophila IMD pathway. *Immunity* 2004;**20**:637–49.
Kaneko T, Silverman N. Bacterial recognition and signalling by the Drosophila IMD pathway. *Cell Microbiol* 2005;**7**:461–9.
Kaneko T, Yano T, Aggarwal K *et al.* PGRP-LC and PGRP-LE have essential yet distinct functions in the drosophila immune response to monomeric DAP-type peptidoglycan. *Nat Immunol* 2006;**7**:715–23.
Kannarkat GT, Boss JM, Tansey MG. The role of innate and adaptive immunity in parkinson's disease. *J Parkinsons Dis* 2013a;**3**:493–514.
Kannarkat GT, Boss JM, Tansey MG. The role of innate and adaptive immunity in parkinson's disease. *J Parkinsons Dis* 2013b;**3**:493–514.
Kanoh H, Kuraishi T, Tong LL *et al.* Ex vivo genome-wide RNAi screening of the Drosophila Toll signaling pathway elicited by a larva-derived tissue extract. *Biochem Biophys Res Commun* 2015;**467**:400–6.
Kapsetaki SE, Tzelepis I, Avgousti K *et al.* The bacterial metabolite 2-aminoacetophenone promotes association of pathogenic bacteria with flies. *Nat Commun* 2014;**5**, DOI: 10.1038/ncomms5401.
Kapsimalis F, Basta M, Varouchakis G *et al.* Cytokines and pathological sleep. *Sleep Med* 2008;**9**:603–14.
Karasov WH, Douglas AE. Comparative Digestive Physiology. *Compr Physiol* 2013;**3**:741–83.
Karpac J, Biteau B, Jasper H. Misregulation of an adaptive metabolic response contributes to the age-related disruption of lipid homeostasis in Drosophila. *Cell Rep* 2013;**4**:1250–61.
Kassinen A, Krogius-Kurikka L, Mäkivuokko H *et al.* The Fecal Microbiota of Irritable Bowel Syndrome Patients Differs Significantly From That of Healthy Subjects. *Gastroenterology* 2007;**133**:24–33.
Kayser MS, Yue Z, Sehgal A. A critical period of sleep for development of courtship circuitry and behavior in Drosophila. *Science (1979)* 2014;**344**:269–74.
Keene AC, Duboué ER, McDonald DM *et al.* Clock and cycle limit starvation-induced sleep loss in drosophila. *Current Biology* 2010;**20**:1209–15.
Keene AC, Joiner WJ. Neurodegeneration: Paying It Off with Sleep. *Current Biology* 2015;**25**:R234–6.
Keith FJ, Gay NJ. *The Drosophila Membrane Receptor Toll Can Function to Promote Cellular Adhesion*., 1990.
Keller M, Mazuch J, Abraham U *et al.* A circadian clock in macrophages controls inflammatory immune responses. *PNAS* 2009;**106**:21407–21412.
Kelly D, Campbell JI, King TP *et al.* Commensal anaerobic gut bacteria attenuate inflammation by regulating nuclear-cytoplasmic shuttling of PPAR-γ and RelA. *Nat Immunol* 2004;**5**:104–12.
Kennedy BK, Berger SL, Brunet A *et al.* Geroscience: Linking aging to chronic disease. *Cell* 2014;**159**:709–13.

Kew O, Morris-Glasgow V, Landaverde M *et al.* Outbreak of poliomyelitis in hispaniola associated with circulating type 1 vaccine-derived poliovirus. *Science (1979)* 2002;**296**:356–9.
Khush RS, Cornwell WD, Uram JN *et al.* A Ubiquitin-Proteasome Pathway Represses the Drosophila Immune Deficiency Signaling Cascade least seven types of antimicrobial peptides that are ac- tive against different classes of microbes. These pep- tides are synthesized in both surface epithelial ti. *Current Biology* 2002;**12**:1728–37.
Kietz C. Regulation of Host-Microbe Interactions and Inflammatory Signalling in Drosophila melanogaster. 2021.
Kietz C, Pollari V, Meinander A. Generating germ-free Drosophila to study gut-microbe interactions: protocol to rear Drosophila under axenic conditions. *Curr Protoc Toxicol* 2018;**77**:e52.
Kim M, Lee JH, Lee SY *et al.* Caspar, a suppressor of antibacterial immunity in Drosophila. *PNAS* 2006;**103**:16358–16363.
Kim S, Kwon SH, Kam TI *et al.* Transneuronal Propagation of Pathologic α-Synuclein from the Gut to the Brain Models Parkinson's Disease. *Neuron* 2019;**103**:627-641.e7.
Kim YK, Yoon IY, Kim JM *et al.* The implication of nigrostriatal dopaminergic degeneration in the pathogenesis of REM sleep behavior disorder. *Eur J Neurol* 2010;**17**:487–92.
King DG. Cellular organization and peritrophic membrane formation in the cardia (proventriculus) of Drosophila melanogaster. *J Morphol* 1988;**196**:253–82.
Kirk RGW. "Life in a Germ-Free World": Isolating Life from the Laboratory Animal to the Bubble Boy. *Bull Hist Med* 2012;**86**:237–75.
Kitani-Morii F, Friedland RP, Yoshida H *et al.* Drosophila as a Model for Microbiota Studies of Neurodegeneration. *Journal of Alzheimer's Disease* 2021;**84**:479–90.
Kleino A, Myllymaki H, Kallio J *et al.* Pirk Is a Negative Regulator of the Drosophila Imd Pathway. *The Journal of Immunology* 2008, DOI: 10.4049/jimmunol.180.8.5413.
Kleino A, Valanne S, Ulvila J *et al.* Inhibitor of apoptosis 2 and TAK1-binding protein are components of the Drosophila Imd pathway. *EMBO Journal* 2005;**24**:3423–34.
Koh K, Evans JM, Hendricks JC *et al. A Drosophila Model for Age-Associated Changes in Sleep:Wake Cycles*., 2006.
Kohl KD, Weiss RB, Cox J *et al.* Gut microbes of mammalian herbivores facilitate intake of plant toxins. *Ecol Lett* 2014;**17**:1238–46.
Kong G, Cao KAL, Judd LM *et al.* Microbiome profiling reveals gut dysbiosis in a transgenic mouse model of Huntington's disease. *Neurobiol Dis* 2020;**135**:104268.
Kounatidis I, Chtarbanova S, Cao Y *et al.* NF-κB Immunity in the Brain Determines Fly Lifespan in Healthy Aging and Age-Related Neurodegeneration. *Cell Rep* 2017;**19**:836–48.
Kounatidis I, Ligoxygakis P. Drosophila as a model system to unravel the layers of innate immunity to infection. *Open Biol* 2012;**2**, DOI: 10.1098/rsob.120075.
Kowalski K, Mulak A, Words K. Brain-Gut-Microbiota Axis in Alzheimer's Disease. *J Neurogastroenterol Motil* 2019;**25**:48–60.
Kripke DF, Garfinkel L, Wingard DL. Mortality associated with sleep duration and insomnia. *Prim Care Companion J Clin Psychiatry* 2002;**4**:34.
Krueger J. The Role of Cytokines in Sleep Regulation. *Curr Pharm Des* 2008;**14**:3408–16.
Krueger JM, Rector DM, Churchill L. Sleep and cytokines. *Sleep Med Clin* 2007;**2**:161–9.
Kuo TH, Pike DH, Beizaeipour Z *et al.* Sleep triggered by an immune response in Drosophila is regulated by the circadian clock and requires the NFκB Relish. *BMC Neurosci* 2010a;**11**, DOI: 10.1186/1471-2202-11-17.

Kuo T-H, Pike DH, Beizaeipour Z *et al.* Sleep triggered by an immune response in Drosophila is regulated by the circadian clock and requires the NFκB Relish. *BMC Neurosci* 2010b;**11**:1–12.
Kuo TH, Williams JA. Increased sleep promotes survival during a bacterial infection in Drosophila. *Sleep* 2014;**37**:1077–86.
Kuraishi T, Binggeli O, Opota O *et al.* Genetic evidence for a protective role of the peritrophic matrix against intestinal bacterial infection in Drosophila melanogaster. *Proceedings of the National Academy of Sciences* 2011;**108**:15966–71.
Kuraishi T, Hori A, Kurata S. Host-microbe interactions in the gut of Drosophila melanogaster. *Front Physiol* 2013a;**4 DEC**:1–8.
Kuraishi T, Hori A, Kurata S. Host-microbe interactions in the gut of Drosophila melanogaster. *Front Physiol* 2013b;**4**:375.
Labzin LI, Heneka MT, Latz E. Innate Immunity and Neurodegeneration. *Annu Rev Med* 2018;**69**:437–49.
Lader M. Sleep and Anxiety Disorders. *Synopsis of Sleep Medicine* 2016:201–12.
Lambert JC, Grenier-Boley B, Chouraki V *et al.* Implication of the immune system in Alzheimer's disease: evidence from genome-wide pathway analysis. *Journal of Alzheimer's Disease* 2010;**20**:1107–18.
Lamiable O, Meignin C, Imler J-L. WntD and Diedel: Two immunomodulatory cytokines in Drosophila immunity. *Fly (Austin)* 2016;**10**:187–94.
Lawrence R. David the "Bubble Boy" and the boundaries of the human. *JAMA* 1985;**253**:74–6.
Lee H-Y, Lee S-H, Lee J-H *et al.* The role of commensal microbes in the lifespan of Drosophila melanogaster. *Aging* 2019;**11**:4611–40.
Lee KZ, Ferrandon D. Negative regulation of immune responses on the fly. *EMBO Journal* 2011;**30**:988–90.
Leftwich PT, Clarke NVE, Hutchings MI *et al.* Gut microbiomes and reproductive isolation in Drosophila. *Proc Natl Acad Sci U S A* 2017;**114**:12767–72.
Lehman RM, Lundgren JG, Petzke LM. Bacterial communities associated with the digestive tract of the predatory ground beetle, poecilus chalcites, and their modification by laboratory rearing and antibiotic treatment. *Microb Ecol* 2009;**57**:349–58.
Lemaitre B, Hoffmann J. The Host Defense of *Drosophila melanogaster*. *Annu Rev Immunol* 2007, DOI: 10.1146/annurev.immunol.25.022106.141615.
Lemaitre B, Kromer-Metzger E, Michaut L *et al. A Recessive Mutation, Immune Deficiency (Imd), Defines Two Distinct Control Pathways in the Drosophila Host Defense (Antibacterial Peptides/Antifungal Peptides/Insect Immunity)*., 1995.
Lemaitre B, Miguel-Aliaga I. The digestive tract of Drosophila melanogaster. *Annu Rev Genet* 2013;**47**:377–404.
Lemaitre B, Nicolas E, Michaut L. *The Dorsoventral Regulatory Gene Cassette Spätzle/Toll/Cactus Controls the Potent Antifungal Response in Drosophila Adults*., 1996.
Lenz O, Xiong J, Nelson MD *et al.* FMRFamide signaling promotes stress-induced sleep in Drosophila. *Brain Behav Immun* 2015;**47**:141–8.
Letiembre M, Hao W, Liu Y *et al.* Innate immune receptor expression in normal brain aging. *Neuroscience* 2007;**146**:248–54.
Leulier F. Tuning Down NF-κB Signaling by DUBs: A Fly Case. *Cell Host Microbe* 2009;**6**:294–6.
Leulier F, Parquet C, Pili-Floury S *et al.* The Drosophila immune system detects bacteria through specific peptidoglycan recognition. *Nat Immunol* 2003;**4**:478–84.

Leulier F, Rodriguez A, Khush RS *et al.* The Drosophila caspase Dredd is required to resist Gram-negative bacterial infection. *EMBO Rep* 2000;**1**:353–8.
Leulier F, Vidal S, Saigo K *et al. Inducible Expression of Double-Stranded RNA Reveals a Role for DFADD in the Regulation of the Antibacterial Response in Drosophila Adults*., 2002.
Levy M, Kolodziejczyk AA, Thaiss CA *et al.* Dysbiosis and the immune system. *Nat Rev Immunol* 2017;**17**:219–32.
Ley RE, Bäckhed F, Turnbaugh P *et al.* Obesity alters gut microbial ecology. *PNAS* 2005;**102**:11070–5.
Lhocine N, Ribeiro PS, Buchon N *et al.* Article PIMS Modulates Immune Tolerance by Negatively Regulating Drosophila Innate Immune Signaling. *Cell Host Microbe* 2008;**4**:147–58.
Li H, Qi Y, Jasper H. Preventing Age-Related Decline of Gut Compartmentalization Limits Microbiota Dysbiosis and Extends Lifespan. *Cell Host Microbe* 2016;**19**:240–53.
Li W, Tapiainen T, Brinkac L *et al.* Vertical Transmission of Gut Microbiome and Antimicrobial Resistance Genes in Infants Exposed to Antibiotics at Birth. *Journal of Infectious Diseases* 2021;**224**:1236–46.
Liang S, Wu X, Jin F. Gut-brain psychology: Rethinking psychology from the microbiota–gut–brain axis. *Front Integr Neurosci* 2018;**12**:1–24.
Liao G-C, Rehm EJ, Rubin GM. Insertion site preferences of the P transposable element in Drosophila melanogaster. *PNAS* 2000;**97**:3347–51.
Liberti J, Engel P. The gut microbiota—brain axis of insects. *Curr Opin Insect Sci* 2020;**39**:6–13.
Liehl P, Blight M, Vodovar N *et al.* Prevalence of local immune response against oral infection in a Drosophila/Pseudomonas infection model. *PLoS Pathog* 2006, DOI: 10.1371/journal.ppat.0020056.
Ligoxygakis P, Ge Pelte N, Hoffmann JA *et al.* Activation of Drosophila Toll During Fungal Infection by a Blood Serine Protease. *Science (1979)* 2002:114–6.
Ligoxygakis P, Hoffmann JA, Reichhart J. Activation of Drosophila Toll During Fungal Infection by a Blood Serine Protease. *ScienceSc* 2002;**297**:114–7.
Lindsay SA, Wasserman SA. Conventional and non-conventional Drosophila Toll signaling. *Dev Comp Immunol* 2014;**42**:16–24.
Linneweber GA, Jacobson J, Busch KE *et al.* Neuronal control of metabolism through nutrient-dependent modulation of tracheal branching. *Cell* 2014;**156**:69–83.
Lipsky MS, King M. Biological theories of aging. *Disease-a-Month* 2015;**61**:460–6.
Liu C, Haynes PR, Donelson NC *et al.* Sleep in populations of Drosophila melanogaster. *eNeuro* 2015;**2**, DOI: 10.1523/ENEURO.0071-15.2015.
Liu RT, Steele SJ, Hamilton JL *et al.* Sleep and suicide: A systematic review and meta-analysis of longitudinal studies. *Clin Psychol Rev* 2020;**81**:101895.
Liu X, Hodgson JJ, Buchon N. Drosophila as a model for homeostatic, antibacterial, and antiviral mechanisms in the gut. *PLoS Pathog* 2017;**13**, DOI: 10.1371/journal.ppat.1006277.
Loch G, Zinke I, Mori T *et al.* Antimicrobial peptides extend lifespan in Drosophila. *PLoS One* 2017;**12**, DOI: 10.1371/journal.pone.0176689.
Loman S, van der Kamp JW. Insulin resistance as key factor for linking modulation of gut microbiome to health claims and dietary recommendations to tackle obesity. *Trends Food Sci Technol* 2016;**57**:306–10.
Lone SR, Potdar S, Srivastava M *et al.* Social experience is sufficient to modulate sleep need of drosophila without increasing wakefulness. *PLoS One* 2016;**11**, DOI: 10.1371/journal.pone.0150596.

Lu Y, Wu LP, Anderson K V. The antibacterial arm of the Drosophila innate immune response requires an IκB kinase. *Genes Dev* 2001;**15**:104–10.
Luczynski P, Neufeld KAMV, Oriach CS *et al.* Growing up in a bubble: Using germ-free animals to assess the influence of the gut microbiota on brain and behavior. *International Journal of Neuropsychopharmacology* 2016;**19**:1–17.
Ludington WB, Ja WW. Drosophila as a model for the gut microbiome. *PLoS Pathog* 2020a;**16**:e1008398.
Ludington WB, Ja WW. Drosophila as a model for the gut microbiome. *PLoS Pathog* 2020b;**16**:1–6.
Lukiw WJ. Bacteroides fragilis lipopolysaccharide and inflammatory signaling in Alzheimer's disease. *Front Microbiol* 2016;**7**:1544.
Lupp C, Robertson ML, Wickham ME *et al.* Host-mediated inflammation disrupts the intestinal microbiota and promotes the overgrowth of Enterobacteriaceae. *Cell Host Microbe* 2007;**2**:119–29.
Luyster FS, Strollo PJ, Zee PC *et al.* Sleep: A health imperative. *Sleep* 2012;**35**:727–34.
Macke E, Tasiemski A, Massol F *et al.* Life history and eco-evolutionary dynamics in light of the gut microbiota. *Oikos* 2017;**126**:508–31.
Macpherson AJ, Harris NL. Interactions between commensal intestinal bacteria and the immune system. *Nat Rev Immunol* 2004;**4**:478–85.
Maier BR, Hentges DJ. Experimental Shigella Infections in Laboratory Animals. *Infect Immun* 1972;**6**:168–73.
Maillet F, Bischoff V, Vignal C *et al.* The Drosophila Peptidoglycan Recognition Protein PGRP-LF Blocks PGRP-LC and IMD/JNK Pathway Activation. *Cell Host Microbe* 2008;**3**:293–303.
Maitra U, Scaglione MN, Chtarbanova S *et al.* Innate immune responses to paraquat exposure in a Drosophila model of Parkinson's disease. *Sci Rep* 2019;**9**:1–17.
Majde JA, Krueger JM. Links between the innate immune system and sleep. *Journal of Allergy and Clinical Immunology* 2005;**116**:1188–99.
Malinen E, Rinttilä T, Kajander K *et al.* Analysis of the Fecal Microbiota of Irritable Bowel Syndrome Patients and Healthy Controls with Real-Time PCR. *Official journal of the American College of Gastroenterology | ACG* 2005;**100**.
Mallon L, Broman JE, Hetta J. Sleep complaints predict coronary artery disease mortality in males: A 12-year follow-up study of a middle-aged Swedish population. *J Intern Med* 2002;**251**:207–16.
Manchanda S, Singh H, Kaur T *et al.* Low-grade neuroinflammation due to chronic sleep deprivation results in anxiety and learning and memory impairments. *Mol Cell Biochem* 2018;**449**:63–72.
Marciano F, Vajro P. Oxidative stress and gut microbiota. *Gastrointestinal Tissue*. Elsevier, 2017, 113–23.
Marianes A, Spradling AC. Physiological and stem cell compartmentalization within the Drosophila midgut. *Elife* 2013;**2**:e00886.
Marika Hedengren, Åsling B, Dushay MS *et al.* Relish, a Central Factor in the Control of Humoral but Not Cellular Immunity in Drosophila. *Molecular Cell* 1999;**4**:827–37.
Martinez J, Longdon B, Bauer S *et al.* Symbionts commonly provide broad spectrum resistance to viruses in insects: a comparative analysis of Wolbachia strains. *PLoS Pathog* 2014;**10**:e1004369.
Martins RR, McCracken AW, Simons MJP *et al.* How to catch a smurf?–Ageing and beyond… In vivo assessment of intestinal permeability in multiple model organisms. *Bio Protoc* 2018;**8**:e2722–e2722.

Mattis J, Sehgal A. Circadian Rhythms, Sleep, and Disorders of Aging Aging of central and peripheral circadian systems Introduction to the circadian system. 2016;**27**:192–203.
Mayer EA, Padua D, Tillisch K. Altered brain-gut axis in autism: Comorbidity or causative mechanisms? *BioEssays* 2014, DOI: 10.1002/bies.201400075.
McClure CD, Hassan A, Aughey GN *et al.* An auxin-inducible, GAL4-compatible, gene expression system for Drosophila. *Elife* 2022;**11**, DOI: 10.7554/eLife.67598.
McFall-Ngai M, Hadfield MG, Bosch TCG *et al.* Animals in a bacterial world, a new imperative for the life sciences. *Proceedings of the National Academy of Sciences* 2013;**110**:3229–36.
McLaughlin CN, Perry-Richardson JJ, Coutinho-Budd JC *et al.* Dying Neurons Utilize Innate Immune Signaling to Prime Glia for Phagocytosis during Development. *Dev Cell* 2019;**48**:506-522.e6.
McMullen JG, Bueno E, Blow F *et al.* Genome-Inferred Correspondence between Phylogeny and Metabolic Traits in the Wild Drosophila Gut Microbiome. *Genome Biol Evol* 2021;**13**, DOI: 10.1093/gbe/evab127.
Meinander A, Runchel C, Tenev T *et al.* Ubiquitylation of the initiator caspase DREDD is required for innate immune signalling. *EMBO Journal* 2012;**31**:2770–83.
Mellroth P, Karlsson J, Steiner H. A scavenger function for a Drosophila peptidoglycan recognition protein. *Journal of Biological Chemistry* 2003;**278**:7059–64.
Menozzi E, Macnaughtan J, Schapira AHV. The gut-brain axis and Parkinson disease: clinical and pathogenetic relevance. *Ann Med* 2021;**53**:611–25.
Metaxakis A, Tain LS, Grönke S *et al.* Lowered Insulin Signalling Ameliorates Age-Related Sleep Fragmentation in Drosophila. *PLoS Biol* 2014a;**12**, DOI: 10.1371/journal.pbio.1001824.
Metaxakis A, Tain LS, Grönke S *et al.* Lowered Insulin Signalling Ameliorates Age-Related Sleep Fragmentation in Drosophila. *PLoS Biol* 2014b;**12**, DOI: 10.1371/journal.pbio.1001824.
Micchelli CA, Perrimon N. Evidence that stem cells reside in the adult Drosophila midgut epithelium. *Nature* 2006;**439**:475–9.
Michel T, Reichhart J-M, Hoffmann JA *et al.* Drosophila Toll is activated by Gram- positive bacteria through a circulating peptidoglycan recognition protein. Nature 414, 756–759 (2001). *Letters to Nature* 2001;**414**:756–9.
Miguel-Aliaga I, Jasper H, Lemaitre B. Anatomy and physiology of the digestive tract of drosophila melanogaster. *Genetics* 2018;**210**:357–96.
Mirmiran M, Scholtens J, van de Poll NE *et al.* Effects of experimental suppression of active (REM) sleep during early development upon adult brain and behavior in the rat. *Brain Res* 1983;**283**:277–86.
Misra S, Hecht P, Maeda R *et al.* Positive and negative regulation of Easter, a member of the serine protease family that controls dorsal-ventral patterning in the Drosophila embryo. *Development* 1998;**125**:1261–7.
Mistry R, Kounatidis I, Ligoxygakis P. Interaction between familial transmission and a constitutively active immune system shapes gut microbiota in Drosophila melanogaster. *Genetics* 2017, DOI: 10.1534/genetics.116.190215.
Molloy JC, Sommer U, Viant MR *et al.* Wolbachia modulates lipid metabolism in Aedes albopictus mosquito cells. *Appl Environ Microbiol* 2016;**82**:3109–20.
Morales-Jiménez J, Zúñiga G, Villa-Tanaca L *et al.* Bacterial community and nitrogen fixation in the red turpentine beetle, dendroctonus valens LeConte (Coleoptera: Curculionidae: Scolytinae). *Microb Ecol* 2009;**58**:879–91.
Moreira LA, Iturbe-Ormaetxe I, Jeffery JA *et al.* A Wolbachia symbiont in Aedes aegypti limits infection with dengue, Chikungunya, and Plasmodium. *Cell* 2009;**139**:1268–78.

Moriyama M, Nikoh N, Hosokawa T *et al.* Riboflavin provisioning underlies Wolbachia's fitness contribution to its insect host. *mBio* 2015;**6**:10–1128.
Morris EK, Caruso T, Buscot F *et al.* Choosing and using diversity indices: insights for ecological applications from the German Biodiversity Exploratories. *Ecol Evol* 2014;**4**:3514–24.
Morrison SJ, Wandycz AM, Akashi K *et al.* The aging of hematopoietic stem cells. *Nat Med* 1996;**2**:1011–6.
Moussian B, Schwarz H, Bartoszewski S *et al.* Involvement of chitin in exoskeleton morphogenesis in Drosophila melanogaster. *J Morphol* 2005;**264**:117–30.
Munford RS, Varley AW. Shield as signal: lipopolysaccharides and the evolution of immunity to gram-negative bacteria. *PLoS Pathog* 2006;**2**:e67.
Murakami R, Shigenaga A, Matsumoto 1Akira *et al.* Novel tissue units of regional differentiation in the gut epithelium of Drosopbila, as revealed by P-element-mediated detection of enhancer. *Roux's archives of developmental biology* 1994;**203**:243–9.
Myllymäki H, Valanne S, Rämet M. The Drosophila Imd Signaling Pathway. *The Journal of Immunology* 2014;**192**:3455–62.
Nagao-Kitamoto H, Kitamoto S, Kuffa P *et al.* Pathogenic role of the gut microbiota in gastrointestinal diseases. *Intest Res* 2016a;**14**:127–38.
Nagao-Kitamoto H, Shreiner AB, Gillilland MG *et al.* Functional Characterization of Inflammatory Bowel Disease-Associated Gut Dysbiosis in Gnotobiotic Mice. *Cmgh* 2016b;**2**:468–81.
Naughton J, Duggan G, Bourke B *et al.* Interaction of microbes with mucus and mucins: recent developments. *Gut Microbes* 2014;**5**:48–52.
Neophytou C, Pitsouli C. How gut microbes nurture intestinal Stem Cells: A Drosophila perspective. *Metabolites* 2022;**12**:169.
Newell PD, Douglas AE. Interspecies interactions determine the impact of the gut microbiota on nutrient allocation in Drosophila melanogaster. *Appl Environ Microbiol* 2014;**80**:788–96.
Neyen C, Poidevin M, Roussel A *et al.* Tissue- and Ligand-Specific Sensing of Gram-Negative Infection in Drosophila by PGRP-LC Isoforms and PGRP-LE. *The Journal of Immunology* 2012;**189**:1886–97.
Neyen C, Runchel C, Schüpfer F *et al.* The regulatory isoform rPGRP-LC induces immune resolution via endosomal degradation of receptors. *Nat Immunol* 2016a;**17**:1150–8.
Neyen C, Runchel C, Schüpfer F *et al.* The regulatory isoform rPGRP-LC induces immune resolution via endosomal degradation of receptors. *Nat Immunol* 2016b;**17**:1150–8.
Nicholson JK, Holmes E, Kinross J *et al.* Host-Gut Microbiota Metabolic Interactions. *The Gut Microbiota* 2012;**108**:1262–8.
Nicholson L, Singh GK, Osterwalder T *et al.* Spatial and Temporal Control of Gene Expression in Drosophila Using the Inducible GeneSwitch GAL4 System. I. Screen for Larval Nervous System Drivers. 2008, DOI: 10.1534/genetics.107.081968.
Nikoh N, Hosokawa T, Moriyama M *et al.* Evolutionary origin of insect–Wolbachia nutritional mutualism. *Proceedings of the National Academy of Sciences* 2014;**111**:10257–62.
Obadia B, Güvener ZT, Zhang V *et al.* Probabilistic Invasion Underlies Natural Gut Microbiome Stability. *Current Biology* 2017;**27**:1999-2006.e8.
O'Hara AM, Shanahan F. The gut flora as a forgotten organ. *EMBO Rep* 2006;**7**:688–93.
Ohlstein B, Spradling A. The adult Drosophila posterior midgut is maintained by pluripotent stem cells. *Nature* 2006;**439**:470–4.
Ondo WG. Sleep / wake problems in Parkinson ' s disease : pathophysiology and clinicopathologic correlations. *J Neural Transm* 2014;**121**:S3–13.

O'Neill SL, M. Pettigrew M, Sinkins SP *et al.* In vitro cultivation of Wolbachia pipientis in an Aedes albopictus cell line. *Insect Mol Biol* 1997;**6**:33–9.
Ooms S, Overeem S, Besse K *et al.* Effect of 1 night of total sleep deprivation on cerebrospinal fluid β-amyloid 42 in healthy middle-aged men a randomized clinical trial. *JAMA Neurol* 2014;**71**:971–7.
O'Riordan KJ, Collins MK, Moloney GM *et al.* Short chain fatty acids: Microbial metabolites for gut-brain axis signalling. *Mol Cell Endocrinol* 2022a;**546**, DOI: 10.1016/j.mce.2022.111572.
O'Riordan KJ, Collins MK, Moloney GM *et al.* Short chain fatty acids: Microbial metabolites for gut-brain axis signalling. *Mol Cell Endocrinol* 2022b;**546**, DOI: 10.1016/j.mce.2022.111572.
Osadchiy V, Martin CR, Mayer EA. The gut–brain axis and the microbiome: mechanisms and clinical implications. *Clinical Gastroenterology and Hepatology* 2019;**17**:322–32.
Osborne SE, Iturbe-Ormaetxe I ½aki, Brownlie JC *et al.* Antiviral protection and the importance of Wolbachia density and tissue tropism in Drosophila simulans. *Appl Environ Microbiol* 2012;**78**:6922–9.
Osterwalder T, Yoon KS, White BH *et al.* A conditional tissue-specific transgene expression system using inducible GAL4. *PNAS* 2001;**98**:12596–601.
Pace-Schott EF, Spencer RMC. Age-related changes in the cognitive function of sleep. *Progress in Brain Research*. Vol 191. Elsevier B.V., 2011, 75–89.
Paik D, Monahan A, Caffrey DR *et al.* SLC46 Family Transporters Facilitate Cytosolic Innate Immune Recognition of Monomeric Peptidoglycans. *The Journal of Immunology* 2017;**199**:263–70.
Pais IS, Valente RS, Sporniak M *et al.* Drosophila melanogaster establishes a species-specific mutualistic interaction with stable gut-colonizing bacteria. *PLoS Biol* 2018;**16**:e2005710.
Pal S, Wu LP. Pattern recognition receptors in the fly. *Fly (Austin)* 2009;**3**:121–9.
Pandi-Perumal SR, Monti JM, Burman D *et al.* Clarifying the role of sleep in depression: A narrative review. *Psychiatry Res* 2020;**291**:113239.
Paredes JC, Welchman DP, Poidevin M *et al.* Negative regulation by Amidase PGRPs shapes the drosophila antibacterial response and protects the Fly from innocuous infection. *Immunity* 2011, DOI: 10.1016/j.immuni.2011.09.018.
Parisky KM, Agosto Rivera JL, Donelson NC *et al.* Reorganization of Sleep by Temperature in Drosophila Requires Light, the Homeostat, and the Circadian Clock. *Current Biology* 2016;**26**:882–92.
Park JT, Uehara T. How Bacteria Consume Their Own Exoskeletons (Turnover and Recycling of Cell Wall Peptidoglycan). *Microbiology and Molecular Biology Reviews* 2008;**72**:211–27.
Parker A, Fonseca S, Carding SR. Gut microbes and metabolites as modulators of blood-brain barrier integrity and brain health. *Gut Microbes* 2020;**11**:135–57.
Pasteur L. Observations relative a la note de M. Duclaux. *Compt Rend Acad Sci* 1885;**100**:68.
Pawelec G. Hallmarks of human "immunosenescence" : Adaptation or dysregulation? *Immunity and Ageing* 2012;**9**, DOI: 10.1186/1742-4933-9-15.
Pédron T, Sansonetti P. Commensals, Bacterial Pathogens and Intestinal Inflammation: An Intriguing Ménage à Trois. *Cell Host Microbe* 2008;**3**:344–7.
Peh A, O'Donnell JA, Broughton BRS *et al.* Gut microbiota and their metabolites in stroke: a double-edged sword. *Stroke* 2022;**53**:1788–801.
Pellegrini C, Antonioli L, Colucci R *et al.* Interplay among gut microbiota, intestinal mucosal barrier and enteric neuro-immune system: a common path to neurodegenerative diseases? *Acta Neuropathol* 2018;**136**:345–61.

Perkins LA, Holderbaum L, Tao R *et al.* The transgenic RNAi project at Harvard medical school: Resources and validation. *Genetics* 2015;**201**:843–52.
Perlman D, Martínez-Álvaro M, Moraïs S *et al.* Concepts and consequences of a core gut microbiota for animal growth and development. *Annu Rev Anim Biosci* 2022;**10**:177–201.
Phelps CB, Brand AH. *Ectopic Gene Expression in Drosophila Using GAL4 System*., 1998.
Pickard JM, Zeng MY, Caruso R *et al.* Gut microbiota: Role in pathogen colonization, immune responses, and inflammatory disease. *Immunol Rev* 2017;**279**:70–89.
St. Pierre SE, Ponting L, Stefancsik R *et al.* FlyBase 102 - Advanced approaches to interrogating FlyBase. *Nucleic Acids Res* 2014;**42**, DOI: 10.1093/nar/gkt1092.
Piper MDW, Partridge L. Drosophila as a model for ageing. *Biochim Biophys Acta Mol Basis Dis* 2018;**1864**:2707–17.
Plovier H, Everard A, Druart C *et al.* A purified membrane protein from Akkermansia muciniphila or the pasteurized bacterium improves metabolism in obese and diabetic mice. *Nat Med* 2017;**23**:107–13.
Politis M, Lahiri N, Niccolini F *et al.* Increased central microglial activation associated with peripheral cytokine levels in premanifest Huntington's disease gene carriers. *Neurobiol Dis* 2015;**83**:115–21.
Purice MD, Speese SD, Logan MA. Delayed glial clearance of degenerating axons in aged Drosophila is due to reduced PI3K/Draper activity. *Nat Commun* 2016;**7**, DOI: 10.1038/ncomms12871.
Qin J, Li Y, Cai Z *et al.* A metagenome-wide association study of gut microbiota in type 2 diabetes. *Nature* 2012;**490**:55–60.
Rahman MM, Islam F, -Or-Rashid MH *et al.* The Gut Microbiota (Microbiome) in Cardiovascular Disease and Its Therapeutic Regulation. *Front Cell Infect Microbiol* 2022;**12**:1–22.
Rajilić-Stojanović M, Smidt H, De Vos WM. Diversity of the human gastrointestinal tract microbiota revisited. *Environ Microbiol* 2007;**9**:2125–36.
Ramakrishna BS. Role of the gut microbiota in human nutrition and metabolism. *J Gastroenterol Hepatol* 2013;**28**:9–17.
Rämet M, Manfruelli P, Pearson A *et al.* Functional genomic analysis of phagocytosis and identification of a Drosophila receptor for E. coli. *Letters to Nature* 2002a;**416**:644–8.
Rämet M, Manfruelli P, Pearson A *et al.* Functional genomic analysis of phagocytosis and identification of a Drosophila receptor for E. coli. *Nature* 2002b;**416**:644–8.
Ranjan R, Rani A, Finn PW *et al.* Multiomic strategies reveal diversity and important functional aspects of human gut microbiome. *Biomed Res Int* 2018;**2018**.
Rault C, Sangaré A, Diaz V *et al.* Impact of sleep deprivation on respiratory motor output and endurance: A physiological study. *Am J Respir Crit Care Med* 2020;**201**:976–83.
Ray A, Speese SD, Logan MA. Glial draper rescues Aβ toxicity in a Drosophila model of Alzheimer's disease. *Journal of Neuroscience* 2017;**37**:11881–93.
Redline S, Kirchner HL, Quan SF *et al.* The Effects of Age, Sex, Ethnicity, and Sleep-Disordered Breathing on Sleep Architecture. *Arch Intern Med* 2004;**164**:406–18.
Reeve S, Sheaves B, Freeman D. Sleep Disorders in Early Psychosis: Incidence, Severity, and Association with Clinical Symptoms. *Schizophr Bull* 2019;**45**:287–95.
De Reggi ML, Cailla HL. Cyclic AMP levels in Drosophila during postembryonic development and in the adults. *J Insect Physiol* 1975;**21**:1671–4.
Ren C, Webster P, Finkel SE *et al.* Increased Internal and External Bacterial Load during Drosophila Aging without Life-Span Trade-Off. *Cell Metab* 2007;**6**:144–52.

Rera M, Clark RI, Walker DW. Intestinal barrier dysfunction links metabolic and inflammatory markers of aging to death in Drosophila. *PNAS* 2012a, DOI: 10.1073/pnas.1215849110.
Rera M, Clark RI, Walker DW. Intestinal barrier dysfunction links metabolic and inflammatory markers of aging to death in Drosophila. *Proc Natl Acad Sci U S A* 2012b;**109**:21528–33.
Rescigno M. The intestinal epithelial barrier in the control of homeostasis and immunity. *Trends Immunol* 2011;**32**:256–64.
Reyniers JA, Sacksteder MR. Tumorigenisis and the Germfree Chicken: a Preliminary Report. *Ann N Y Acad Sci* 1959;**78**:328–53.
Riegler M, Sidhu M, Miller WJ *et al.* Evidence for a global Wolbachia replacement in Drosophila melanogaster. *Current biology* 2005;**15**:1428–33.
Riesenfeld CS, Schloss PD, Handelsman J. Metagenomics: genomic analysis of microbial communities. *Annu Rev Genet* 2004;**38**:525–52.
Rohrscheib CE, Bondy E, Josh P *et al.* Wolbachia influences the production of octopamine and affects Drosophila male aggression. *Appl Environ Microbiol* 2015;**81**:4573–80.
Romaní-Pérez M, Bullich-Vilarrubias C, López-Almela I *et al.* The Microbiota and the Gut–Brain Axis in Controlling Food Intake and Energy Homeostasis. *Int J Mol Sci* 2021;**22**:5830.
Rooks MG, Garrett WS. Gut microbiota, metabolites and host immunity. *Nat Rev Immunol* 2016;**16**:341–52.
Rossi DJ, Bryder D, Seita J *et al.* Deficiencies in DNA damage repair limit the function of haematopoietic stem cells with age. *Nature* 2007;**447**:725–9.
Rossi DJ, Bryder D, Zahn JM *et al.* Cell intrinsic alterations underlie hematopoietic stem cell aging. *Proceedings of the National Academy of Sciences* 2005;**102**:9194–9.
Rossi DJ, Jamieson CHM, Weissman IL. Stems cells and the pathways to aging and cancer. *Cell* 2008;**132**:681–96.
Rothschild D, Weissbrod O, Barkan E *et al.* Environment dominates over host genetics in shaping human gut microbiota. *Nature* 2018;**555**:210–5.
Round JL, Mazmanian SK. The gut microbiota shapes intestinal immune responses during health and disease. *Nat Rev Immunol* 2009;**9**:313–23.
Royet J, Dziarski R. Peptidoglycan recognition proteins: Pleiotropic sensors and effectors of antimicrobial defences. *Nat Rev Microbiol* 2007;**5**:264–77.
Royet J, Gupta D, Dziarski R. Peptidoglycan recognition proteins: Modulators of the microbiome and inflammation. *Nat Rev Immunol* 2011;**11**:837–51.
Royet J, Reichhart JM, Hoffmann JA. Sensing and signaling during infection in Drosophila. *Curr Opin Immunol* 2005;**17**:11–7.
Rudman SM, Greenblum S, Hughes RC *et al.* Microbiome composition shapes rapid genomic adaptation of Drosophila melanogaster. *Proc Natl Acad Sci U S A* 2019;**116**:20025–32.
Ruesten A von, Weikert C, Fietze I *et al.* Association of sleep duration with chronic diseases in the european prospective investigation into cancer and nutrition (epic)-potsdam study. *PLoS One* 2012;**7**:1–9.
Ruiz A, Cerdó T, Jáuregui R *et al.* One-year calorie restriction impacts gut microbial composition but not its metabolic performance in obese adolescents. *Environ Microbiol* 2017;**19**:1536–51.
Rutschmann S, Jung AC, Zhou R *et al. Role of Drosophila IKKγ in a Toll-Independent Antibacterial Immune Response*., 2000.
Rutschmann S, Kilinc A, Ferrandon D. Cutting Edge: The Toll Pathway Is Required for Resistance to Gram-Positive Bacterial Infections in Drosophila. *The Journal of Immunology* 2002;**168**:1542–6.

Ryu J, Kim S, Lee H *et al.* Innate Immune Homeostasis by the Homeobox Gene Caudal and Commensal-Gut Mutualism in Drosophila. *Science (1979)* 2008;**319**:777–82.
Sabat D, Johnson EM. A Protocol to Generate Germ Free Drosophila for Microbial Interaction Studies. *Adv Tech Biol Med* 2015;**s1**, DOI: 10.4172/2379-1764.s1-001.
Sabia S, Fayosse A, Dumurgier J *et al.* Association of sleep duration in middle and old age with incidence of dementia. *Nat Commun* 2021;**12**:2289.
Saha S, Pupo E, Zariri A *et al.* Lipid A heterogeneity and its role in the host interactions with pathogenic and commensal bacteria. *microLife* 2022;**3**:uqac011.
Salih DA, Bayram S, Guelfi S *et al.* Genetic variability in response to amyloid beta deposition influences Alzheimer's disease risk. *Brain Commun* 2019;**1**:1–13.
Salvioli S, Monti D, Lanzarini C *et al. Immune System, Cell Senescence, Aging and Longevity-Inflamm-Aging Reappraised*., 2013.
Sampson TR, Debelius JW, Thron T *et al.* Gut microbiota regulate motor deficits and neuroinflammation in a model of Parkinson's disease. *Cell* 2016;**167**:1469–80.
Sannino DR, Dobson AJ, Edwards K *et al.* The Drosophila melanogaster gut microbiota provisions thiamine to its host. *mBio* 2018;**9**:10–1128.
Sansonetti PJ, Puhar A. Overview of Bacterial Pathogens. *The Immune Response to Infection* 2010:155–64.
Santana PT, Rosas SLB, Ribeiro BE *et al.* Dysbiosis in Inflammatory Bowel Disease: Pathogenic Role and Potential Therapeutic Targets. *Int J Mol Sci* 2022;**23**, DOI: 10.3390/ijms23073464.
Sanuki R, Tanaka T, Suzuki F *et al.* Normal aging hyperactivates innate immunity and reduces the medical efficacy of minocycline in brain injury. *Brain Behav Immun* 2019;**80**:427–38.
Sarubbo F, Cavallucci V, Pani G. The influence of gut microbiota on neurogenesis: evidence and hopes. *Cells* 2022;**11**:382.
Schirmer M, Franzosa EA, Lloyd-Price J *et al.* Dynamics of metatranscription in the inflammatory bowel disease gut microbiome. *Nat Microbiol* 2018;**3**:337–46.
Schneider DS, Ayres JS. Two ways to survive infection: what resistance and tolerance can teach us about treating infectious diseases. *Nat Rev Immunol* 2008;**8**:889–95.
Schneider DS, Jin Y, Morisato D *et al.* A processed form of the Spätzle protein defines dorsal-ventral polarity in the Drosophila embryo. *Development* 1994;**120**:1243–50.
Schretter CE, Vielmetter J, Bartos I *et al.* A gut microbial factor modulates locomotor behaviour in Drosophila. *Nature* 2018;**563**:402–6.
Schuijt TJ, van der Poll T, de Vos WM *et al.* The intestinal microbiota and host immune interactions in the critically ill. *Trends Microbiol* 2013;**21**:221–9.
Seganfredo FB, Blume CA, Moehlecke M *et al.* Weight-loss interventions and gut microbiota changes in overweight and obese patients: a systematic review. *Obesity Reviews* 2017;**18**:832–51.
Sehgal A, Mignot E. Genetics of sleep and sleep disorders. *Cell* 2011;**146**:194–207.
Sekirov I, Russell SL, Caetano L *et al.* Gut Microbiota in Health and Disease. *Physiol Rev* 2010;**90**:859–904.
Sekiya M, Wang M, Fujisaki N *et al.* Integrated biology approach reveals molecular and pathological interactions among Alzheimer's Aβ42, Tau, TREM2, and TYROBP in Drosophila models. *Genome Med* 2018;**10**, DOI: 10.1186/s13073-018-0530-9.
Selkrig J, Mohammad F, Ng SH *et al.* The Drosophila microbiome has a limited influence on sleep, activity, and courtship behaviors. *Sci Rep* 2018;**8**:10646.
Seugnet L, Suzuki Y, Donlea JM *et al. Sleep Deprivation During Early-Adult Development Results in Long-Lasting Learning Deficits in Adult Drosophila*., 2011.

Shandilya S, Kumar S, Jha NK *et al.* Interplay of gut microbiota and oxidative stress: Perspective on neurodegeneration and neuroprotection. *J Adv Res* 2022;**38**:223–44.
Shang Y, Griffith LC, Rosbash M. Light-arousal and circadian photoreception circuits intersect at the large PDF cells of the Drosophila brain. *PNAS* 2008;**105**:19587–94.
Sharon G, Segal D, Ringo JM *et al.* Commensal bacteria play a role in mating preference of Drosophila melanogaster. *Proc Natl Acad Sci U S A* 2010;**107**:20051–6.
Shaw PJ, Cirelli C, Greenspan RJ *et al.* Correlates of Sleep and Waking in Drosophila melanogaster. *Science (1979)* 2000;**287**:1834–7.
Shibata T, Sekihara S, Fujikawa T *et al.* Transglutaminase-catalyzed protein-protein cross-linking suppresses the activity of the NF-κB-like transcription factor relish. *Sci Signal* 2013;**6**:1–11.
Shukla AK, Spurrier J, Kuzina I *et al.* Hyperactive Innate Immunity Causes Degeneration of Dopamine Neurons upon Altering Activity of Cdk5. *Cell Rep* 2019;**26**, DOI: 10.1016/j.celrep.2018.12.025.
Silva YP, Bernardi A, Frozza RL. The Role of Short-Chain Fatty Acids From Gut Microbiota in Gut-Brain Communication. *Front Endocrinol (Lausanne)* 2020;**11**:1–14.
Silverman N, Zhou R, Stöven S *et al.* A Drosophila IκB kinase complex required for relish cleavage and antibacterial immunity. *Genes Dev* 2000;**14**:2461–71.
Simhadri RK, Fast EM, Guo R *et al.* The gut commensal microbiome of Drosophila melanogaster is modified by the endosymbiont Wolbachia. *mSphere* 2017;**2**:10–1128.
Singh A, Irvine KD. Drosophila as a model for understanding development and disease. *Developmental Dynamics* 2012;**241**:1–2.
Singh SR, Zeng X, Zheng Z *et al.* The adult Drosophila gastric and stomach organs are maintained by a multipotent stem cell pool at the foregut/midgut junction in the cardia (proventriculus). *Cell Cycle* 2011;**10**:1109–20.
Smith CJ, Emsley HC, Udeh CT *et al.* Interleukin-1 receptor antagonist reverses stroke-associated peripheral immune suppression. *Cytokine* 2012a;**58**:384–9.
Smith JA, Das A, Ray SK *et al.* Role of pro-inflammatory cytokines released from microglia in neurodegenerative diseases. *Brain Res Bull* 2012b;**87**:10–20.
Socała K, Doboszewska U, Szopa A *et al.* The role of microbiota-gut-brain axis in neuropsychiatric and neurological disorders. *Pharmacol Res* 2021;**172**, DOI: 10.1016/j.phrs.2021.105840.
Sofola O, Kerr F, Rogers I *et al.* Inhibition of GSK-3 ameliorates Aβ pathology in an adult-onset Drosophila model of Alzheimer's disease. *PLoS Genet* 2010;**6**, DOI: 10.1371/journal.pgen.1001087.
Solana R, Tarazona R, Gayoso I *et al.* Innate immunosenescence: Effect of aging on cells and receptors of the innate immune system in humans. *Semin Immunol* 2012;**24**:331–41.
Spira AP, Gamaldo AA, An Y *et al.* Self-reported sleep and β-amyloid deposition in community-dwelling older adults. *JAMA Neurol* 2013;**70**:1537–43.
Spradling AC, Stern D, Beaton A *et al. The Berkeley Drosophila Genome Project Gene Disruption Project: Single P-Element Insertions Mutating 25% of Vital Drosophila Genes*., 1999.
Staubach F, Baines JF, Künzel S *et al.* Host Species and Environmental Effects on Bacterial Communities Associated with Drosophila in the Laboratory and in the Natural Environment. *PLoS One* 2013;**8**, DOI: 10.1371/journal.pone.0070749.
Stavitsky K, Neargarder S, Bogdanova Y *et al.* The impact of sleep quality on cognitive functioning in Parkinson's disease. *Journal of the International Neuropsychological Society* 2012;**18**:108–17.
Stefani A, Högl B. Sleep in Parkinson's disease. *Neuropsychopharmacology* 2020;**45**:121–8.

Stenbak CR, Ryu J-H, Leulier F *et al. Peptidoglycan Molecular Requirements Allowing Detection by the Drosophila Immune Deficiency Pathway 1*., 2004.
Stoffolano Jr JG, Haselton AT. The adult Dipteran crop: a unique and overlooked organ. *Annu Rev Entomol* 2013;**58**:205–25.
Storch K, Lipan O, Leykin I *et al.* Liver and brain mitochondria preparation. 2002;**417**:0–6.
Storelli G, Defaye A, Erkosar B *et al.* Lactobacillus plantarum promotes drosophila systemic growth by modulating hormonal signals through TOR-dependent nutrient sensing. *Cell Metab* 2011;**14**:403–14.
Storelli G, Strigini M, Grenier T *et al.* Drosophila perpetuates nutritional mutualism by promoting the fitness of its intestinal symbiont Lactobacillus plantarum. *Cell Metab* 2018;**27**:362–77.
Stöven S, Ando I, Kadalayil L *et al. Activation of the Drosophila NF-KB Factor Relish by Rapid Endoproteolytic Cleavage*., 2000.
Stöven S, Silverman N, Junell A *et al.* Caspase-mediated processing of the Drosophila NF-B factor Relish. *PNAS* 2003;**100**:5991–6.
Strand M, Micchelli CA. Quiescent gastric stem cells maintain the adult Drosophila stomach. *Proceedings of the National Academy of Sciences* 2011;**108**:17696–701.
Stuart LM, Ezekowitz RA. Phagocytosis and comparative innate immunity: Learning on the fly. *Nat Rev Immunol* 2008, DOI: 10.1038/nri2240.
Su X, Maguire-Zeiss KA, Giuliano R *et al.* Synuclein activates microglia in a model of Parkinson's disease. *Neurobiol Aging* 2008;**29**:1690–701.
Sun Y, Sommerville NR, Liu JYH *et al.* Intra-gastrointestinal amyloid-β1–42 oligomers perturb enteric function and induce Alzheimer's disease pathology. *J Physiol* 2020;**598**:4209–23.
Sundman MH, Chen N, Subbian V *et al.* The bidirectional gut-brain-microbiota axis as a potential nexus between traumatic brain injury, inflammation, and disease. *Brain Behav Immun* 2017;**66**:31–44.
Surana NK, Kasper DL. Moving beyond microbiome-wide associations to causal microbe identification. *Nature* 2017;**552**:244–7.
Takashima S, Mkrtchyan M, Younossi-Hartenstein A *et al.* The behaviour of Drosophila adult hindgut stem cells is controlled by Wnt and Hh signalling. *Nature* 2008;**454**:651–5.
Takehana A, Katsuyama T, Yano T *et al.* Overexpression of a pattern-recognition receptor, peptidoglycan-recognition protein-LE, activates imd/relish-mediated antibacterial defense and the prophenoloxidase cascade in Drosophila larvae. *PNAS* 2002;**99**:13705–10.
Takehana A, Yano T, Mita S *et al.* Peptidoglycan recognition protein (PGRP)-LE and PGRP-LC act synergistically in Drosophila immunity. *EMBO Journal* 2004;**23**:4690–700.
Takiishi T, Fenero CIM, Câmara NOS. Intestinal barrier and gut microbiota: Shaping our immune responses throughout life. *Tissue Barriers* 2017;**5**:e1373208.
Tamura T, Chiang A-S, Ito N *et al.* Aging Specifically Impairs amnesiac-Dependent Memory in Drosophila Genetic studies of memory formation in Drosophila. *Neuron* 2003;**40**:1003–11.
Tan L, Schedl P, Song HJ *et al.* The Toll→NFκB signaling pathway mediates the neuropathological effects of the human Alzheimer's Aβ42 polypeptide in Drosophila. *PLoS One* 2008;**3**, DOI: 10.1371/journal.pone.0003966.
Tang H. Regulation and function of the melanization reaction in Drosophila. *Fly (Austin)* 2009;**3**:105–11.
Tang H, Kambris Z, Lemaitre B *et al.* Two Proteases Defining a Melanization Cascade in the Immune System of Drosophila *. *J Biol Chem* 2006;**281**:28097–104.

Tang W, Zhu H, Feng Y *et al.* The impact of gut microbiota disorders on the blood–brain barrier. *Infect Drug Resist* 2020:3351–63.
Tarasoff-Conway JM, Carare RO, Osorio RS *et al.* Clearance systems in the brain - Implications for Alzheimer disease. *Nat Rev Neurol* 2015;**11**:457–70.
Teixeira L, Ferreira Á, Ashburner M. The bacterial symbiont Wolbachia induces resistance to RNA viral infections in Drosophila melanogaster. *PLoS Biol* 2008;**6**:e1000002.
Thimgan MS, Suzuki Y, Seugnet L *et al.* The Perilipin homologue, Lipid storage droplet 2, regulates sleep homeostasis and prevents learning impairments following sleep loss. *PLoS Biol* 2010;**8**:29–30.
Tobaldini E, Costantino G, Solbiati M *et al.* Sleep, sleep deprivation, autonomic nervous system and cardiovascular diseases. *Neurosci Biobehav Rev* 2017;**74**:321–9.
Tomari Y, Zamore PD. Perspective: Machines for RNAi. *Genes Dev* 2005;**19**:517–29.
Tomasello G, Mazzola M, Leone A *et al.* Nutrition, oxidative stress and intestinal dysbiosis: Influence of diet on gut microbiota in inflammatory bowel diseases. *Biomed Pap Med Fac Univ Palacky Olomouc Czech Repub* 2016;**160**:461–6.
Tononi G, Cirelli C. Sleep and synaptic homeostasis: A hypothesis. *Brain Res Bull* 2003;**62**:143–50.
Tononi G, Cirelli C. Sleep function and synaptic homeostasis. *Sleep Med Rev* 2006;**10**:49–62.
Towb P, Bergmann A, Wasserman SA. The protein kinase Pelle mediates feedback regulation in the Drosophila Toll signaling pathway. *Development* 2001;**128**:4729–36.
Van Treuren W, Dodd D. Microbial contribution to the human metabolome: implications for health and disease. *Annual Review of Pathology: Mechanisms of Disease* 2020;**15**:345–69.
Trinder M, Daisley BA, Dube JS *et al.* Drosophila melanogaster as a High-Throughput Model for Host – Microbiota Interactions. *Front Microbiol* 2017;**8**:1–8.
Tsichritzis T, Gaentzsch PC, Kosmidis S *et al.* A Drosophila ortholog of the human cylindromatosis tumor suppressor gene regulates triglyceride content and antibacterial defense. *Development* 2007;**134**:2605–14.
Tsuda M, Langmann C, Harden N *et al.* The RING-finger scaffold protein Plenty of SH3s targets TAK1 to control immunity signalling in Drosophila. *EMBO Rep* 2005;**6**:1082–7.
Tu W, Rao S. Mechanisms underlying T cell immunosenescence: Aging and cytomegalovirus infection. *Front Microbiol* 2016;**7**, DOI: 10.3389/fmicb.2016.02111.
Turnbaugh PJ, Ley RE, Mahowald MA *et al.* An obesity-associated gut microbiome with increased capacity for energy harvest. *Nature* 2006;**444**:1027–31.
Tzou P, de Gregorio E, Lemaitre B. How Drosophila combats microbial infection: A model to study innate immunity and host-pathogen interactions. *Curr Opin Microbiol* 2002, DOI: 10.1016/S1369-5274(02)00294-1.
Tzou P, Ohresser S, Ferrandon D *et al.* Tissue-Specific Inducible Expression of Antimicrobial Peptide Genes in Drosophila Surface Epithelia. *Immunity* 2000;**13**:737–48.
Ugur B, Chen K, Bellen HJ. Drosophila tools and assays for the study of human diseases. *Dis Model Mech* 2016;**9**:235–44.
Vaccaro A, Dor YK, Nambara K *et al.* Sleep loss can cause death through accumulation of reactive oxygen species in the gut. *Cell* 2020;**181**:1307–28.
Valanne S, Wang J-H, Rämet M. The Drosophila Toll Signaling Pathway. *The Journal of Immunology* 2011;**186**:649–56.
Valdes AM, Walter J, Segal E *et al.* Role of the gut microbiota in nutrition and health. *BMJ (Online)* 2018;**361**:36–44.
Vale PF, Jardine MD. Sex-specific behavioural symptoms of viral gut infection and Wolbachia in Drosophila melanogaster. *J Insect Physiol* 2015;**82**:28–32.

Venu I, Durisko Z, Xu J *et al.* Social attraction mediated by fruit flies' microbiome. *Journal of Experimental Biology* 2014;**217**:1346–52.
Verkasalo PK, Lillberg K, Stevens RG *et al.* Sleep duration and breast cancer: A prospective cohort study. *Cancer Res* 2005;**65**:9595–600.
Vgontzas AN, Pejovic S, Zoumakis E *et al.* Daytime napping after a night of sleep loss decreases sleepiness, improves performance, and causes beneficial changes in cortisol and interleukin-6 secretion. *Am J Physiol Endocrinol Metab* 2007;**292**:253–61.
Vidal PM, Pacheco R. The cross-talk between the dopaminergic and the immune system involved in schizophrenia. *Front Pharmacol* 2020;**11**:394.
Visconti A, Le Roy CI, Rosa F *et al.* Interplay between the human gut microbiome and host metabolism. *Nat Commun* 2019;**10**:1–10.
Vuong HE, Yano JM, Fung TC *et al.* The Microbiome and Host Behavior. *Annu Rev Neurosci* 2017a;**40**:21–49.
Vuong HE, Yano JM, Fung TC *et al.* The Microbiome and Host Behavior. *Annu Rev Neurosci* 2017b;**40**:21–49.
Wang C, Holtzman DM. Bidirectional relationship between sleep and Alzheimer's disease: role of amyloid, tau, and other factors. *Neuropsychopharmacology* 2020;**45**:104–20.
Wang L, Gilbert RJC, Atilano MaL *et al.* Peptidoglycan recognition protein-SD providesversatility of receptor formation inDrosophilaimmunity. *PNAS* 2008;**105**:11881–6.
Wang Q, Luo Y, Ray Chaudhuri K *et al.* The role of gut dysbiosis in Parkinson's disease: Mechanistic insights and therapeutic options. *Brain* 2021a;**144**:2571–93.
Wang X, Quinn PJ. Endotoxins: lipopolysaccharides of gram-negative bacteria. *Endotoxins: structure, function and recognition* 2010:3–25.
Wang Y, Kasper LH. The role of microbiome in central nervous system disorders. *Brain Behav Immun* 2014, DOI: 10.1016/j.bbi.2013.12.015.
Wang Z, Zhang Q, Lin JR *et al.* Deep post-GWAS analysis identifies potential risk genes and risk variants for Alzheimer's disease, providing new insights into its disease mechanisms. *Sci Rep* 2021b;**11**, DOI: 10.1038/s41598-021-99352-3.
Warner N, Núñez G. MyD88: A Critical Adaptor Protein in Innate Immunity Signal Transduction. *The Journal of Immunology* 2013;**190**:3–4.
Weber ANR, Tauszig-Delamasure S, Hoffmann JA *et al.* Binding of the Drosophila cytokine Spätzle to Toll is direct and establishes signaling. *Nat Immunol* 2003;**4**:794–800.
Wen J, Ding Y, Wang L *et al.* Gut microbiome improves postoperative cognitive function by decreasing permeability of the blood-brain barrier in aged mice. *Brain Res Bull* 2020;**164**:249–56.
Werner T, Liu G, Kang D *et al.* A family of peptidoglycan recognition proteins in the fruit fly Drosophila melanogaster. *PNAS* 2000;**97**:13772–7.
Werren JH, Baldo L, Clark ME. Wolbachia: master manipulators of invertebrate biology. *Nat Rev Microbiol* 2008;**6**:741–51.
Westfall S, Lomis N, Id SP *et al. A Novel Synbiotic Delays Alzheimer's Disease Onset via Combinatorial Gut-Brain-Axis Signaling in Drosophila Melanogaster.*, 2019.
Wilches D, Coghlin P, Floate K. Next generation sequencing, insect microbiomes, and the confounding effect of Wolbachia: a case study using Drosophila suzukii Matsumura (Diptera: Drosophilidae). 2021.
Wiley NC, Dinan TG, Ross RP *et al.* The microbiota-gut-brain axis as a key regulator of neural function and the stress response: Implications for human and animal health. *J Anim Sci* 2017;**95**:3225–46.
Williams JA, Sathyanarayanan S, Hendricks JC *et al.* Interaction between sleep and the immune response in Drosophila: a role for the NFκB relish. *Sleep* 2007;**30**:389–400.

Williams SCP. Gnotobiotics. *Proc Natl Acad Sci U S A* 2014;**111**:1661.
Wong AC, Luo Y, Jing X *et al.* The Host as the Driver of the Microbiota in the Gut and External Environment of Drosophila melanogaster. *Appl Environ Microbiol* 2015;**81**:6232–40.
Wong ACN, Chaston JM, Douglas AE. The inconstant gut microbiota of Drosophila species revealed by 16S rRNA gene analysis. *ISME J* 2013;**7**:1922–32.
Wong ACN, Vanhove AS, Watnick PI. The interplay between intestinal bacteria and host metabolism in health and disease: Lessons from Drosophila melanogaster. *DMM Disease Models and Mechanisms* 2016;**9**:271–81.
Wong CNA, Ng P, Douglas AE. Low-diversity bacterial community in the gut of the fruitfly Drosophila melanogaster. *Environ Microbiol* 2011;**13**:1889–900.
Wong ZS, Hedges LM, Brownlie JC *et al.* Wolbachia-mediated antibacterial protection and immune gene regulation in Drosophila. *PLoS One* 2011;**6**:e25430.
World Population Prospects: the 2019 Revision. 2019.
Wright AL, Zinn R, Hohensinn B *et al.* Neuroinflammation and Neuronal Loss Precede Aβ Plaque Deposition in the hAPP-J20 Mouse Model of Alzheimer's Disease. *PLoS One* 2013;**8**, DOI: 10.1371/journal.pone.0059586.
Wu J, Wang K, Wang X *et al.* The role of the gut microbiome and its metabolites in metabolic diseases. *Protein Cell* 2021;**12**:360–73.
Wu JS, Luo L. A protocol for dissecting Drosophila melanogaster brains for live imaging or immunostaining. *Nat Protoc* 2006;**1**:2110–5.
Wu SC, Cao ZS, Chang KM *et al.* Intestinal microbial dysbiosis aggravates the progression of Alzheimer's disease in Drosophila. *Nat Commun* 2017;**8**:1–8.
Wulff K, Gatti S, Wettstein JG *et al.* Sleep and circadian rhythm disruption in psychiatric and neurodegenerative disease. *Nature Reviews* 2010;**11**:1–11.
Xia S, Zhang X, Zheng S *et al.* An Update on Inflamm-Aging: Mechanisms, Prevention, and Treatment. *J Immunol Res* 2016;**2016**, DOI: 10.1155/2016/8426874.
Xie L, Kang H, Xu Q *et al.* Sleep drives metabolite clearance from the adult brain. *Science (1979)* 2013;**342**, DOI: 10.1126/science.1241224.
Yamamoto S, Jaiswal M, Charng WL *et al.* A drosophila genetic resource of mutants to study mechanisms underlying human genetic diseases. *Cell* 2014;**159**:200–14.
Yamamoto-Hino M, Goto S. In vivo RNAi-based screens: studies in model organisms. *Genes (Basel)* 2013;**4**:646–65.
Yamanaka K, Chun SJ, Boillee S *et al.* Astrocytes as determinants of disease progression in inherited amyotrophic lateral sclerosis. *Nat Neurosci* 2008;**11**:251–3.
Yano T, Mita S, Ohmori H *et al.* Autophagic control of listeria through intracellular innate immune recognition in drosophila. *Nat Immunol* 2008;**9**:908–16.
Younes S, Al-Sulaiti A, Nasser EAA *et al.* Drosophila as a Model Organism in Host–Pathogen Interaction Studies. *Front Cell Infect Microbiol* 2020;**10**:1–16.
Yun J-H, Roh SW, Whon TW *et al.* Insect gut bacterial diversity determined by environmental habitat, diet, developmental stage, and phylogeny of host. *Appl Environ Microbiol* 2014;**80**:5254–64.
Zachar Z, Savage DC. Microbial interference and colonization of the murine gastrointestinal tract by Listeria monocytogenes. *Infect Immun* 1979;**23**:168–74.
Zengler K, Toledo G, Rappé M *et al.* Cultivating the uncultured. *Proceedings of the National Academy of Sciences* 2002;**99**:15681–6.
Zhang G, Li J, Purkayastha S *et al.* Hypothalamic programming of systemic ageing involving IKK-β, NF-κB and GnRH. *Nature* 2013;**497**:211–6.

Zhang SL, Yue Z, Arnold DM *et al.* A Circadian Clock in the Blood-Brain Barrier Article A Circadian Clock in the Blood-Brain Barrier Regulates Xenobiotic Efflux. *Cell* 2018;**173**:130–9.
Zhang Y, Ren R, Yang L *et al.* Sleep in Huntington's disease: A systematic review and meta-analysis of polysomongraphic findings. *Sleep* 2019;**42**, DOI: 10.1093/sleep/zsz154.
Zhang Y, Ren R, Yang L *et al.* Sleep in Alzheimer's disease: a systematic review and meta-analysis of polysomnographic findings. *Transl Psychiatry* 2022;**12**:136.
Zhao D-X, Zhang X-F, Chen D-S *et al.* Wolbachia-host interactions: host mating patterns affect Wolbachia density dynamics. *PLoS One* 2013;**8**:e66373.
Zhao HY, Wu HJ, He JL *et al.* Chronic Sleep Restriction Induces Cognitive Deficits and Cortical Beta-Amyloid Deposition in Mice via BACE1-Antisense Activation. *CNS Neurosci Ther* 2017;**23**:233–40.
Zhao L. The gut microbiota and obesity: From correlation to causality. *Nat Rev Microbiol* 2013;**11**:639–47.
Zhao Y, Lukiw WJ. Microbiome-generated amyloid and potential impact on amyloidogenesis in Alzheimer's disease (AD). *J Nat Sci* 2015;**1**.
Zhou H, Sun J, Yu B *et al.* Gut microbiota absence and transplantation affect growth and intestinal functions: an investigation in a germ-free pig model. *Animal Nutrition* 2021;**7**:295–304.
Zhu S, Jiang Y, Xu K *et al.* The progress of gut microbiome research related to brain disorders. *J Neuroinflammation* 2020;**17**:1–20.
Zimmerman JE, Chan MT, Jackson N *et al.* Genetic background has a major impact on differences in sleep resulting from environmental influences in Drosophila. *Sleep* 2012;**35**:545–57.
Zoetendal EG, Vaughan EE, De Vos WM. A microbial world within us. *Mol Microbiol* 2006;**59**:1639–50.
Zug R, Hammerstein P. Still a host of hosts for Wolbachia: analysis of recent data suggests that 40% of terrestrial arthropod species are infected. *PLoS One* 2012;**7**:e38544.